# The regulation of deubiquitinases by oxidative stress in *Saccharomyces cerevisiae*.

Faye Elizabeth Jade Curtis

Thesis submitted for the degree of Doctor of Philosophy

Institute for Cell and Molecular Biosciences

Faculty of Medical Sciences

Newcastle University

September 2018

# Declaration

I certify that this thesis is my own work, except where acknowledged. Work in this thesis has not been previously submitted for another degree or qualification at this or any other university.

## Abstract

Reactive oxygen species (ROS) are produced as by-products of cellular processes. In eukaryotes high levels of ROS cause oxidative stress, leading to intracellular damage and age-related diseases, whereas low levels of ROS are vital for many cellular functions including signal transduction and cell proliferation. It is therefore essential that cells can sense the different types and levels of ROS to ensure that they respond in an appropriate manner. Ubiquitination is a post-translational modification which plays vital roles in fundamental cellular processes, including protein degradation and many signalling pathways. Ubiquitination of substrates occurs in a cycle involving the coordinated activity of conjugation and deconjugation enzymes and, interestingly, most ubiquitin pathway enzymes utilise catalytic cysteines for function. Recent work from our lab and others has begun to reveal that the relative sensitivity of these cysteines to oxidation is important for sensing the different types and levels of ROS. In the present study we hypothesised that deubiquitinases (dUbs), which remove ubiquitin from substrates through the activity of an active site catalytic cysteine, may also be regulated by ROS. Hence to test this hypothesis, the tractability and powerful genetic tools available in the model eukaryote *Saccharomyces cerevisiae* were utilised to investigate the potential regulation and function of all dUbs in this organism in response to different oxidising agents. Excitingly, an initial screen of available *S. cerevisiae* dUb gene deletion mutants and strains expressing epitope-tagged dUbs identified wide and varied responses of dUbs to different oxidising agents. For example, several dUbs were found to be important for cell survival under different oxidative stress conditions. Furthermore, specific dUbs were also found to be modified in response to specific oxidising agents. In particular, further investigations into specific dUbs observed that Ubp12 was reversibly oxidised into a HMW intramolecular disulphide complex in response to $H_2O_2$ but no other oxidising agents tested. Significantly, the catalytic cysteine of Ubp12 was shown to be essential for this complex, suggesting that oxidation regulates Ubp12 activity. Another dUb, Ubp2, was also found to be oxidised in response to $H_2O_2$. Other work has shown that Ubp2 and Ubp12 regulate mitochondrial dynamics, and therefore the present study led to a model

suggesting that the regulation of Ubp12 and Ubp2 by $H_2O_2$ may regulate mitochondrial dynamics in response to different levels of $H_2O_2$. In contrast to Ubp2 and Ubp12, further investigations into another dUb, Ubp15, was found to be oxidised into HMW complexes in response to both $H_2O_2$ and diamide. Interestingly, these Ubp15 HMW complexes have different mobilities suggesting differences in the way Ubp15 responds to different oxidising agents. Significantly, similar to Ubp12, the catalytic cysteine of Ubp15 was essential for the formation of the $H_2O_2$-induced HMW complex. Ubp15 has previously been implicated in the regulation of cell cycle progression, and consistent with this link the present results suggest that Ubp15 may be important for regulating G1 phase arrest/delay, and for regulating the release into S phase, following $H_2O_2$ treatment. Collectively, the work described here has begun to provide insight into how cells sense and respond to different types and levels of ROS by regulating specific dUbs. Furthermore, the yeast dUbs are conserved in higher eukaryotes and hence these studies have potential implications for the regulation of fundamental processes such as the cell cycle and mitochondrial dynamics.

# Acknowledgements

Firstly, I would like to thank my supervisor Brian Morgan, for his constant support, advice, enthusiasm, and total confidence in me throughout this PhD. I would also like to acknowledge the BBSRC for funding my research, and David Stead at Aberdeen University for completing the mass spectrometry and computational analysis.

Secondly, I would like to thank everyone in the Morgan, Quinn, Whitehall, and Veal labs, past and present, for helping with ideas and insight in this project. But more importantly for providing cake, chocolate and for making the four years fun! I would especially like to thank Callum- for keeping me sane (ish!), and Zoe-for the much needed coffee breaks, wine nights and random chat.

Thirdly, I would like to thank my family, Mam and Dad, and even you Scall, for the encouragement and support over all the years and for providing endless love (and gin) to get me to here.

Finally, I would like to thank Luke. You have been there to celebrate the good days and to cheer me up after the bad days. You have made everything better, and I definitely couldn't have done it without you.

# Table of Contents

# Abbreviations

| | |
|---|---|
| 8-oxoG | 8-oxoguanine |
| ·OH | Hydroxyl radical |
| AGE | Advanced glycation end product |
| APC/C | anaphase-promoting complex/cyclosome |
| ATP | Adenosine triphosphate |
| BCA | Bicinchoninic acid |
| bp | Base pair |
| BSA | Bovine serum albumin |
| BSO | Buthionine sulfoximine |
| CDK | Cyclin dependent kinase |
| CRL | Cullin-RING ligases |
| $dH_2O$ | Deionised $H_2O$ |
| DIC | Differential interference contrast |
| DNA | Deoxyribonucleic acid |
| dUb | De-ubiquitinases |
| *E. coli* | *Escherichia coli* |
| EDTA | Ethylenediaminetetraacetic acid |
| ER | Endoplasmic Reticulum |
| Gpx | Glutathione peroxidases |
| Grx | Glutaredoxins |
| GSH | Glutathione |
| $H_2O_2$ | Hydrogen Peroxide |
| HEPES | 4-(2-hydroxyethyl)-1-piperazineethanesulfonic acid |
| HRP | Horseradish Peroxidase |
| HU | Hydroxy Urea |
| JAMM | JAB1/MPN/Mov34 metalloenzyme |
| kDa | kilodalton |
| MW | Molecular weight |
| NEM | N-Ethylmaleimide |
| $nH_2O$ | Nano $H_2O$ |
| $O_2^{\cdot -}$ | Superoxide |

| | |
|---|---|
| OTU | Ovarian tumour-related |
| PBS | Phosphate-buffered saline |
| PCNA | Proliferating cell nuclear antigen |
| PCR | Polymerase chain reaction |
| PEG | Polyethylene glycol |
| PMSF | phenylmethylsulfonyl fluoride |
| Prx | Peroxiredoxins |
| PTM | Post translational modification |
| RBR | Ring-in-between-RING |
| RNA | Ribonucleic acid |
| ROS | Reactive oxygen species |
| Rpm | Revolutions per minute |
| SCF | Skp, Cullin, F-box containing complex |
| *S. cerevisiae* | *Saccharomyces cerevisiae* |
| SD | Synthetic dextrose |
| SDS | Sodium dodecyl sulphate |
| SUMO | Small Ubiquitin-like modifier |
| TAP | Tandem affinity purification |
| TBS | Tris-buffered saline |
| TBST | Tris-buffered saline tween |
| TCA | Tricholoracetic acid |
| TE | Tris EDTA |
| Tpx | Thioredoxin peroxidases |
| Trx | Thioredoxins |
| Ub | Ubiquitin |
| Ubl | Ubiquitin-like |
| UCH | ubiquitin carboxy-terminal hydrolases |
| USP | ubiquitin specific protease |
| UV | Ultra violet |
| WT | Wild Type |
| YPD | Yeast extract peptone dextrose |

# List of Figures

# List of Tables

# Chapter One: Introduction

## 1.1. Ubiquitin and ubiquitin-like modifications

Post translational modifications (PTMs) regulate proteins by altering their physical properties, including regulating protein localisation, abundance and activity. There are many examples of PTM including methylation, phosphorylation, glycosylation, acetylation, ubiquitin and ubiquitin-like modifications (Walsh Christopher *et al.*, 2005; Paula and Uwe, 2012). Ubiquitination is a classic example of a PTM which, upon addition onto target protein substrates, regulates protein function in several different ways. Ubiquitin is a 76 amino acid peptide, with a mass of approximately 8.5 kDa (Hochstrasser, 2009; Jadhav and Wooten, 2009), which is conjugated onto substrates via an isopeptide bond, historically to target the substrate for degradation. Since ubiquitination was discovered (Goldknopf *et al.*, 1977; Ciehanover *et al.*, 1978; Swatek and Komander, 2016) other proteins similar to ubiquitin, ubiquitin-like modifications, with a similar 3D structure including the characteristic β-grasp fold and a conserved di-glycine motif (Hochstrasser, 2009) have been identified. These ubiquitin-like modifications include proteins such as SUMO and Rub1/NEDD8 among others (Table 1.1). Ubiquitin and ubiquitin-like modifications are highly conserved across all eukaryotes (for example the yeast and mammalian ubiquitin protein differs in only three amino acids) and are essential in many cases. Although ubiquitin and ubiquitin-like modifications were thought not to be present in prokaryotes, more recently ubiquitin-like modifications have been identified, including Pupylation, Sampylation and Ttub, which share a similar β-grasp fold and that are linked to target proteins by isopeptide bonds (Maupin-Furlow, 2014). Ubiquitin and ubiquitin-like modifications have been linked to the regulation of cellular processes. Furthermore, in human cells the dysregulation of ubiquitination has been implicated in several diseases, including cancers and neurodegenerative disorders. Thus it is important to understand the mechanisms underlying the regulation of ubiquitination.

| Ubiquitin-like modifier | Encoding genes | E1 | E2 | E3 | Targets |
|---|---|---|---|---|---|
| Ubiquitin | *UBI1-UBI4 (UBA52, UBA80, UBB, UBC)* | Uba1 (UBA1, UBA6) (Jin *et al.*, 2007) | Ubc1-13 (~40 E2s (Stewart *et al.*, 2016) | ~60 – 100 (>600 in mammalian cells) (Bassermann *et al.*, 2014) | Many |
| SUMO | *SMT3 (SUMO1-4 )* | Aos1/Uba2 (SAE1/UBA2) | Ubc9 | Siz1, Siz2, Mms21, and Zip3 (15 in mammalian cells) (Watts, 2013) | Many |
| Rub1 (NEDD8) | *RUB1 (NEDD8)* | Ula1/Uba3 (Uba3/APPB1) (Ehrentraut *et al.*, 2016) | Ubc12 (UBE2M) | Many | Cullin family in SCF E3s |
| Urm1 | *URM1* | Uba4 (MOCS3) | - | - | Many |
| Atg8 (LC3) | *ATG8* (7 in mammalian) | Atg7 | Atg3 | Atg12/Atg5 (Otomo *et al.*, 2013) | Phosphatidylethanolamine (Otomo *et al.*, 2013) |
| Atg12 | *ATG12* | Atg7 | Atg10 | - | Atg5 (Otomo *et al.*, 2013) |

**Table 1.1: The conjugation pathways of Ub/Ubl modifications.** The encoding genes and conjugation pathway enzymes of ubiquitin and the ubiquitin-like modifiers SUMO, Rub1, Urm1, Atg8, and Atg12 in *S. cerevisiae*; mammalian homologs are included in brackets. Adapted from (Jentsch and Pyrowolakis, 2000; Hochstrasser, 2009; Veen and Ploegh, 2012).

### *1.1.1. Ubiquitin and ubiquitin-like conjugation*

Ubiquitin and ubiquitin-like modifiers are generally conjugated onto target proteins by the coordinated activity of three enzymes which function in a cascade; termed E1, E2 and E3 (Figure 1.1). E1 activating enzymes initiate the cycle by forming a high energy ubiquitin/ubiquitin-like adenylate intermediate which is donated to the catalytic cysteine of the E1 within the active site. The activated ubiquitin/ubiquitin-like modifier forms a thioester bond between the carboxyl group of the terminal glycine residue of the ubiquitin/ubiquitin-like modifier, and a cysteine residue in the E1 in an ATP-dependent manner (Finley *et al.*, 2012). The ubiquitin/ubiquitin-like modifier is then transferred to the active site cysteine of E2 conjugating enzymes through transesterification (Bedford *et al.*, 2010). E2s are characterised by the presence of a catalytic fold (UBC domain) which are highly conserved regions of ~200 amino acids (van Wijk and Timmers, 2010) that allow binding of both E1s and E3s along with the activated ubiquitin/ubiquitin-like modifier. In the final step of the conjugation cycle, ubiquitin/ubiquitin-like modifiers are conjugated to lysine residues on target proteins with the aid of E3 ligase enzymes (Hershko and Ciechanover, 1998; Nguyen *et al.*, 2015). An isopeptide bond between a lysine receptor residue on the substrate binds to the previously activated carboxyl group of the ubiquitin/ubiquitin-like molecule. The specific enzymes involved in ubiquitin and ubiquitin-like conjugation in *S. cerevisiae*, including mammalian homologs where known, are listed in Table 1.1.

#### *1.1.1.1. Ubiquitin conjugation*

In mammalian and *S. cerevisiae* cells four genes encode ubiquitin; *UBA52, UBA80, UBB*, and *UBC* (Kobayashi *et al.*, 2016) and *UBI1, UBI2, UBI3,* and *UBI4* (Finley *et al.*, 2012) respectively. *UBI1, UBI2* and *UBI3* produce transcripts encoding ubiquitin attached to an unrelated tail protein, which must be removed to produce mature ubiquitin (Ozkaynak *et al.*, 1987). In the case of *UBI1* and *UBI2*, this tail protein is an identical ribosomal protein precursor (Finley *et al.*, 1989). The poly-ubiquitin *UBI4* gene transcript encodes five ubiquitin repeats arranged head to tail (Ozkaynak *et al.*, 1987). In order to produce mature

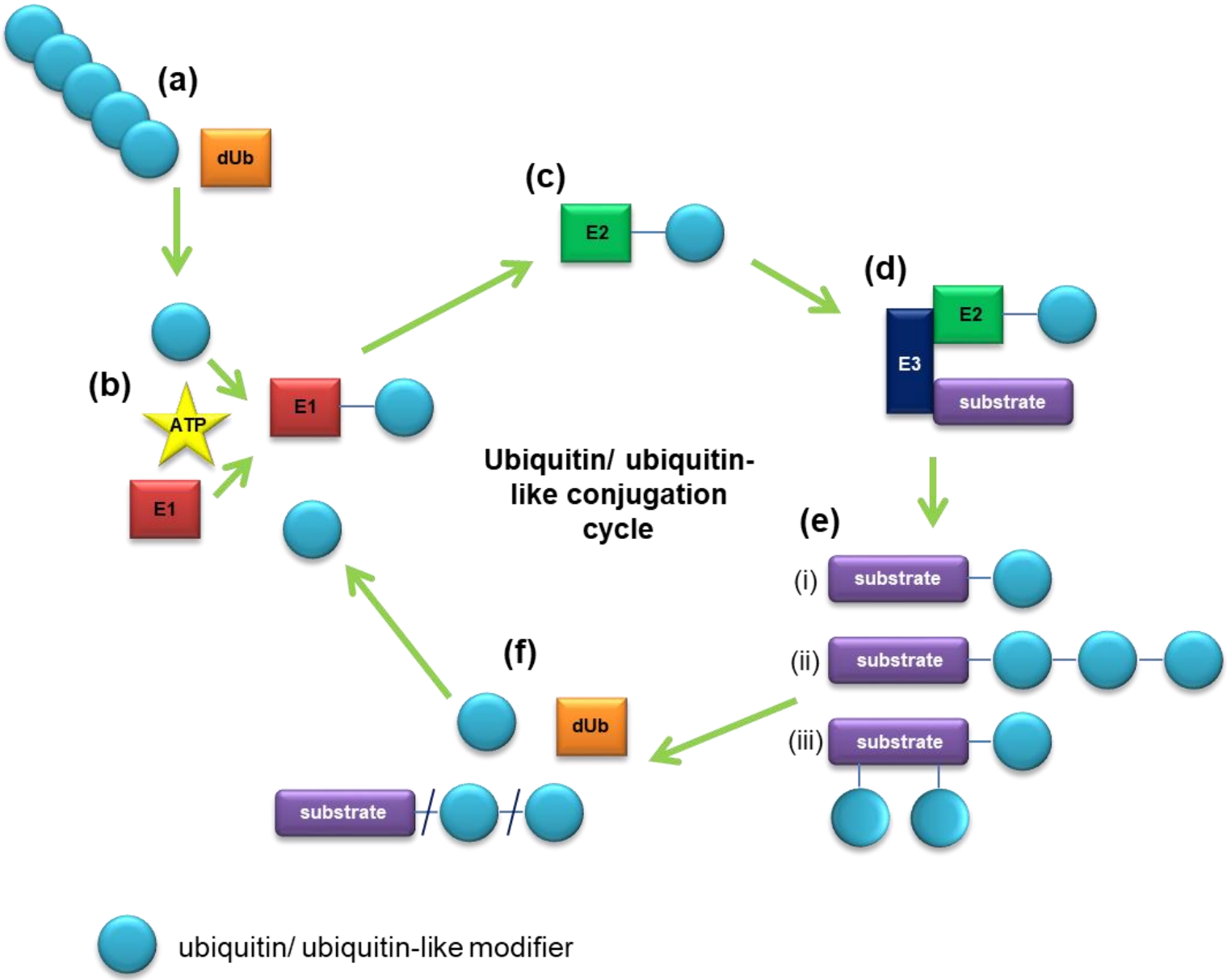
(a)
dUb
(b)
ATP
E1
E1
(c)
E2
(d)
E2
E3
substrate
Ubiquitin/ ubiquitin-like conjugation cycle
(e)
(i)
substrate
(ii)
substrate
(iii)
substrate
(f)
dUb
substrate
ubiquitin/ ubiquitin-like modifier

[4]

**Figure 1.1: Ubiquitin/ ubiquitin-like modification conjugation cycle.** (a) Immature ubiquitin/ ubiquitin-like modifiers are processed by isopeptidases (dUbs) before they are (b) activated by E1 enzymes in an ATP-dependent manner and joined to the E1 by a thioester bond. (c) Transesterification transfers the activated ubiquitin/ ubiquitin-like modifier to an E2 enzyme which (d) conjugates the ubiquitin/ ubiquitin-like modifier to a substrate with the help of an E3 ligase enzyme. (e) Ubiquitin/ ubiquitin-like modifiers can be conjugated to substrates in multiple ways after repetitive rounds of conjugation (e); (i) mono-, (ii) poly-, and (iii) multi-. (f) Ubiquitin/ ubiquitin-like modifiers are removed from substrates by dUbs which cleave the isopeptide bond between either the ubiquitin/ ubiquitin-like modifier and substrate, or between two ubiquitin/ ubiquitin-like modifiers. The cleaved ubiquitin is then able to be reused in another cycle.

ubiquitin to allow conjugation to substrates the precursors must undergo proteolytic processing (see section 1.1.2) whereby the tail regions are removed. In the case of Ubi1-3 proteins this exposes the C-terminal glycine carboxylate which is essential for activation. In the case of Ubi4, the five ubiquitin chain repeats are cleaved to produce mature ubiquitin moieties (Finley *et al.*, 1987; Gemayel *et al.*, 2017). Interestingly *UBI4* is not essential under unstressed conditions, but is specifically required for heat stress, nutrient starvation, and oxidative stress responses (Finley *et al.*, 1987).

Mature ubiquitin is covalently attached to target proteins via a pathway containing three enzymes; E1, E2, and E3 (see Figure 1.1). *S. cerevisiae* contains one ubiquitin-specific, monomeric E1 named Uba1 (Table 1.1), which is essential for viability (McGrath *et al.*, 1991). This is in contrast to mammalian cells which express two ubiquitin E1s, UBA1 and UBA6 (Schulman and Harper, 2009). Uba1 can bind two ubiquitin molecules at the same time; one in the adenyl-intermediate form, and one as activated ubiquitin bound by a thioester bond to the catalytic cysteine of Uba1 (Haas *et al.*, 1982; Groen and Gillingwater, 2015). The ability to bind two ubiquitin molecules not only allows rapid activation of ubiquitin molecules, but the conformation of the E1 associated with two ubiquitin molecules allows favourable transfer of the activated ubiquitin to E2 enzymes (Schulman and Harper, 2009). Uba1 is essential for viability in *S. cerevisiae* and interestingly there have been many diseases associated with mutations in the mammalian Uba1 (Balak *et al.*, 2017). Mutations in Uba1 have been linked to many neurodegenerative disorders and spinal muscular atrophy. As such Uba1 has been proposed as a therapeutic target for these diseases (Groen and Gillingwater, 2015).

*S. cerevisiae* expresses 11 ubiquitin-specific E2 enzymes, Ubc1-8, 10, 11, and 13 (Finley *et al.*, 2012), whereas mammalian cells contain ~40 known ubiquitin E2 enzymes (Stewart *et al.*, 2016). E2 enzymes interact with Uba1 and E3s, but in addition must be able to transfer ubiquitin to substrates. Hence E2 enzymes have different binding domains for each specific interaction. Interestingly, the binding site for Uba1 and E3 enzymes overlap, thus preventing E2 enzymes becoming loaded with ubiquitin again before conjugation of the previous ubiquitin

molecule has been completed (Eletr *et al.*, 2005). Importantly, it is E2 enzymes that are critical for ensuring unidirectional ubiquitin cycling. This directionality is determined by the different binding affinity of Uba1 and the E3 enzymes to E2 enzymes. In particular, Uba1 has a higher binding affinity to unloaded E2 enzymes, rather than E2-ubiquitin conjugates. Conversely, E3 enzymes have a higher binding affinity to E2-ubiquitin conjugates so will preferentially bind to E2s which are loaded with ubiquitin resulting in conjugation of ubiquitin to the substrate (Finley *et al.*, 2012). Of the 11 *S. cerevisiae* E2 enzymes only one, Cdc34, is essential for viability. For example, a $Cdc34^{ts}$ mutant was found to arrest at the G1-S phase boundary at the non-permissive temperature (Schwob *et al.*, 1994). Cdc34 has many substrates which are mostly targeted by the SCF ubiquitin ligase complex of which Cdc34 is the associating E2 (described in more detail below). Examples of Cdc34 ubiquitination substrates are histone ubiquitination, and regulating the protein quality control pathway (Finley *et al.*, 2012). More details on Cdc34 substrates and the remaining *S. cerevisiae* E2s can be found in Table 1.2.

In the final step of the cycle, ubiquitin is conjugated to lysine residues in target substrates with the aid of E3 enzymes. E3 ligases catalyse the formation of an isopeptide bond between the ε-amino groups of lysine residues in the substrate, and the carboxyl group of ubiquitin and hence must be able to bind to E2 enzymes and substrates. E3's are the largest group of enzymes in the ubiquitin conjugation cascade; in *S. cerevisiae* ~100 E3 enzymes have been identified (for a comprehensive list see (Finley *et al.*, 2012)), and more than 600 are present in mammalian cells (Bassermann *et al.*, 2014). E3 enzymes are divided into 2 major groups depending on domain architecture and functional mechanism; RING domain E3s (which also include U-box domain E3s) and HECT domain E3s (Finley *et al.*, 2012). Only five HECT domain E3 enzymes are present in *S. cerevisiae*, all of which have a catalytic cysteine within their HECT domain (Rodriguez *et al.*, 2003). This cysteine forms a thioester with ubiquitin donated from the E2 enzyme, which is then attached to the substrate (Rotin and Kumar, 2009). The five HECT domain E3s currently identified in *S. cerevisiae* are Rsp5, Ufd4, Hul4, Hul5, and Tom1 (Finley *et al.*, 2012). Interestingly, only Rsp5 is essential for viability. Rsp5 has many substrates in a wild range of pathways,

| E2 | Function |
|---|---|
| Ubc1 | Vesicle biogenesis, ER-associated degradation, nuclear protein quality control, E2 for APC |
| Ubc2/Rad6 | DNA repair, H2B mono-ubiquitination, regulator of K63 |
| Cdc34 | Cell cycle regulation, E2 for SCF E3s, nuclear protein quality control pathway, histone regulation, methionine expression regulation |
| Ubc4 | E2 for APC, cytoplasmic protein quality control, promotes efficient DNA replication |
| Ubc5 | Paralog of Ubc4 |
| Ubc6 | ER-associated degradation, K11 synthesis |
| Ubc7 | ER-associated degradation, inner nuclear membrane-associated degradation |
| Ubc8 | Gluconeogenesis regulation, histone ubiquitination |
| Ubc9 | E2 for SUMO conjugation |
| Ubc10/Pex4 | Peroxisome biogenesis |
| Ubc11 | Function unknown |
| Ubc12 | E2 for Rub1 conjugation |
| Ubc13 | DNA repair, synthesises K63 when in a dimer with a non-catalytic partner protein, Mms2 |

**Table 1.2: *S. cerevisiae* E2 enzymes and their cellular roles.** Table adapted from (Finley *et al.*, 2012).

including lipid biosynthesis, regulation of unsaturated fatty acids and regulation of specific transcription factors (Kaliszewski and Zoladek, 2008; Finley *et al.*, 2012). In contrast to HECT domain E3 enzymes, RING domain E3s do not form a direct thioester with ubiquitin, but instead mediate ubiquitin transfer from the E2 enzyme to the substrate by activating the E2, and facilitating ubiquitination by positioning E2-ubiquitin in proximity to the target lysine in the substrate (Deshaies and Joazeiro, 2009). RING domain E3 enzymes constitute the majority of *S. cerevisiae* E3s, including the distinct subgroup RING-in-between-RING (RBR) E3 enzymes. RBRs function as hybrids of RING and HECT E3 enzymes. In this case one RING domain binds to the E2 enzyme and allows transfer of ubiquitin onto a cysteine residue in the other RING domain forming an E3-ubiquitin thioester before the ubiquitin molecule is conjugated onto a target lysine (Wenzel and Klevit, 2012). There are currently 44 *S. cerevisiae* proteins identified which encode RING domain E3s, however the most prominent members of the RING domain E3s are the APC/C RING E3, and the cullin-RING ligases (CRLs) (Finley *et al.*, 2012). The APC/C E3 comprises 13 subunits in *S. cerevisiae* (Finley *et al.*, 2012), and includes a RING domain which binds to the associating E2s Ubc1 and Ubc4 (Rodrigo-Brenni and Morgan, 2007). The APC/C core includes three activators which bind to substrates and are critical for targeting specific substrates. These activators are Cdh1, Cdc20 and Ama1, and interaction with the APC/C with the activators directs specific substrate targeting (Finley *et al.*, 2012). CRLs comprise the largest group of ubiquitin ligases in all eukaryotes. CRLs consist of four subunits, a RING protein, a linker and a substrate receptor. The specific cullin aspect of CRLs (*S. cerevisiae* has three cullins, Cdc53, Cul3, and Rtt101 (Finley *et al.*, 2012)) depends on the type of CRL, for example the cullin Cdc53 assembles SCF ligases, which have F-box proteins as the substrate receptor (Yen *et al.*, 2012). The RING domain subunit interacts with, and activates, the SCF associating E2, Cdc34 (Petroski and Deshaies, 2005).

Specificity of ubiquitin conjugation to substrates is achieved through the particular combination of E2 and E3 enzymes used. This specificity is often achieved by the E3 enzyme, which has recognition domains distinct from catalytic domains which can direct the E2-ubiquitin conjugate (Jackson *et al.*, 2000). The large number of E3 enzymes and their interaction with specific E2s allows for greater specificity of

ubiquitination. Interestingly, this specificity can be influenced further by the requirement for certain chaperones to direct certain substrates to the specific E3 enzyme (Rosser *et al.*, 2007). Specificity can also be directed to substrates by recognising previously modified or marked lysines of the target protein. E4 enzymes are a small subclass of E3 ligases that are responsible for ubiquitinating substrates which have previously been ubiquitinated, thus adding to substrate-specific ubiquitination (Koegl *et al.*, 1999; Hoppe, 2005).

#### *1.1.1.2. Types of ubiquitin conjugation*

Ubiquitin can be conjugated to substrates in several different ways; mono-ubiquitination, multi-ubiquitination and poly-ubiquitination. Significantly, each individual type of ubiquitination initiates different fates for the substrate (Figure 1.2). Investigations of the effects of different types of ubiquitination revealed that ubiquitination is much more complex than initially proposed, and can in fact have many more consequences than simply targeting proteins for degradation. E2 enzymes often have a preference for promoting ubiquitin initiation on substrates rather than elongation which is regulated by the interaction between the E2s and E3s (Ye and Rape, 2009). This is thought to be achieved by the turnover rates of the substrate and E2-E3 binding. Mono-ubiquitination is achieved by E3s which quickly release the product, but that have a slow E2 turnover. However for poly-ubiquitination, E3s which turn over E2s rapidly but release the substrate more slowly seem to be preferable (Eletr *et al.*, 2005)

##### *1.1.1.2.1. Mono- and multi-ubiquitination*

Mono-ubiquitination is the addition of one ubiquitin moiety onto target lysine residues. Mono-ubiquitination is not often linked to protein degradation, which is proposed to be due to one ubiquitin molecule not presenting enough of a signal to target substrates for protein degradation (Hicke, 2001). Instead mono-ubiquitination has been linked to other non-proteolytic pathways including regulating endocytosis, protein localisation, retrovirus budding, and histone ubiquitination (Hicke, 2001; Sadowski *et al.*, 2011) (Figure 1.2). Interestingly, *S. cerevisiae* cells that are unable to mono-ubiquitinate the specific histone H2B are unable to undergo meiosis (Robzyk *et al.*, 2000).

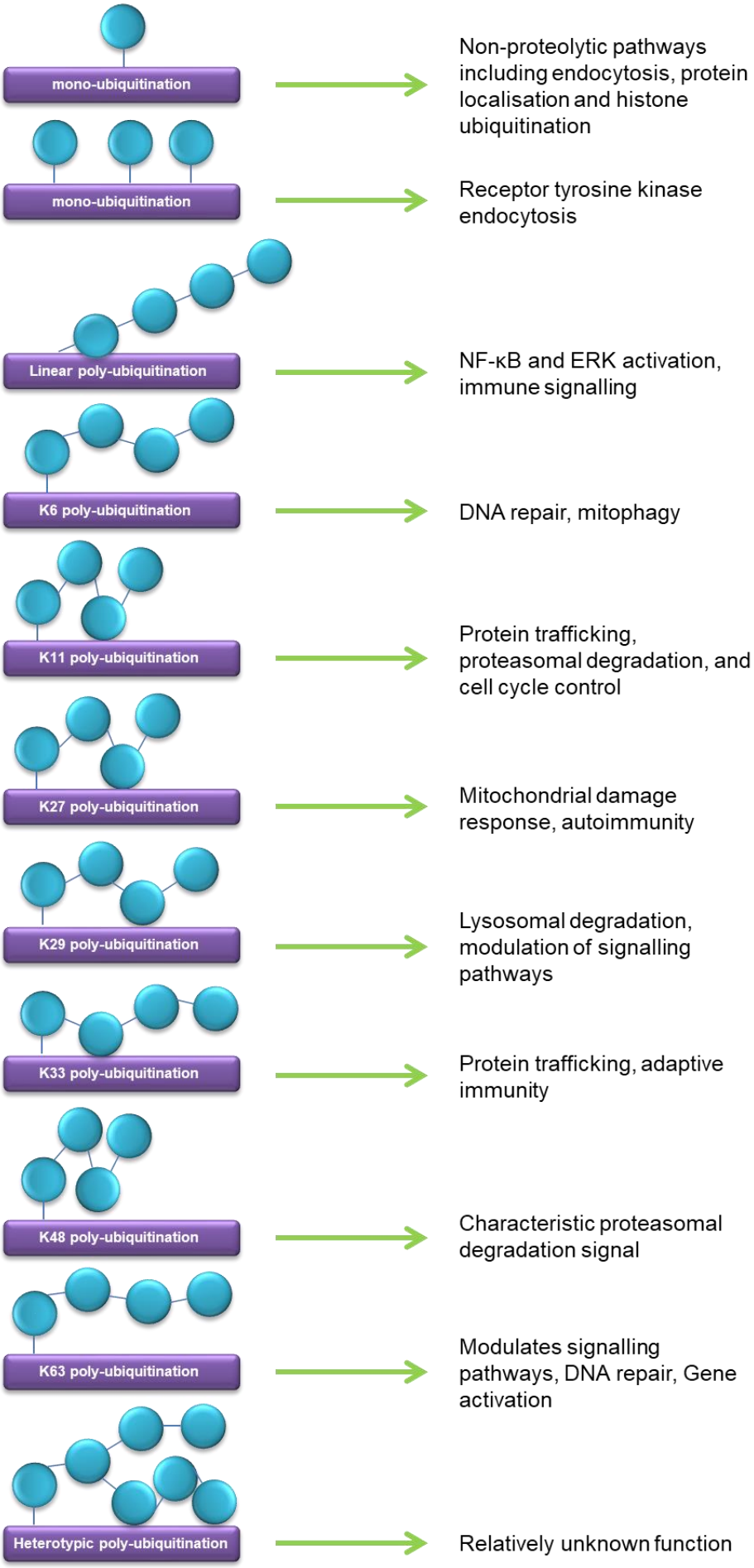
mono-ubiquitination
Non-proteolytic pathways including endocytosis, protein localisation and histone ubiquitination
mono-ubiquitination
Receptor tyrosine kinase endocytosis
Linear poly-ubiquitination
NF-κB and ERK activation, immune signalling
K6 poly-ubiquitination
DNA repair, mitophagy
K11 poly-ubiquitination
Protein trafficking, proteasomal degradation, and cell cycle control
K27 poly-ubiquitination
Mitochondrial damage response, autoimmunity
K29 poly-ubiquitination
Lysosomal degradation, modulation of signalling pathways
K33 poly-ubiquitination
Protein trafficking, adaptive immunity
K48 poly-ubiquitination
Characteristic proteasomal degradation signal
K63 poly-ubiquitination
Modulates signalling pathways, DNA repair, Gene activation
Heterotypic poly-ubiquitination
Relatively unknown function

[11]

**Figure 1.2: Schematic of poly-ubiquitin chain conjugation and known cellular roles.** Ubiquitin can be conjugated to substrates in different ways. Mono- and multi-ubiquitination occurs when ubiquitin is conjugated to lysine residues in the substrate. Poly-ubiquitin chains can be formed in 8 mechanisms including linear Met1 linkages and through conjugation onto the 7 lysine residues in ubiquitin; K6, K11, K27, K29, K33, K48, and K63. Heterotypic ubiquitination can occur when different types of ubiquitination are present on one substrate, e.g. branched or forked chains of different linkages. Adapted from (Komander, 2009; Klein *et al.*, 2016; Lafont *et al.*, 2018; Kulathu and Komander, 2012)

Multi-ubiquitination is the attachment of multiple, single ubiquitin molecules to a number of lysine acceptors of the substrate protein. Multi-ubiquitination is not well characterised, however multi-ubiquitination signals have been shown to trigger internalisation of cell-surface receptors. This internalisation results in degradation or recycling to the cell membrane for example, the regulation of receptor tyrosine kinase endocytosis (Haglund *et al.*, 2003) (Figure 1.2). The multi-ubiquitin signal is recognised by the conserved endosomal sorting complex required for transport (ESCRT) complexes, which recognises multi-ubiquitinated substrates and facilitates their transport from endosomes to lysosomes (Williams and Urbé, 2007).

*1.1.1.2.2. Poly-ubiquitination*

Poly-ubiquitination occurs when the ubiquitin molecule itself is ubiquitinated. There are 7 lysine residues present in the ubiquitin molecule; K6, K11, K27, K29, K33, K48 and K63, all of which can act as isopeptide bond acceptors to be ubiquitinated, primarily in a chain. The location of each specific lysine in ubiquitin is important. The shape the chain takes when attached is thought to initiate specific pathways. Proteins which bind ubiquitin molecules have ubiquitin binding domains which recognise hydrophobic parts of ubiquitin. However these interactions are weak and often need other associating proteins to strengthen the bonds (Chen and Sun, 2009). The different shapes of the ubiquitin chains may be a mechanism by which specific proteins are able to bind. For example, the globular nature of K48 may bind preferentially to proteasomal subunits which initiate proteasomal degradation. However, other non-proteolytic proteins may preferentially bind to the linear shape of K63 chains (Chen and Sun, 2009). For example, the yeast E2 enzyme Ubc13 forms K63 poly-ubiquitin chains when in a heterodimer with a non-catalytic subunit Mms2. Binding of Mms2 to the acceptor ubiquitin allows only the K63 residue to be in proximity to the active site of Ubc13 and thus be ubiquitinated (Eddins *et al.*, 2006).

An 8$^{th}$ type of chain linkage occurs when ubiquitin is attached to the N-terminus of another ubiquitin molecule (Kirisako *et al.*, 2006; Iwai *et al.*, 2014). This type of linkage, termed Met1 or linear ubiquitination, has been linked to many signalling cascades including ERK and NF-κB activation in mammalian cells (Sasaki *et al.*,

2013). Interestingly, when lysine and Met1 sites are unavailable, ubiquitination can occur on serine, threonine and cysteine residues (McDowell and Philpott, 2013). These alternative ubiquitination signals on non-lysines may have different outcomes for substrates, for example ubiquitination of cysteine residues may play an important role in mitosis (Vosper *et al.*, 2009). Interestingly, it has also been identified that some E2 enzymes are able to conjugate poly-ubiquitin chains *en bloc* onto substrate lysines. An example here is the yeast Ubc7 and its mammalian homolog Ube2g2 (Finley *et al.*, 2012). While non-lysine types of poly-ubiquitination can occur *in vivo*, lysine residues remain the most common targets. Interestingly, each of type of lysine chain can initiate a different response in substrates (Figure 1.2). Additionally, poly-ubiquitination is not limited to one type of chain linkage on a substrate (homotypic ubiquitination). Heterotypic poly-ubiquitination can occur where multiple types of poly-ubiquitin chains are present on substrates, often in a branched or forked shape whereby a single ubiquitin moiety is ubiquitinated at two or more sites (Figure 1.2) (Kulathu and Komander, 2012).

K48 linkages are the only type of poly-ubiquitination which are essential for viability (Spence *et al.*, 1995). K48 ubiquitination is the characteristic degradation signal, where four ubiquitin moieties form a globular chain that targets substrates to the proteasome (Spence *et al.*, 1995). K48 poly-ubiquitination accounts for the majority of poly-ubiquitination; however this is still only approximately 30% of all ubiquitin linkages (Bremm and Komander, 2011). The remaining ubiquitin lysine residues can be mutated to understand the specific function for each linkage (Spence *et al.*, 1995). This genetic manipulation and the improving mass spectrometric techniques have allowed understanding of the many emerging roles of poly-ubiquitination.

One of the more recently emerging roles of poly-ubiquitination is a non-proteolytic signalling role. Here, substrates are not targeted to the proteasome, but can have other roles, such as in signalling cascades or protein localisation. One of the main poly-ubiquitin linkages associated with non-proteolytic roles is K63, which has recently been observed to be important in many signalling pathways (Spence *et al.*, 1995). Further research into yeast K63 function has highlighted links with

autophagy signalling (Ferreira *et al.*, 2015), multi-vesicular body protein sorting (Erpapazoglou *et al.*, 2012), and stress response signalling (Silva *et al.*, 2015b). Interestingly, recent work in mammalian cells identified that a serine/threonine protein kinase involved in transcriptional regulation of cell death pathways, HIPK2, was stabilised by K63 ubiquitination. After slight heat shock HIPK2 was stabilised by K63 and translocated to the cytoplasm, inhibiting its association with the cell death response and therefore allowing the cell to recover from this stress (Upadhyay *et al.*, 2016). At high lethal temperatures, HIPK2 was not ubiquitinated by K63 and was able to re-enter the nucleus and initiate a cell death response (Upadhyay *et al.*, 2016), indicating that K63 ubiquitination of this protein is vital to determine when cell death occurs.

#### *1.1.1.3. Targets and functions of ubiquitination*

Ubiquitination has been linked with almost all cellular pathways and indeed it is thought that most proteins will, at some point, be ubiquitinated (Swatek and Komander, 2016). Although ubiquitination of substrates often results in degradation through 26S proteasome activity, more and more non-proteolytic roles are emerging, often depending on the type of ubiquitin signal on substrates (see Section 1.1.1.2). Details of all ubiquitin substrates are not feasible in this introduction (for further reviews see (Finley *et al.*, 2012; Ciechanover, 2015; Mansour, 2018)). However it has been identified previously that ubiquitination is vital for cell cycle progression, DNA repair and replication, protein localisation, and mitochondrial regulation and examples of these are discussed below.

##### *1.1.1.3.1. Ubiquitination and cell cycle regulation*

Ubiquitination regulates many important cell cycle proteins. For example use of a temperature sensitive Cdc34 mutant identified that Cdc34 is critical for cell cycle progression as *cdc34*-ts strains arrest at the G1-S phase boundary at the non-permissible temperature (Schwob *et al.*, 1994). Cdc34 regulates the cell division cycle by ubiquitinating the cyclin dependent kinase (CDK) inhibitor Sic1 (Schwob *et al.*, 1994), subsequently marking it for degradation and thus allowing cell cycle progression. The timing of the degradation of many cell cycle regulating proteins is important. For example, Sic1 is only ubiquitinated and thus targeted for degradation when it has six independent phosphorylation signals (Cross *et al.*,

2007). Ubiquitin is also critical in regulating the cell cycle in many other ways. For example K48 poly-ubiquitination is crucial for G1-S transition by marking key CDK's for degradation by the proteasome to allow progression through the checkpoint (Mocciaro and Rape, 2012), Interestingly, non-proteolytic K63 poly-ubiquitination is also important for activating certain cell cycle check points. K63 chains are often assembled at sites of DNA damage and inhibit G2-M transition when this damage is present (Mocciaro and Rape, 2012). The APC/C and SCF protein ligase complexes are also important to regulate the cell cycle. The importance for the SCF complex to ubiquitinate substrates and regulate the cell cycle is demonstrated by investigating temperature sensitive mutants of each component of the complex, and Cdc34. All of these mutants display cell cycle arrest at non-permissive temperatures, and cells are unable to undergo DNA replication due to their inability to degrade Sic1 (Schwob *et al.*, 1994; Seol *et al.*, 1999). Regulation of the cell cycle by the APC/C complex is dependent on the specific activator subunit bound to the ligase (Krek, 1998). For example APC/$C^{Cdc20}$ is activated in early mitosis and regulates mitotic progression, and also degrades B-type cyclins Clb2 and Clb5 (Wäsch and Cross, 2002). In contrast APC/$C^{Cdh1}$ is only active in G1 phase and maintains cells in a stable G1 phase by downregulating many target proteins including the F-box protein Skp2 (Skaar and Pagano, 2009).

#### *1.1.1.3.2. Ubiquitination and DNA repair*

Identification that the *S. cerevisiae* Rad6 enzyme (a key enzyme for post replication DNA repair) was a ubiquitin E2 enzyme initiated the link between DNA damage repair and ubiquitination (Jentsch *et al.*, 1987; Jackson and Durocher, 2013). Post replication repair allows the replication of DNA after stress, and is therefore a mechanism by which DNA damage can be tolerated (Jackson and Durocher, 2013). PCNA, an important protein for DNA post replication repair, is a nuclear complex made up of 3 monomers of identical proteins, in *S. cerevisiae* these are Pol30 (Fan and Xiao, 2016). The sub-units of PCNA form a ring, which is large enough for the double helix of DNA to pass through the centre. Ubiquitination of PCNA, by the E2 and E3 Rad6 and Rad18 respectively at the K164 residue (Fan and Xiao, 2016), is upregulated after exposure to DNA

damaging agents and UV radiation. Mono-ubiquitination causes PCNA to initiate translesion synthesis (TLS) through recruitment of specialised polymerases, which allows areas of DNA damage to be bypassed and subsequently allows DNA replication to continue (Xu *et al.*, 2015).

#### *1.1.1.3.3. Ubiquitination and protein localisation*

Protein localisation can also be regulated by ubiquitination. The mammalian transcription factor p53 is known to be important for control of many pathways including cell cycle arrest and apoptosis, and is known to be an important tumour suppressor in many cancers (Muller and Vousden, 2013; Meek, 2015). p53 can be poly-ubiquitinated by the E3 ligase Msl2 which promotes nuclear export but does not initiate degradation of p53 (Kruse and Gu, 2009). Subsequent mono-ubiquitination of p53 removes p53 from the cytoplasm into the mitochondria, effectively stopping p53 from entering the nucleus where it would act as a transcription factor for many downstream genes, and also initiating apoptosis (Marchenko *et al.*, 2007). This mono-ubiquitination also inhibits any further poly-ubiquitination of p53 which may cause p53 degradation. A further example whereby protein localisation is regulated by ubiquitination is the ubiquitination state of PLK1. PLK1 regulates many factors of mitosis, including mitotic entry, chromosome alignment and sister chromatid segregation (Sumara *et al*., 2004). When PLK1 is not ubiquitinated it localises to the kinetochore, where it promotes chromosomal alignment. Ubiquitination of PLK1 at Lys492 by the E3 ligase CUL3 results in disassociation from the kinetochores (Beck *et al*., 2013). Therefore, the balance of ubiquitinated PLK1 is critical for the chromosomal alignment and timely sister chromatid segregation during metaphase (Lui and Zhang, 2017).

#### *1.1.1.3.4. Ubiquitination and mitochondrial regulation*

Mitochondria are organelles with many important roles within the cell. For example, they are important in iron sulphur cluster formation (Rouault and Tong, 2005), ATP production via the electron transport chain (García-Ruiz *et al.*, 1995), and are intrinsically linked to multiple cell signalling pathways (Duchen, 2000; Hancock *et al.*, 2001; Fleury *et al.*, 2002). Mitochondria are very dynamic organelles, constantly changing shape and size to create a homeostatic balance between fission and fusion depending on cellular environment. This constant

change in shape is known as mitochondrial dynamics. In mammalian cells ubiquitination of key mitochondrial proteins has been shown regulate mitochondrial dynamics. The mammalian E3 ubiquitin ligase MITOL was found to ubiquitinate outer membrane fission proteins FIS1 and DRP1 (Yonashiro *et al.*, 2006). This modification is important in Drp1-dependent mitochondrial fission as inactivation of MITOL inhibits mitochondrial fission (Heo and Rutter, 2011). Another E3 ligase, Parkin has also been associated with mitochondria quality control. Depolarised mitochondria enable stabilised PINK1, a serine-threonine protein kinase, to recruit Parkin which poly-ubiquitinates PINK1 with either K63 or K27 linkages in a proteasome-independent manner. This signal mediates the transport of the mitochondria to the autophagosome where mitochondria are degraded. Mutations or loss of function in either PINK1 or Parkin result in Parkinson's disease, which highlights the importance of removing damaged organelles for cell survival. Parkin has also been associated with K48 linked poly-ubiquitination of MFN1 and MFN2 (key mitofusins) for targeting to the proteasome, resulting in MFN1 and MFN2 loss and subsequent mitochondrial fragmentation. Investigations into the roles of ubiquitin in the regulation of mitochondrial dynamics in *S. cerevisiae* found that in *S*. *cerevisiae* Mdm30 is a vital E3 ligase that maintains fusion (Fritz *et al.*, 2003). For example, in *mdm30*Δ cells, mitochondria were found to be very aggregated and unable to form networks. However, mitochondria were restored to wild type morphology in a *dnm1*Δ *mdm30*Δ double mutant (Fritz *et al.*, 2003). Further studies found that Mdm30, similar to Parkin in mammalian cells, controls the degradation of Fzo1 (a mitofusin which is the homolog to MFN1/MFN2) by ubiquitinating it and targeting it for destruction through the proteasome pathway (Fritz *et al.*, 2003).

#### *1.1.1.4. Ubiquitin-like modifications*

There are many ubiquitin-like modifiers in eukaryotes and the discussion of these is beyond the scope of this introduction. However, for reviews see (Kerscher *et al.*, 2006; Hochstrasser, 2009; van der Veen and Ploegh, 2012; Wang *et al.*, 2017). This section will focus on two ubiquitin-like modifiers SUMO and Rub1.

Rub1 (NEDD8 in mammalian cells) is an example of a ubiquitin-like modifier which is attached to substrates in similar cycle to that described for ubiquitin

(Liakopoulos *et al.*, 1998; Boase and Kumar, 2015). Of all the ubiquitin-like modifiers, Rub1 has the highest sequence similarity to ubiquitin (van der Veen and Ploegh, 2012). However, while ubiquitin is essential for viability in *S. cerevisiae*, *rub1*Δ strains are viable (Liakopoulos *et al.*, 1998). Similar to ubiquitin, Rub1 is initially expressed as an inactive precursor which must be processed and in *S. cerevisiae,* this is performed by Yuh1 (Linghu *et al.*, 2002b). Once processed Rub1 is then activated by an E1 heterodimer consisting of Ula1 and Uba3 (in humans Uba3 and APPB1 (Ehrentraut *et al.*, 2016)). Activated Rub1 is transferred to the E2 Ubc12 in *S. cerevisiae*, and subsequently conjugated onto lysine residues in target substrates with the aid of several E3 enzymes (Linghu *et al.*, 2002b). Interestingly, although Rub1 is similar in sequence to ubiquitin, it differs in the target substrates. In contrast to ubiquitin, only a few substrates have been identified as Rub1 targets. Furthermore, Rub1 modifications are targeted to the cullin family (van der Veen and Ploegh, 2012), and indeed the first Rub1 target identified in *S. cerevisiae* was Cdc53. In mammalian cells NEDD8 is required for maximum functionality of the cullin subunit in the SCF group of E3's. Rub1 is removed from substrates by the conserved multi-subunit COP9 signalosome (CSN) (Deshaies *et al.*, 2010), for a review of COP9 see (Wei and Deng, 2003).

The Small Ubiquitin-like Modifier (SUMO) is involved in many cellular processes including DNA repair, replication, and transcription. SUMO is attached to substrates via a similar cycle to that described for ubiquitin and Rub1 (Hay, 2005; Kroetz, 2005). *S. cerevisiae* contains a single SUMO encoding gene, *SMT3*, however mammalian cells contain four; *SUMO1*-4 (van der Veen and Ploegh, 2012). Similar to Rub1, SUMO is transcribed as an immature precursor which is processed by SUMO-specific proteases before being activated by a heterodimer E1 consisting of Aos1 and Uba2 (Melchior, 2000). Activated SUMO is then transferred to a single E2; Ubc9 (Johnson and Blobel, 1997). Although, in contrast to ubiquitin and Rub1, SUMO can be conjugated directly to substrates from Ubc9, E3 enzymes also confer specificity. In *S. cerevisiae* SUMO specific E3 enzymes identified are Siz1, Siz2, Mms21, and Zip3 (Jalal *et al.*, 2017). SUMO is removed from substrates by the SUMO-specific proteases. In *S. cerevisiae* there are two SUMO specific proteases, Ulp1, which is essential for

viability, and Ulp2 (Jalal *et al.*, 2017), whereas mammalian cells express nine SUMO-specific proteases (Nayak and Müller, 2014).

### *1.1.2. Deubiquitination*

Deubiquitination enzymes (dUbs) are responsible for removing ubiquitin molecules from substrate proteins by catalysing the breakdown of the isopeptide bond between the target substrate lysine and the ubiquitin molecule. This recycles ubiquitin to reuse in subsequent ubiquitin conjugation, and adds an extra level of control in protein regulation. dUbs are highly conserved from yeast to humans, however, while mammalian cells express approximately 100 known dUbs (Turcu *et al.*, 2009), *S. cerevisiae* encodes only 20 (Finley et al., 2012). dUbs are functionally diverse in their substrate specificity and subcellular localisation, as the small number of *S. cerevisiae* dUbs need to be able to deubiquitinate the large number of ubiquitinated substrates (Table 1.3). dUbs are linked to almost all cellular processes, and have the potential to regulate the stability, activity, and localisation of target proteins through ubiquitin removal. Interestingly, certain pathogens have acquired dUb encoding genes, suggesting that they may trigger the dysregulation of the ubiquitin pathway as a mechanism of attacking a host (Rytkonen and Holden, 2007; Edelmann and Kessler, 2008).

DUbs main function is to remove ubiquitin from substrates, but their mechanism of action can vary between dUbs; some have preferences for removing mono-ubiquitin, some prefer to remove chains *en bloc*, and some have preferences for editing chain lengths. As described previously ubiquitin is expressed initially as an immature precursor attached to unrelated tail proteins (section 1.1.1.1). Hence, one role of dUbs is to process immature ubiquitin into mature ubiquitin that can be activated by E1s and used in the ubiquitin cycle (Grou *et al.*, 2015). Early mammalian studies identified that UCHL3 and UCHL1 were involved in processing ubiquitin attached to ribosomal precursors, and USP5 was implicated in poly-ubiquitin processing (Grou *et al.*, 2015). However mouse models lacking both UCHL3 and UCHL1 were viable suggesting that other dUbs may be involved. It has also been suggested that ubiquitin may be processed co-

| Group | dUb | Mammalian homolog | Biological role |
|---|---|---|---|
| USP | Ubp1 | USP19* | Endocytosis (Schmitz *et al.*, 2005) |
| | Ubp2 | USP28* | Cargo sorting of membrane proteins and multi-vesicular biogenesis (Lam *et al.*, 2009), mitochondrial morphology regulation (Anton *et al.*, 2013) |
| | Ubp3 | USP10 | Osmotic response (Baker *et al.*, 1992), ribophagy and autophagy (Kraft *et al.*, 2008), inhibitor of gene silencing (Moazed and Johnson, 1996) |
| | Ubp4 (Doa4) | USP4/USP8 | Paralog of Ubp5. Recycles ubiquitin from proteasome-bound proteins and vacuolar degradation (Swaminathan *et al.*, 1999), maintains monomeric ubiquitin levels (Nikko and Andre, 2007) |
| | Ubp5 | USP4/USP8 | Paralog of Ubp4 |
| | Ubp6 | USP14 | Degrades ubiquitin chains at the proteasome (Hanna *et al.*, 2006) |
| | Ubp7 | USP21 | Paralog of Ubp11 |
| | Ubp8 | USP22 | Deubiquitination of histone H2B (Henry *et al.*, 2003) |
| | Ubp9 | USP12/ USP1 | Paralog of Ubp13. Mitochondrial biogenesis (Kanga *et al.*, 2012) |
| | Ubp10 | USP20/ USP36 | Ribosome biogenesis (Richardson *et al.*, 2012), PCNA deubiquitination (Gallego-Sanchez *et al.*, 2012), histone H2BK123 deubiquitination (Schulze *et al.*, 2011) |
| | Ubp11 | USP21 | Paralog of Ubp7 |
| | Ubp12 | USP15 | Mitochondrial morphology regulation (Anton *et al.*, 2013) |
| | Ubp13 | USP46 | Paralog of Ubp9. Suppresses cold sensitivity (Hernandez-Lopez *et al.*, 2011), mitochondrial biogenesis (Kanga *et al.*, 2012) |

| | | | |
|---|---|---|---|
| USP | Ubp14 | USP5 | Specifically deubiquitinates unanchored ubiquitin chains (Amerik *et al.*, 1997; Hu *et al.*, 2005) |
| | Ubp15 | USP7 | Peroxisome biogenesis (Debelyy *et al.*, 2011), methionine synthesis (Benschop *et al.*, 2010) |
| | Ubp16 | USP16 | Anchored to mitochondrial membrane, function unknown (Kinner and Kolling, 2003) |
| OTU | Otu1 | OTU1 | ER-associated degradation (Stein *et al.*, 2014) |
| | Otu2 | OTUD6B | Unknown function, may interact with ribosomes |
| UCH | Yuh1 | UCHL3 | Cleaves Rub1 preferentially, but will cleave ubiquitin (Linghu *et al.*, 2002a) |
| JAMM | Rpn11 | POH1 | Essential for *S. cerevisiae* viability. Bound to 26S proteasome lid, cleaves ubiquitin *en bloc* (Mevissen and Komander, 2017) |

**Table 1.3: *S. cerevisiae* dUbs and their biological functions.** Mammalian homologs listed are suggested by protein sequence similarity using NCBI BLASTp, * denotes low sequence homology. Adapted from (Huseinovic *et al.*, 2018).

translationally due to the fast nature of the processing in vivo. It has been observed that USP9 and USP7 are also linked to processing ubiquitin bound to ribosomal precursors, and Otulin has been shown to be involved with processing poly-ubiquitin precursors (Grou et al., 2015). However, despite these studies the roles of the respective homologs in S. cerevisiae remain unknown. dUbs are separated into two distinct categories based on sequence, structure and catalytic activity; zinc metalloproteases and cysteine proteases (Finley et al., 2012). In S. cerevisiae the cysteine proteases are broken down into three further subgroups, USP, OTU, UCH, whereas there is only one member of the JAMM type zinc metalloprotease (Table 1.3).

*1.1.2.1. JAMM family*

The JAMM family are the only known group of dUb enzymes that are zinc metalloproteinases. These enzymes have active site $Zn^{2+}$ ions which function in coordination with a water molecule and two specific conserved histidines, and one specific conserved glutamate residues (Shrestha *et al.*, 2014). One $Zn^{2+}$ ion, in conjunction with the glutamate residue, activates the water molecule to attack the isopeptide bond between the substrate lysine and the ubiquitin molecule (Komander *et al.*, 2009; Fuchs *et al.*, 2018), whilst another $Zn^{2+}$ ion aids stabilisation of the motif that recognises the distal ubiquitin (Maytal-Kivity *et al.*, 2002).

In mammalian cells there are 14 members of the JAMM family, whereas *S. cerevisiae* has only one, Rpn11 (Table 1.3). Rpn11 is situated within the 26S proteasome lid, directly adjacent to the entry channel of the proteasome core and targets proximal ubiquitin on substrates to remove ubiquitin chains *en bloc* (Mevissen and Komander, 2017). Rpn11 is the only essential dUb in *S. cerevisiae* (Finley *et al.*, 2012) and knockdown of the human homolog, POH1, inhibits cellular growth, and causes ineffective substrate degradation and proteasomal activity, and an increase in poly-ubiquitinated substrates (Gallery *et al.*, 2007). Interestingly, non-lethal *rpn11* mutations in *S. cerevisiae* result in over-replication of DNA and severe growth impairment, and cause an increase of ubiquitinated proteins (Gallery *et al.*, 2007). Interestingly, an active site mutant version of Rpn11 disrupts protein degradation but cells remain viable, suggesting

that the role Rpn11 plays in maintaining proteasome stability is more important than its deubiquitinase activity (Guterman and Glickman, 2004).

*1.1.2.2. USP family*

The remaining groups of dUbs are thiol proteases, however can be further classified into subgroups depending on protease domain and structure (Nijman *et al.*, 2005). The main group of thiol proteases in both mammalian cells and *S. cerevisiae* are the ubiquitin specific proteases (USP). All USP dUbs have two highly conserved catalytic regions, the Cys and His boxes, which reside in the USP domain of the proteins. Crucially it is these boxes that allow deprotonation of the catalytic cysteine found within the conserved active site (Amerik and Hochstrasser, 2004). Importantly, the catalytic cysteine is situated in a cleft located close to conserved histidine and aspartic acid residues found in the His box and it is the activity of this triad which deprotonates the catalytic cysteine in order to allow deubiquitination (Figure1.3). Although the USP domain in each dUbs contains two highly conserved active site Cys and His motifs, the size of each USP domain can vary due to unrelated sequences located between the two conserved motifs (Nijman *et al.*, 2005). Although these unrelated sequences have been suggested to have a regulatory function, no evidence exists to support this hypothesis. The crystal structures of many dUbs have been solved, and generally all USP domains have a very similar structure consisting of a palm, a thumb, and finger-like regions, with the catalytic cysteine positioned between the palm and thumb domains (Hu *et al.*, 2002). Interestingly, in many dUbs, the USP domain is not catalytically active when not bound to substrates. In these cases when substrates bind to the dUb, either conformational changes bring the catalytic triad together to allow catalytic activity (Komander *et al.*, 2009), or substrate binding removes inhibiting structures which normally block catalytic activity (Amerik and Hochstrasser, 2004).

In mammalian cells 56 USP members have been described (Guo *et al.*, 2018), whilst *S. cerevisiae* expresses 16, Ubp1-Ubp16 (Table1.3). Although the active site Cys and His residues of all *S. cerevisiae* USP dUbs are highly conserved (Figure 1.3), the specific cellular roles of each dUb are highly divergent. Indeed, defining the roles of each dUb is a large ongoing are of research. Specific

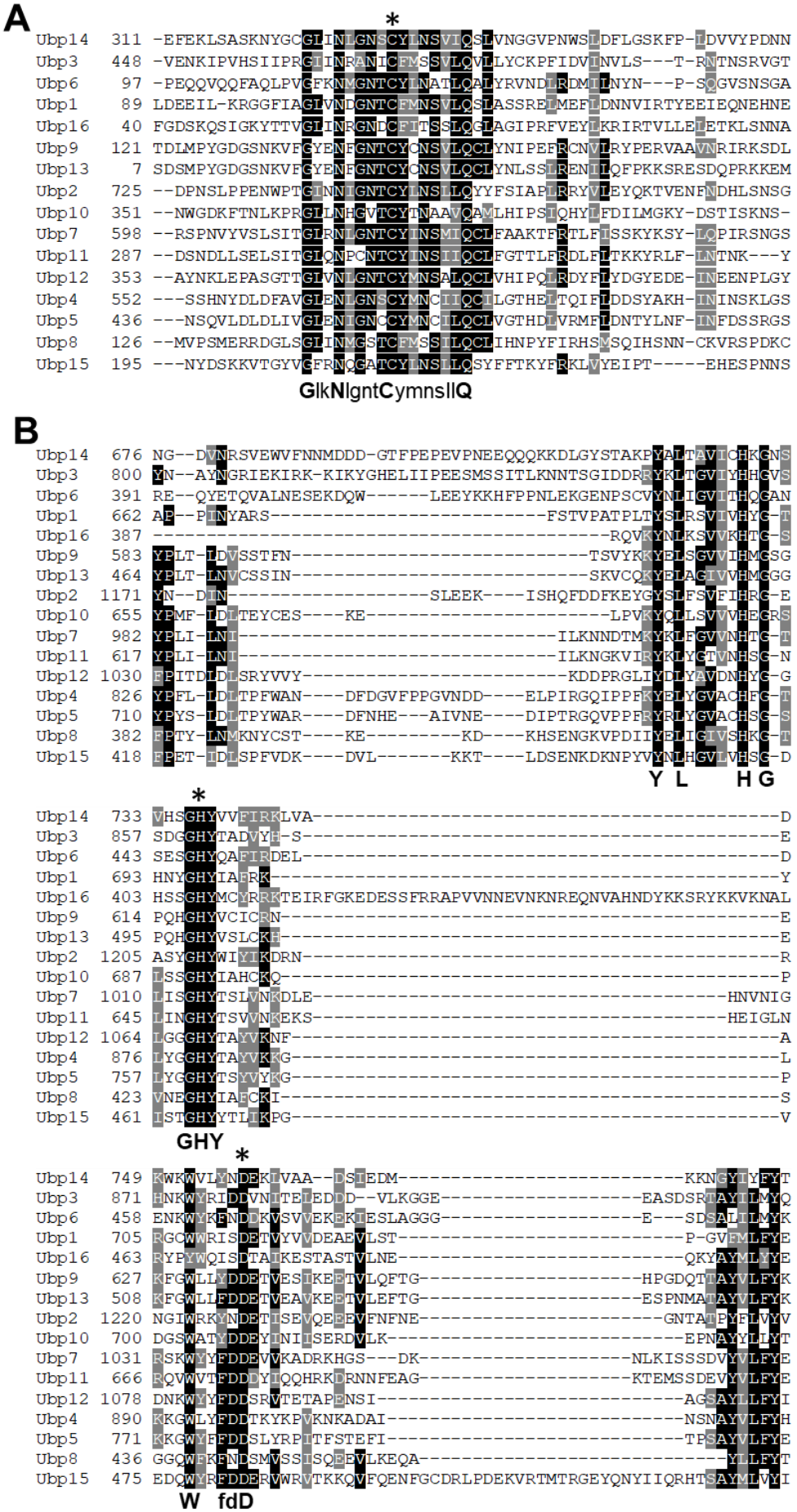
A
B
GlkNlgntCymnsllQ
Y L H G
GHY
W fdD

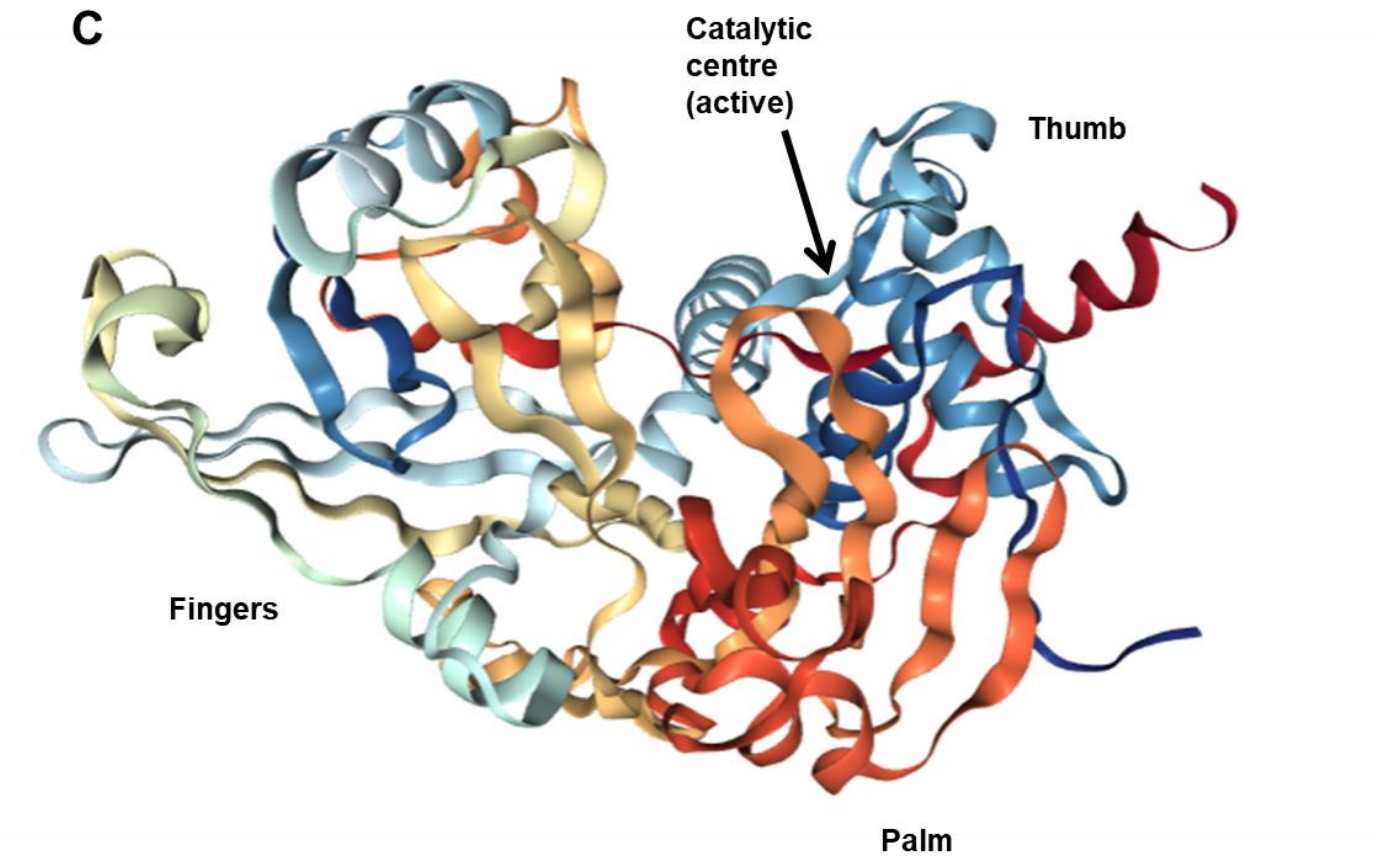


**Figure 1.3: Alignment of the active sites of *S. cerevisiae* USP dUbs.** (A) Alignment of the conserved cys box active site which contains the active site catalytic cysteine (denoted by *). (B) Alignment of the conserved His box, containing the histidine and aspartic acid residues (denoted by *) which form the catalytic triad along with the active site cysteine. The histidine deprotonates the cysteine to allow breakage of the isopeptide bond in ubiquitinated proteins. Dub sequences were obtained from the *Saccharomyces cerevisiae* genome database, and the alignments were conducted using Clustal Omega, and annotated by Boxshade. The shadings represent the similarity between amino acid residues. (C) Structure of an active USP dub (USP7) from the Protein Data Bank (identifier 1nbf (Hu *et al*, 2002)) edited to show the catalytic core in relation to the palm, thumb, and fingers in USP dub active sites. The catalytic core (containing amino acids denoted by * in A and B) is identified by the arrow.

functions of the *S. cerevisiae* dUbs that have been identified to date are shown in Table 1.3 (for reviews of mammalian dUbs and their cellular roles see (Nijman *et al.*, 2005; Ventii and Wilkinson, 2008).

*1.1.2.3. UCH family*

Another group of dUbs which are cysteine proteases is termed the ubiquitin carboxy-terminal hydrolases (UCH). Generally, UCH dUbs contain a 230 amino acid catalytic core which consists of a catalytic triad and has a 3D structure similar to USP dUbs, with which they share catalytic activity (Turcu *et al.*, 2009).Interestingly, the catalytic cysteine of UCH dUbs is located in a narrow groove in the protein (Amerik and Hochstrasser, 2004). UCH dUbs were initially found to have catalytic activity towards small amide groups and esters located at the C-terminus of ubiquitin (hence their name). Indeed, their affinity for small substrates is suggested by their structure which contains a crossover loop close that covers the active site. Substrates must pass through this loop to reach the catalytic core, effectively preventing binding of larger substrates (Nijman *et al.*, 2005; Komander *et al.*, 2009).

In mammalian cells there are 4 members of the UCH family, whist *S. cerevisiae* expresses only 1, Yuh1 (Finley *et al.*, 2012) (Table 1.3). Mammalian UCH dUbs are thought to be involved in ubiquitin processing due to their affinity for smaller substrates, and also their ability to act on peptide conjugates as well as isopeptide bonds. In *S. cerevisiae* although Yuh1 is thought to primarily act on Rub1 modifications (Linghu *et al.*, 2002b), it can also cleave ubiquitin chains (Finley *et al.*, 2012).

*1.1.2.4. OTU family*

Ovarian tumour-related (OTU) proteases are the final group of cysteine protease dUbs in *S. cerevisiae*. Although the OTU catalytic core resembles those of the USP and UCH dUbs, the catalytic core in the OTU dUbs resides in a 130 amino acid domain conserved between OTU family members (Messick *et al.*, 2008) consisting of a 5-stranded β-sheet surrounded by helical domains (Nanao *et al.*, 2004). The catalytic core deubiquitinates substrates in a similar manner to the USP and UCH groups whereby the His residue within the catalytic triad

deprotonates the catalytic cysteine to enable cleavage of the isopeptide bond (Messick *et al.*, 2008). The OTU protease family has members which contain an OTU domain residing in a USP family domain, which initially suggested the OTU deubiquitinating activity.

In mammalian cells there are 18 known OTU dUbs, although only 14 have had their dUb activity confirmed (Komander *et al.*, 2009). *S. cerevisiae* expresses two OTU dUbs; Otu1 and Otu2 (Table 1.3). The targets of Otu1 have only recently begun to emerge, and although specific roles of Otu2 remain unknown, they are hypothesised to be ribosome-related (Huseinovic *et al.*, 2018). The recent studies of Otu1 revealed it to have preferences for K48 linkages, and to have links to ER-associated degradation (Stein *et al.*, 2014).

*1.1.2.5. DUb specificity*

Although dUbs, especially those in the USP group, have a similar active site and mode of cleavage, many dUbs have specific substrates and regulate specific pathways and chain linkages. The specificity of dUbs can be achieved in multiple ways; recognition of ubiquitin or ubiquitin-like moieties, the type of ubiquitin modification (for example lysine mono-ubiquitination or the type of poly-ubiquitination), the target protein onto which the ubiquitin moiety is attached, and the necessity for partner proteins. It must also be noted that a combinatorial effect of multiple mechanisms may aid in dUb specificity.

*1.1.2.5.1. Ubiquitin vs ubiquitin-like specificity*

Most dUbs primarily catalyse ubiquitin specific linkages only, but to do this they must be able to differentiate between ubiquitination and other ubiquitin-like modifications such as SUMO and Rub1 (NEDD8) (Nijman *et al.*, 2005). This is achieved by the interaction between the distal ubiquitin moiety and the dUb. For catalysis the distal ubiquitin extends towards the catalytic centre of the dUb, where it interacts with approximately 40% of the dUb surface (Komander *et al.*, 2009). DUbs can recognise the amino acids that cover the surface as the C-terminal amino acids of ubiquitin (L71, R72, L73, R74, G75, G76) differ to other ubiquitin-like modifiers (Komander *et al.*, 2009), with R74 and G75 residues critical for dUb recognition. However, while the majority of dUbs cleave only

ubiquitin, some do cleave other ubiquitin-like modifiers from substrates. For example, although Yuh1 primarily cleaves Rub1 linkages, it also has catalytic activity towards ubiquitin (Finley *et al.*, 2012). In mammalian cells the dUb USP21 also cleaves the Rub1 homolog NEDD8 (Gong *et al.*, 2000), and the dUb USP7 can remove SUMO chains (Lecona *et al.*, 2016). Furthermore, similar to ubiquitin, many ubiquitin-like modifications have their own deconjugating enzymes, for example SENPs specifically recognise and remove SUMO (Drag and Salvesen, 2008).

*1.1.2.5.2. Substrate specificity*

As described previously (see Section 1.1.1.2), ubiquitin can be conjugated to substrates in multiple different forms to elicit different outcomes. Mono-ubiquitination is the attachment on one ubiquitin moiety onto a substrate lysine residue. Hence, to cleave this type of ubiquitination dUbs must be able to bind to the specific substrate directly. This type of substrate specificity is potentially regulated by domain(s) outside of the catalytic core of the dUb (Nijman *et al.*, 2005), directing binding of the dUb and the substrate, leaving the catalytic triad within the dUb free to hydrolyse the isopeptide bond. Detailed investigations of substrate specificity are scarce due to the difficulty to identify mono-ubiquitinated substrates. However, it has been suggested that dUbs may recognise the actual ubiquitination sites on the substrate. Interestingly, one investigation using *S. cerevisiae* revealed that Ubp8 can directly recognise mono-ubiquitinated histone H2B in the SAGA complex (Morgan *et al.*, 2016), however further studies into the exact mechanism of this are needed. Additionally some dUbs may potentially bind to the substrate and remove poly-ubiquitin chains *en bloc* in a single-step chain removal (Heride *et al.*, 2014). In these cases dUbs may remove the whole chain leaving the substrate free from ubiquitin, or may actually leave the substrate mono-ubiquitinated (Komander *et al.*, 2009) which would then need the activity of a different dUb to remove the final ubiquitin moiety.

*1.1.2.5.3. Type of chain linkage*

In addition to distinguishing substrates that are mono-ubiquitinated, dUbs must also have specificity for the different types of poly-ubiquitination linkage. In this

category, dUbs can be termed endo-dUbs, which can cleave ubiquitin within a chain, or exo-dUbs, which cleave ubiquitin from the end of the chain (Heride *et al.*, 2014). Endo- cleavage is very efficient at removing an entire ubiquitin chain from the substrate resulting in the release of an unanchored chain which requires further processing. However, endo-dUbs are also able to bind to ubiquitin moieties in the middle of specific chains. In contrast, exo-dUbs cleave single ubiquitin molecules from the distal end of ubiquitin chains, producing mono-ubiquitin (He *et al.*, 2016). The action of exo-dUbs can thus trim the lengths of the chain to, for example, regulate the ubiquitin signal, or alternatively they can act repeatedly to remove whole poly-ubiquitin chains. The specificity of dUbs to cleave at certain points in the poly-ubiquitin chain is often dependent on the conformation of the chain itself. For example, K48 linkages form a globular shaped chain (Ronau *et al.*, 2016) which can be recognised by dUbs such as Rpn11 and Ubp6. In contrast, K63-linked ubiquitin chains have a much more linear structure (Ronau *et al.*, 2016) thus requiring different recognition. Interestingly, some dUbs can also act in an endo- and an exo- manner depending on the chain linkages. For example, the mammalian dUb USP21 is able to cleave K63 chains at any linkage, whereas it is only able to cleave the terminal ubiquitin moiety from K6-linked chains (Mevissen and Komander, 2017). When dUbs remove chains of poly-ubiquitin from substrates, these chains then need to be further processed into single mono-ubiquitin moieties which can ultimately be reused in the conjugation cycle. In mammalian cells this further processing is performed by USP5 and USP13, which recognise the C-terminal di-glycine motif in unanchored poly-ubiquitin chains (Reyes-Turcu *et al.*, 2006; Komander *et al.*, 2009) In *S. cerevisiae*, Ubp14 processes these unanchored chains, and *ubp14*Δ mutants show an increase in free poly-ubiquitin chains (Amerik *et al.*, 1997). However, *ubp14*Δ mutant cells are still viable; suggesting that either the build-up of poly-ubiquitin chains is not detrimental to cell survival under normal conditions, or that another dUb is also able to contribute to the degradation of these chains.

Although dUbs demonstrate specificities in their substrate recognition, they also show redundancy and overlapping roles with other dUbs. This significantly adds to the number of substrates for each dUb, and also inhibits attempts to elucidate substrates. In *S. cerevisiae* only one dUb, Rpn11, is essential for viability (Finley

*et al.*, 2012), and moreover, when the other dUbs are individually removed surprisingly few growth defects are observed under normal conditions (Amerik *et al.*, 2000), suggesting that many dUbs can fulfil overlapping cellular roles. Indeed, a mutant strain with 5 dUbs deleted (*ubp1*Δ*, ubp2*Δ*, ubp3*Δ*, ubp7*Δ*, ubp8*Δ) displayed the same growth phenotype as a single *ubp8*Δ deletion strain suggesting a large redundancy of dUb functions (Amerik *et al.*, 2000).

*1.1.2.5.4. Protein partners*

While many dUbs can bind directly to the substrate, it has been found that some dUbs may need the activity of a binding or interaction partner (Ventii and Wilkinson, 2008). Furthermore, many dUbs have a low affinity for binding ubiquitin, suggesting that binding partners may also be a mechanism for regulating dUb specificity. For example, in mammalian cells TRAF2 (an E3 ligase important for cell survival and apoptosis) can bind to USP2, an interaction that stops USP2 from deubiquitinating K48 chains, but does not interfere with K63 deubiquitination (McClurg and Robson, 2015). Additionally, the mammalian dUb USP1, a key dUb involved in the DNA damage response, requires interaction with the WD40 interacting partner UAF1 to activate its enzymatic activity (McClurg and Robson, 2015). In *S. cerevisiae*, Ubp3 (mammalian homolog USP10) forms a complex with Bre5 to enable deubiquitination of subunits in COPII and COPI complexes (Cohen *et al.*, 2003) and for vacuole trafficking (Li *et al.*, 2007). Bre5 is an essential positive regulator of Ubp3 catalytic function. Interestingly, Bre5 does not complement a catalytically inactive mutant of Ubp3 and is not involved in substrate recognition (Cohen *et al.*, 2003), suggesting that Bre5 is necessary for Ubp3 substrate targeting or regulating catalytic activity (Li *et al.*, 2007). It has also been suggested that Ubp16 requires a binding partner, unknown at present, to enable deubiquitination of H2A (Turcu *et al.*, 2009).

The necessity for certain dUbs to utilise binding partners or cofactors suggests a potential mechanism for targeting and inhibiting specific dUb activity, without inhibiting the role of the dUb in other cellular roles independent of the binding partner (McClurg and Robson, 2015).

*1.1.2.5.5. Outstanding questions about dUb specificity*

New forms of ubiquitination are constantly emerging, bringing with them the possibility that new roles of dUbs (and maybe new dUbs) are yet to be identified. For example it has been found that multi-ubiquitination can occur at different lysine residues on ubiquitin, forming complex branched chains. Such branches may interfere with dUb cleavage, as they could interrupt endo-dUbs from recognising chain links. At this stage it is unclear whether any dUbs recognise specifically branched ubiquitin chains, or even whether these are processed by the same dUbs, but at a slower rate (Mevissen and Komander, 2017). Models have identified phosphorylation sites on ubiquitin (at Ser65 (Wauer *et al.*, 2015), or di-ubiquitin phosphorylated at Ser20 or Ser57 (Huguenin-Dezot *et al.*, 2016)) which could inhibit dUb binding. However no specific dUbs have been currently identified to recognise phosphorylated ubiquitin (Mevissen and Komander, 2017).

*1.1.2.6. DUbs in disease*

The dysregulation of mammalian dUbs has been linked to many diseases (for reviews see (Hanpude *et al.*, 2015; Heideker and Wertz, 2015; Magraoui *et al.*, 2015; Wei *et al.*, 2015)). Indeed, many dUbs were originally identified due to their links with disease progression. dUbs have been linked to the progression of many cancers, for example CYLD is a mammalian USP dUb which has been linked to the NF-κB and JNK pathways. Mutations in CYLD are highly prevalent in familial cylindromatosis, patients of which are prone to developing skin tumours (Bignell *et al.*, 2000). USP6 has been identified as an oncogene in Ewing's sarcoma that causes aneurismal bone cysts (Oliveira *et al.*, 2005). dUbs are also important in regulating tumour suppressors and oncogenes, disruption of which can also lead to cancer progression. One of the most studied dUb which regulates tumour suppressor and oncogenes genes is USP7. USP7 has been found to regulate the tumour suppressors PTEN (Song *et al.*, 2008) and p53, and also the oncogene Mdm2 (Sheng *et al.*, 2006). Initially USP7 was identified as a tumour suppressor as it was shown to be a dUb acting on p53 (Zhou *et al.*, 2018), allowing the stabilisation of p53 and inducing cell growth depression apoptosis in a p53-dependent mechanism. However more recent work revealed USP7 can also deubiquitinate Mdm2, an E3 which ubiquitinates p53. USP7

stabilises Mdm2 which the subsequently ubiquitinates p53 to maintain low cellular p53 levels (Hu *et al.*, 2006). Hence, removal of USP7 can result in activated P53 which can lead to cell cycle arrest and apoptosis (Zhou *et al.*, 2018). Interestingly, upregulation of USP7 has been identified in many cancers; such as prostate cancer (Song *et al.*, 2008), gliomas (Bhattacharya and Ghosh, 2014), and neuroblastoma (Fan *et al.*, 2013). The connection between USP7 function and cancer is further emphasised by the observations that high expression levels of USP7 in these tumours is linked to tumour aggressiveness and poor prognosis (Zhou *et al.*, 2018). Hence, there is much interest in investigating targeting USP7 for many cancer therapies. Another dUb noted for its link to cancers is USP15. USP15 removes ubiquitin and subsequently stabilises the oncogene TGF-β. Similar to USP7, high expression levels of USP15 have been found in certain cancers such as glioblastomas, and breast and ovarian cancers. Furthermore, loss of USP15 has been linked to reducing the oncogenic capacity of certain gliomas in mouse models, due to the downregulation of TGF-β (Eichhorn *et al.*, 2012). Interestingly, dUb dysregulation is linked to other aspects of human health. For example, USP16 has been linked with Down's syndrome phenotypes. Down's syndrome occurs upon trisomy of chromosome 21 and it has been proposed that the severe phenotypes are partly due to the upregulation of USP16 (Adorno *et al.*, 2013) which is expressed from this chromosome. Given the linkage of dysregulation of dUbs to many diseases, it is vital that dUbs (and other ubiquitin and ubiquitin-like modification pathway enzymes) are tightly controlled. It is therefore essential to understand the regulation and functions of specific dUbs in eukaryotes.

### *1.1.3. Regulation of ubiquitin/ubiquitin-like pathway enzymes*

Due to the large presence of ubiquitin and ubiquitin-like modifications in the cell, and the potential for dysregulation of the modifications to lead to disease, the modifications must be tightly regulated. In addition to conjugation and deconjugation of the moiety onto substrates, there are many layers of regulation which work together to control these modifications. For example, ubiquitin itself can be SUMOylated (Guzzo and Matunis, 2013) which can inhibit further ubiquitination of the substrate and also inhibit dUb recognition of the chain.

Indeed ubiquitin can be SUMOylated at 5 different lysine residues; K6, K11, K27, K48, and K63 (Swatek and Komander, 2016). The specific nature of SUMOylation of ubiquitin remains unknown. However, it has been identified that K6 and K27 SUMOylation is upregulated after heat shock (Hendriks *et al.*, 2014). Ubiquitin can also be modified by other PTMs such as phosphorylation and acetylation. Indeed, all lysine residues except for K29 in ubiquitin have been shown to be acetylated, and 11 different residues have been observed to be phosphorylated (Swatek and Komander, 2016). Both acetylation and phosphorylation change the surface properties of ubiquitin. Although most of the phosphorylation of ubiquitin has unknown physiological functions, it is interesting to note that phosphorylation at S65 (S65-phosphoUb) has been linked to Parkinson's disease and mitophagy (Okatsu *et al.*, 2015; Ordureau *et al.*, 2015). Thus, it is likely that PTM of ubiquitin has important functions in cells.

DUbs are a key regulator of ubiquitination as they remove the ubiquitin chains from substrates. It is therefore necessary to regulate dUb activity as without regulation dUbs could potentially indiscriminately remove ubiquitin thus dysregulating cellular ubiquitination (Sahtoe and Sixma, 2015). The regulation of dUbs can be broken into two main categories: the regulation of abundance and localisation of dUbs, and regulation of dUb catalytic activity (Mevissen and Komander, 2017). DUb localisation can be regulated by certain PTM's in the dUbs themselves, for example when the normally cytoplasmic mammalian dUb USP10 is phosphorylated it induces translocation to the nucleus, whereby USP10 deubiquitinates p53 (Yuan *et al.*, 2010). For further reviews covering regulatory mechanisms of dUbs and other ubiquitin and ubiquitin-like modifier pathway enzymes see (Petroski and Deshaies, 2005; Hickey *et al.*, 2012; Sahtoe and Sixma, 2015; Swatek and Komander, 2016; Mevissen and Komander, 2017). Interestingly, due to the presence of catalytic cysteines in many ubiquitin and ubiquitin-like modifier pathway enzymes, including dUbs, an important mechanism by which the catalytic activity of ubiquitin and ubiquitin-like modifications can be regulated is through the oxidation of these conserved cysteines by reactive oxygen species (ROS). Hence ROS, and the regulation by ROS, will be the focus of the remainder of this introduction.

## 1.2. Reactive oxygen species

Reactive oxygen species (ROS) are highly reactive molecules that contain one or more unpaired electrons in their outer orbit. Cells can be exposed to ROS from the environment, or from by-products of intracellular biological processes. Due to the damaging nature of ROS, high levels of oxidative stress are associated with the ageing process and many diseases and consequently cells have mechanisms that respond to the presence of these stress conditions to repair damage and restore homeostasis. These defences include enzymatic and non-enzymatic mechanisms. In contrast low levels of ROS are important components of many signalling pathways. Hence ROS levels must be tightly regulated to maintain equilibrium between the damaging high concentrations, and the important low concentrations of ROS, and cells must be able to distinguish both levels and types of ROS to respond in an appropriate manner.

### *1.2.1. Types and sources of ROS*

ROS encompass many different types of oxygen containing molecules, most of which have an unpaired electron in their outer shell producing highly reactive radicals (eg superoxide radicals: $O_2^{\cdot -}$ and hydroxyl radicals: $^{\cdot}OH$), however other non-radical forms have also been identified (eg hydrogen peroxide: $H_2O_2$) (Ray *et al.*, 2012; Phaniendra *et al.*, 2015). Superoxide is produced intracellularly through leakage in the electron transport chain (1.2.1.1). While $O_2^{\cdot -}$ is able to cause damage itself, it is comparatively stable when compared to other radicals. However $O_2^{\cdot -}$ is readily converted to $H_2O_2$ either spontaneously or through the action of superoxide dismutase enzymes (SODs) after $O_2^{\cdot -}$ interaction with $H^+$ (Fridovich, 1986). Although $H_2O_2$ has only weak oxidising abilities, it is classed as a cause of ROS due to high permeability across hydrophobic membranes (Kohen and Nyska, 2002), and ability to produce $^{\cdot}OH$ after interaction with metal ions (1.2.1.2). $^{\cdot}OH$ is the most highly reactive type of ROS (Valko *et al.*, 2006) and causes the majority of damage to cells, including DNA damage. $^{\cdot}OH$ has a short half-life (less than 1 ns) and as such tends to attack other molecules close to its site of formation (Valko *et al.*, 2006).

ROS are produced from many sources, including the production of different types of ROS from other radicals as described above. Other intracellular sources include electron leakage from the electron transport chain in normal respiration in the mitochondria, ROS production from transition metals, ROS production from the immune response. Extracellular sources include UV radiation and xenobiotics. Examples of intracellular and extracellular sources are described below.

*1.2.1.1. The mitochondrial electron transport chain*

Cellular energy is produced by respiration and the final step in this process is oxidative phosphorylation at the electron transport chain which occurs on the inner membrane of mitochondria (Nickel *et al.*, 2014). Although mitochondria are very efficient (human mitochondria reduce ~95% of total $O_2$ (Halliwell, 2006)) 0.1-2% electrons can escape from complexes, primarily complexes I and III in the electron transport chain (Bertaux *et al.*, 2018). Furthermore, electron leakage from complex III (in *S. cerevisiae* cytochrome *bcl* complex (Lemesle-Meunier *et al.*, 1993)) can result in electrons passing directly to $O_2$ producing $O_2^{\cdot-}$ . Significantly, this specific production of $O_2^{\cdot-}$ is classed as one of the major intracellular sources of $O_2$ radicals (Jastroch *et al.*, 2010). *S. cerevisiae* does not have complex I, but instead has three rotenone insensitive NADH dehydrogenases (Bakker *et al.*, 2001; Herrero *et al.*, 2008). Two of these enzymes have active sites which face the intermembrane space rather than the matrix. The rotenone insensitive NADH dehydrogenases oxidise NADH and transfer electrons to ubiquinone, and in doing so can transfer electrons directly to $O_2$ producing $O_2^{\cdot-}$ (Fang and Beattie, 2003). $O_2^{\cdot-}$ is converted to $H_2O_2$ via the action of mitochondrial superoxide dismutase (mtSOD) (Ansenberger-Fricano *et al.*, 2013), which in turn can be detoxified by enzymes such as catalase and glutathione peroxidase. If not detoxified, $H_2O_2$ can be converted into $^{\cdot}OH$, for example after interaction with iron (1.2.1.2) through the Haber Weiss and Fenton reactions.

*1.2.1.2. Transition metals*

Eukaryotes use several different transition metals such as iron (Fe), copper (Cu), zinc (Zn), manganese (Mn), nickel (Ni), and cobalt (Co) for many biological processes (Rodrigo-Moreno *et al.*, 2013). For example Fe, one of the most abundant metals on earth, is crucial for iron-sulphur clusters (Fe-S) which are important for several key cellular processes including electron transfer (Lill, 2009). Transition metals are also important for protein folding (Palm-Espling *et al.*, 2012), and are critical for function in the electron transport chain via association with complexes I-III. Hence, it is not surprising that transition metals are essential for cellular viability and highly abundant within cells. Indeed, ~30-40% proteins in the Protein Data Bank (PBD) contain a metal ion associated with the protein (Andreini *et al.*, 2013). Moreover, many of these proteins are catalytic enzymes where the metal ion is essential for function. For example, manganese mitochondrial SOD (MnSOD) carries one Mn ion per protein which is located in the active site, and donates an electron to the positively charged $O_2$ which is attracted to the SOD (Murphy, 2009). The ability of transition metals to recycle their redox state which is important for their catalytic role also means that they can reduce oxygen species to ROS. Hence, it is important that metal pools within cells are tightly regulated to reduce the production of $^{\cdot}OH$ through the Fenton reaction. In the Fenton reaction $Fe^{2+}$ interacts with $H_2O_2$ to produce $^{\cdot}OH$ and $OH^-$ (Figure 1.4). The resulting ferric ion $Fe^{3+}$ is also able to react with $O_2^{\cdot-}$ in the Haber Weiss reaction to produce $O_2$, in a redox cycle (reviewed in (Kehrer, 2000)). Thus, due to their ability to produce ROS in this manner, metal homeostasis is tightly regulated prevent aberrant ROS production.

*1.2.1.3. The immune response*

The immune response is an important defence mechanism against infection. One aspect of such responses is phagocytosis where cells in the immune system engulf invading pathogens and produce ROS to kill the trapped organism. In the initial stages of phagocytosis a large uptake of $O_2$, known as the respiratory burst occurs (Forman and Torres, 2002). NADPH oxidase (NOX2) then reduces the $O_2$ to $O_2^{\cdot-}$ which can be catalysed to $H_2O_2$ by dismutases (Dupré-Crochet *et al.*, 2013). NOX2 acts at a critical step in pathogen removal, suggesting that the

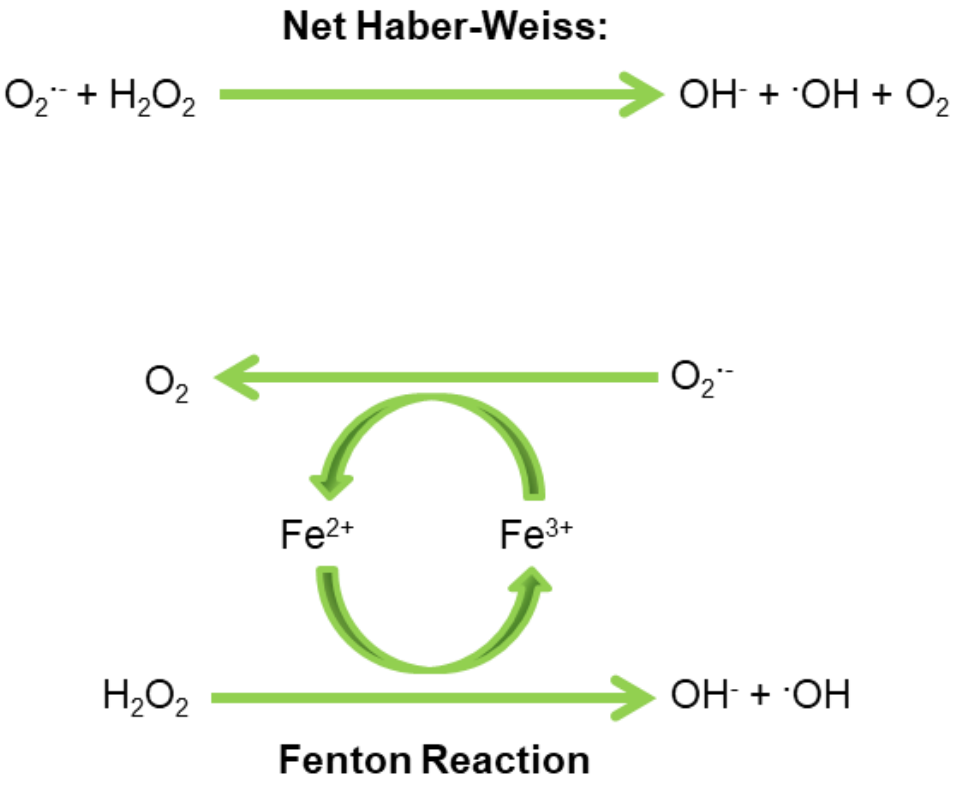


**Figure 1.4: The Haber-Weiss and Fenton reaction.** The Haber-Weiss reaction consists of a series of redox cycling reactions of iron (Fe) during $O_2^{\cdot-}$ oxidation to $O_2$, and $H_2O_2$ reduction to $OH^-$ + $\cdot OH$ (Fenton reaction). The net Haber-Weiss reaction produces OH-, $\cdot OH$ and $O_2$ from $O_2^{\cdot-}$ and $H_2O_2$. Adapted from (Kehrer, 2000).

production of the $O_2^{\cdot -}$ radical and subsequent $H_2O_2$ production are important for this process (Dupré-Crochet *et al.*, 2013). The ROS produced from NOX2 have been shown to be important for pathogen resistance as patients with mutations in NOX2 can acquire chronic granulomatous disease (CGD). These patients have neutrophils which cannot create ROS and as such suffer recurrent bacterial and fungal infections (Klebanoff, 2005), highlighting the importance of ROS production in the immune response. The ROS produced by neutrophil NOX2 can attack and oxidise DNA, proteins, and lipids of the pathogen. NOX2 produced ROS are also secreted specifically into the phagolysosome creating a charge gradient and influx of $K^+$, which initiates protease release that degrade ingested pathogens allowing a dual attack by ROS (Murphy and DeCoursey, 2006).

#### *1.2.1.4. Xenobiotics*

Xenobiotics are chemicals found within an organism that originate from the external environment. There are many examples of xenobiotics, for example environmental toxins, drugs, and metal ions, which can cause oxidative stress either by increasing the production of ROS within the cell (Klotz and Steinbrenner, 2017), or by attacking the intracellular antioxidant mechanisms. Quinones are a general term for a group of compounds produced from various xenobiotics which produce ROS and can remove cellular antioxidants. Quinones are potent redox-active compounds which can undergo enzymatic or non-enzymatic redox cycling, both of which can produce hydroxyl radicals (Bolton *et al.*, 2000). There are many types of cellular quinones, and one example is ubiquinone. Ubiquinone is present in all eukaryotic cells, where it is an essential component of the electron transport chain. Ubiquinone can exist in three redox states: fully oxidised, partially reduced (ubisemiquinone), and fully reduced. Importantly, it is this redox cycling that enables ubiquinone to shuttle electrons from complexes I and II to complex III (Hirst, 2013). However, the partially reduced ubisemiquinone can also interact with $O_2$ to produce superoxide radicals (Turrens *et al.*, 1985; Samoilova *et al.*, 2011). Another essential nutrient associated with quinones is vitamin K. Vitamin K is catalysed by NAD(P)H:quinone oxidoreductase 1 and NRH:quinone oxidoreductase 2 into vitamin K hydroquinone (Gong *et al.*, 2008) which is an important component of

blood clotting and bone metabolism. Vitamin K can be redox-cycled through one electron reduction to semiquinone, which after reacting with $O_2$ can be oxidised back to vitamin K (Gong *et al.*, 2008). However, this cycling of vitamin K produces superoxide. Interestingly, this ROS production can have certain beneficial roles in human health. For example, vitamin K can be used as a cancer therapy whereby the ROS produced by this redox cycling can be used to attack cancerous cells. Menadione is an exogenous polycyclic aromatic ketone which can act as a precursor for vitamin K production (Loor *et al.*, 2010), and hence can be classed as a superoxide producer (Fukui *et al.*, 2012). Low concentrations of menadione initiates redox-dependent gene expression (Chuang *et al.*, 2002), however high concentrations of menadione has been shown to cause mitochondrial DNA damage and tissue injury, and subsequently activate programmed cell death (Loor *et al.*, 2010).

#### *1.2.1.5. UV and ionising radiation*

UV light can cause cellular damage either directly, for example DNA damage, or indirectly by ROS production. The DNA damage induced by UVB rays of UV light is primarily the stimulation of pyrimidine dimers in adjacent bases on the DNA strand and such damage has been linked with skin cancer (Marrot and Meunier, 2008). UVB also can produce $H_2O_2$ in cells, which can in turn form hydroxyl radicals (Halliwell, 2006). However, although UV light is known to cause damage to cells, the oxidising potential is relatively low. In contrast, the oxidising potential of ionising radiation is high, for example, X-rays can directly ionise $H_2O$ to $H^{\cdot}$ and $OH^{\cdot}$ (Halliwell, 2006).

### ***1.2.2. Effects of ROS***

Due to the reactive nature of ROS described above, intracellular ROS can cause damage to DNA, proteins, and lipids. The nature and consequences of such oxidative damage will be discussed below.

#### *1.2.2.1. DNA*

ROS damage to DNA is a common event in humans. Indeed the human genome is continually exposed to ROS and it is thought that $10^5$ lesions/cell/day occur

due to ROS (Bridge *et al.*, 2014). These lesions include single- and double-stranded breaks, inter- and intra-crosslinking of DNA and/or DNA-associated proteins, attack of the deoxyribose backbone, and base attacks (Jena, 2012). Over 100 different DNA lesions have already been identified in mammalian DNA (Cadet and Wagner, 2013). However, one of the most characterised type of DNA damage caused by ROS is the introduction of 8-oxoG in the place of guanine bases (David *et al.*, 2007). Guanine bases have the least oxidative potential, and hence they are easily modified by ROS (Aguiar *et al.*, 2013). When guanine residues undergo one-electron oxidation to 8-oxoG, base miss-matches can occur whereby 8-oxoG pairs with adenine causing a transversion mutation in the template strand on DNA during DNA replication (Bridge *et al.*, 2014). Mutations such as these happen throughout the genome and are usually kept under control by base excision repair mechanisms (David *et al.*, 2007). Significantly, 8-oxoG has been found to be the most abundant mutation in certain melanomas. Furthermore, due to the common occurrence of this type of mutation, 8-oxoG is often used as a biomarker of DNA damage due to oxidative stress (David *et al.*, 2007). However, it is important to note that due to the lack of specificity of 8-oxoG mutation, it can only be used a measure of global oxidative DNA damage. Interestingly, using 8-oxoG as a marker it has been shown that mitochondrial DNA accumulates much more oxidative damage than nuclear DNA. It has been observed that there is approximately 16 times more 8-oxoG in mitochondrial DNA that nuclear DNA (Richter *et al.*, 1988). However, it has been argued that the higher accumulation of DNA damage in mitochondrial DNA is expected due to the rate of ROS production from the electron transport chain (it is known that ·OH have a very short half-life and tend to attack molecules close to the production of the radical). Also, mitochondrial DNA has no histones to aid in DNA protection (Richter *et al.*, 1988). It is also known that mitochondria have a high mutation and subsequent evolutionary rate, possibly due to the lack of DNA repair mechanisms within the organelle.

#### *1.2.2.2. Proteins*

Proteins are also damaged by ROS, which can attack them either at the peptide backbone, or at amino acid side chains (Berlett and Stadtman, 1997). Hydroxyl

radicals can attack hydrogen atoms on the polypeptide chain which, after a series of redox reactions results in an alkoxyl derivative and subsequent peptide fragmentation at that site (Stadtman, 2006). Peptide cleavage can also occur when hydroxyl radicals directly attack proline or glutamic acid side chains (Uchida *et al.*, 1990; Stadtman, 2006).The amino acid side chains on proteins can also be oxidised, either reversibly or irreversibly. An example of irreversible protein oxidation is protein carbonylation. This type of protein oxidation occurs much more readily than other forms of protein oxidation, and is often used as a biomarker of ROS-induced protein damage (Dalle-Donne *et al.*, 2003). Protein carbonylation occurs at proline, arginine, lysine, and threonine residues, whereby they become oxidised to aldehyde or ketone groups (Berlett and Stadtman, 1997). Carbonylation occurs by three mechanisms. In the first mechanism, the amino acid side chains of proline, arginine, lysine and threonine can be directly oxidised resulting in carbonyl derivatives (Stadtman and Levine, 2006). Secondly, α,β-unsaturated aldehydes from lipid peroxidation (see Section 1.2.2.3) can react with proteins through the 'Michael addition' reaction (Refsgaard *et al.*, 2000). Thirdly, the reaction of reducing sugars or oxidation products with lysine residues can result in advanced glycation end products (AGEs) (Cho *et al.*, 2007), which are large branched molecules that can block proteasome activity (Chondrogianni *et al.*, 2014). A large portion of proteasomal function is to remove proteins which have been damaged by oxidative stress. Hence, when the proteasome is blocked by AGEs damaged proteins, which would usually undergo degradation, accumulate resulting in larger amounts of ROS damaged proteins than normal within cells. Lysine carbonylation can also play a role in the regulation of post translational modifications. For example, lysine residues are sites for acetylation, methylation, and ubiquitin and ubiquitin-like modifications (Santos and Lindner, 2017), however lysine carbonylation prevents these modifications.

Proteins can also undergo reversible oxidation. For example, methionine residues can be oxidised by ROS into methionine sulphoxide which prevents methionine acting as a methyl donor (Kim *et al.*, 2014). However, methionine oxidation is reversible via the action of reductases, which reduce methionine sulphoxide back to methionine (Drazic and Winter, 2014). Cysteine residues can also be reversibly oxidised by ROS. Cysteines are sulphur containing residues

which play important roles in protein structure and function. For example, cysteine residues can form disulphide bonds, either intra- or inter-molecular, which can change the shape of proteins, and form covalent protein interactions. Cysteine residues can be oxidised in multiple ways, both reversibly and, after further oxidation, irreversibly (Figure 1.5). Upon initial oxidation, cysteine residues are oxidised into a sulphenic form. The sulphenic acid is reversible and can be reduced back to its initial state. This form is often classed as a cysteine oxidation gateway form, as from here the cysteine residue can undergo further oxidation or modifications (Finkel, 2011). For example, the sulphenic acid can form a reversible disulphide with another cysteine residue, which can be reduced back to a reduced thiol state. Sulphenic forms can also undergo reversible glutathiolation after reaction with glutathione, is a protective mechanism, which can also be reduced to its original state (Finkel, 2011). However, further oxidation of the sulphenic form produces a sulphinic and sulphonic acid sequentially which are generally irreversible. However, in specific proteins, 2-cys peroxiredoxins, sulphinic acids can be reduced by the sulphiredoxin (Srx) back to a sulphenic form (Biteau *et al.*, 2003). However, in all cases to date, sulphonic acids are irreversible and thus initiate degradation of the oxidised protein. This redox cycling of cysteine residues and the multiple redox states (reversible or irreversible) lends cysteine thiols to be important in ROS sensing and redox pathways (see Section 1.2.5). Furthermore, only cysteine thiols with a low pKa value (lower than the usual 8-8.5 pKa (Hoffman *et al.*, 2015; Poole, 2015)) are susceptible to oxidation. Thus, only certain cysteine residues are able to act as ROS sensors. Moreover, it also enables mechanisms that lower the pKa values of cysteine residues, such as de-protonation, to regulate when cysteines could be oxidised, thus resulting in regulation of oxidative stress response pathways (Finkel, 2011). Also many defences against ROS such as ROS scavengers of other enzymes use redox sensitive cysteine thiols for function (see Section 1.2.4).

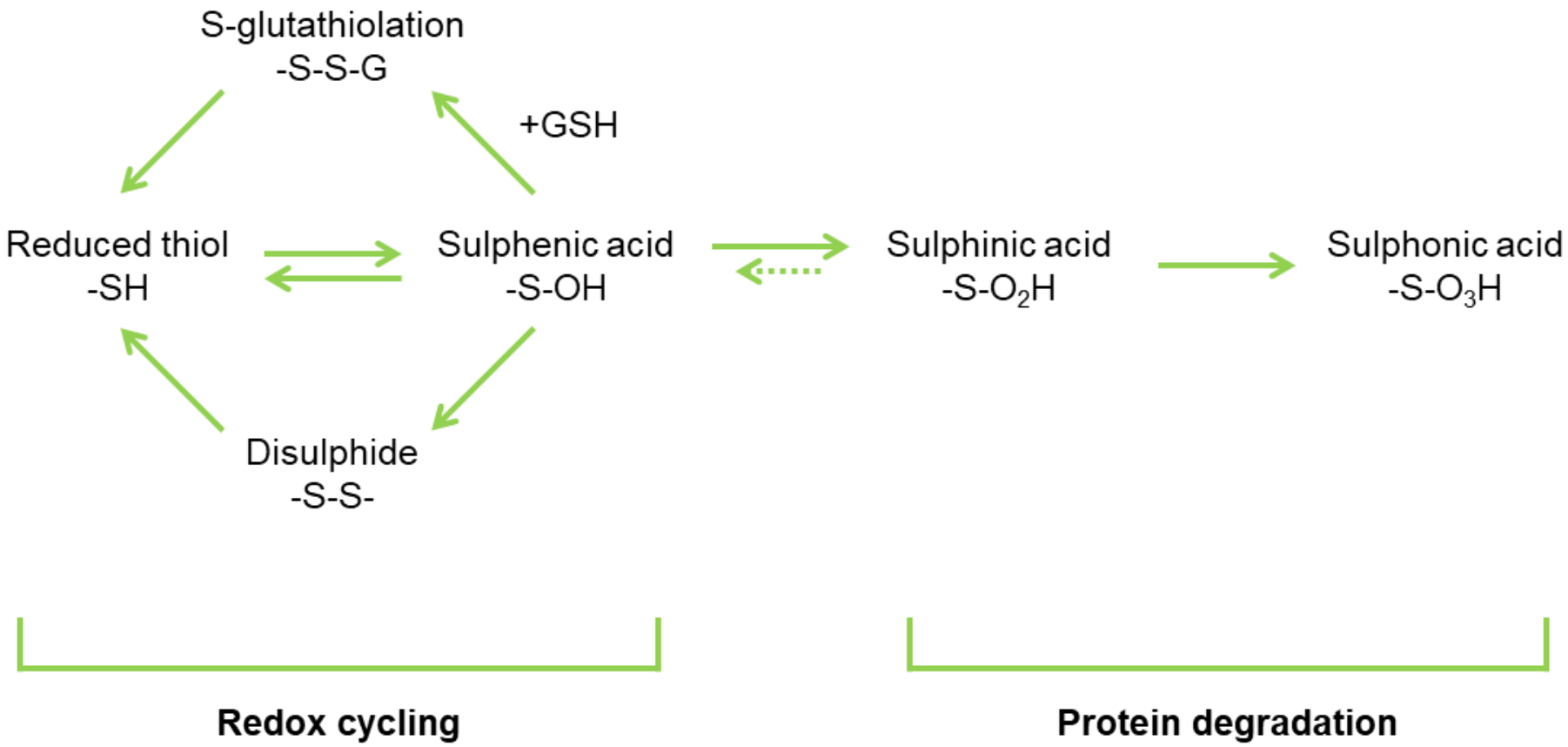


**Figure 1.5: The oxidation states of reactive protein thiols.** A reduced thiol can be reversibly oxidised into a sulphenic acid. Redox cycling reduces the sulphenic acid to its original state, and also enables disulphides to form with other reactive thiols. S-glutathiolation protects sulphenic acids from being oxidised further and can also be reduced to the original protein state. Sulphenic acids can be further oxidised into sulphinic acids and sulphonic acids. Sulphinic acids in 2-cys peroxiredoxins can be reduced by sulphiredoxin, however in most cases sulphinic and sulphonic acids are irreversible oxidation states and can initiate protein degradation.

*1.2.2.3. Lipids*

Lipids are large molecules consisting of a phosphate or sugar head-group and a hydrophobic fatty acid chain that make up the bilayer that forms cellular and intracellular membranes. In addition to acting as a physical barrier for organelles and cells due to their hydrophobic chain, lipids can be used as a source of energy by utilising the phosphate/ sugar head-group. The head-group of lipids can link together neighbouring lipids to form large structures which enable them to encase organelles. Due to their hydrophobic lipid nature, ROS including $^{\cdot}OH$, but not $O_2^{\cdot-}$ and $H_2O_2$ (Catalá, 2010), are able to oxidise lipids. Moreover, polyunsaturated lipids are the most vulnerable to attack by ROS due to the presence of a C=C double bond, absent from saturated hydrocarbon chains. ROS can attack the hydrogen atoms in the methylene group leaving an unpaired radical on the carbon. This radical then stimulates a chain reaction of lipid peroxidation through abstracting further hydrogen atoms from neighbouring hydrocarbon chains (Buettner, 1993). Importantly, the high propensity of polyunsaturated fatty acids to stabilise radicals means that they can produce a wide range of oxidised intermediates and end products. Lipid oxidation can have disastrous consequences for membranes as it can perturb membrane assembly and potentially damage membrane-bound proteins (Catalá, 2010).

### *1.2.3. ROS in ageing and disease*

As described above, oxidative stress can damage DNA, proteins, and lipids and as a consequence has been linked with many disease states and the aging process. Indeed, ROS have been linked to lifespan in multiple ways and there are many theories of ageing surrounding ROS. The first theory, the 'Free radical theory of ageing,' was proposed in 1956 (Harman, 1956). The basis of this hypothesis was that the causes of ageing were similar in all living things, and could be explained by the presence of ROS (Harman, 1956). Indeed, the link between ROS and ageing has been identified in many instances. For example, in *S. cerevisiae*, aged mother cells, but not younger daughter cells, were found to have increased levels of oxidative stress in the absence of external stress, suggesting that the mother cells contained oxidising molecules originating from the mitochondria (Laun *et al.*, 2001). A similar link between increased levels of

ROS and ageing has been observed in more complex models. For example, when supplemented with synthetic defences against ROS, the lifespan of wild type *C. elegans* increased dramatically, suggesting that pharmacological supplements to reduce ROS levels may increase lifespan (Melov *et al.*, 2000). Consistent with these findings, other studies of the relationship between ROS defences and lifespan found that mutations in antioxidant pathways shortened lifespan. For example, deletion of a primary defence against ROS, the mitochondrial superoxide dismutase MnSOD, leads to the build-up of ROS produced from the mitochondria in *S. cerevisiae* (Longo *et al.*, 1999). This causes inactivation of iron sulphur cluster containing enzymes which results in a reduction of mitochondrial function and can cause an increase in DNA mutation rates, leading to a loss of cell viability (Longo *et al.*, 1999). In higher eukaryotes the presence of ROS has also been linked to shortened telomeres. Telomeres are often referred to as a biological clock, and shortened telomeres results in cellular senescence or apoptosis (Titen and Golic, 2008). Furthermore, telomeres are particularly susceptible to oxidative stress, which has been shown to cause telomere shortening in mammalian cell cultures (von Zglinicki, 2000). Indeed, a recent study in cancer cell lines suggested this shortening is due to the inhibition of telomerase function by ROS (Ahmed and Lingner, 2018). However, while studies linking ROS to lifespan are extensive, more recent work has contradicted established theories surrounding ROS and ageing. For example, mitochondrial mutations in *C. elegans* which lead to an increased production of superoxide have actually been shown to be necessary for longevity (Yang and Hekimi, 2010). Furthermore, mitohormesis (Tapia, 2006) is the theory that ROS produced by the mitochondria are required for an increased lifespan, due the activation of antioxidant protective mechanisms. It has also been proposed that ROS from different cellular compartments may play varied roles in the ageing process (Ristow and Schmeisser, 2014). For example, mitochondrial ROS have been linked to increased lifespan in *C. elegans*, while the same study found that increased levels of cytoplasmic ROS actually led to a decreased lifespan (Schaar *et al.*, 2015). Hence, while the links between ROS and lifespan remain unclear, it is possible that the type and source of ROS, and potentially a culmination of many cellular processes in response to ROS, influence the ageing response.

While the links between ROS and lifespan are not fully understood, ROS have also been linked to many diseases, including cancers (Liou and Storz, 2010a), neurodegenerative disorders (Kim *et al.*, 2015) and other age-related diseases. For example, neurodegenerative diseases are connected given the propensity of the brain to be targeted by oxidative stress due to the necessity for high levels of oxygen and iron for normal functions (Kim *et al.*, 2015). Indeed, neurodegenerative disorders such as Alzheimer's disease are often associated with increased levels of ROS (Huang *et al.*, 2016). Alzheimer's disease is usually diagnosed by the presence of amyloid plaques or tau tangles in a post mortem biopsy (Melov *et al.*, 2007). Interestingly, mitochondrial specific oxidative stress has been found to be linked to tau phosphorylation, suggesting that oxidative stress is a causative factor to Alzheimer's disease (Melov *et al.*, 2007). Furthermore, protein carbonyls and 8-oxoG, both of which are used as biomarkers for oxidative stress, have been observed to occur at higher levels than normal in Alzheimer's brains (Sliwinska *et al.*, 2016). However, whether ROS are a cause and/or a consequence of Alzheimer's progression remains unknown. Indeed it has also been demonstrated that β-amyloid can increase ROS production by reducing electron transport chain efficiency (Luque-Contreras *et al.*, 2014), thereby creating a potential positive feedback loop to further induce the disease. This complex relationship between ROS and a potential cause and/or consequence in disease progression is also observed in cancers. ROS have been linked with almost all cancers studied (Liou and Storz, 2010a) and indeed one hallmark of cancer is the 'oxidative switch', where cancerous cells have an increased intracellular level of ROS (Liou and Storz, 2010a). Using the biomarker 8-oxoG, it has also been found that cancerous cells have an increased level of ROS induced DNA damage. However ROS levels are also manipulated in clinical treatments of cancers. Indeed, many chemotherapy and radiation strategies increase intracellular ROS to attempt to initiate tumour cell apoptosis (Liou and Storz, 2010a). Due to the links between ROS and ageing and disease, it is highly important to understand the mechanisms behind sensing ROS levels, and signal transduction in response to ROS, in both prevention and treatment of diseases.

### *1.2.4. Defences against ROS*

Cells utilise many mechanisms to maintain the balance of ROS levels in order to prevent cellular damage. These defences include enzymatic defences, such as SODs, catalases, and peroxidases, and non-enzymatic defences, such as glutathione, glutaredoxins, thioredoxins, and Vitamins C and E. Another component of cellular defences involves transcriptional regulation of antioxidants. For example in *S. cerevisiae* the transcription factors Yap1, Skn7 and Sod1 play important roles (Herrero *et al.*, 2008). Lower levels of antioxidants function to maintain redox homeostasis under normal conditions. However, in response to increased ROS levels these defences are increased to remove ROS before damage occurs and also to participate in repair mechanisms. The antioxidant defences of *S. cerevisiae* will be discussed below.

#### *1.2.4.1. Enzymatic defences against ROS*

Examples of *S. cerevisiae* enzymatic defences against oxidative stress, which function by directly detoxifying ROS, are discussed below.

##### *1.2.4.1.1. Superoxide dismutase*

Superoxide dismutases (SODs) detoxify superoxide by catalysing $O_2^{\cdot-}$ to $H_2O_2$ and $O_2$ with the aid of metal ions (Fukai and Ushio-Fukai, 2011). In *S. cerevisiae* there are two SODs, Cu/ZnSOD (Sod1) and MnSOD (Sod2) (Rattanawong *et al.*, 2015). These enzymes differ in their localisation and the metal ion they require for function. The predominantly cytoplasmic Sod1 requires a zinc ion and a catalytic copper ion, the latter of which is donated by the copper chaperone Ccs1. Ccs1 also facilitates the formation of a disulphide bond between two cysteines in Sod1 which is critical for Sod1 activity (Furukawa *et al.*, 2004). A proportion of Sod1 localises to the nucleus (Rona *et al.*, 2015) and Sod1, along with Ccs1, is also localised to the mitochondrial intermembrane space where it can scavenge mitochondrial ROS (Sturtz *et al.*, 2001). In contrast to Sod1, Sod2 localises to the mitochondrial matrix (Muid *et al.*, 2014) as a tetramer, and requires one manganese ion per subunit for function which is donated by the manganese chaperone Mtm1 (Luk *et al.*, 2005). Both *sod1*Δ and *sod2*Δ null mutants display increased sensitivity to external sources of superoxide, and also have slow

growth phenotypes and decreased lifespan (Chung, 2017). Furthermore, Sod2 has been suggested to be essential for defences against mitochondrial ROS generated from the electron transport chain (Herrero *et al.*, 2008). Indeed, consistent with this suggestion, *sod2*Δ mutants are unable to grow under respiratory conditions, and are also hyper sensitive to hyperoxia (Herrero *et al.*, 2008).

*1.2.4.1.2. Catalase*

Catalases are heme-containing tetrameric enzymes that detoxify $H_2O_2$ into $O_2$ and $H_2O$ (Kirkman and Gaetani, 1984). *S. cerevisiae* expresses two catalases, Cta1 and Ctt1 (Martins and English, 2014). Similar to SODs these proteins differ in their localisation; Cta1 localises to mitochondria, and also the peroxisome, where it detoxifies $H_2O_2$ produced during fatty acid oxidation (Martins and English, 2014), whereas Ctt1 is cytoplasmic and is important for protecting against oxidative stress however the precise role is unclear (Herrero *et al.*, 2008). In unstressed conditions, the *cta1*Δ and *ctt1*Δ single mutants, and the *ctt1*Δ *cta1*Δ double mutant, grow similarly to wild type cells, suggesting these catalases are not essential to maintain normal redox balance (Martins and English, 2014). However when cells are exposed to $H_2O_2$, Ctt1, but not Cta1, activity is stimulated, which subsequently increases cell survival (Martins and English, 2014). Taken together, these data suggest that Ctt1 is essential for protection against exogenous $H_2O_2$. However, the observation that catalase does not appear to be required raises the possibility that catalases may have overlapping roles with other intracellular antioxidants (Martins and English, 2014).

*1.2.4.1.3. Peroxidases*

In contrast to SODs and catalases, peroxidases do not use metal groups to reduce substrates (Herrero *et al.*, 2008). Instead peroxidases use electron donors to reduce $H_2O_2$ to $H_2O$ by the activity of cysteine thiol residues. Depending on the electron donor, peroxidases are divided into two classes: glutathione peroxidases (Gpx) which utilise glutathione, and thioredoxin peroxidases (peroxiredoxins (Prx)) which utilise thioredoxins as a reductant.

There are two types of Prx enzyme, 1-Cys or 2-Cys classified by their catalytic activity (Zhu *et al.*, 2012). The 2-Cys enzymes are subdivided into two further groups, typical and atypical. Typical 2-Cys Prxs have two cysteine residues at the active site, the peroxidatic cysteine and the resolving cysteine. The activity of typical 2-Cys Prxs first requires oxidation of the peroxidatic cysteine into a sulphenic group. This oxidised cysteine then forms a disulphide with a resolving cysteine from another Prx, which protects the enzyme from further oxidation (Zhu *et al.*, 2012; Angelucci *et al.*, 2013). Atypical 2-Cys Prxs initially function in a similar manner to typical 2-Cys Prxs, where the peroxidatic cysteine is first oxidised to a sulphenic group. However, in the case of atypical Prxs, the peroxidatic cysteine then forms an intramolecular disulphide with a resolving cysteine within the same Prx (Seo *et al.*, 2000; Zhu *et al.*, 2012). 1-Cys Prxs only have one cysteine at their active site, and subsequently cannot form an intramolecular disulphide (Wood *et al.*, 2003). Here, it is thought that the sulphenic form of the cysteine is then reduced by a thiol containing electron donor, which in yeast is glutathione (Greetham and Grant, 2009). In all the examples above, the redox cycling of the cysteines within the active site of Prxs allows the reduction of $H_2O_2$. However, multi-oxidation states of Prxs have also been identified. In these examples, following the initial oxidation of the peroxidatic cysteine further oxidation can occur, resulting in formation of a sulphinic group, which inhibits protein activity. Interestingly, this oxidation is not irreversible as it can be reduced back to a sulphenic group through the activity of sulphiredoxin (Srx) (Jeong *et al.*, 2012). However, further oxidation of the sulphinic group results in the formation of an irreversible sulphonic group (Lian *et al.*, 2012). Interestingly, Srx levels increase after $H_2O_2$ incubation (Biteau *et al.*, 2003) suggesting that the redox cycling of Prxs are important for stress responses. In *S. cerevisiae* there are 5 Prxs: Tsa1 (cTpxI), Tsa2 (cTpxII), and Ahp1 (cTpxIII) which are cytoplasmic; Dot5 (nTpx) which is nuclear; and Prx1 (mTpx) which is mitochondrial (Wong *et al.*, 2004). Although all Prxs have similar and often overlapping anti-oxidant roles, they are differentially expressed and usually are present in different cellular locations. For example, both Tsa1 and Tsa2 are highly homologous typical 2-Cys peroxidases that are required for the cellular responses to $H_2O_2$ (Garrido and Grant, 2002). The *tsa2*Δ mutants are more sensitive to exogenous $H_2O_2$ than the *tsa1*Δ mutants, suggesting they have

different roles (Wong *et al.*, 2002). However the double *tsa1*Δ *tsa2*Δ displays greater sensitivity to $H_2O_2$ than either of the single mutants, suggesting they have overlapping functions to provide resistance to peroxide stress (Wong *et al.*, 2002). Although Ahp1 has been historically classified as a typical 2-Cys Prx, recent studies have suggested that Ahp1 may be classed in a new, separate group of typical 2-Cys Prxs based on to its structural similarity to atypical and 1-Cys Prxs, but mechanistic similarity to typical 2-Cys Prxs (Lian *et al.*, 2012). In *S. cerevisiae* the 1-Cys mitochondrial Prx1 has been found to detoxify cadmium and $H_2O_2$ within mitochondria (Greetham and Grant, 2009). In conclusion, Prxs have specific individual roles and localisations within the cell, but also have overlapping roles. Moreover, all of the Prxs have been deleted simultaneously in *S.* cerevisiae and yet the cells remain viable (Wong *et al.*, 2004), suggesting there is redundancy with other cellular mechanisms. Indeed the quintuple mutant displays increased sensitivity when glutathione is depleted (Wong *et al.*, 2004), suggesting that glutathione linked pathways have overlapping functions with the Tpxs.

Gluathione peroxidases (Gpx) function similarly to Tpxs, except that tthey predominantly use glutathione as an electron donor. In *S. cerevisiae* there are three Gpxs, Gpx1, Gpx2, and Gpx3, all of which are atypical 2-Cys peroxidases (Delaunay *et al.*, 2002; Tanaka *et al.*, 2005; Ohdate *et al.*, 2010). In contrast to higher eukaryotes, which have both classical Gpxs (cGpx), which use glutathione as an electron donor, and phospholipid hydroperoxide Gpxs (PHGpx) which can use other electron donors, *S. cerevisiae* has only PHGpxs (Avery and Avery, 2001; Avery *et al.*, 2004). Indeed Gpx2 predominantly uses thioredoxin as an electron donor, rather than glutathione (Ukai *et al.*, 2011). Although *gpx1*Δ and *gpx2*Δ mutants show no altered sensitivities in response to exogenous peroxide stress, *gpx3*Δ strains display increased sensitivity (Inoue *et al.*, 1999), suggesting that Gpx3 has a larger role in peroxide response. Interestingly a fraction of Gpx3 has been observed to localise to the mitochondrial intermembrane space where it has been suggested that Gpx3 plays a role in $H_2O_2$ detoxification (Kritsiligkou *et al.*, 2017). Gpx3 has also been observed to be a major mediator of $H_2O_2$ signalling by the transcription factor Yap1 (See section 1.2.4.3).

*1.2.4.2. Non-enzymatic defences against ROS*

Eukaryotes have two major systems within the cell to defend against oxidative stress, the glutathione system (Grx) and the thioredoxin system (Trx). Both systems use NADPH produced from the pentose phosphate pathway as an electron donor in order to reduce oxidised proteins via the redox cycling of either glutathione reductase (Glr) and glutaredoxin (Grx), or thioredoxin (Trx) and thioredoxin reductase (Trr) respectively. Both systems, together with glutathione, are discussed below in the context of *S. cerevisiae*; for further reviews see (Fernandes and Holmgren, 2004; Lu and Holmgren, 2014).

*1.2.4.2.1. Glutathione*

Glutathione is a highly abundant tripeptide thiol found mainly in the cytoplasm, but which also localises to other organelles (Hwang *et al.*, 1992; Lu, 2013). The thiol group on the cysteine allows glutathione to act as a ROS scavenger to directly detoxify chemicals including free radicals, peroxides, and xenobiotics (Toledano *et al.*, 2013). However, it also allows glutathione to protect proteins from oxidation by formation of a disulphide bond between this cysteine and the substrate. This results in protein S-glutathiolation, which protects the protein from irreversible oxidative damage (Shenton and Grant, 2003). Glutathione is predominantly found in its reduced GSH state within the cell (Hwang *et al.*, 1992; Couto *et al.*, 2016), however oxidation of the active site cysteine in GSH allows formation of a disulphide bond to oxidised GSSG, subsequently reducing intracellular GSH levels (Lu, 2013). GSSG is reduced back to the GSH state through the activity of Glr utilising NADPH as an electron donor (Grant *et al.*, 1996a) (see 1.2.4.2.2). This oxidation and reduction forms a redox cycle which enables glutathione to act as a ROS scavenger or to protect substrate proteins from oxidation.

Intracellular GSH is synthesised through two ATP-dependent reactions (Figure 1.6), (Couto *et al.*, 2016). Firstly, γ-glutamylcysteine synthetase (encoded by *GSH1* in *S. cerevisiae*) catalyses L-glutamate and L-cysteine into the intermediate L-γ-glutamyl-L-cysteine. Secondly, glutathione synthetase (encoded by *GSH2* in *S. cerevisiae*) converts L-γ-glutamyl-L-cysteine and glycine into

glutathione (GSH) (Ohtake and Yabuuchi, 1991; Grant, 2001; Tang *et al.*, 2015). In *S. cerevisiae* glutathione is essential (Grant *et al.*, 1996b), and *gsh1*Δ mutants are inviable unless supplemented with exogenous glutathione in media. Interestingly, *gsh2*Δ strains can grow in glutathione depletion conditions, suggesting that γ-glutamylcysteine can partially substitute for GSH (Wheeler *et al.*, 2002). The inability of *gsh1*Δ strains to grow in glutathione lacking media cannot be rescued by reducing agents, suggesting that the essential role of glutathione is not due to a general role as a reductant.

*1.2.4.2.2. Glutaredoxins*

Glutaredoxins (Grx) are small soluble proteins involved in the reduction of oxidised GSH-protein disulphides (Figure 1.7A). Grxs are divided into two subgroups, either dithiol or monothiol, depending on the number of active site cysteines they have (Hanschmann *et al.*, 2013). Dithiol Grxs have two cysteine residues located in a CPYC motif, and *S. cerevisiae* expresses three dithiols, Grx1, Grx2, and Grx8 which localise to the cytosol (Li *et al.*, 2010; Tang *et al.*, 2014). Interestingly Grx2 contains an alternative start codon which can alter its localisation to the mitochondria. Although Grx2 has the most oxidoreductase ability, both Grx1 and Grx2 are important for $H_2O_2$ response. In contrast, only Grx1 is necessary for the response to the superoxide generating drug menadione, indicating the specific roles for each Grx (Luikenhuis *et al.*, 1998). Grx8 is not necessary for a general oxidative stress response, and also does not enhance the phenotypes displayed by *grx1*Δ and *grx2*Δ mutants (Eckers *et al.*, 2009; Tang *et al.*, 2014). Monothiol Grxs have one cysteine located in a CGFS motif (Zhang *et al.*, 2013), and *S. cerevisiae* expresses five monothiol Grxs; Grx3 and Grx4 which are nuclear (Pujol-Carrion *et al.*, 2006), and also regulate actin dynamics (Pujol-Carrion and de la Torre-Ruiz, 2010), Grx5 which is mitochondrial(Zhang *et al.*, 2013), and Grx6 and Grx7 which localise to the ER and Golgi membrane (Izquierdo *et al.*, 2008). Grx3 and Grx4 are involved in the maintenance of intracellular iron levels by regulating the transcription factor Aft1 (Pujol-Carrion *et al.*, 2006). For example, the double *grx3*Δ *grx4*Δ mutant displays an increased iron accumulation due to the nuclear accumulation of Aft1 (Pujol-Carrion *et al.*, 2006). Iron homeostasis is important for maintaining oxidative

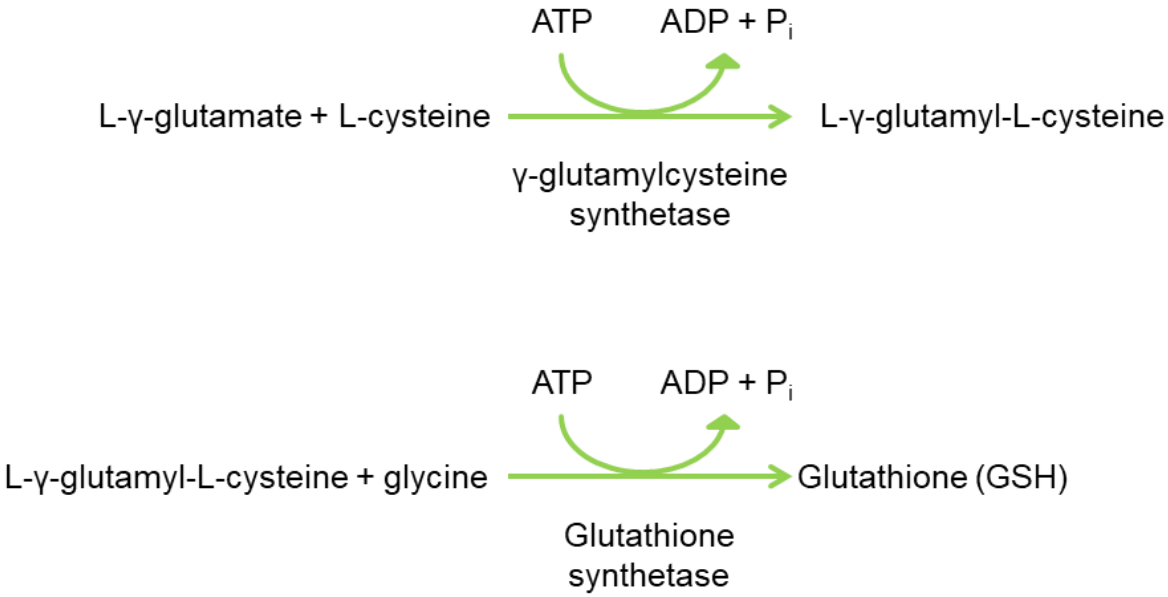


**Figure 1.6: Glutathione production is a two-step process.** GSH is synthesised through two enzyme controlled reactions, catalysed by γ-glutamylcysteine synthetase and glutathione synthetase. See text for details.

**A**

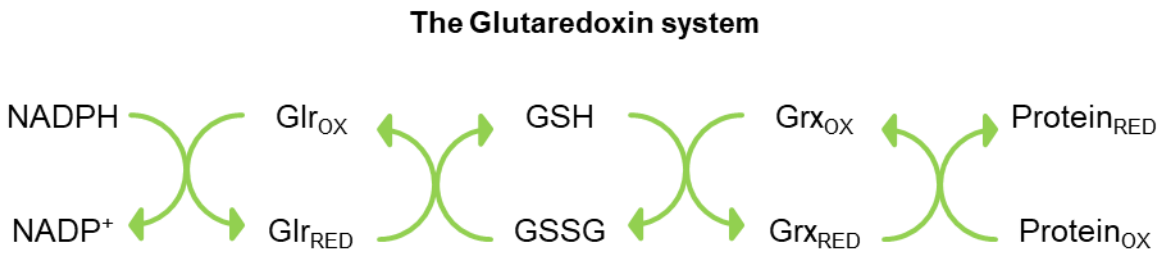


**B**

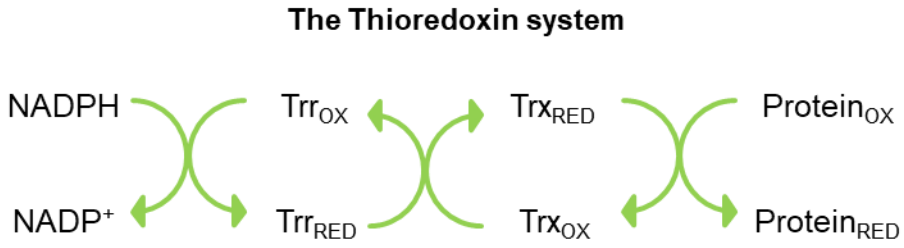


**Figure 1.7: The redox cycling of the Glutaredoxin and Thioredoxin systems.** (A) In the glutaredoxin system NADPH reduces $Glr_{OX}$ to produce $Glr_{RED}$, which subsequently reduces oxidised glutathione (GSSG) to reduced glutathione (GSH). GSH then reduces $Grx_{OX}$ to produce $Grx_{RED}$ which is able to reduce oxidised target proteins. (B) The thioredoxin system is shown in B. NADPH reduces $Trr_{OX}$ to $Trr_{RED}$ which subsequently reduces Trx $_{OX}$ to $Trx_{RED}$. Reduced Trx is then able to reduce oxidsed target proteins.

balance as iron is a critical factor in the Fenton reaction (1.2.1.2) which can increase oxidative stress. In contrast to Grx3 and Grx4, mitochondrial Grx5 is important for the response to $H_2O_2$ and menadione (Rodríguez-Manzaneque *et al.*, 1999), and for the biogenesis of Fe-S clusters (Rodriguez-Manzaneque *et al.*, 2002). Thus, the roles of Grx's within cells seem different, while dithiols possibly have a more generic response to oxidative stress; monothiols appear to act on more specific protein targets.

*1.2.4.2.3. Thioredoxins*

Thioredoxins (Trx) proteins contain two conserved active site cysteines which redox cycle by reduction by thioredoxin reductases (Trr) (Pedrajas *et al.*, 1999) (Figure 1.7B). *S. cerevisiae* expresses three Trxs, Trx1 and Trx2 which are cytoplasmic together with the thioredoxin reductase Trr1, and Trx3 which is mitochondrial together with the thioredoxin reductase Trr2 (Pedrajas *et al.*, 1999). Intriguingly, while t*rx1*Δ*, trx2*Δ*, trr1*Δ, and t*rr2*Δ single mutants all show increased sensitivity to $H_2O_2$, the single *trx3*Δ mutant does not (Trotter and Grant, 2005), suggesting that Trr2 has antioxidant functions in mitochondria that are different to Trx3. Interestingly, although the thioredoxin system is distinct from the glutaredoxin system, Trx3 accumulates in a *glr1*Δ mutant strain, suggesting that the systems overlap and that Glr1 may regulate Trx3 (Trotter and Grant, 2005). This overlap of roles is also consistent with the observation that a *trx1*Δ *trx2*Δ double mutant is viable, and a *trx1*Δ *trx2*Δ g*rx1*Δ *grx2*Δ quadruple mutant is inviable (Garrido and Grant, 2002), indicating that at least one of these systems is necessary for viability.

*1.2.4.3. Transcriptional regulation in response to ROS*

Oxidative stress causes a change in RNA levels of many genes. A study by Gasch *et al* (2000) found that 900 genes were regulated by multiple different types of stress, including osmotic stress, heat stress, and oxidative stress among others (Gasch *et al.*, 2000; Taymaz-Nikerel *et al.*, 2016). Many genes were downregulated, for example those with products involved in RNA metabolism and protein and DNA synthesis, while genes which were upregulated included those with products necessary for protein degradation, DNA damage repair,

signalling, ROS breakdown and redox control (Gasch *et al.*, 2000). Two transcription factors are mainly involved with the response by *S. cerevisiae* to oxidative stress, Yap1 and Skn7, although other transcription factors have roles in transcriptional response to oxidative stress (for reviews see (Herrero *et al.*, 2008; Morano *et al.*, 2012; Taymaz-Nikerel *et al.*, 2016).

Yap1 is a member of the conserved AP-1 transcription factor family (Moye-Rowley *et al.*, 1989; Delaunay *et al.*, 2000), and binds to Yap1 recognition elements (YREs) which are present in many gene promoters (Lee *et al.*, 1999; Herrero *et al.*, 2008). Interestingly, certain Yap1 targets do not contain YREs, suggesting that there are additional recognition sites (Herrero *et al.*, 2008). In *S. cerevisiae* Yap1 has been found to be activated by a number of stress conditions including different types of oxidation, metals and drugs (Delaunay *et al.*, 2002; Rodrigues-Pousada *et al.*, 2004). Indeed, Yap1 is the main cellular regulator of responses to different oxidants in *S. cerevisiae* (Herrero *et al.*, 2008). Yap1 is activated by the different oxidants due to the subcellular localisation, more specifically by regulating Yap1 nuclear export. In unstressed conditions Yap1 localises to the cytoplasm, where it is kept in a reduced form by the Trx system, and bound to the nuclear exportin Crm1 (Yan *et al.*, 1998). Oxidants inhibit the interaction between Yap1-Crm1 by disrupting the Yap1 nuclear export signal, therefore enabling Yap1 to accumulate in the nucleus. While oxidation by the different oxidants such as $H_2O_2$ and diamide both induce nuclear accumulation of Yap1, the mechanism behind Yap1 activation by the different oxidants is different. In response to diamide, intramolecular disulphide bridges occur between closely located cysteines in the C-terminal (C598, C620, and C629) (Azevedo *et al.*, 2003). However, $H_2O_2$ addition triggers the formation of an intramolecular disulphide between two cysteine residues (C303 and C598) in Yap1 (Delaunay *et al.*, 2000), which requires Gpx3 and Ybp1 (Veal *et al.*, 2003). Gpx3 senses $H_2O_2$ in the environment and transduces the signal to Yap1 by binding and forming an intermolecular disulphide between C36 in Gpx3 and C598 in Yap1 (Delaunay *et al.*, 2002). This is then resolved into the Yap1 intramolecular disulphide of C303 and C598 which enables Yap1 to accumulate in the nucleus (Delaunay *et al.*, 2002). This poses a 2-component system where Gpx3 senses intracellular $H_2O_2$, and relays the signal to Yap1. Yap1 then

disassociates from Crm1 and accumulates in the nucleus, whereby it can transcribe downstream stress response genes. Ybp1 is also required for Yap1 nuclear accumulation in response to $H_2O_2$ (Veal *et al.*, 2003). More recent data has elucidated the molecular mechanism for the role of Ybp1 in the formation of the Yap1 disulphide complex. Bersweiler *et al* (2017) identified that Ybp1 forms a ternary complex with the Gpx3-Yap1 intermolecular disulphide complex (Bersweiler *et al*, 2017). This in turn promotes the formation of the Yap1 intermolecular disulphide complex between C303 and C598 by impeding the formation of an intramolecular disulphide complex within Gpx3. The importance of Ybp1 in the oxidation of Yap1 is highlighted by the fact that the Gpx3-Yap1 intermolecular disulphide cannot be formed in a *ybp1*Δ delete strain (Veal *et al.*, 2003). It is interesting to note that certain *S. cerevisiae* strain backgrounds do not have a fully functional Ybp1 gene. The W303 strain background of *S. cerevisiae* encodes a truncated and therefore non-functional version of Ybp1, which is therefore unable to form the Yap1-Ybp1 complex (Veal *et al.*, 2003). In the W303 strain background Yap1 is activated independently of Gpx3 whereby the Tpx Tsa1 is required for activation of Yap1 (Veal *et al.*, 2003). The difference in regulation of Yap1 by the different strain backgrounds of *S. cerevisiae* causes an increase in sensitivity to $H_2O_2$, but not diamide (Veal *et al.*, 2003). Therefore it is intriguing to note the strain specific differences in the response to oxidative stress in cerevisiae. Interestingly, Yap1 is constitutively oxidised in *trr1*Δ mutants, and remains nuclear (Ragu *et al.*, 2014). Nuclear Yap1 initiates the transcription of approximately 70 genes, including important components of the Grx and Trx systems for example *GSH1, GPX3, TSA1, TRX1* and *TRR1* (Mulford and Fassler, 2011).

While many genes involved in the oxidative stress response are regulated by Yap1, the expression of several genes depend on Yap1 together with another transcription factor Skn7 (Mulford and Fassler, 2011). Interestingly there are only two genes that are dependent on Skn7 alone, *DNM1* (a mitochondrial GTPase involved in morphology) and *OLA1* (an ATPase linked to the proteasome) suggesting that Skn7 is not distinct from Yap1 in the oxidative stress response (Mulford and Fassler, 2011). In contrast to Yap1, Skn7 localises to the nucleus in both non stress and stress conditions (Raitt *et al.*, 2000). After stress, Yap1

localises to the nucleus, where it can interact with Skn7 directly and bind to the promoters of specific genes to activate transcription (Mulford and Fassler, 2011). Consistent with the interaction between Yap1 and Skn7 cooperating to activate gene expression, single *yap1*Δ and *skn7*Δ mutants are extremely sensitive to $H_2O_2$ and superoxide producers, whilst the double *yap1*Δ *skn7*Δ mutant has no additional defects (Morgan *et al.*, 1997; Ohdate *et al.*, 2010; Yi *et al.*, 2016).

Sod1, a superoxide dismutase which detoxifies superoxide by catalysing $O_2^{\cdot-}$ to $H_2O_2$ and $O_2$ (section 1.2.4.1.1) has recently been characterised as a transcription factor important for resistance to oxidative stress (Tsang *et al.*, 2014; Chung, 2017). After superoxide and $H_2O_2$ stress the predominantly cytoplasmic Sod1 became nuclear due to phosphorylation of Sod1 in a Mec1/Dun1-dependent manner. Once nuclear, Sod1 has been identified to be important in regulating the transcription of 123 genes, which are involved in a variety of stress responses (Tsang *et al.*, 2014). Interestingly, changes in the localisation of Sod1 were not observed with agents that induce DNA damage, suggesting that Sod1 localisation is specifically sensitive to oxidation by superoxide and $H_2O_2$ (Tsang *et al.*, 2014). It is also intriguing that $H_2O_2$ regulates Sod1 localisation, yet is not actually a target of Sod1 dismutase activity, possibly suggesting that the transcriptional role of Sod1 is distinct from detoxifying roles (Tsang *et al.*, 2014).

### *1.2.5. ROS sensing and signalling*

High levels of ROS are largely associated with causing damage to cellular components such as DNA, proteins, and lipids which can result in age-related diseases such as cancer and neurodegenerative disorders, and decrease lifespan (see previous sections and Figure 1.8). However, low levels of ROS also play essential roles in signal transduction mediating cellular functions such as proliferation, apoptosis and cell migration (Veal *et al.*, 2007). However, as the levels of ROS increase from low to high, different response mechanisms are activated that induce the activation of defences to ROS, including the upregulation of antioxidants (Herrero *et al.*, 2008). These antioxidants act to

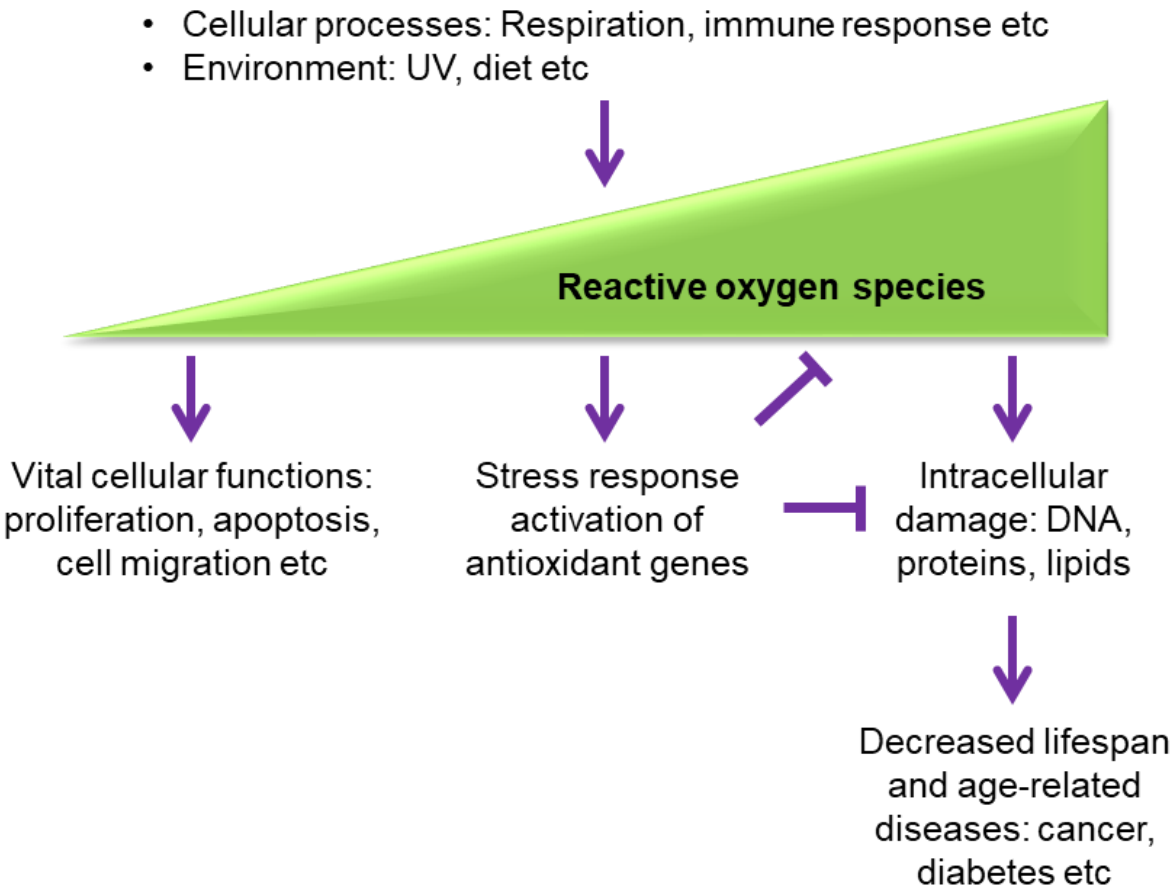


**Figure 1.8: The concentration-dependent effects of different levels of ROS.** Different cellular and environmental processes can produce ROS, which have different effects depending on the concentration and type of ROS. For example, high levels of ROS can cause damage to DNA, proteins and lipids which can cause decreased lifespan and age-related diseases. However, low ROS levels are critical for many vital cellular processes including proliferation, apoptosis, and cell migration. As levels increase cells must be able to sense the change in ROS concentration and initiate the appropriate cellular responses. These responses include the activation of antioxidants which can reduce the intracellular ROS levels and also repair damage.

reduce levels of ROS within the cell and repair any damage to cellular components (Liou and Storz, 2010b) (Figure 1.8). Thus, cells require sensing mechanisms that can detect ROS levels, and also the types of ROS, to trigger the appropriate responses.

Three important characteristics are important for ROS to be able to effectively act as a signalling molecule: production must be rapid and close to the site of action, the signal initiated must be able to be detected easily in order to initiate the appropriate response, and the signal must be able to be removed rapidly to attenuate the signalling cascade when necessary (Hancock, 2009). In this respect $H_2O_2$ is an especially good candidate for a signalling molecule. $H_2O_2$ can be produced rapidly by NADPH oxidases which produce $O_2^{\cdot-}$ by the transfer of electrons to oxygen (Landry and Cotter, 2014). Rapid dismutation by SODs produce $H_2O_2$ (section 1.2.1) which is much more stable than $O_2^{\cdot-}$ and able to cross intracellular membranes (Bienert *et al.*, 2006), allowing $H_2O_2$ to be close to most sites of action (Lassegue and Griendling, 2010). $H_2O_2$ is also able to initiate different cellular responses depending on concentration and localisation. $H_2O_2$ can be detected by $H_2O_2$ sensor proteins, often with the use of cysteine residues with a low pKa which increases their susceptibility to oxidation (Section 1.2.2.2). Not all proteins have cysteines with a pKa low enough to be able to be easily oxidised, thus the oxidation of only certain cysteines allows specific targeting of downstream responses (Rhee *et al.*, 2005). After the desired response has been initiated by $H_2O_2$ the signal must be blocked at some point to inhibit the signalling cascade. With respect to this inhibition, firstly $H_2O_2$ itself must be removed from the cell to prevent further oxidation. Mechanisms here include the use of antioxidants which are able to remove $H_2O_2$ (Section 1.2.4). Secondly, cysteine residues oxidised by $H_2O_2$ must be reduced, to revert the protein back to its normal reduced state (Hancock, 2009). In many cases reduction of oxidised cysteine residues is performed by the Grx and/or Trx pathways (Section 1.2.4).

In addition to distinguishing different levels of ROS, cells also need to be able to respond to different types of oxidising agents. As described previously (Section 1.2.4.3), Yap1 is a transcription factor that is activated after oxidative stress. The nuclear accumulation and transcriptional activity of Yap1 is triggered by many

types of oxidising agent and at least two different sensing mechanisms are involved (Azevedo *et al.*, 2003). For example, $H_2O_2$ addition to yeast cells triggers the formation of an intramolecular disulphide between two cysteine residues (C303 and C598) in Yap1. However in contrast, oxidation by other thiol reactive chemicals, such as diamide, caused the formation of disulphides between three different cysteines (C598, C620, and C629) (Azevedo *et al.*, 2003) (see Section 1.2.4.3). Interestingly menadione is able to oxidise Yap1 through both mechanisms (Azevedo *et al.*, 2003). These different sensing mechanisms in Yap1 that detect different types of stress highlight the abilities of proteins to sense different types of ROS.

Cells must also be able to distinguish between low and high levels of oxidising agents. One example of this is that the oxidation status of the Peroxiredoxin Tpx1 in the fission yeast *S. pombe* can regulate specific transcription factors depending on the concentration of $H_2O_2$ (Veal *et al.*, 2007). Two different transcription factors are important for regulating gene expression in response to $H_2O_2$ in *S. pombe*, and the concentration of $H_2O_2$ regulates which transcription factors are activated thus regulating which genes are upregulated (Veal *et al.*, 2007). At low concentrations of $H_2O_2$, the peroxidatic cysteine in Tpx1 is oxidised into a sulphenic acid, which results in activated Tpx1. Activated Tpx1 subsequently activates Pap1 which induced the expression of Pap1 dependent genes (Quinn *et al.*, 2002). In contrast, high levels of $H_2O_2$ hyperoxidises the peroxidatic cysteine of Tpx1 which activates the MAPK Sty1 which in turn phosphorylates Atf1 (Quinn *et al.*, 2002; Day *et al.*, 2012). Phosphorylated Atf1 induces the transcription of Atf1 dependent genes. Interestingly, Atf1 results in the transcription of the sulphiredoxin Srx1. Srx1 reduces the sulphinic acid of hyperoxidised Tpx1 to a sulphenic acid, which results in the activation of Tpx1 and the subsequent Pap1 activation (Vivancos *et al.*, 2005). In conclusion, the differential oxidation status of Tpx1 to different concentrations of $H_2O_2$ in *S. pombe* exemplifies an effective mechanism whereby the levels of oxidative stress are sensed to allow the appropriate downstream response.

Protein tyrosine phosphatases (PTPs) have important roles in many signalling pathways including those stimulated by growth factors and cytokines. In

particular, PTPs de-phosphorylating tyrosine residues which can inactivate MAPKs and activate CDKs (Veal *et al.*, 2007). PTPs have a catalytic cysteine residue at their active site (H-C-$X_5$-R (Tabernero *et al.*, 2008)) which has a low pKa value. This feature allows the cysteine to act as a nucleophile to attack substrates, but also renders the cysteine susceptible to oxidation. Indeed oxidation of the catalytic cysteine inactivates PTP function (Liou and Storz, 2010a), inhibiting its role in signalling pathways. Thus in order to maintain PTP roles in signalling, further irreversible oxidation must be prevented. One mechanism by which this is achieved is exemplified by the oxidation that a cyclic sulphenylamide forms in the PTP PTP1B which changes protein conformation (Salmeen *et al.*, 2003). This conformational change prevents further oxidation of PTP1B, and also exposes the catalytic cysteine to reducing agents, which allows the redox cycling important for ROS-dependent signalling (Salmeen *et al.*, 2003; van Montfort *et al.*, 2003). More recently it has been identified that Trx1 reactivates oxidised PTP1B into its reduced form (Schwertassek *et al.*, 2014). This mechanism is not the case for all PTPs. For example, oxidation of Cdc25 causes the formation of an intramolecular disulphide between the catalytic cysteine with another cysteine residue in the protein, which protects the catalytic cysteine from further irreversible oxidation (Buhrman *et al.*, 2005). Similar to PTP1B this protective disulphide is reduced by thioredoxin (Seth and Rudolph, 2006).

Recently ubiquitin and ubiquitin-like pathways have been linked to ROS sensing and signalling, and these will be discussed in more depth in the next section.

### 1.3. Regulation of ubiquitin and ubiquitin-like modifications by ROS

As described previously (see Section1.1) many of the ubiquitin and ubiquitin-like modifier pathway enzymes use catalytic cysteines for function. Ubiquitin and ubiquitin-like E1 and E2 enzymes use catalytic cysteines to form a thioester with the C-terminal glycine residue of the ubiquitin and ubiquitin-like moiety. To act this way the catalytic cysteine must first be deprotonated to reduce the pKa. However, as a consequence this reduction in pKa also potentially increases their

susceptibility to oxidation by ROS. Interestingly, under normal physiological conditions the pKa of E2 catalytic cysteines is relatively high (Tolbert *et al.*, 2005), thus allowing specific regulation of E2s by oxidation only when the cysteine is deprotonated (Stankovic-Valentin and Melchior, 2018). When ubiquitin and ubiquitin-like modifiers are transferred from the E1 enzymes to E2 enzymes, the catalytic cysteines from the E1 and the E2 come into close proximity allowing nucleophilic attack of the C-terminal glycine residue of the ubiquitin and ubiquitin-like modifier by the E2 catalytic cysteine (Stankovic-Valentin and Melchior, 2018). Interestingly, in addition to the conjugation machinery, isopeptidases which catalyse the cleavage of ubiquitin (dUbs) and SUMO (SENPs) utilise a catalytic cysteine which is deprotonated to allow cleavage of the isopeptide bond between the ubiquitin and ubiquitin-like modifiers and lysine residues. This deprotonation lowers the pKa of the cysteine, thus increasing their potential to be oxidised. Indeed, there is increasing evidence that enzymes in ubiquitin and ubiquitin-like modification pathways are regulated by ROS, and this is discussed below.

### *1.3.1. SUMO*

Regulation of the ubiquitin-like modification pathway SUMO by ROS has been described previously. Bossis and Melchior (2006) found that in mammalian cells the addition and removal of SUMO through the conjugation and deconjugation cycle is differentially affected by $H_2O_2$ in a manner that is capable of distinguishing low and high levels of ROS (Figure 1.9). In this study, global SUMOylation was found to be reduced at low levels of $H_2O_2$ (1 mM $H_2O_2$) but increased at high levels (100 mM $H_2O_2$). Analysis of the SUMO conjugation pathway revealed that an intermolecular disulphide bond forms between the catalytic cysteine residues of Uba2 and Ubc9 (E1 and E2 respectively) at both low and high levels of $H_2O_2$ preventing SUMOylation (Bossis and Melchior, 2006). However at low levels of $H_2O_2$, SENPS are still active, leading to global SUMO deconjugation and the accumulation of free SUMO (Bossis and Melchior, 2006). Interestingly, it was also observed that the glutathione system reduced the Uba2-Ubc9 dimer (Bossis and Melchior, 2006). In contrast, increasing $H_2O_2$ concentrations also inhibited the deconjugation machinery, preventing the removal of SUMO from substrates and consequently maintaining SUMOylation

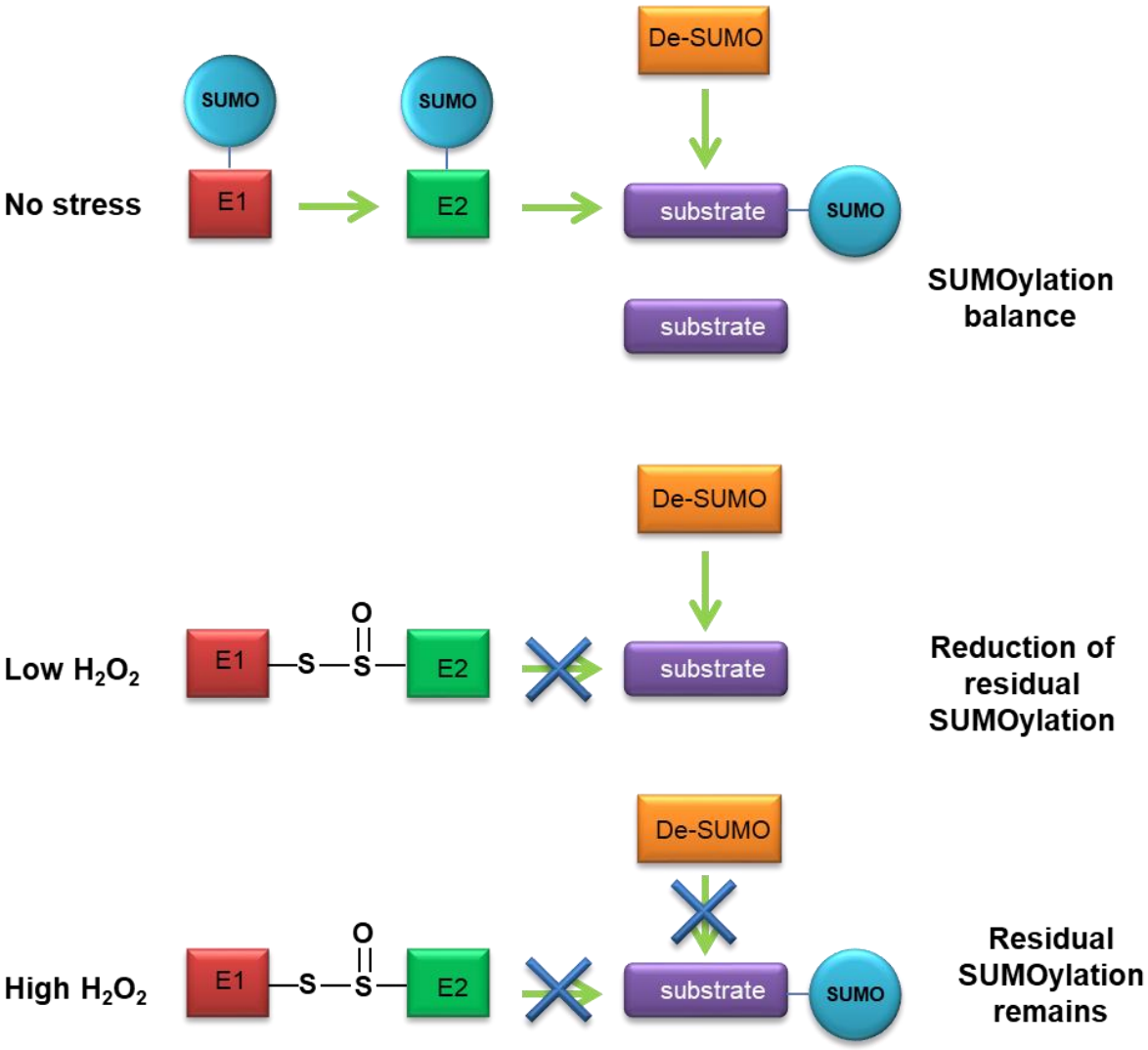


**Figure 1.9: ROS sensing by SUMO pathway enzymes in mammalian cells.** In unstressed cells both the SUMO conjugation and deconjugation machinery function as normal, creating a balance of SUMOylation of substrates. At low levels of $H_2O_2$ SUMO conjugating enzymes are oxidised and form a disulphide complex between the E1 and E2, whereas the deSUMOylases are still active thereby causing a reduction of residual levels of SUMOylated substrates. However at higher $H_2O_2$ concentrations the deSUMOylases are also inhibited, thus maintaining global SUMOylation.

under higher concentrations of $H_2O_2$ (Bossis and Melchior, 2006). Interestingly, in response to $H_2O_2$ the mammalian SENP1 forms an intramolecular disulphide between the catalytic cysteine (C603) and a neighbouring cysteine (C613) (Xu *et al.*, 2008; Stankovic-Valentin and Melchior, 2018). This disulphide, which is reversible, is suggested to be a protective mechanism to prevent further sulphydryl oxidation. The oxidation of SENP1 is also conserved in *S. cerevisiae* Ulp1 (Xu *et al.*, 2008). The differential sensitivity of different components in the SUMO conjugation/ deconjugation pathway to oxidation identifies a ROS sensing mechanism, whereby different concentrations of ROS result in different outcomes for SUMO substrates. Importantly, after reduction the E1 and E2 enzymes which formed a disulphide complex in response to $H_2O_2$ were still catalytically active, revealing that oxidation was reversible (Stankovic-Valentin and Melchior, 2018). More recent investigations of the physiological importance of regulating SUMO pathway enzymes in this way found that the reversible oxidation of SUMO E1 and E2 enzymes was critical for cell survival after DNA damage by oxidative stress (Stankovic-Valentin and Melchior, 2018). Importantly this was seen not only after incubation with exogenous $H_2O_2$ which can sometimes be seen as not physiologically relevant, but after chronic oxidative stress in older cells caused by cultivation in 20% oxygen (Stankovic-Valentin and Melchior, 2018).

### *1.3.2. NEDD/ Rub1*

The NEDD8 ubiquitin-like modification pathway in mammalian cells has also been found to be regulated by ROS. In response to bacterial infection mammalian epithelial cells can produce ROS as a defensive mechanism. Interestingly, this bacterially-induced ROS has been linked to the oxidation of the NEDD8 E2 Ubc12 which forms a high molecular weight complex (Kumar *et al.*, 2007). This observation suggests that NEDD8 may be regulated in a similar mechanism to the SUMO pathway described above. Further analysis of Cul1, a NEDD8 substrate that is a subunit of the $SCF^{\beta\text{-}TrCP}$ E3 ubiquitin ligase, revealed that after oxidation of Ubc12, NEDDylation of Cul1 was abolished potentially inactivating $SCF^{\beta\text{-}TrCP}$ (Kumar *et al.*, 2007). In contrast to the SUMO pathway where Ubc9 formed a disulphide complex with Uba2, it remains unknown whether

Ubc12 forms a disulphide complex with another enzyme, as the E1 is not part of the Ubc12 oxidised complex (Kumar *et al.*, 2007).

### *1.3.3. Ubiquitination*

Initial studies of global ubiquitination after different concentrations of $H_2O_2$ were added to mammalian cells suggested that ubiquitin conjugation/ deconjugation was not affected by $H_2O_2$ (Bossis and Melchior, 2006). However, in contrast to SUMO conjugation, many more E2s and dUbs are involved in ubiquitination pathways, thus raising the possibility that specific ubiquitin pathways may be sensitive to ROS. Interestingly, studies in *S. cerevisiae* revealed that one particular ubiquitin pathway E2 does indeed form a disulphide complex in response to oxidative stress similar to that seen in the SUMO and NEDD8 pathways in mammalian cells (Bossis and Melchior, 2006; Kumar *et al.*, 2007). Studies from our lab showed that exposure of cells to different oxidising agents, the E2 Cdc34, but not other ubiquitin E2 enzymes, formed a HMW intermolecular disulphide complex with the E1, Uba1 (Doris *et al.*, 2012). As described previously, Cdc34 regulates cell cycle progression in late G1 phase via the ubiquitination of the CDK inhibitor Sic1 (Section 1.1.1.3.1). In wild type, unstressed cells, Uba1 and Cdc34 ubiquitinate Sic1 which is subsequently degraded by the proteasome system, allowing normal cell cycle progression from G1 to S phase (Verma *et al.*, 1997). However, after oxidation by $H_2O_2$ or diamide Cdc34 forms a disulphide complex. The kinetics of the formation of the disulphide complex coincides with an increase in Sic1 stability (Doris *et al.*, 2012). Thus, these data suggest that the Cdc34-Uba1 disulphide complex cannot ubiquitinate Sic1, which is subsequently not degraded, resulting in cell cycle arrest (Figure 1.10).

At the beginning of this thesis studies it was unknown whether dUbs are differentially oxidised in response to ROS in *S. cerevisiae*. dUb oxidation in other organisms prior to this thesis studies is discussed below.

#### *1.3.3.1. Deubiquitination*

As many dubs are thiol proteases which use deprotonation of a catalytic cysteine for function, they also have the potential to be regulated by ROS. Prior to the

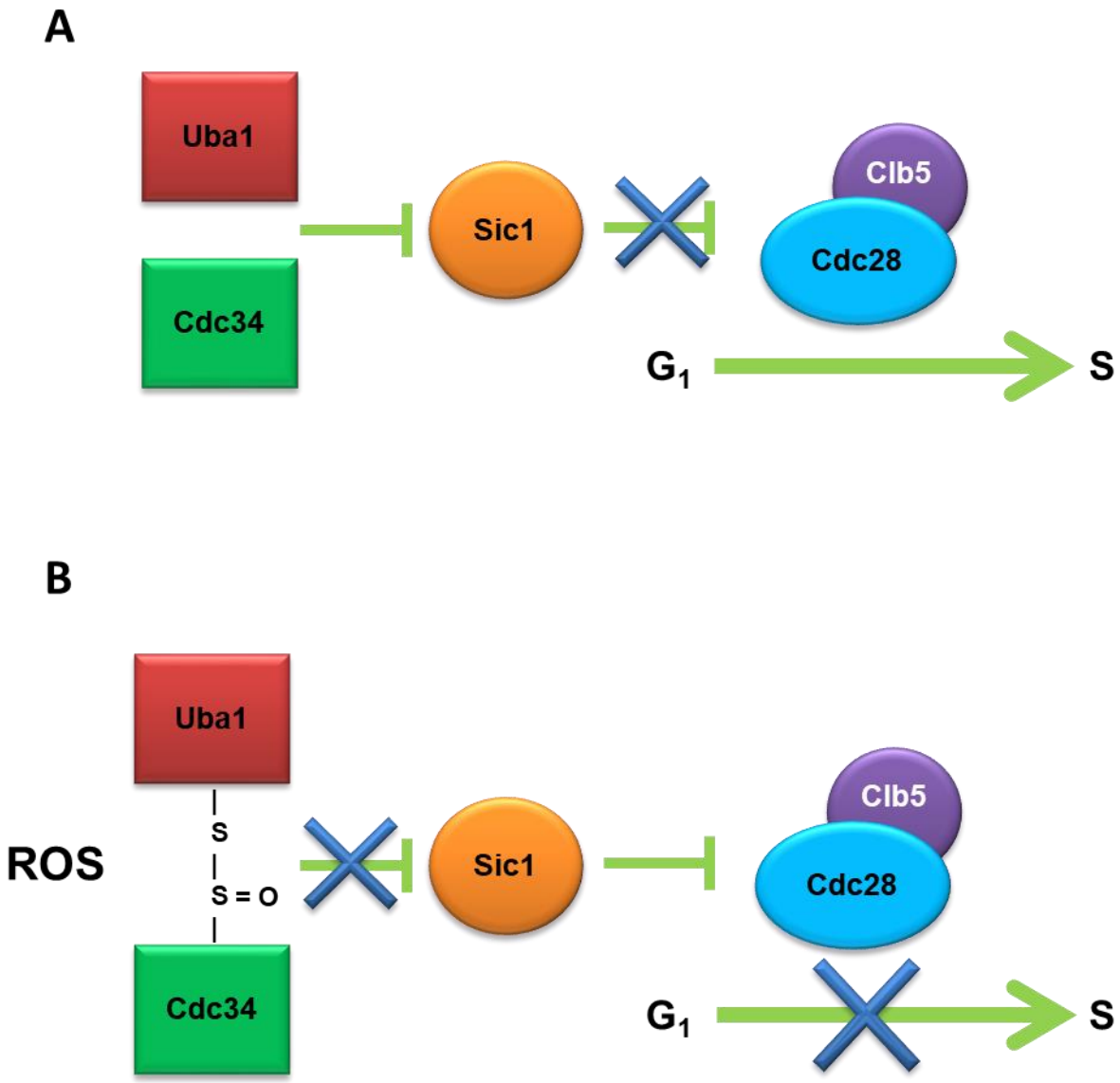


**Figure 1.10: Schematic for the regulation of cell cycle progression by oxidation of Cdc34-Uba1 in *S. cerevisiae*.** Under unstressed conditions Cdc34 and Uba1 ubiquitinate the CDK inhibitor Sic1, targeting it for degradation and allowing cell cycle progression. However after oxidation Cdc34 and Uba1 form a disulphide complex which subsequently inhibits ubiquitination of Sic1. Thus, Sic1 is not degraded by the proteasome and inhibits cell cycle progression from G1 to S phase by inhibiting the CDK complex Cdc20/Clb5.

initiation of this thesis work, a study into the regulation of the ubiquitin pathway by ROS in mammalian cells revealed that many mammalian dUbs were activated, or had enhanced activity, when incubated with the reducing agent DTT *in vitro*, suggesting that oxidation inhibits dUb activity (Lee *et al.*, 2013). Interestingly, it was also shown that different dUbs had different responses to $H_2O_2$, as many of the dUbs showed increased resistance to ROS. For example, while the mammalian USP19 was sensitive to inactivation by $H_2O_2$, USP1 and UCH-L1 were found to be comparatively more resistant to oxidation by $H_2O_2$ (Lee *et al.*, 2013). Further evidence for regulation of dUbs by ROS was identified recently, where authors identified that USP1 (which removes removing mono-ubiquitin signals from PCNA at K164) was reversibly inactivated by ROS (Cotto-Rios *et al.*, 2012). In this case USP1 is responsible for removing mono-ubiquitin signals from PCNA at K164. Ubiquitination of PCNA allows for TLS to occur after DNA damage response (Section 1.1.2). Inactivation of USP1 by oxidation allows stabilisation of PCNA by mono-ubiquitination thus allowing DNA replication to be maintained after 1 mM $H_2O_2$ stress (Cotto-Rios *et al.*, 2012). In the same study, the authors also describe the reversible oxidation of USP7 catalytic cysteine resulted in a decrease in the deubiquitination of USP7 substrates. Thus suggesting that oxidation inhibited USP7 function (Cotto-Rios *et al.*, 2012). It was also shown that certain OTU dUbs are susceptible to reversible oxidation at the catalytic cysteine by $H_2O_2$ in order to regulate their catalytic activity (Kulathu *et al.*, 2013). Importantly, it was identified that certain OTU enzymes were more susceptible to oxidation than others, for example the mammalian OTU dUb Cezanne was much more sensitive to oxidation than OTUD2 (Kulathu *et al.*, 2013). This study highlighted the importance of differential sensitivity of OTU dUbs to oxidative stress, however a cellular situation which was dependent on OTU oxidation was not defined (Kulathu *et al.*, 2013).

In conclusion, although dUbs have conserved domain regions, in particular the active site domains which contain the catalytic triad, dUbs do differ in the remaining regulatory regions. It has also been observed in mammalian cells that different dUbs appear to be more readily oxidised than others. It is also interesting that specific dUbs have also been observed to be oxidised differently depending on the concentration of oxidising agent. As such the differential

sensitivity of dUbs may be a key mechanism by which specific cellular outcomes are regulated.

## 1.4. Aims and objectives

Ubiquitination is a post-translational modification that is present in almost all cellular pathways. Ubiquitination has historically been associated with targeting substrates to the proteasome for degradation, however recently other signalling roles have been identified. Ubiquitin is removed from substrates by dUbs. dUbs are highly conserved in eukaryotes and cleave ubiquitin from proteins using an active site catalytic cysteine. This removal of ubiquitin from substrates recycles ubiquitin for further use, but importantly adds another level of control to the cycle, and of the function/activity of ubiquitinated substrates. The use of a catalytic cysteine for ubiquitin cleavage by dUbs, suggests that dUbs have the potential to be oxidised by ROS, as seen in other ubiquitin/ ubiquitin like pathway enzymes in order to regulate their activity. Thus, the aim of this thesis was to use the model organism *S. cerevisiae* to explore the potential functions and regulation of dUbs in response to oxidative stress.

Specific objectives were:

1. To investigate the relative requirements and modifications of dUbs in response to different oxidising agents.

2. To investigate the potential roles and regulation of the dUb, Ubp12, in oxidative stress responses.

3. To investigate the potential roles and regulation of the dUb, Ubp15, in oxidative stress responses and cell cycle regulation.

# Chapter Two: Materials and Methods

## 2.1. Yeast strains

The *S. cerevisiae* strains used in this study are derived from W303 (*ade2-1*, *can1-100*, *his3-11,15*, *leu2-3,112*, *trp1-1*, *ura3-1*), BY4741 (*his3Δ1*, *leu2Δ0*, *met15Δ0*, *ura3Δ0*), or BY4742 (*his3Δ1*, *leu2Δ0, ura3Δ0,* lys2Δ0).

All strains used in this study are listed in Table 2.1.

## 2.2. Yeast techniques

### *2.1.1 Growth conditions*

Strains were grown in either rich YPD complete media (1% w/v Bacto-yeast extract, 2% w/v Bacto-peptone, 2% w/v glucose, +/- 2% w/v agar), or SD minimal media (0.67% w/v Bacto-yeast nitrogen base without amino acids, 2% w/v glucose, +/- 2% w/v agar). For selective growth, SD was supplemented with adenine sulphate (20 mg/L, L-histidine hydrochloride (10 mg/L), L-leucine (20 mg/L), L-tryptophan (10 mg/L), uracil (8 mg/L), L-methionine (10 mg/L), and L-lysine hydromonochloride (30 mg/L) as required (all supplied by Sigma). G418 antibiotic (Formedium) was supplemented in YPD at 400 µg/ml. Strains were grown at 30 °C unless otherwise stated.

### *2.1.2 Transformation*

DNA was introduced into *S. cerevisiae* using a protocol based on the high efficiency lithium acetate method (Schiestl and Gietz, 1989). 50 ml of mid-log phase growing cells were pelleted (2000 rpm, 3 minutes), washed with 50 ml sterile water, and pelleted again. Cells were resuspended in 1 ml LiAc/TE (0.1 M LiAc/ 10 mM Tris-HCl pH 7.4, 1 mM EDTA pH8). 200 µl cells were added to 5 µg of salmon sperm DNA (Ambion), and 0.1 - 10 µg transforming DNA. 1.2 ml of LiAc/TE/PEG solution (0.1 M LiAc/ 10 mM Tris-HCl pH 7.4, 1 mM EDTA pH8/

| Strain ID | Genotype | Reference |
|---|---|---|
| FCC1 * | *MATa ade2-1 can1-100 his3-11,15 leu2-3,112 trp1-1 ura3-1* | Lab Stock |
| FCC2 * | *MATα ade2-1 can1-100 his3-11,15 leu2-3,112 trp1-1 ura3-1* | Lab Stock |
| FCC10 * | *MATa ade2-1 can1-100,15 his3-11 leu2-3,112 trp1-1 ura3-1 ubp12::HIS3* | This study |
| FCC23 # | *MATa his3Δ1 leu2Δ0 met15Δ0 ura3Δ0* | Lab Stock |
| FCC60 * | *MATa ade2-1 can1-100,15 his3-11 leu2-3,112 trp1-1 ura3-1 ubp15::HIS3* | This study |
| FCC63 # | *MATα his3Δ1 leu2Δ0 lys2Δ0 ura3Δ0* | Lab Stock |
| FCC70 # | *leu2Δ0/leu2Δ0 his3Δ1/his3Δ1 ura3Δ0/ura3Δ0 met15Δ0/MET15 lys2Δ0/LYS2 UBP12/UBP12-TAP:HIS3* | This study |
| FCC73 # | *MATa his3Δ1 leu2Δ0 met15Δ0 ura3Δ0 ubp2::KanMX* | Newcastle University High throughput service |
| FCC74 # | *MATa his3Δ1 leu2Δ0 met15Δ0 ura3Δ0 ubp3::KanMX* | Newcastle University High throughput service |
| FCC75 # | *MATa his3Δ1 leu2Δ0 met15Δ0 ura3Δ0 ubp12::KanMX* | Newcastle University High throughput service |
| FCC80 * | *MATa ade2-1 can1-100 his3-11,15 leu2-3,112 trp1-1 ura3-1 FZO1-3HA:HIS3* | This study |
| FCC93 * | *MATa ade2-1 can1-100 his3-11,15 leu2-3,112 trp1-1 ura3-1 UBP12-3HA:KanMX* | This study |
| FCC96 # | *MATa his3Δ1 leu2Δ0 met15Δ0 ura3Δ0 ubp1::KanMX* | Newcastle University High throughput service |
| FCC97 # | *MATa his3Δ1 leu2Δ0 met15Δ0 ura3Δ0 ubp5::KanMX* | Newcastle University High throughput service |
| FCC98 # | *MATa his3Δ1 leu2Δ0 met15Δ0 ura3Δ0 ubp6::KanMX* | Newcastle University High throughput service |
| FCC99 # | *MATa his3Δ1 leu2Δ0 met15Δ0 ura3Δ0 ubp7::KanMX* | Newcastle University High throughput service |
| FCC100 # | *MATa his3Δ1 leu2Δ0 met15Δ0 ura3Δ0 ubp8::KanMX* | Newcastle University High throughput service |

| | | |
|---|---|---|
| FCC101 # | *MATa his3Δ1 leu2Δ0 met15Δ0 ura3Δ0 ubp9::KanMX* | Newcastle University High throughput service |
| FCC102 # | *MATa his3Δ1 leu2Δ0 met15Δ0 ura3Δ0 ubp10::KanMX* | Newcastle University High throughput service |
| FCC103 # | *MATa his3Δ1 leu2Δ0 met15Δ0 ura3Δ0 ubp11::KanMX* | Newcastle University High throughput service |
| FCC104 # | *MATa his3Δ1 leu2Δ0 met15Δ0 ura3Δ0 ubp13::KanMX* | Newcastle University High throughput service |
| FCC106 # | *MATa his3Δ1 leu2Δ0 met15Δ0 ura3Δ0 ubp15::KanMX* | Newcastle University High throughput service |
| FCC107 # | *MATa his3Δ1 leu2Δ0 met15Δ0 ura3Δ0 ubp16::KanMX* | Newcastle University High throughput service |
| FCC108 # | *MATa his3Δ1 leu2Δ0 met15Δ0 ura3Δ0 otu1::KanMX* | Newcastle University High throughput service |
| FCC109 # | *MATa his3Δ1 leu2Δ0 met15Δ0 ura3Δ0 otu2::KanMX* | Newcastle University High throughput service |
| FCC110 # | *MATa his3Δ1 leu2Δ0 met15Δ0 ura3Δ0 yuh1::KanMX* | Newcastle University High throughput service |
| FCC123 # | *MATa his3Δ1 leu2Δ0 met15Δ0 ura3Δ0 OTU1-TAP:HIS3* | (Ghaemmaghami *et al.*, 2003b) |
| FCC124 # | *MATa his3Δ1 leu2Δ0 met15Δ0 ura3Δ0 OTU2-TAP:HIS3* | (Ghaemmaghami *et al.*, 2003b) |
| FCC125 # | *MATa his3Δ1 leu2Δ0 met15Δ0 ura3Δ0 RPN11-TAP:HIS3* | (Ghaemmaghami *et al.*, 2003b) |
| FCC130 * | *MATa ade2-1 can1-100,15 his3-11 leu2-3,112 trp1-1 ura3-1 UBP15-3HA:HIS3* | (Ghaemmaghami *et al.*, 2003b) |
| FCC135 # | *MATa his3Δ1 leu2Δ0 met15Δ0 ura3Δ0 CEX1-TAP:HIS3* | (Ghaemmaghami *et al.*, 2003b) |
| FCC145 * | *MATa leu2Δ0 met15Δ0 ura3Δ0 CDC34-TAP:HIS3* | (Ghaemmaghami *et al.*, 2003b) |
| FCC146 # | *MATa his3Δ1 leu2Δ0 met15Δ0 ura3Δ0 HIS4-TAP:HIS3* | (Ghaemmaghami *et al.*, 2003b) |
| FCC147 # | *MATa his3Δ1 leu2Δ0 met15Δ0 ura3Δ0 CDC19-TAP:HIS3* | (Ghaemmaghami *et al.*, 2003b) |
| FCC148 # | *MATa his3Δ1 leu2Δ0 met15Δ0 ura3Δ0 PDC1-TAP:HIS3* | (Ghaemmaghami *et al.*, 2003b) |

| | | |
|---|---|---|
| FCC149 # | *MATa his3Δ1 leu2Δ0 met15Δ0 ura3Δ0 TEF2-TAP:HIS3* | (Ghaemmaghami *et al.*, 2003b) |
| FCC150 # | *MATa his3Δ1 leu2Δ0 met15Δ0 ura3Δ0 ACO1-TAP:HIS3* | (Ghaemmaghami *et al.*, 2003b) |
| FCC151 # | *MATa his3Δ1 leu2Δ0 met15Δ0 ura3Δ0 TOM1-TAP:HIS3* | (Ghaemmaghami *et al.*, 2003b) |
| FCC152 # | *MATa his3Δ1 leu2Δ0 met15Δ0 ura3Δ0 MDN1-TAP:HIS3* | (Ghaemmaghami *et al.*, 2003b) |
| FCC154 # | *MATa his3Δ1 leu2Δ0 met15Δ0 ura3Δ0 UBP12-6HA:HIS3* | (Gödderz *et al.*, 2017) |
| FCC156 * | *MATa ade2-1 can1-100 his3-11,15 leu2-3,112 trp1-1 ura3-1 CDC34-13Myc:KanMX* | Lab Stock |
| FCC157 * | *MATα ade2-1 can1-100 his3-11,15 leu2-3,112 trp1-1 ura3-1 CDC34-13Myc:KanMX* | Lab Stock |
| FCC158 # | *MATa his3Δ1 leu2Δ0 met15Δ0 ura3Δ0 UBP12-TAP:HIS3, UBP12-3HA:KanMX* | This study |
| FCC161 | *MAT? ade2-1 can1-100,15 his3-11 leu2-3,112 trp1-1 ura3-1 ubp15::HIS3, CDC34-13Myc:KanMX* | This study |
| FCC162 FCC163 * | *MAT? ade2-1 can1-100,15 leu2-3,112 trp1-1 ura3-1 trr1::HIS3, UBP15-3HA:HIS3* | This study |
| FCC167 * | *MATa ade2-1 can1-100 his3-11,15 leu2-3,112 trp1-1 ura3-1 trr1::HIS3* | Lab Stock |
| FCC171 FCC172 FCC175 * | *MATa ade2-1 can1-100 his3-11,15 leu2-3,112 trp1-1 ura3-1 trr1::HIS3, UBP12-3HA:KanMX* | This study |
| FCC176 # | *MATa leu2Δ0 met15Δ0 ura3Δ0 PUF3-TAP:HIS3* | (Ghaemmaghami *et al.*, 2003b) |
| FCC178 # | *MATa his3Δ1leu2Δ0 met15Δ0 ura3Δ0 GCN5-TAP:HIS3* | (Ghaemmaghami *et al.*, 2003b) |
| FCC179 # | *MATa his3Δ1leu2Δ0 met15Δ0 ura3Δ0 FKH1-TAP:HIS3* | (Ghaemmaghami *et al.*, 2003b) |
| ELR28 # | *MATa his3Δ1 leu2Δ0 met15Δ0 ura3Δ0 UBP1-TAP:HIS3* | (Ghaemmaghami *et al.*, 2003b) |
| ELR29 # | *MATa his3Δ1 leu2Δ0 met15Δ0 ura3Δ0 UBP2-TAP:HIS3* | (Ghaemmaghami *et al.*, 2003b) |
| ELR30 # | *MATa his3Δ1 leu2Δ0 met15Δ0 ura3Δ0 UBP3-TAP:HIS3* | (Ghaemmaghami *et al.*, 2003b) |
| ELR31 # | *MATa his3Δ1 leu2Δ0 met15Δ0 ura3Δ0 UBP4-TAP:HIS3* | (Ghaemmaghami *et al.*, 2003b) |
| ELR32 # | *MATa his3Δ1 leu2Δ0 met15Δ0 ura3Δ0 UBP5-* | (Ghaemmaghami |

| | | |
|---|---|---|
| | *TAP:HIS3* | *et al.*, 2003b) |
| ELR33 # | *MATa his3Δ1 leu2Δ0 met15Δ0 ura3Δ0 UBP6-TAP:HIS3* | (Ghaemmaghami *et al.*, 2003b) |
| ELR34 # | *MATa his3Δ1 leu2Δ0 met15Δ0 ura3Δ0 UBP8-TAP:HIS3* | (Ghaemmaghami *et al.*, 2003b) |
| ELR35 # | *MATa his3Δ1 leu2Δ0 met15Δ0 ura3Δ0 UBP9-TAP:HIS3* | (Ghaemmaghami *et al.*, 2003b) |
| ELR36 # | *MATa his3Δ1leu2Δ0 met15Δ0 ura3Δ0 UBP10-TAP:HIS3* | (Ghaemmaghami *et al.*, 2003b) |
| ELR37 # | *MATa his3Δ1 leu2Δ0 met15Δ0 ura3Δ0 UBP11-TAP:HIS3* | (Ghaemmaghami *et al.*, 2003b) |
| ELR38 # | *MATa his3Δ1 leu2Δ0 met15Δ0 ura3Δ0 UBP12-TAP:HIS3* | (Ghaemmaghami *et al.*, 2003b) |
| ELR39 # | *MATa his3Δ1 leu2Δ0 met15Δ0 ura3Δ0 UBP13-TAP:HIS3* | (Ghaemmaghami *et al.*, 2003b) |
| ELR40 # | *MATa his3Δ1 leu2Δ0 met15Δ0 ura3Δ0 UBP14-TAP:HIS3* | (Ghaemmaghami *et al.*, 2003b) |
| ELR41 # | *MATa his3Δ1 leu2Δ0 met15Δ0 ura3Δ0 UBP15-TAP:HIS3* | (Ghaemmaghami *et al.*, 2003b) |
| ELR42 # | *MATa his3Δ1 leu2Δ0 met15Δ0 ura3Δ0 UBP16-TAP:HIS3* | (Ghaemmaghami *et al.*, 2003b) |

**Table 2.1: Yeast strains used in this study.** Strains with * are in the W303 strain background, and strains with # are in the BY strain background. Where mating type is unknown it is shown as *MAT?*.

40% w/v PEG-4000) were added and gently mixed, before incubation at 30 °C with agitation for 30 minutes, followed by a heatshock at 42 °C for 15 minutes. Cells were pelleted (8000 rpm, 1 minute), resuspended in 150 µl n$H_2O$ and plated onto appropriate selective media. Plates were incubated for 3-5 days at 30 °C to allow for growth of transformants. For G418 selection of KanMX strains, the transformation mixture was spread onto a YPD plate and grown for 2 days at 30 °C. The resulting lawns were replica plated using a wooden block and Wattman filter paper onto YPD plates supplemented with G418, and incubated for a further 3 days at 30 °C to allow for growth of colonies.

### *2.1.3 Strain construction*

#### *2.1.3.1 Gene deletion*

Genes were substituted with a selectable marker in the genome of *S. cerevisiae* using the one-step homologous recombination method previously described (Rothstein, 1991) (Figure 2.1). The specific gene was replaced in *S. cerevisiae* using the appropriate forward and reverse deletion oligonucleotide primers (Table 2.2), and YDp-H plasmid (Table 2.3) as a template (Berben *et al.*, 1991). The forward primer contains 90 nucleotides homologous to the region located directly upstream of the ATG of the target gene, and 20 nucleotides homologous to the region directly upstream to the 5' end of the selectable marker gene in the YDp-H plasmid. The reverse primer contains 90 nucleotides homologous to the DNA sequence located directly downstream of the stop codon of the target gene to be deleted and 20 nucleotides homologous to the 3' end of the selectable marker gene. PCR fragments were then transformed into the relevant strain and successful transformants were selected by growth of colonies on media lacking histidine. Gene replacement was verified using the respective check forward and reverse primers (Check primer F and Check primer R) flanking the region of interest.

Where strains were obtained from the deletion collection library (Newcastle University High throughput service) correct deletion of the gene from the chromosome was verified using a specific forward primer to the gene of interest and a reverse primer located in the kanamycin selectable marker (Kan909R).

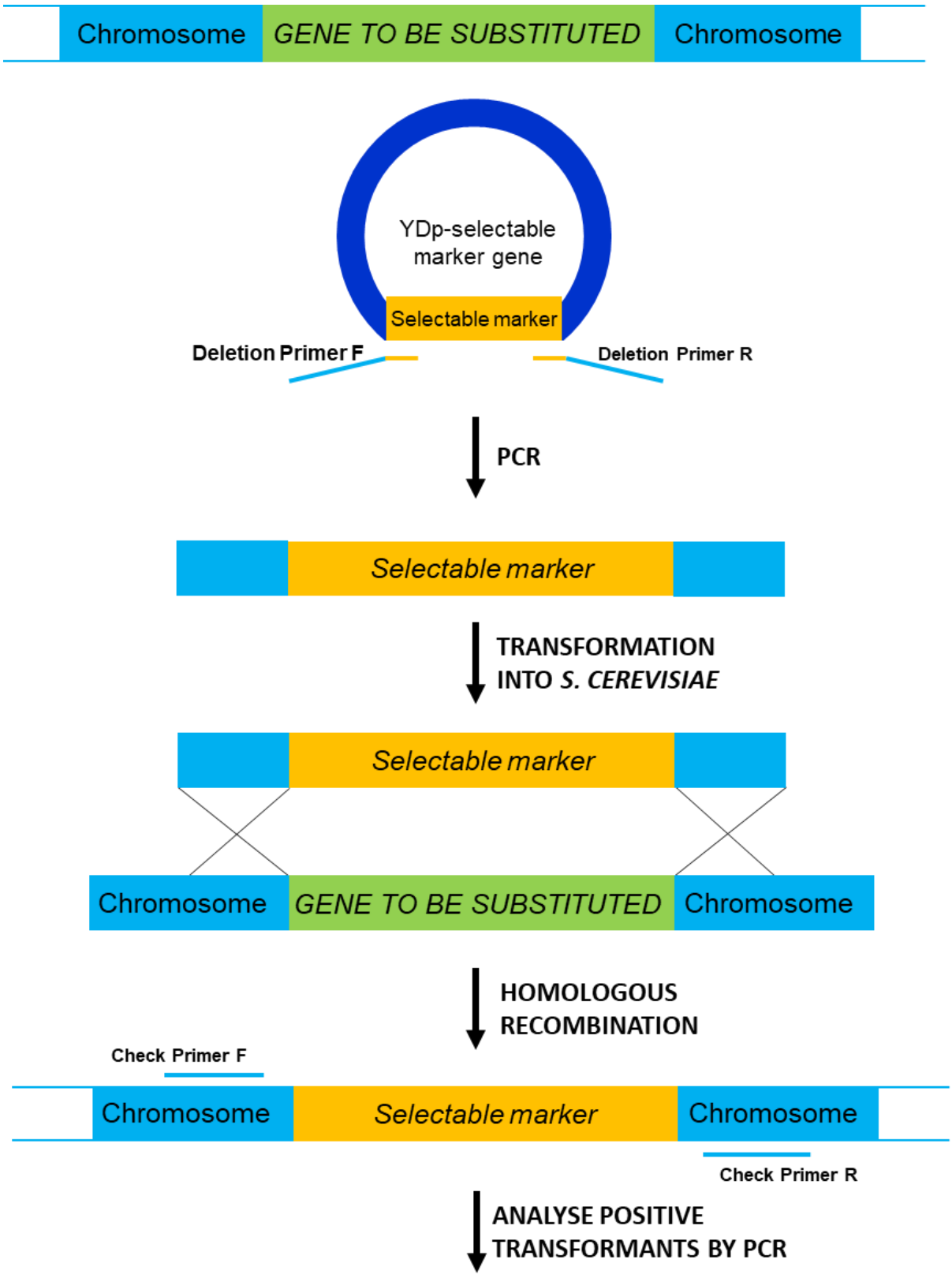
Chromosome
GENE TO BE SUBSTITUTED
Chromosome
YDp-selectable marker gene
Selectable marker
Deletion Primer F
Deletion Primer R
PCR
Selectable marker
TRANSFORMATION INTO S. CEREVISIAE
Selectable marker
Chromosome
GENE TO BE SUBSTITUTED
Chromosome
HOMOLOGOUS RECOMBINATION
Check Primer F
Chromosome
Selectable marker
Chromosome
Check Primer R
ANALYSE POSITIVE TRANSFORMANTS BY PCR

**Figure 2.1: Schematic diagram of gene deletion in *S. cerevisiae*.** Deletion Primer F contains 90 base pairs homologous to the chromosome sequence directly upstream of the start codon of the gene to be deleted and 20 base pairs homologous to the 5' end of the selectable marker gene in the YDp plasmid. Deletion Primer R contains 90 base pairs homologous to the chromosome sequence directly downstream of the stop codon of the gene to be deleted and 20 base pairs homologous to the 3' end of the selectable marker gene in the YDp plasmid. PCR using deletion Primer F and deletion Primer R and the YDp plasmid containing the selectable marker gene as a template generates a PCR fragment of the selectable marker and 90 base pairs homologous to the chromosome on either side of the gene. The cassette is transformed into wild type *S. cerevisiae* and homologous recombination results in the substitution of the gene to be deleted with the selectable marker gene onto the chromosome. Transformants were plated onto minimal media to select for the presence of the marker. Successful deletion was then verified by a check PCR using check Primer F and check Primer R which bind further upstream and downstream of the gene that has been deleted.

| ***Primer Name*** | ***Sequence 5' → 3'*** |
|---|---|
| *ubp1ChkDelF* | CACATTCAAAGAATAGAAGC |
| *ubp1ChkTagF* | GAAGGATGATTTGGAAGCTATTCAG |
| *ubp2ChkDelF* | GTTCATAGTCTAAGGGTG |
| *ubp2ChkTagF* | ACTATTGGATATATATCAAGG |
| *ubp2ChkTagR* | TTACGCAACCTATCTAC |
| *ubp3ChkDelF* | GTATATAGGTGAACGGTAATAAG |
| *ubp3TagChkF2* | CATTGAAAAACAACACCTC |
| *ubp3TagChkR2* | GAAATAATTGGTTTCGTGG |
| *ubp4ChkTagF* | GTATGGTGGTCATTATACAGCC |
| *ubp5ChkDelF* | CTTCAACACATCAAGTAAAC |
| *ubp5ChkTagF* | CATGAAGCTATTGTTAATGAGGAC |
| *ubp6ChkDelF* | CTGCAAGTAATTGGTGC |
| *ubp6ChkTagF* | GATCGGTGTCATTACACATCAAG |
| *ubp7ChkDelF* | CGCTAGGAAATAGGTAC |
| *ubp7ChkTagF* | GGAGTGGTTAACCATACAGG |
| *ubp8ChkDelF* | CAACTGGCTGTCATAATTTTG |
| *ubp8ChkTagF* | GAAAATGGCAAGGTTCCAG |
| *ubp9ChkDelF* | GCTTGAACAAGCTTGAATG |
| *ubp9ChkTagF* | GGTTAAGGGATCGTAAATTGAGG |
| *ubp10ChkTagF* | CTCCTATACACGAGGCTAAC |
| *ubp11ChkDelF* | GTTGATTATAAGCTCTGAAAG |
| *ubp11ChkTagF* | GAGCCATGAAATTGGACTG |
| *ubp12ChkDelF* | TATAATCAGGTATATTTCG |
| *ubp12ChkDelR* | TTGCTTCGTTTATGTAATT |
| *ubp12ChkTagF* | GACGAAGATGACAATG |
| *ubp12ChkTagR* | TTGCTTCGTTTATGTAATT |
| *ubp13ChkTagF* | CTAATCAAGTACGATGATTGGC |
| *ubp13TagChkF2* | GAATGATCGTGAAAATATGG |
| *ubp13TagChkR2* | CTTGCATGCCTAAATACTTC |
| *ubp14ChkDelF* | GATCAAATTTATCACTTGATG |
| *ubp14DelChkF2* | GATGAAATCACAGTGAAAAG |
| *ubp14DelChkR2* | CTCGATAGATTTGATCATAC |
| *ubp14ChkTagF* | GTAAACTAGTGGCAGACAAATG |
| *ubp15ChkDelF* | GGATTAATCAGTTACACAGG |
| *ubp15ChkDelR* | CTGCTCTATAGTTTGTGTTC |
| *ubp15ChkTagF2* | CTTCATGCAAAATTTGGTC |
| *ubp15ChkTagR2* | CCTTTTAGCTACGGGTC |
| *ubp16ChkDelF* | CAAAGTCCAGCTATAAAAC |
| *ubp16ChkTagF* | GCACCAGTTGTCAACAATG |
| *otu1ChkDelF* | GGTAGTAACTAATAGTAAAGG |
| *otu1ChkTagF* | CTGGCCTCAAATTTGAAGC |

| | |
|---|---|
| *otu2ChkDelF* | GTATTATTATGCGTCGCG |
| *otu2ChkTagF* | GATTTTGGCTCTCTCTCACG |
| *yuh1ChkDelF* | GTCGACTATAAAGGTGGAAG |
| *rpn11DelChkF2* | CAAATTCACAAGAAAAGCC |
| *rpn11DelChkR2* | CTACCAGTAGCCATTTC |
| *rpn11ChkTagF* | GAGTATGGTTAAGATAGCCGAAC |
| *TapTagChkR* | AACCCGGGGATCCGTCGACC |
| *kan909R* | ATCACGCTAACATTTGATTAAAATAG |
| *ubp12TagF2* | AAGTCGCTGATTTGAATTTAAAAAATGGTGTGACACTAGAA TCGCCAGAACGGATCCCCGGGTTAATTAA |
| *ubp12TagR2* | TTATACATGTGGAAATTTATTAATTTTATCTATCATATAAAC TCATGTCAGAATTCGAGCTCGTTTAAAC |
| *ubp15DelF* | CCCTACGTTTTGCCCCTTTGATCAAACTATCAGTTAAGATA TTAATTTTTTTGAGAAAACGATTCTTTGATTAGTCTCTTCAA ACAAACAGAATTCCCGGGGATCCGGTG |
| *ubp15DelR* | GTGTGGAAGTGATGGCGGCTGAGAGATTATCATAAAAAAA CATAAAAAAAATGGAGAAAACATCAAAGCTAAACATAGTC GTAAGACGTAAAGCTAGCTTGGCTGCAGGT |
| *ubp15TagSF* | ATAGATTGAGATCGCATTCTTCCTATGATAGACCAATGATC ATTAAAAACCGGATCCCCGGGTTAATTAA |
| *ubp15TagSR* | CATAAAAAAAATGGAGAAAACATCAAAGCTAAACATAGTC GTAAGACGTAGAATTCGAGCTCGTTTAAAC |
| *ubp12DelF* | TGAAGATAAAAGATGGGATTACTGGAAAAATAAAGGGAGG AAAATCCTGCAGAACGTTGTTGTTTCAATCGAAGGTTTCTT CATTCGAAAGAATTCCCGGGGATCCGGTG |
| *ubp12DelR* | GCCTAGGCAGTAAATAGTAGGCGAAAAAGATTGAAAAGTA TTATACATGTGGAAATTTATTAATTTTATCTATCATATAAAC TCATGTCAAAGCTAGCTTGGCTGCAGGT |
| *trr1DelChkF* | GCTTGTAGATTAATTTCTG |
| *trr1DelChkR* | GTATTGGCTTTCTCTAATAATG |
| *Cex1ChkTagF* | GCTTTCTATCAAGAAGAAG |
| *Cex1ChkTagR* | GATGACTCTTCTTGCTTATG |
| *His4ChkTagF* | CTAACCATACATTACCAAC |
| *Cdc19ChkTagF* | CCAATCATCTTGGTTACC |
| *Pdc1ChkTagF* | CTTGAAGCCATACTTGTTC |
| *Tef2ChkTagF* | CCAAAGTTCTTGAAGTCC |
| *Aco1ChkTagF* | CTGACTATGACAAGATCAAC |
| *Tom1ChkTagF* | CTTATGTTAATTACACCGC |
| *Mdn1ChkTagF* | CGAAGACCATGAAACAATAC |
| *Ubp12F1* | GGGCCCCCCCTCGAGGTCGACGGTATCGATAGAGATACG TCTACGATAGCATGTAAC |
| *Ubp12R1* | AAACCAGTAGTACCTGATGCTGGTTCGAGTTTATTATAAG |
| *Ubp12F2* | GAACCAGCATCAGGTACTACTGGTTTGGTCAATTTG |

| | |
|---|---|
| *Ubp12R2* | TCTGGCTCTGTACTTGCATCTTCTTCAACATC |
| *Ubp12F3* | GAAGAAGATGCAAGTACAGAGCCAGAATTAACAGATAAG |
| *Ubp12R3* | CCCGGGCTGCAGGAATTCGATATCACCAGTCCTTCTGTTT TGTTTTTTTC |
| *Ubp12CCR1* | AGAATTCATGTAAGATGTATTTCCCAAATTGACC |
| *Ubp12CCF2* | TGGGAAATACATCTTACATGAATTCTGCGTTG |
| *Ubp12ccTagR3* | TTCTGGCGATTCTAGTGTCACACCATTTTTTAAATTC |
| *HA-Prs316 TagR* | CCCGGGCTGCAGGAATTCGATATCAAGATCTATATTACCC TGTTATCCCTA |
| *Ubp15F1* | GGGCCCCCCCTCGAGGTCGACGGTATCGATATGTGTATT ACGATATAGTTAATAGTTGATAG |
| *Ubp15R1* | TTAATATCCTATTCAATTCCTGCACATCGTG |
| *Ubp15F2* | TGTGCAGGAATTGAATAGGATATTAATGGACAGGC |
| *Ubp15R2* | TCATATATATTTCATTTATGGTACCAGGTTGG |
| *Ubp15F3* | TGGTACCATAAATGAAATATATATGAAGGAGACAATATATG |
| *Ubp15R3* | CCCGGGCTGCAGGAATTCGATATCAACCACTGAAACTTCA TTTACTTTATG |
| *Ubp15CCR1* | CGAATTCAAATAAGATGTGGAACCCTGATTTCGG |
| *Ubp15CCF2* | CAGGGTGCCACATCTTATTTGAATTCGTTATTGC |
| *Ubp15ccTagR3* | GTTTTTAATGATCATTGGTCTATCATAGGAAGAATG |
| *M13F* | GTAAAACGACGGCCAGTG |
| *M13R* | CAGGAAACAGCTATGACC |
| *fkh1ChkTagF* | GAGAAATACCTGCTCCTG |
| *fkh1ChkTagR* | CTGGCGGTTTCCTTAATC |
| *puf3ChkTagF* | CAAGGATCAATTTGCCAAC |
| *Puf3ChkTagR* | GCAGAAAAATAGAGATGAGG |
| *gcn5ChkTagF* | CCGTTAATAAAGAGGAGGTC |
| *gcn5ChkTagR* | CAGAAAGTCCAGAAGAAGC |
| *emw1ChkTagF* | GATACAGTGGATGCTTGTG |
| *emw1ChkTagR* | CGAGGTGATAAAGAAAAGGC |
| *cdc34TagChkF* | GGTCCGTCATTTTACAAG |
| *cdc34TagChkR* | CCTGTCAATCTCAGATTATC |
| *fzo1TagF* | AACTTGTTGTCAATCAAATTCTTCCAATCTCTATACGAAGG AACCGTGGCTCAAAAATTGATGGTGGAAGAAATAAATTTA GACATCGATCGGATCCCCGGGTTAATTAA |
| *fzo1TagR* | GTGAAAAAAAAAATGGACCTGCTTGGAATAAAATAATAAGT AACATTATGTATATTGATTTGAAAAGACCTCATATATTTACA AGAATATGAATTCGAGCTCGTTTAAAC |
| *fzo1ChkTagF* | TGTTTTGCGTGTACCTAC |
| *fzo1ChkTagR* | TTGCTCATTTTTCGTTCCG |

**Table 2.2: DNA sequence of oligonucleotide primers used in this study.** All primers were supplied by Sigma Aldrich.

| ***Plasmid name*** | ***Comments*** | ***Reference*** |
|---|---|---|
| *YDP-H* | Deletion plasmid containing HIS3 disruption cassette | (Berben *et al.*, 1991) |
| *pFA6a-HIS3* | Epitope tagging plasmid containing HIS3 selectable marker | (Longtine *et al.*, 1998) |
| *pFA6a-KanMX6* | Epitope tagging plasmid containing Kanamycin resistance selectable marker | (Longtine *et al.*, 1998) |
| *pRS316* | Cen plasmid with URA3 marker | Lab stock |
| *pRS426* | 2 micron plasmid with URA3 marker | Lab stock |
| *pRS426-UBP12-3HA* | Ubp12-3HA epitope tag, 2 micron plasmid | This study |
| *pRS426-UBP12$^{C373S}$-3HA* | Ubp12-3HA epitope tag, C373S mutant, 2 micron plasmid | This study |
| *pRS426-UBP12* | Ubp12, 2 micron plasmid | This study |
| *pRS316-UBP15$^{C214S}$-3HA* | Ubp15-3HA epitope tag, C214S mutant, CEN plasmid | This study |
| *pRS426-UBP15* | Ubp15, 2 micron plasmid | This study |

**Table 2.3: Plasmids used in this study.**

*2.1.3.2 Gene tagging*

Chromosomal gene tagging was achieved by using the method described previously (Longtine et al., 1998) (Figure 2.2). Ubp12 and Ubp15 were epitope-tagged on the C-terminus by integration of a PCR-amplified cassette at the normal chromosomal locus for each gene, using the appropriate TagF and TagR primers (Table 2.2), with either the pFA6-3HA-KanMX6 or pFA6-3HA-HIS3 plasmid as a template (Table 2.3). The forward primer (TagF) contains 50 nucleotides homologous to the region located at the end of the 3' region of the gene, immediately upstream of but excluding the stop codon, and 20 nucleotides homologous to the 5' sequence of the plasmid used as the template for tagging. The reverse primer (TagR) contains 50 nucleotides homologous to the DNA sequence located directly after the stop codon of the gene to be epitope-tagged and 20 nucleotides homologous to the 3' sequence of the plasmid used as the template for tagging. PCR fragments were then transformed into the relevant strain and successful transformants were selected by growth on media lacking histidine or by kanamycin resistance. The integration of the PCR cassette encoding the epitope-tag at the correct chromosomal location was verified using the respective check forward and reverse primers (TagChkF and TagChkR) flanking the region of interest.

Where strains were obtained from the TAP tag library (Ghaemmaghami et al., 2003) (Newcastle University High throughput service) correct epitope tagging of the gene was verified using a specific forward primer to the gene of interest, and a reverse primer homologous to a sequence encoding the TAP epitope tag.

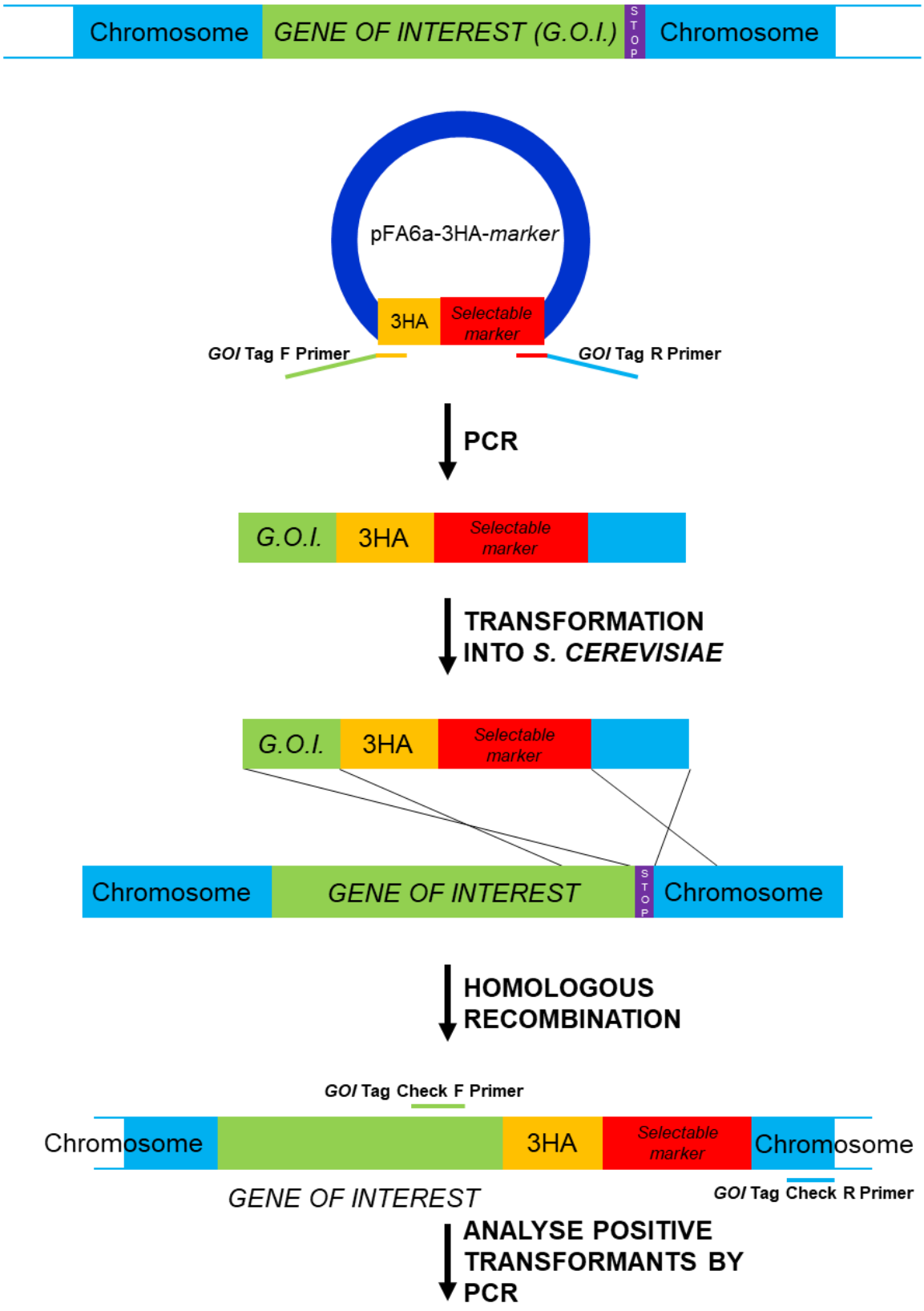
Chromosome
GENE OF INTEREST (G.O.I.)
STOP
Chromosome
pFA6a-3HA-marker
3HA
Selectable marker
GOI Tag F Primer
GOI Tag R Primer
PCR
G.O.I.
3HA
Selectable marker
TRANSFORMATION INTO S. CEREVISIAE
G.O.I.
3HA
Selectable marker
Chromosome
GENE OF INTEREST
STOP
Chromosome
HOMOLOGOUS RECOMBINATION
GOI Tag Check F Primer
Chromosome
3HA
Selectable marker
Chromosome
GENE OF INTEREST
GOI Tag Check R Primer
ANALYSE POSITIVE TRANSFORMANTS BY PCR

**Figure 2.2: Schematic diagram for epitope tagging genes at their normal chromosomal locus.** The gene of interest Tag F primer contains 50 base pairs homologous to the chromosome sequence directly upstream of the stop codon of the gene to be epitope tagged, and 20 base pairs homologous to the 5' end of the 3HA sequence in the pFA6a plasmid. The gene of interest Tag R primer contains 50 base pairs homologous to the chromosome sequence directly downstream of the stop codon of the gene to be epitope tagged, and 20 base pairs homologous to the 3' end of the selectable marker in the pFA6a plasmid. PCR with the TagF and TagR primers and the plasmid pFA6a-3HA-*marker* plasmid as a template generates a PCR fragment encoding the 3HA epitope tag with the selectable marker and 50 base pairs homologous to the chromosome on either side of the stop codon of the gene of interest. The cassette is transformed into wild type *S. cerevisiae* and homologous recombination results in the replacement of the stop codon with the sequence encoding the 3HA epitope tag in frame with the gene to be tagged. Transformants were plated onto minimal media to select for the presence of the marker. Successful epitope tagging was verified by a check PCR using GOI Tag Check F (TagChkF) and GOI Tag check R (TagChkR) Primers.

#### *2.1.3.3 Diploid and haploid strain construction*

Strains of opposite mating type were crossed on YPD agar and the resulting diploids were sporulated on sporulation media (1% w/v potassium acetate, 0.1% w/v yeast extract, 0.05% glucose) by incubation for 2 days at 30 °C. Cells were resuspended in 100 µl 5% v/v glusulase (PerkinElmer) and incubated at 30 °C for 30 minutes. The cell suspension was gently mixed with 900 µl water and 100 µl were pipetted onto a YPD plate. Tetrads containing four spores were then separated using a tetrad dissector (Singer instruments) and the plates incubated at 30 °C for 3 days.

### *2.1.4 Plasmid manipulations*

#### *2.1.4.1 Plasmid construction*

Plasmids were constructed using the *in vivo* recombination ability of *S. cerevisiae* described previously (Oldenburg *et al.*, 1997): Figure 2.3. Wild type DNA (FCC1) was used as a template for PCR reactions to construct fragments with over-lapping regions of the gene of interest; including 20 nucleotides homologous to the pRS426 plasmid (Table 2.3) either side of the *HindIII* restriction site. The forward primer for Fragment 1 (F1) (Table 2.2) was designed with 20 nucleotides homologous to the plasmid (at one side of the *HindIII* site) and 30 nucleotides homologous to the 5' end of the gene of interest. The internal primers (R1, F2, R2, and F3) were designed to have 20 nucleotides overlapping to produce three separate cassettes with internal overlapping regions. The reverse primer for fragment 3 (R3) was designed to have 30 nucleotides homologous to the 3' end of the gene of interest, and 20 nucleotides homologous to the plasmid (at the other side of the *HindIII* cut site). The linearised plasmid (cut at the *HindIII* site), and the three overlapping fragments produced by PCR using the primers described above, were co-transformed into the yeast using the LiAc method described previously (2.2.2) with a vector: insert ratio of 1:3. Transformants were plated onto selective media lacking uracil whereby growth of colonies suggests uptake of the uracil gene within the plasmid. Positive colonies were checked for the full recombined plasmid using the universal M13 primers (M13F and M13R, Table 2.2). Plasmids from colonies which were identified to be of the correct size

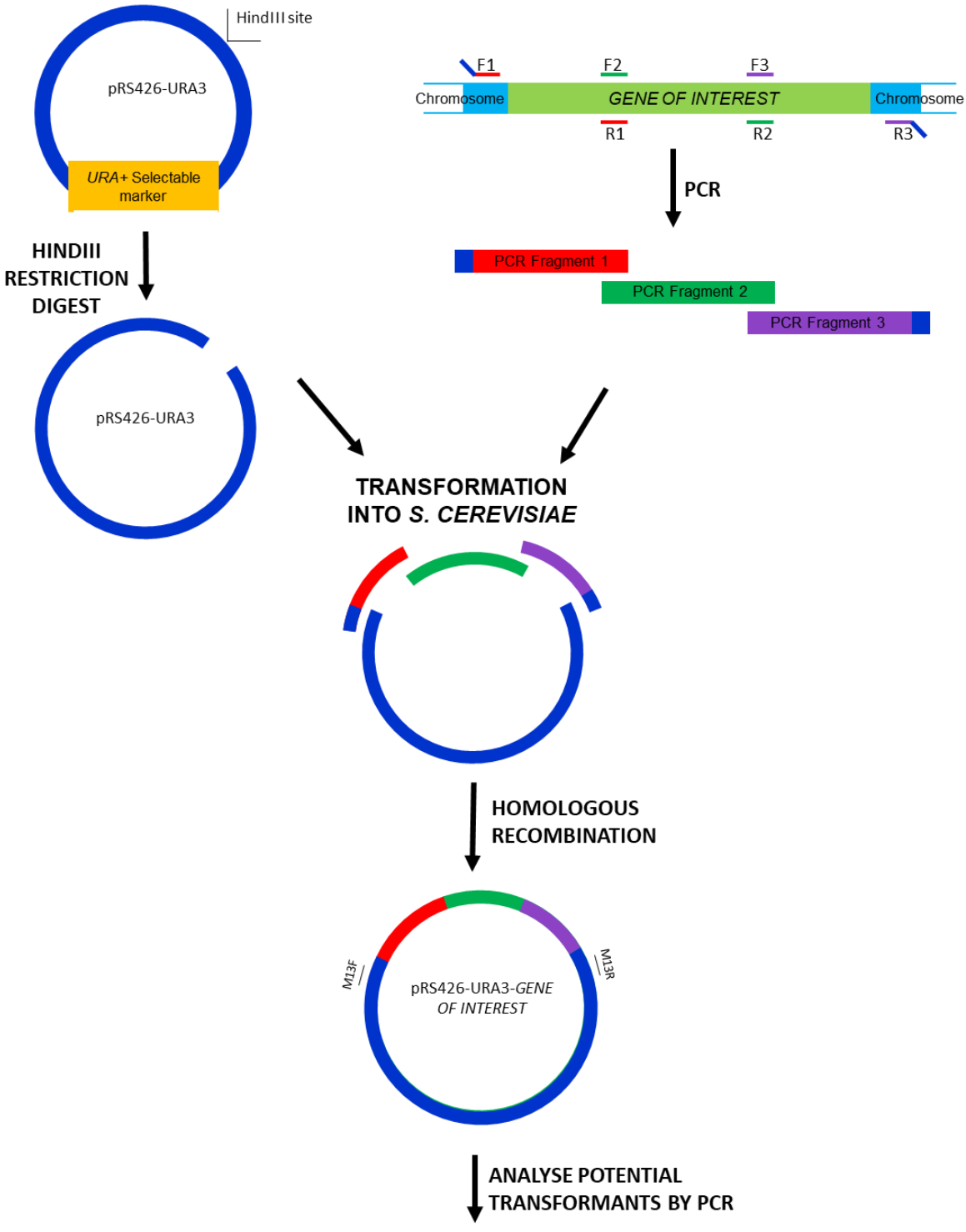
HindIII site
pRS426-URA3
URA+ Selectable marker
HINDIII RESTRICTION DIGEST
pRS426-URA3
F1
F2
F3
Chromosome
GENE OF INTEREST
Chromosome
R1
R2
R3
PCR
PCR Fragment 1
PCR Fragment 2
PCR Fragment 3
TRANSFORMATION INTO S. CEREVISIAE
HOMOLOGOUS RECOMBINATION
M13F
M13R
pRS426-URA3-GENE OF INTEREST
ANALYSE POTENTIAL TRANSFORMANTS BY PCR

**Figure 2.3: Schematic diagram for plasmid construction in the pRS426 plasmid.** The plasmid pRS426 was linearised with the restriction enzyme *HindIII* in the multiple cloning site. Three fragments with overlapping regions were produced using three sets of primers. Fragment 1 forward primer (F1) had 20 nucleotides homologous to the pRS426 plasmid directly before the *HindIII* cut site, and 30 nucleotides homologous to the 5' end of the gene of interest, and the reverse primer (R1) is situated ~1500 base pairs into the gene of interest. Fragment 2 is produced using a forward primer (F2) which binds in the same position as R1 to produce 20 base pairs homology between the fragments, and a reverse primer (R2) which binds to the gene of interest to produce a fragment of ~1500 base pairs. Fragment 3 is produced by a forward primer (F3) which binds at the same position as R2 to produce 20 base pairs homology between the fragments, and a reverse primer (R3) which has 30 nucleotides homologous to the 3' end of the gene of interest, and 20 nucleotides homologous to the pRS426 plasmid directly after the *HindIII* cut site. The fragments and the linearised plasmid were co-transformed into S. cerevisiae and homologous recombination of the overlapping regions of the DNA results in the construction of the pRS426 plasmid containing the gene of interest in the correct orientation. Cells containing the potential constructs were selected on minimal $ura^-$ media as $URA^+$ colonies. Colonies were tested for correct recombination using the universal M13 primers (M13F and M13R) located either side of the multiple cloning site. Plasmids of the correct size were extracted from S. cerevisiae (1.2.3.4) and transformed into E. coli. Plasmids were extracted from E.coli and sequenced to verify correct recombination.

using the check PCR were extracted (1.2.4.2) and transformed into *E.coli* (1.3.4). Plasmids were extracted from *E.coli* and sequenced to confirm proper construction of the plasmid.

#### *2.1.4.2 Plasmid recovery from yeast*

Plasmid recovery from yeast was adapted from the GenElute Plasmid Miniprep kit (SigmaAldrich). Cultures were grown overnight in appropriate media to select for the plasmid, and then pelleted by centrifugation (3000 rpm, 5 minutes). Cells were resuspended in 200 µl resuspension buffer (GenElute Plasmid Miniprep kit), and the cells lysed with glass beads using a Mini Beadbeater. The supernatant was collected, and 400 µl lysis buffer (GenElute Plasmid Miniprep kit) were added and incubated at room temperature for 5 minutes. 300 µl neutralisation buffer (GenElute Plasmid Miniprep kit) were added to the samples and gently mixed, before the samples were centrifuged at 13000 rpm for 10 minutes. The lysate was divided over two GenElute Spin Columns and the plasmid isolated and washed per the manufacturer's instructions. The plasmids were eluted in 75 µl elution buffer (GenElute Plasmid Miniprep kit), concentrated by ethanol precipitation, resuspended in 20 µl sterile $H_2O$, and then transformed into *E. coli* (1.3.4).

### *2.1.5 Stress sensitivity testing*

For stress sensitivity assays cells were grown to exponential phase and 5-fold serial dilutions were spotted using a 48 pin tool (Sigma) onto the indicated agar plates. Plates were incubated at 30 °C for 3 days unless otherwise indicated. For UV sensitivity cells were spotted onto plates and then treated with the appropriate UV dose by a Stratalinker, before being incubated in the dark at 30 °C for 3 days unless otherwise indicated.

### *2.1.6 Genomic DNA extraction*

DNA was extracted from cells using a protocol described previously (Hoffman and Winston, 1987). 10 ml of culture were grown overnight, pelleted by centrifugation (3000 rpm, 2 minutes), washed in 1 ml sterile $dH_2O$ and resuspended in 200 µl STET solution (2% w/v Triton X-100, 1% w/v SDS, 100

mM NaCl, 10 mM Tris-HCl pH8). 200 µl phenol/chloroform/isoamyl alcohol (25:24:1, pH8) were added and the cells lysed with glass beads using a Mini Beadbeater (Biospec Products). 200 µl TE solution were added to the samples, which were then pelleted by centrifugation (13000 rpm, 5 minutes). The upper aqueous phase was placed in a fresh Eppendorf tube with 1 ml 100% ethanol, and DNA was pelleted by centrifugation (13000 rpm, 2 minutes). The DNA pellet was resuspended in TE solution containing 75 µg/ml RNase (Sigma) and incubated at 37 °C for 5 minutes. 10 µl of 4 M ammonium sulphate and 1 ml 100% ethanol were added and the DNA precipitated (13000, 5 minutes). The DNA pellet was resuspended in 50 µl TE and stored at -20 °C.

### *2.1.7 Protein extraction*

For soluble protein extraction, 50 ml of mid-log phase growing cells were pelleted by centrifugation (3000 rpm, 3 minutes). The pellet was snap frozen in liquid nitrogen and kept at -80°C. The pellet was thawed at room temperature and resuspended in 150 µl protein lysis buffer (20 mM HEPES, 350 mM NaCl, 10% v/v glycerol, 0.1% v/v Tween-20) containing aprotinin (0.097 trypsin inhibitor units/ml aprotinin), 2 µg/ml leupeptin, pepstatin (2 µg/ml pepstatin A), and 105 µg/ml PMSF. Cells were lysed with 1 ml ice cold glass beads with a Mini Beadbeater (Biospec Products) and proteins were collected by centrifugation (13000 rpm, 10 minutes) at 4 °C. Protein concentrations were calculated using Bradford Assay (Pierce) following manufacturer's instructions.

When investigating protein oxidation, the TCA protein extraction method was used. 5 ml of mid-log phase cells were collected with 5 ml 20% (w/v) TCA, pelleted at 3000 rpm for 2 minutes, and the pellet frozen in liquid nitrogen. Pellets were thawed on ice and resuspended in 200 µl 10% (w/v) TCA before being lysed with ice-cold glass beads using a Mini Beadbeater (Biospec Products). After lysis, each pellet was centrifuged (13000 rpm, 15 minutes) and washed 3 times with 200 µl acetone. Pellets were solubilised with TCA buffer (100 mM Tris-HCl pH8, 1% w/v SDS, 1 mM EDTA) containing 5% (v/v) NEM and incubated at 25 °C for 30 minutes followed by 37 °C for 5 minutes. The protein concentration was calculated using the BCA protein assay kit (Thermo Scientific) following the manufacturer's instructions.

### *2.1.8 Western blotting*

Samples were prepared for analysis by adding 4 x sample buffer (0.5% w/v bromophenol blue, 10 % w/v SDS, 625 mM Tris-HCl pH 6.8, 50% v/v glycerol, +/- 10% v/v β-mercaptoethanol) and denaturing at 100 °C for 3 minutes. Proteins were separated on 6%, 8% or 15% SDS-polyacrylamide gels with a lane of PageRuler Prestained Protein Ladder (ThermoScientific) or HiMark™ Pre-stained Protein Standard (ThermoScientific) included allowing estimation of molecular weight. Separated proteins were transferred onto Protran® nitrocellulose membrane (Amersham) for 120 minutes at 400 mA, and blocked for non-specific binding by incubating in 10% w/v BSA in 1x TBST (1 mM Tris-HCl pH 8, 15 mM NaCl, 0.01% v/v Tween-20) for 30 minutes. The membrane was incubated at 4 °C overnight with agitation with the indicated primary antibody. Antibodies were diluted (dilutions shown in Table 2.3) in 5% (w/v) BSA in 1x TBST. The membrane was washed with 1x TBST (3x5 minutes) and then incubated for 1 hour at room temperature with the appropriate secondary antibody (anti-mouse HRP, or anti-rabbit HRP) diluted 1:2000 in 5x (w/v) BSA in 1x TBST. After washes (3 x 5 minutes) proteins were visualised with either ECL detection system (Amersham) onto film, or ECL plus Chemiluminescent kit (GE Healthcare) and scanned on a Typhoon FLA 9500 (GE Healthcare). Scanned images were quantified using ImageQuantTL software. To re-probe the nitrocellulose membrane with different antibodies, membranes were stripped by 30 minute incubation at 50 °C with stripping buffer (2% w/v SDS, 62.5 mM Tris-HCl pH 6.7, 100 mM β-mercaptoethanol). The membrane was washed 4x 10 minutes in 1x TBST before being blocked again in 10% BSA w/v in 1x TBST before reprobing.

| *Antibody Name* | *Dilution used in 5% w/v BSA* | *Supplier* | *Raised in* |
|---|---|---|---|
| *Peroxidase Anti-peroxidase* | 1:1000 | Sigma Aldrich (P1291) | Rabbit |
| *Anti-HA* | 1:1000 | Thermo Scientific (26183) | Mouse |
| *Anti-Myc* | 1:1000 | Sigma Aldrich | Mouse |
| *Anti-TAP* | 1:1000 | Thermo Scientific (CAB1001) | Rabbit |
| *Anti-tubulin* | 1:1000 | DSHB, University of Iowa | Mouse |
| *Anti-Ub (F-11)* | 1:1000 | SantaCruz Biotechnology (sc-271289) | Mouse |
| *Anti-Rabbit HRP* | 1:2000 | Sigma Aldrich | - |
| *Anti-Mouse HRP* | 1:2000 | Sigma Aldrich | - |

**Table 2.3: Antibodies used in this study.**

### *2.1.9 TAP purification*

500 ml cells were grown to mid-log phase and either incubated with or without 2 mM $H_2O_2$ for 10 minutes. Cells were pelleted (5000 rpm, 6 minutes), washed in ice cold PBS (137 mM NaCl, 2.7 mM KCl, 10 mM $Na_2HPO_4$, 1.8 mM $KH_2PO_4$, pH 7.4), before pelleting again (3000 rpm, 5 minutes) and snap freezing in liquid nitrogen. Pellets were stored at -80°C. Pellets were resuspended in ice cold TMN150 buffer (50 mM Tris-HCl pH 7.8, 150 mM NaCl, 1.5 mM $MgCl_2$, 0.1% v/v NP-40) containing aprotinin (0.097 trypsin inhibitor units/ml aprotinin), 2 µg/ml leupeptin, pepstatin (2 µg/ml pepstatin A), 105 µg/ml PMSF and 5% (v/v) NEM, and allowed to thaw. Cells were lysed with 3 ml ice cold glass beads by vortexing (1 minute, followed by 1 minute in ice, repeated 5 times). 4 ml ice cold TMN150 buffer were added to samples which were vortexed again for 10 seconds, followed by pelleting by centrifugation (4500 rpm, 28 minutes). The supernatants were transferred to fresh eppendorfs and samples were centrifuged again (13000 rpm, 26 minutes) to remove cell debris. The supernatant was collected, 1% sample was taken for direct analysis by western blotting (1.2.8), and the remaining lysate was snap frozen in liquid nitrogen and stored at -80 °C. 150 µl of IgG sepharose slurry (Sigma Aldrich) were washed twice with 1.5 ml ice cold TMN150 buffer, and incubated with lysates for 2 hours at 4 °C with rolling. The beads were collected by gently pelleting (1000 rpm, 30 seconds). 1% supernatant was taken for direct analysis by western blotting (1.2.8). Beads were washed 4 times with 10 ml ice cold TMN150. The beads were then resuspended in 50 µl TCA buffer (100 mM Tris-HCl pH8, 1% w/v SDS, 1 mM EDTA) containing 5% (v/v) NEM and boiled for 1 minute, mixed and boiled again for 1 minute. Samples were pelleted by centrifugation (2000 rpm, 1 minute) and lysates were stored at -20 °C. Proteins were precipitated by mixing the lysate with an equal volume of 20% (w/v) TCA and incubating on ice for 30 minutes. Precipitated proteins were pelleted by centrifugation (13000, 4 minutes, 4°C), washed with acetone, and resuspended in 20 µl TCA buffer with 5 % (v/v) NEM. Proteins were separated on a precast 4-15% Criterion™ Tris-HCl Protein Gel (BioRad), stained with InstantBlue™ Protein Stain (Expedeon), and excised for analysis.

### *2.1.10 DNA content analysis*

Approximately 5 x $10^6$ mid-log phase cells were pelleted by centrifugation (3000 rpm, 2 minutes), washed in 1 ml $H_2O$ and pelleted again. Cells were then fixed in 1 ml (v/v) 70% ethanol and stored at 4 °C. Cells were sonicated for 5 seconds and pelleted (13000 rpm, 1 minute). The pellet was washed with 800 µl 50 mM sodium citrate (pH 7.2), pelleted again, resuspended in 500 µl RNase A solution (50 mM sodium citrate pH 7.2, 0.25 mg/ml RNase A from Thermo Scientific) and incubated at 37 °C overnight. 50 µl of proteinase K (20 mg/ml from Ambion) were added and cells incubated for 1 hour at 50 °C. Cells were sonicated for 5 seconds and incubated with 500 µl Sytox Green solution (50 mM sodium citrate pH7.2, 4 µM Sytox Green from LifeTechnologies) for 1 hour in the dark at room temperature. DNA content analysis was performed using a FACSCanto™ II flow cytometer (BD Life Sciences) and DIVA software (BD Life Sciences).

## 2.2 Molecular biology and bacterial techniques

### *2.2.1 PCR*

DNA amplifications were carried out using either Phusion® High-Fidelity Polymerase (NEB) (2.3.1.1) or DreamTaq Green DNA Polymerase (ThermoScientific) (2.3.1.2). Primers used for PCR are shown in Table 2.2.

#### *2.2.1.1 Phusion High-Fidelity Polymerase (NEB)*

For PCR reactions where the amplified product was used for cloning or sequencing and required DNA proofreading, Phusion® High-Fidelity Polymerase (NEB) was used. Typical reaction conditions were: 0.5 µl Phusion® Polymerase (0.02 U), 0.1-1 ng template DNA, 0.5 µl forward and reverse primer (10 µM), 0.5 µl dNTP mix (10 mM), 1.5 µl $MgCl_2$ (1.5 mM), 10 µl 5x Phusion HF or GC buffer (supplied by manufacturer), made up to 50 µl with sterile $dH_2O$. The reactions were placed in a thermocycler with the following conditions:

Step 1: Initial denaturation 2 minutes, 94 °C

| | |
|---|---|
| Step 2: Denaturation | 30 seconds, 94 °C |
| Step 3: Annealing | *30 seconds, 50 - 60 °C |
| Step 4: Extension: | **0.5 – 3 minutes, 72 °C |
| Step 5: Final extension: | 10 minutes, 72 °C |

Steps 2-4 were cycled 35 times.

* Annealing temperature was defined by the specific melting temperature of the primers used.

** Extension time was defined by the length of the PCR product: 1 minute per 1 kb DNA.

*2.2.1.2 DreamTaq Green DNA Polymerase (ThermoScientific)*

For check PCR reactions, DreamTaq Green DNA Polymerase (ThermoScientific) was used with the following conditions: 0.25 µl DreamTaq Green DNA Polymerase (0.1 U), 5 µl DreamTaq Green buffer (supplied by manufacturer), 0.1-1 ng template DNA, 0.5 µl forward and reverse primer (10 µM), 0.5 µl dNTP mix (10 mM), made up to 50 µl with sterile $dH_2O$. The reactions were placed in a thermocycler with the following conditions:

| | |
|---|---|
| Step 1: Initial denaturation | 10 minutes, 94 °C |
| Step 2: Denaturation | 30 seconds, 94 °C |
| Step 3: Annealing | *30 seconds, 50 - 60 °C |
| Step 4: Extension: | **0.5 – 3 minutes, 72 °C |
| Step 5: Final extension: | 10 minutes, 72 °C |

Steps 2-4 were cycled 35 times.

* Annealing temperature was defined by the specific melting temperature of the primers used.

** Extension time was defined by the length of the PCR product: 1 minute per 1 kb DNA.

### *2.2.2 Restriction enzyme digests*

Plasmid DNA was digested using the relevant restriction enzymes and buffers according to the manufacturer's instructions (ThermoScientific). Digested plasmids were visualised on an agarose gel (see 2.3.3).

### *2.2.3 Agarose gel electrophoresis, DNA purification and DNA sequencing*

DNA was separated by electrophoresis using 1 % w/v agarose gels using TAE buffer (40 mM Tris acetate, 1 mM EDTA pH8) and containing 5 µg/ml ethidium bromide. Where needed, DNA was extracted and purified using a QIAquick gel extraction kit (QIAGEN) as per manufacturer's instructions. DNA concentrations were determined using a Nanodrop spectrophotometer (Labtech). Sequencing reactions were performed by GATC Biotech

### *2.2.4 Escherichia coli transformation and plasmid isolation*

Plasmids were propagated by introducing them into *E. coli* SURE competent cells (Agilent Technologies) (*e14$^-$ [McrA$^-$] Δ[mcrCB$^-$hsdSMR$^-$mrr] 171 endA1 supE44 thi-1 gyrA96 relA1 lac recB recJ sbcC umuC::Tn5 [Kan$^r$] uvrC[F'proAB lac$^Q$ZΔm15 Tn10 [Tet$^R$]])* using the standard $CaCl_2$ transformation method described previously (Maniatis *et al.*, 1985) onto LB agar (2 % w/v Bacto tryptone, 1 % w/v Bacto yeast extract, 1 % w/v NaCl pH7.2) containing 0.1 mg/ml ampicillin. Plates were incubated at 37 °C overnight. *E. coli* SURE cells containing plasmids with the Ampicillin resistance gene were grown in LB media containing 0.1 mg/ml ampicillin (SigmaAldrich). A GenElute Plasmid Miniprep kit (SigmaAldrich) was used to isolate plasmid DNA as per manufacturer's instructions.

# Chapter Three: Analyses of the relative contribution of yeast dUbs to ROS responses

## 3.1. Introduction

It is well characterised that high levels of ROS causes oxidative stress, however low ROS levels also play essential roles in signal transduction. It is therefore essential that cells can sense and distinguish the different levels and types of ROS so they respond in an appropriate manner (see Section1.2.5). Many signalling pathways utilise the reversible oxidation of cysteine thiol residues to regulate their activity (Veal *et al.*, 2007). Catalytic cysteine thiols are widespread in the ubiquitination pathway, whereby catalytic activity is used for the conjugation and deconjugation of ubiquitin from target substrates (Finley *et al.*, 2012; Ronau *et al.*, 2016). Recently it has been shown that the ubiquitin, SUMO, and NEDD8 pathways are important for sensing ROS levels (see Section1.3). Although many dUbs have been identified, and much research is focussed on finding their downstream targets, very little is known about dUb regulation and specificity. In *S. cerevisiae* 19 of the 20 known dUbs are cysteine thiols (Finley et al., 2012) suggesting a number of them could be regulated by ROS. Indeed investigations into mammalian SENPS (see Section 1.3.1) and dUbs (see Section 1.3.3.1) suggest reversible oxidation by ROS inhibits protein activity (Bossis and Melchior, 2006, Lee et al., 2013). Hence it is suggested that that oxidation of dUbs, and in particular the differential sensitivities of certain dUbs to specific oxidative stresses/ROS could potentially be a mechanism by which ubiquitination is linked to stress responses within cells. However the regulation of specific dUbs by different types and levels of stress remains unknown.

To investigate the possibility that dUbs are regulated by ROS we decided to use the tractability of the model organism *S. cerevisiae* and the available genetic tools, to take a systematic approach to investigate all the yeast dUbs in response to a range of different oxidative stresses. The objective in this chapter was to investigate the potential modifications and roles of the yeast dubs to different

types of oxidative stresses in order to move towards an understanding of the response of dUbs to oxidative stresses at an organism-wide level.

## 3.2. Results

### *3.2.1. Confirmation of dUb deletion strains and strains expressing epitope tagged dUbs.*

Much work has been done in both mammalian and yeast cells to try and understand the response of specific dUbs to ROS; however extensive investigations into the global response of dUbs to a variety of types of oxidative stress have not previously been carried out. In order to begin analyses of all the *S. cerevisiae* dUbs all of the available dUb gene deletion mutants were obtained from the *S. cerevisiae* gene deletion collection (Giaever *et al.*, 2002). In addition all of the available TAP epitope tagged dUbs were obtained from the TAP epitope tag strain collection (Ghaemmaghami *et al.*, 2003a). Of the 20 dUbs in *S. cerevisiae*, 17 individual gene deletion mutants and 19 strains expressing individual TAP epitope tagged dUbs from their normal genome locus were obtained.

Next, all of the deletion strains were checked by PCR to confirm they were correct using a generic reverse primer homologous to the kanamycin resistance cassette and a specific primer homologous to the individual dUb genome. Only successful deletion of the target gene would allow the PCR to produce a product as the wild-type locus would not allow annealing of the kanamycin reverse primer and therefore no extension would occur (Figure. 3.1A). A positive result for gene deletion is indicated by a band present at approximately 1500bp depending on the precise position of the specific forward primer (Figure 3.1B). Positive results were observed for all the obtained strains with the exception of *ubp14*Δ. It was possible the *UBP14* gene was deleted and that the PCR had simply failed. Hence to test whether the *UBP14* gene was deleted further PCR analyses, using a specific forward and specific reverse primer, were performed (Figure 3.1C). With these primers gene deletion was predicted to produce a PCR product for the

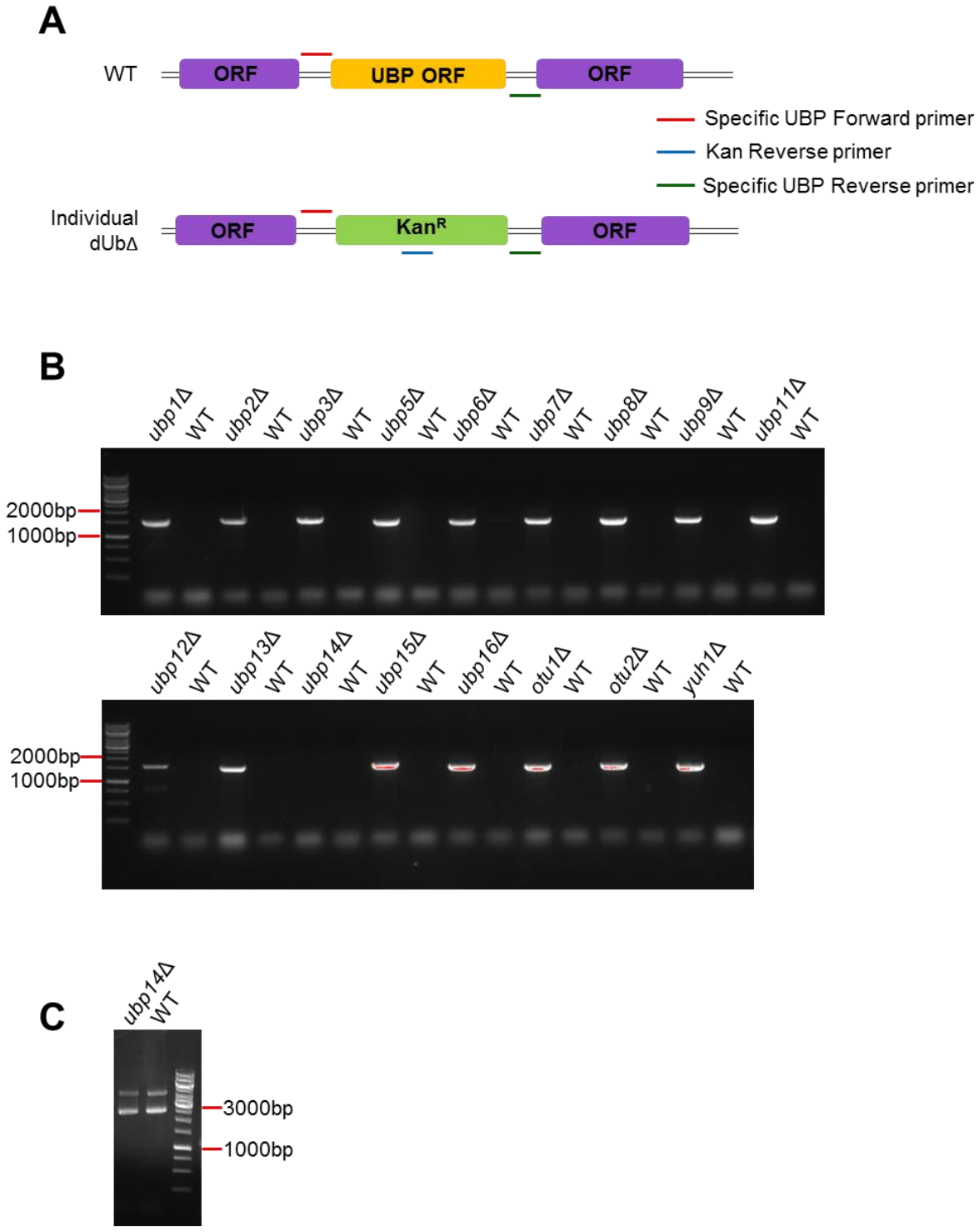
A
WT
ORF
UBP ORF
ORF
Specific UBP Forward primer
Kan Reverse primer
Specific UBP Reverse primer
Individual dUbΔ
ORF
KanR
ORF
B
ubp1Δ WT ubp2Δ WT ubp3Δ WT ubp5Δ WT ubp6Δ WT ubp7Δ WT ubp8Δ WT ubp9Δ WT ubp11Δ WT
2000bp
1000bp
ubp12Δ WT ubp13Δ WT ubp14Δ WT ubp15Δ WT ubp16Δ WT otu1Δ WT otu2Δ WT yuh1Δ WT
2000bp
1000bp
C
ubp14Δ WT
3000bp
1000bp

**Figure 3.1: PCR analyses of the dUb gene deletion mutants.** (A) PCR using a generic KAN reverse primer and a gene-specific forward primer, was performed with DNA isolated from each deletion strain obtained from the *Saccharomyces cerevisiae* genome deletion collection (FCC73-FCC75, FCC96-FCC110) and a WT control (FCC23). Successful deletion produces a PCR product of approximately 1500bp. (B) Using DNA from each potential dUb deletion mutant, PCR products were analysed on a 1% agarose gel together with a wild type control using the same primers. (C) *ubp14*Δ showed no PCR product when using the generic KAN reverse primer and was repeated with both specific forward and reverse primers for the deleted gene (see A). Correct gene deletion yields a band of approximately 1900bp, whereas the expected band size for wild type *UBP14* gene is 2550bp.

kanamycin cassette at approximately 1900bp, whilst the presence of the wild-type gene was predicted to produce a product of approximately 2550bp. As can be seen the PCR analyses indicated the presence of the wild-type gene (Figure 3.1C). These analyses confirmed the majority of the deletion strains, with the exception of the *ubp14*Δ strain, from the deletion library are correctly deleted and could be used in the rest of the investigation.

Next, all TAP epitope-tagged strains were checked to confirm the presence of a TAP epitope tag, in frame at the C-terminus of the individual dUb protein. Firstly, an initial PCR check of all 19 strains was performed. A specific forward primer to each gene and a generic reverse primer homologous to the TAP epitope tag cassette were used. Only strains with the TAP epitope tag cassette integrated at the individual dUb gene locus would allow annealing of the TAP reverse primer and therefore extension of the product (Figure 3.2.A). A positive result is indicated by the presence of a band at approximately 200-500bp, depending on the precise binding position of the specific forward primer on the chromosome (Figure 3.2B). Positive results were obtained for the majority of strains, with the exception of Ubp2-TAP, Ubp3-TAP, Ubp15-TAP and Ubp13-TAP (Figure 3.2B). It was possible the results for these four strains were not correct. Hence, further PCR analyses using gene-specific forward and reverse primers were performed (Figure 3.2C). Using these primers, strains containing the TAP epitope tag cassette at the correct location were predicted to produce PCR products of approximately 3000bp, whilst the wild-type strains were predicted to produce PCR products of approximately 200-500bp. These analyses indicated that the Ubp2-TAP, Ubp3-TAP and Ubp15-TAP strains were correct whereas the Ubp13-TAP strain produced a PCR product indicative of a wild type strain (Figure 3.2C)

The PCR analyses of the epitope tagged strains confirmed the presence of the TAP epitope tag cassette. However, although the epitope tag cassette was located in the dUb gene loci, it was possible the cassette had integrated out of frame with the dUb ORF. In addition, it was also possible that the successfully tagged proteins might be difficult to detect due to low abundance and/or low stability. Hence, the TAP epitope-tagged dUbs were examined by western blot analyses. Protein extracts isolated from each of the strains were examined using

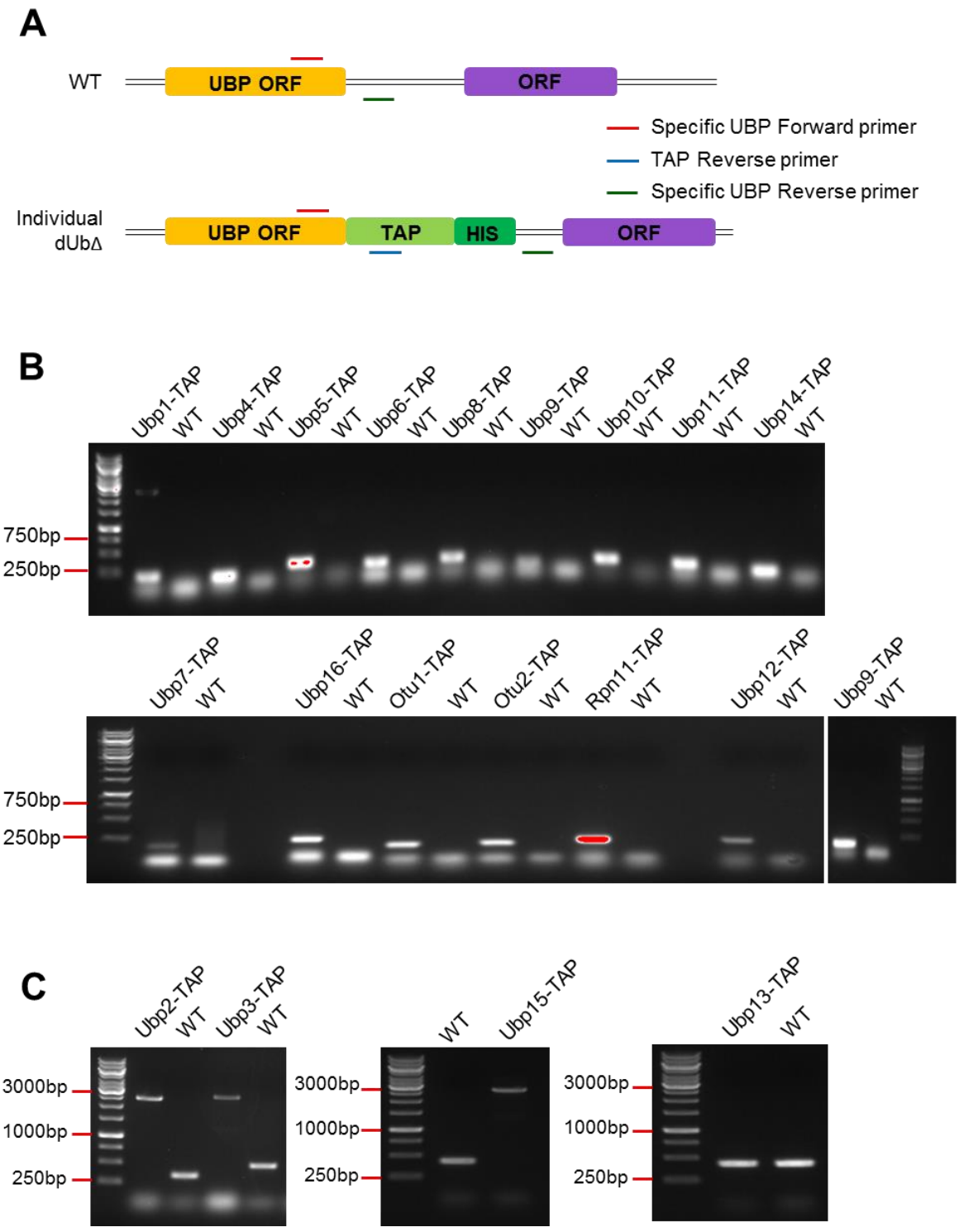
A
WT
UBP ORF
ORF
Specific UBP Forward primer
TAP Reverse primer
Specific UBP Reverse primer
Individual dUbΔ
UBP ORF
TAP
HIS
ORF
B
Ubp1-TAP
WT
Ubp4-TAP
WT
Ubp5-TAP
WT
Ubp6-TAP
WT
Ubp8-TAP
WT
Ubp9-TAP
WT
Ubp10-TAP
WT
Ubp11-TAP
WT
Ubp14-TAP
WT
750bp
250bp
Ubp7-TAP
WT
Ubp16-TAP
WT
Otu1-TAP
WT
Otu2-TAP
WT
Rpn11-TAP
WT
Ubp12-TAP
WT
Ubp9-TAP
WT
750bp
250bp
C
Ubp2-TAP
WT
Ubp3-TAP
WT
3000bp
1000bp
250bp
WT
Ubp15-TAP
3000bp
1000bp
250bp
Ubp13-TAP
WT
3000bp
1000bp
250bp

**Figure 3.2: PCR analyses of the TAP epitope-tagged dUb strains.** (A) PCR using a generic TAP reverse primer and a gene-specific forward primer, was performed with DNA isolated from each TAP epitope-tagged strain obtained from the *Saccharomyces cere*visiae TAP-tag collection (FCC123-FCC125, ELR28-ELR42), and a WT control (FCC23). Successful integration of the TAP epitope tag cassette at each individual dUb gene locus produces a PCR product of approximately 200-500bp depending on the position of the specific forward primer. (B) The PCR products using DNA from each potential TAP epitope tagged dUb strain were analysed on a 1% agarose gel together with a wild type control using the same primers. (C) PCR analyses using DNA isolated from strains that showed no PCR product when using the generic TAP reverse primer were repeated with both gene-specific forward and gene-specific reverse primers for the tagged locus.

the PαP antibody which recognises the TAP epitope (Figure 3.3). Importantly, a specific band was detected in protein extracts from the majority of strains (Figure 3.3). In most cases, the band detected has a slower mobility than expected. The basis for this altered mobility is not clear but is likely associated with the effects of the TAP epitope tag. No specific band was detected in the extract from the Ubp7-TAP strain. The basis for this lack of detection remains unclear, but may be related to decreased stability of the epitope-tagged protein and/or due to the failure to accurately insert the epitope tag cassette. It is unlikely that it is due to the relative expression of Ubp7, as Ubp8, which is predicted to have a lower abundance than Ubp7 (Kulak *et al.*, 2014) (Figure 3.3), can be readily detected. No further work was performed with Ubp7-TAP due to the lack of detection of the protein. It is intriguing that the relative protein abundances of the TAP epitope tagged strains do not always correlate with the predicted protein abundance by Kulak *et al* (2014) as stated in Figure 3.3D. For example, the protein abundance predicted for Ubp4 is 294 molecules per cell (Kulak *et al.*, 2014), however the western blot analyses show a specific band for Ubp4-TAP as fainter than the specific band for Ubp5-TAP, which is predicted to have only 125 molecules per cell (Kulak *et al.*, 2014). It has been reported previously that the TAP epitope tag may affect protein abundance (Gloeckner *et al.*, 2007) which and that certain proteins are more susceptible to TAP epitope tag interference than other proteins. This may explain discrepancies between the abundance predicted by Kulak *et al* (2014) and the present data (Figure 3.3). Curiously, a specific band of the expected mobility was detected in extracts from the Ubp13-TAP strain (Figure 3.3B-C). In contrast the PCR analysis described above suggested that the Ubp13-TAP strain did not contain the TAP epitope cassette at the correct location (Figure 3.2C). Hence, due to these conflicting results no further work was performed using the Ubp13-TAP strain.

In conclusion, the initial analyses of the dUb deletion strains and the dUb TAP epitope tagged strains confirmed that 16 dUb gene deletion strains and 17 TAP epitope tagged dUb strains were available for further investigations.

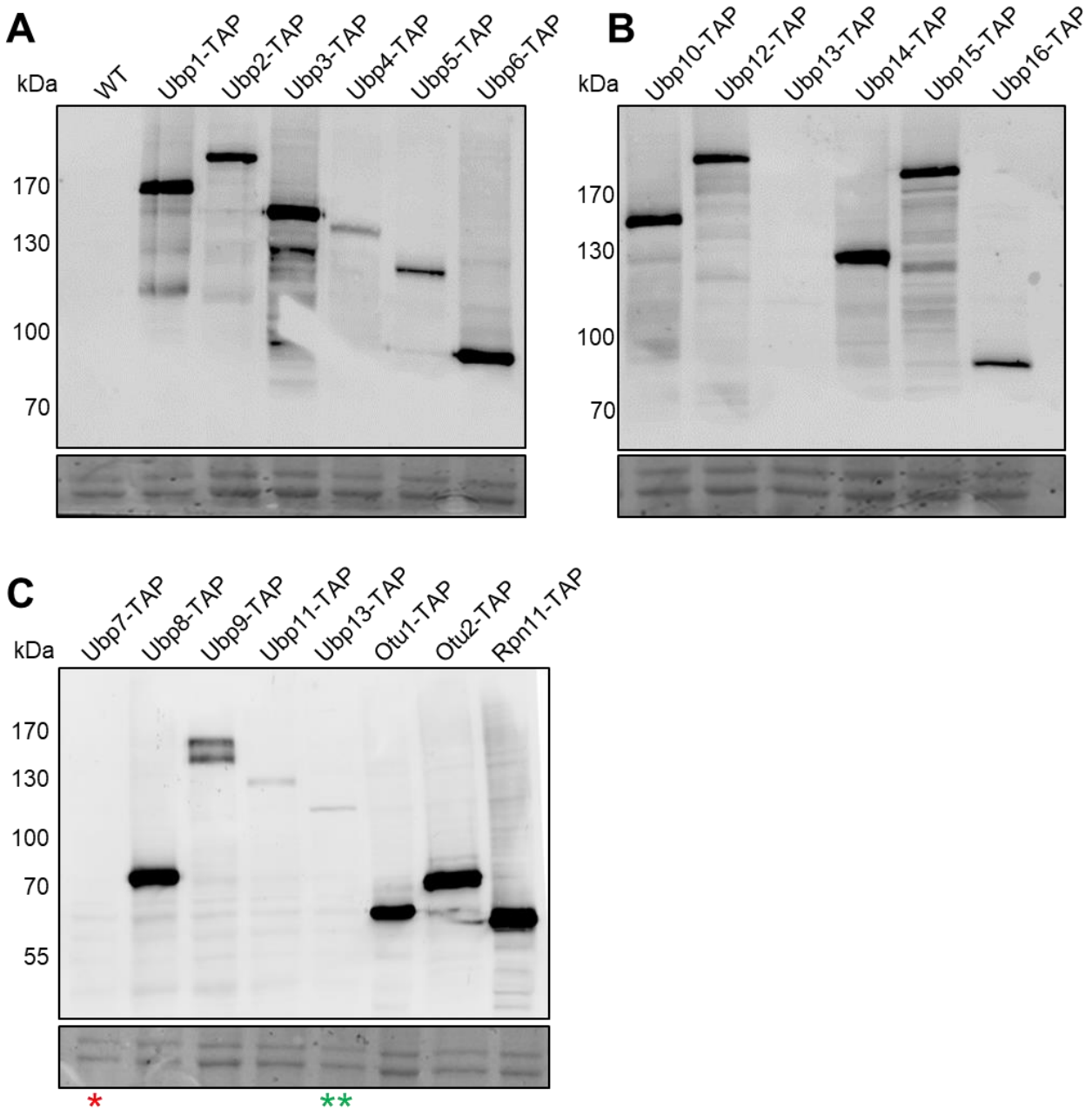


**D**

| dUb | MW (+ 21 kDa for TAP tag) | Expected protein abundance Molecules/cell | dUb | MW (+ 21 kDa for TAP tag) | Expected protein abundance Molecules/cell |
|---|---|---|---|---|---|
| Ubp1 | 113.7 | 1434 | Ubp11 | 103.7 | 12 |
| Ubp2 | 167.3 | 1355 | Ubp12 | 164.2 | 577 |
| Ubp3 | 122.9 | 2679 | Ubp13 | 104.9 | 446 |
| Ubp4 | 126.2 | 294 | Ubp14 | 109.6 | 924 |
| Ubp5 | 113.3 | 125 | Ubp15 | 164.6 | 1194 |
| Ubp6 | 78.1 | 8978 | Ubp16 | 77.9 | 89 |
| Ubp7 | 144.1 | 221 | Otu1 | 54.5 | 2699 |
| Ubp8 | 74.6 | 545 | Otu2 | 57.1 | 2822 |
| Ubp9 | 107.2 | 29 | Yuh1 | Not in Library | 1626 |
| Ubp10 | 109.5 | 521 | Rpn11 | 55.4 | 7827 |

**Figure 3.3: Epitope tagged dUbs can be visualised by western blot analysis.** (A)(B)(C) Protein extracts from all dUb strains expressing TAP epitope tags (FCC123-FCC125, ELR28-ELR42), and a WT control (FCC23) were analysed by western blot using a PαP primary antibody. Ponceau S stain was used as a loading control * indicates no epitope-tagged protein after western blot analysis. ** indicates potential Ubp13-TAP. (D) The table shows the expected sizes of each TAP epitope-tagged strain and the expected protein abundance. Protein abundance was taken from (Kulak *et al.*, 2014).

### *3.2.2. Different dUbs have specific responses to oxidative stress*

Having obtained most of the dUb deletion strains the next step was to investigate the relative contribution of the individual dUbs to responses to oxidative stress. Ubiquitin pathway enzymes have previously been shown to be regulated by oxidative stress, and recent work suggested that dUbs could also be regulated by ROS (Lee *et al.*, 2013). However studies of the roles of all the dUbs in *S. cerevisiae* in response to a variety of stresses were limited. Indeed, although the roles of the dUbs in response to temperature and the toxic amino acid homolog canavanine (Amerik *et al.*, 2000) had been studied, no large scale analyses of their linkage to oxidative stress had been performed. Here a systematic approach was undertaken to further the understanding of the roles of yeast dUbs in response to different oxidising agents. In particular, the relative sensitivities of each of the individual dUb deletion mutants was examined when exposed to the oxidising agents $H_2O_2$, diamide, and menadione. These three oxidising agents act through different mechanisms, and trigger different responses within cells (see introduction for details).

#### *3.2.2.1. $H_2O_2$ sensitivity*

To investigate the specific roles of dUbs to $H_2O_2$, the dUb deletion strains and a wild-type control were grown to mid-log phase and spotted onto YPD media containing increasing amounts of $H_2O_2$ (Figure 3.4). Interestingly, a diverse range of requirements for the dUbs was observed. For example the mutants displaying the greatest increase in sensitivity to $H_2O_2$ were *ubp2*Δ, *ubp3*Δ, and *otu2*Δ (Figure 3.4), suggesting that the three dUbs encoded by these genes are vital for the cells' survival in the presence of $H_2O_2$. Indeed, this increased sensitivity of *ubp3*Δ has been reported previously (Jin, 2017), validating the present results. In contrast, the *ubp1*Δ mutant showed increased $H_2O_2$ resistance (Figure 3.4). Ubp1 has been linked to the endocytic pathway as a component of protein transport machinery (Schmitz *et al.*, 2005), however the role of Ubp1 in stress responses has not been well characterised.

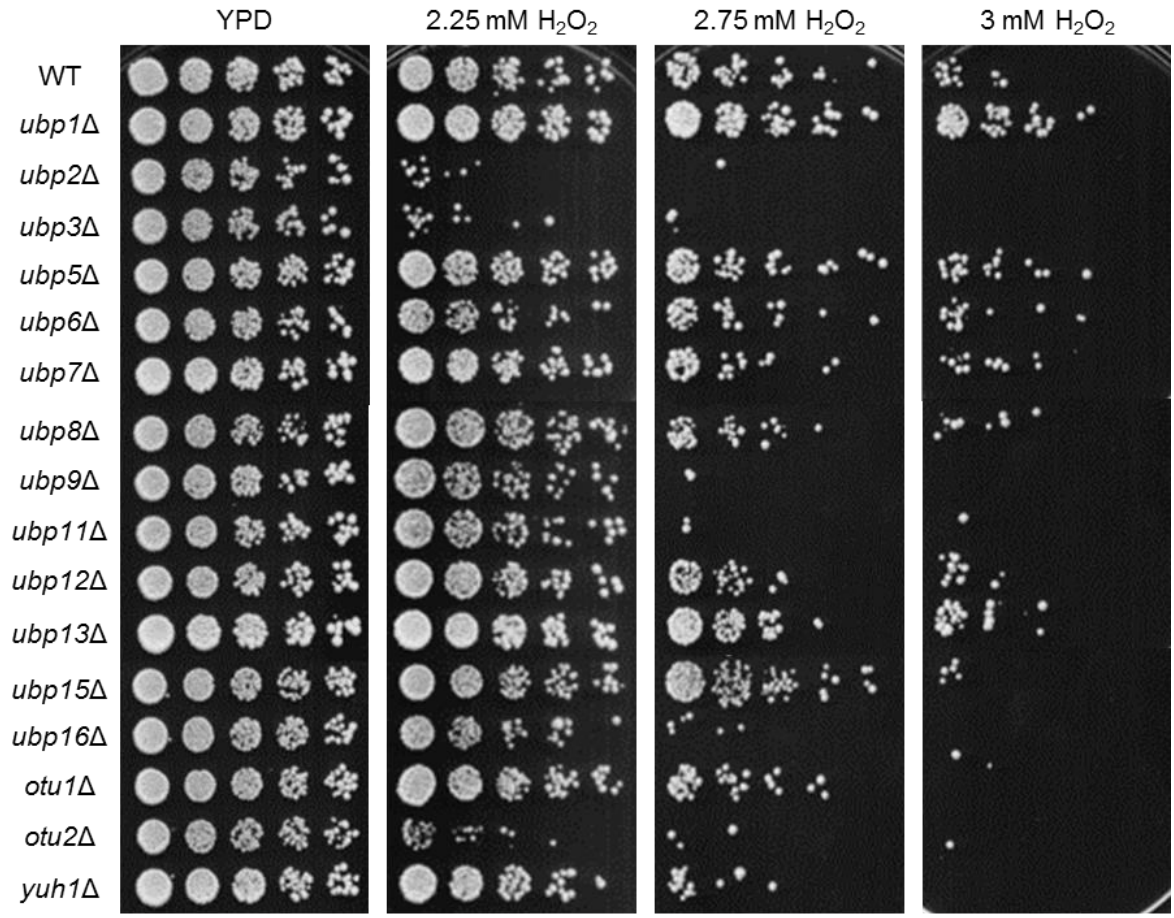


**Figure 3.4: dUbs have specific responses to $H_2O_2$ stress.** The dUb deletion strains (FCC73-FCC75, FCC96-FCC110) and a WT control (FCC23) were grown to mid-log phase in YPD and 5 fold serial dilutions were spotted onto YPD media containing increasing concentrations of $H_2O_2$. Plates were incubated at 30 °C for 3 days before imaging.

### *3.2.2.2. Diamide sensitivity*

Next, the role of the different dUbs in response to diamide was examined. Diamide is a drug which permeates the plasma membrane and reversibly oxidises GSH into GSSG. Deletion strains and a wild type control were grown to mid-log phase and spotted onto YPD media containing increasing amounts of diamide (Figure 3.5). Similar to the results obtained using $H_2O_2$, a variety of different sensitivities was observed. Similar to the results with $H_2O_2$, *ubp3*Δ cells displayed increased sensitivity to diamide. Previous work indicated that *ubp3*Δ cells are more sensitive to diamide (Dodgson et al., 2016), however the present result (Figure 3.5) shows a greater increase in sensitivity than was previously reported. The basis of this difference is not known but is possibly due to the use of different strain background. Nevertheless, the fact that *ubp3*Δ cells display increased sensitivity to both $H_2O_2$ and diamide suggests a wide role of the Ubp3 protein in responses to oxidative stress. The *ubp15*Δ strain showed increased sensitivity to diamide but not $H_2O_2$, suggesting Ubp15 has specific oxidative stress functions. Interestingly *ubp5*Δ, *ubp8*Δ, and *ubp12*Δ strains display increased resistance to diamide (Figure 3.5). The basis of this increase in resistance is not clear but suggests that these three dUbs inhibit the response to diamide.

### *3.2.2.3. Menadione sensitivity*

To investigate whether any of the dUbs have specific roles in responses to menadione, the dUb deletion strains and a wild type control were grown to mid-log phase and spotted onto YPD media containing increasing amounts of menadione (Figure 3.6). Consistent with the $H_2O_2$ and diamide sensitivity analyses the *ubp3*Δ mutant displayed increased sensitivity to menadione. Hence Ubp3 appears to have roles in responses to a range of oxidative stress conditions. Interestingly the *ubp15*Δ mutant showed increased sensitivity to menadione and to diamide, but not $H_2O_2$, whereas the *yuh1*Δ mutant showed increased sensitivity to menadione and $H_2O_2$, suggesting specific dUbs roles in certain stress responses. Furthermore, the *ubp13*Δ mutant showed increased sensitivity to menadione but not $H_2O_2$ or diamide, indicating a specific role in responses to menadione.

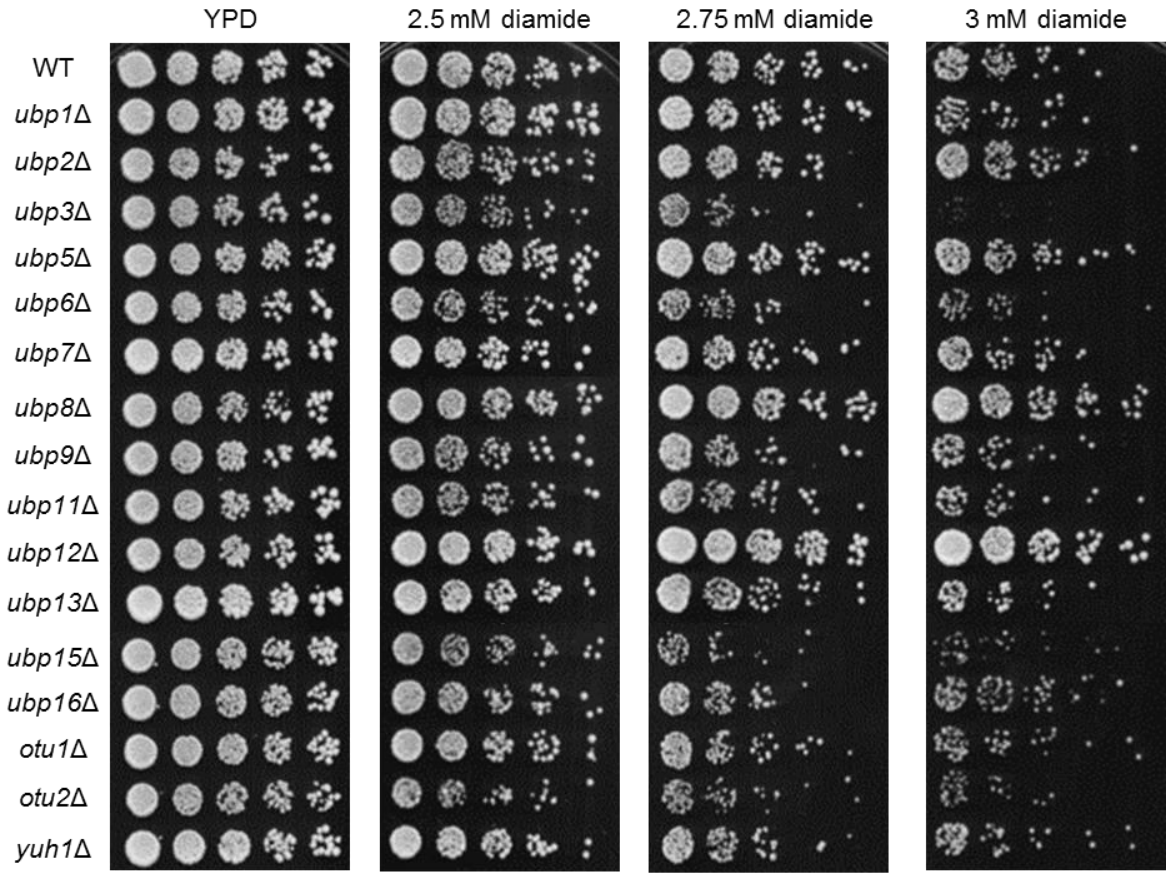


**Figure 3.5: dUbs have specific responses to diamide stress.** The dUb deletion strains (FCC73-FCC75, FCC96-FCC110) and a WT control (FCC23) were grown to mid-log phase in YPD and 5 fold serial dilutions were spotted onto YPD media containing increasing concentrations of diamide. Plates were incubated at 30 °C for 3 days before imaging.

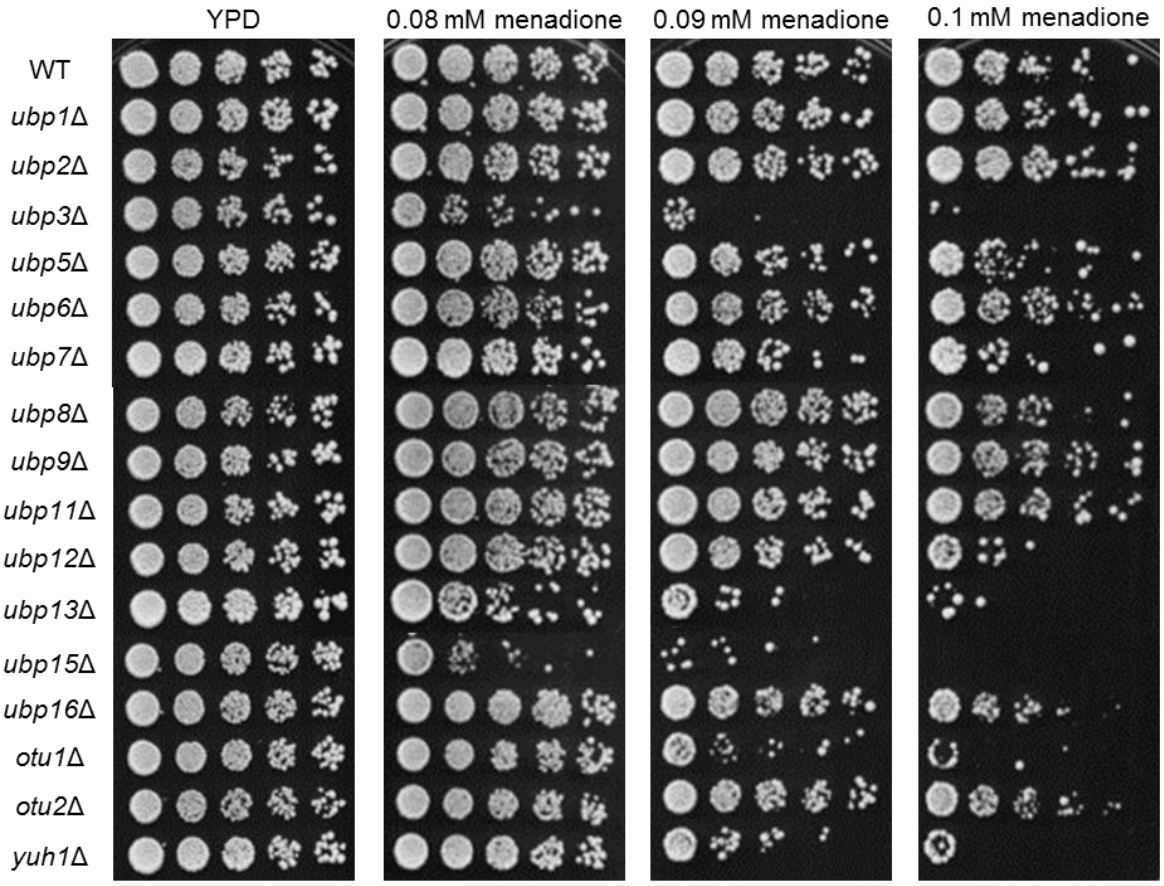


**Figure 3.6: dUbs have specific responses to menadione stress.** The dUb deletion strains (FCC73-FCC75, FCC96-FCC110) and a WT control (FCC23) were grown to mid-log phase in YPD and 5 fold serial dilutions were spotted onto YPD media containing increasing concentrations of menadione. Plates were incubated at 30 °C for 3 days before imaging.

The data presented suggests that dUbs play a range of roles in response to specific and several different oxidative stress conditions (summarised in Table 3.1). Using different oxidising agents has provided insight into the fact that all dUbs investigated in this chapter show some increased sensitivity or resistance to at least one of the oxidative stresses. However, it is important to note that dUbs have similar domain architecture, particularly in their active site, leading to the potential for redundancy of function.

| dUb | Response to oxidising agents | | |
|---|---|---|---|
| | $H_2O_2$ | diamide | menadione |
| Ubp1 | +++ | WT | WT |
| Ubp2 | - - - - - | + | WT |
| Ubp3 | - - - - | - - - | - - - - |
| Ubp4 | N/A | N/A | N/A |
| Ubp5 | ++ | ++ | WT |
| Ubp6 | WT | - | WT |
| Ubp7 | WT | WT | - |
| Ubp8 | WT | + + | - |
| Ubp9 | - - | WT | WT |
| Ubp10 | N/A | N/A | N/A |
| Ubp11 | - - | WT | WT |
| Ubp12 | WT | +++ | - - |
| Ubp13 | + | WT | - - - |
| Ubp14 | N/A | N/A | N/A |
| Ubp15 | WT | - - | - - - - - |
| Ubp16 | - | WT | - |
| Otu1 | - | WT | - - - |
| Otu2 | - - - | - | - |
| Yuh1 | - - | WT | - - - - |
| Rpn11 | N/A | N/A | N/A |

**Table 3.1: Summary of the differential dUb sensitivities in response to ROS.** Blue columns show a summary of all the relative sensitivities of dUb deletion mutants to the different oxidising agents tested when grown on YPD media, - indicates level of sensitivity, + indicates level of resistance, and WT indicates the strain responded the same as wild type. N/A indicates that the strain was either not present in the collection, or was found to be an incorrect strain.

### *3.2.3. Specific dUbs are modified in response to oxidative stress*

Having established the responses of the dUb deletion mutants to different oxidative stress conditions, the next step involved investigation into whether any of the dUb proteins were modified in response to oxidative stress. Previous work from our lab revealed that an E2 enzyme in the ubiquitin conjugation cycle, Cdc34, was oxidised into a high molecular weight complex in response to specific oxidising agents (Doris *et al.*, 2012) (see Section 1.3.3). Given that many of the yeast dUbs utilise catalytic cysteine residues it was possible that one or more of the dUbs may also form disulphide complexes in response to oxidative stress. Indeed a previous study (Lee *et al.*, 2013) demonstrated that dUbs can be inhibited by $H_2O_2$ and subsequently were either activated, or had their activity enhanced in the presence of the reducing agent DTT. Furthermore, it was also observed that a specific dUb, USP19, was oxidised into a sulphenylamide form by $H_2O_2$, and also formed a HMW disulphide complex (~250 kDa) (Lee *et al.*, 2013). Although that study suggested that dUbs can indeed be modified in response to $H_2O_2$ those experiments were undertaken in mammalian cells *in vitro*, and only examined a portion of the mammalian dUbs and only with $H_2O_2$. Hence here we examined whether there is any evidence for modifications of the different dUbs in *S. cerevisiae* in response to different oxidising agents.

#### *3.2.3.1. Analyses of dUb modification in response to $H_2O_2$*

To examine whether any of the dUbs were modified in response to $H_2O_2$ the different TAP epitope-tagged dUb strains (see Section 3.2.1) and a wild-type control strain were grown to mid log phase and incubated with 2 mM $H_2O_2$. Proteins were extracted in the presence of NEM, which maintains oxidation states by binding to reduced cysteines, resulting in no reduction of oxidised cysteines, and analysed via western blot (Figure 3.7). Interestingly, of the 17 dUbs tested, 4 showed repeatable shifts in mobility suggesting post translational modification in response to $H_2O_2$. The nature of these potential modifications remains unclear but it is reasonable to speculate that small changes of mobility, for example Ubp5-TAP and Ubp6-TAP, may be phosphorylation. Indeed, both proteins contain potential phosphorylation sites (Albuquerque *et al.*, 2008; Swaney *et al.*, 2013). Ubp6 contains 4 ubiquitination sites (Swaney *et al.*, 2013)

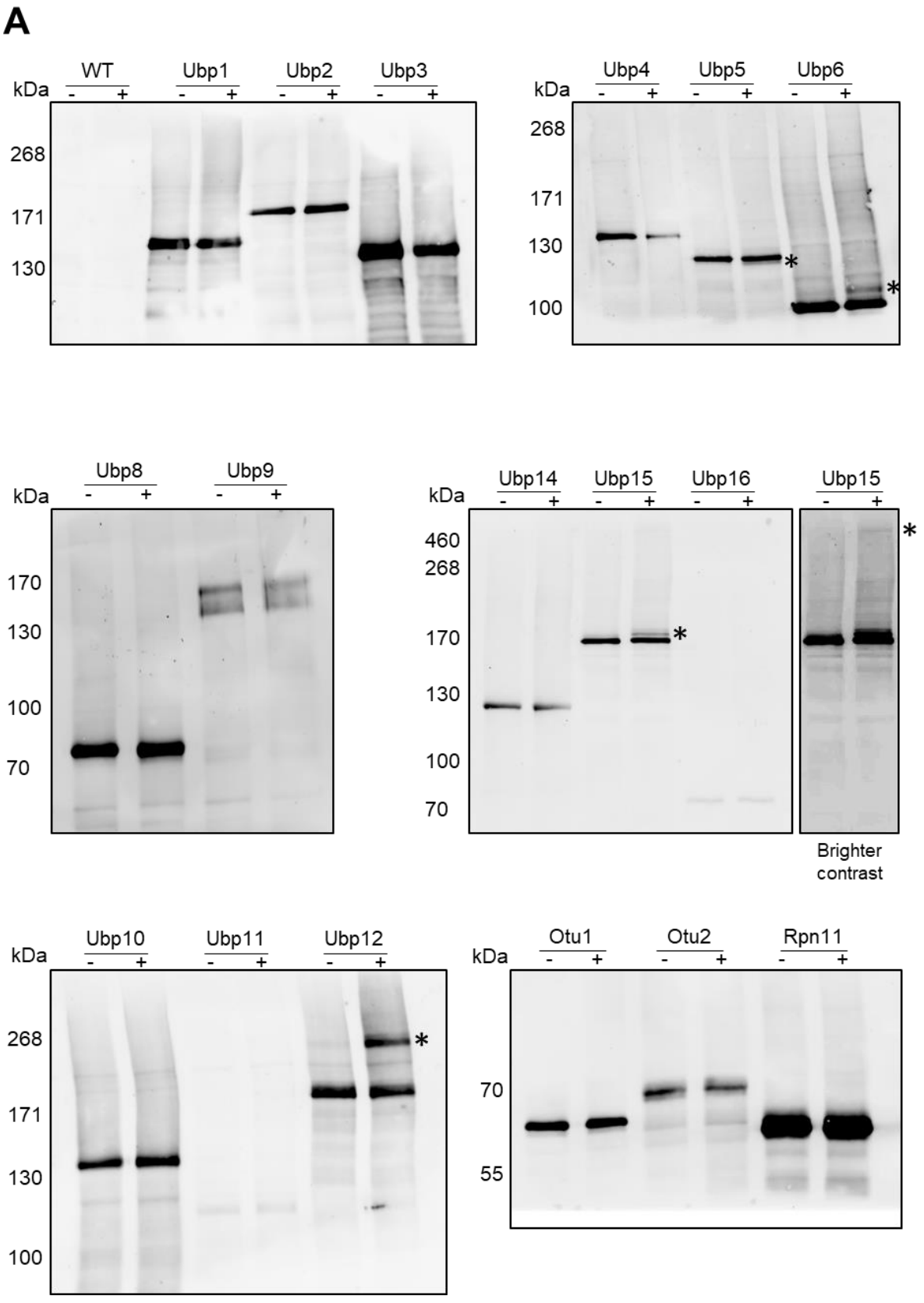
A
WT
Ubp1
Ubp2
Ubp3
kDa
- +
268
171
130
Ubp4
Ubp5
Ubp6
100
*
Ubp8
Ubp9
170
100
70
Ubp14
Ubp15
Ubp16
460
Brighter
contrast
Ubp10
Ubp11
Ubp12
Otu1
Otu2
Rpn11
55

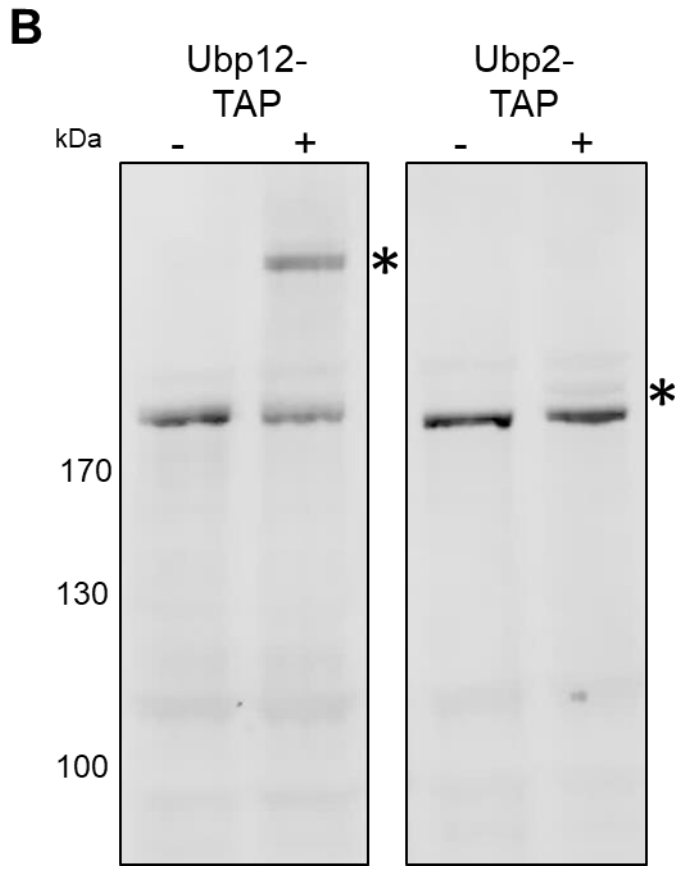


**Figure 3.7: Specific dUbs are modified in response to $H_2O_2$.** (A)(B) Cells expressing TAP-tagged dUbs (FCC123-FCC125, ELR28-ELR42), and a WT control (FCC23) were incubated with 2 mM $H_2O_2$ for 0 (-) and 10 minutes (+). Protein extracts were prepared in non-reducing conditions and separated by SDS-PAGE. Proteins were visualised using PαP antibodies. * denotes $H_2O_2$ induced modifications.

and a succinylation site (Weinert *et al.*, 2013), raising the possibility that the $H_2O_2$ induced slower mobility forms may be due to ubiquitination or succinylation (Figure 3.7). Interestingly, $H_2O_2$ treatment of cells expressing Ubp12-TAP produced a high molecular weight (HMW) band at approximately 250 kDa, an increase in the normal molecular weight by approximately 50 kDa (Figure 3.7). Furthermore, approximately 50% of the Ubp12-TAP protein is in this HMW form, suggesting the possibility that Ubp12-TAP is forming some sort of disulphide containing complex analogous to Cdc34 (Doris *et al.*, 2012) or USP19 (Lee *et al.*, 2013). Intriguingly, treatment of Ubp15-TAP expressing cells also resulted in the formation of a HMW Ubp15-TAP complex (Figure 3.7). However a smaller shift in mobility was also detected following $H_2O_2$ treatment which may be due to a modification such as phosphorylation and/or ubiquitination. Indeed Ubp15 contains five lysine residues that are susceptible to ubiquitination (Swaney *et al.*, 2013). Interestingly, $H_2O_2$ induced a HMW complex in Ubp2-TAP cells (Figure 3.7B); however this modification was not seen consistently. It is possible that the specific concentration or the short time frame used in these analyses, or the potentially transient formation of the complex, may miss the formation of the HMW complex.

*3.2.3.2. Analyses of dUb modification in response to diamide*

The potential modification of the dUbs in response to diamide was explored next. Similar to the $H_2O_2$ studies, cells expressing TAP epitope-tagged dUbs and a wild type control were grown to mid-log phase and incubated with 3 mM diamide. Proteins were extracted in the presence of NEM and analysed via western blot under non-reducing conditions (Figure 3.8). Interestingly, of the 17 dUbs tested, Ubp14-TAP and Ubp15-TAP showed repeatable diamide-induced shifts of mobility suggesting both proteins became modified (figure 3.8). For Ubp14-TAP the diamide-induced band has a faster mobility on the western blot (figure 3.8). Although the nature of this change in mobility is unknown it is tempting to speculate that diamide has induced an intramolecular disulphide(s) changing the folding which is causing the protein to have a faster mobility. In contrast the diamide induced band in the Ubp15-TAP cells has a much slower mobility than the TAP epitope tagged protein (Figure 3.8). This appears analogous to the effects of $H_2O_2$ on Ubp15 (see figure 3.7) where a HMW band is also induced.

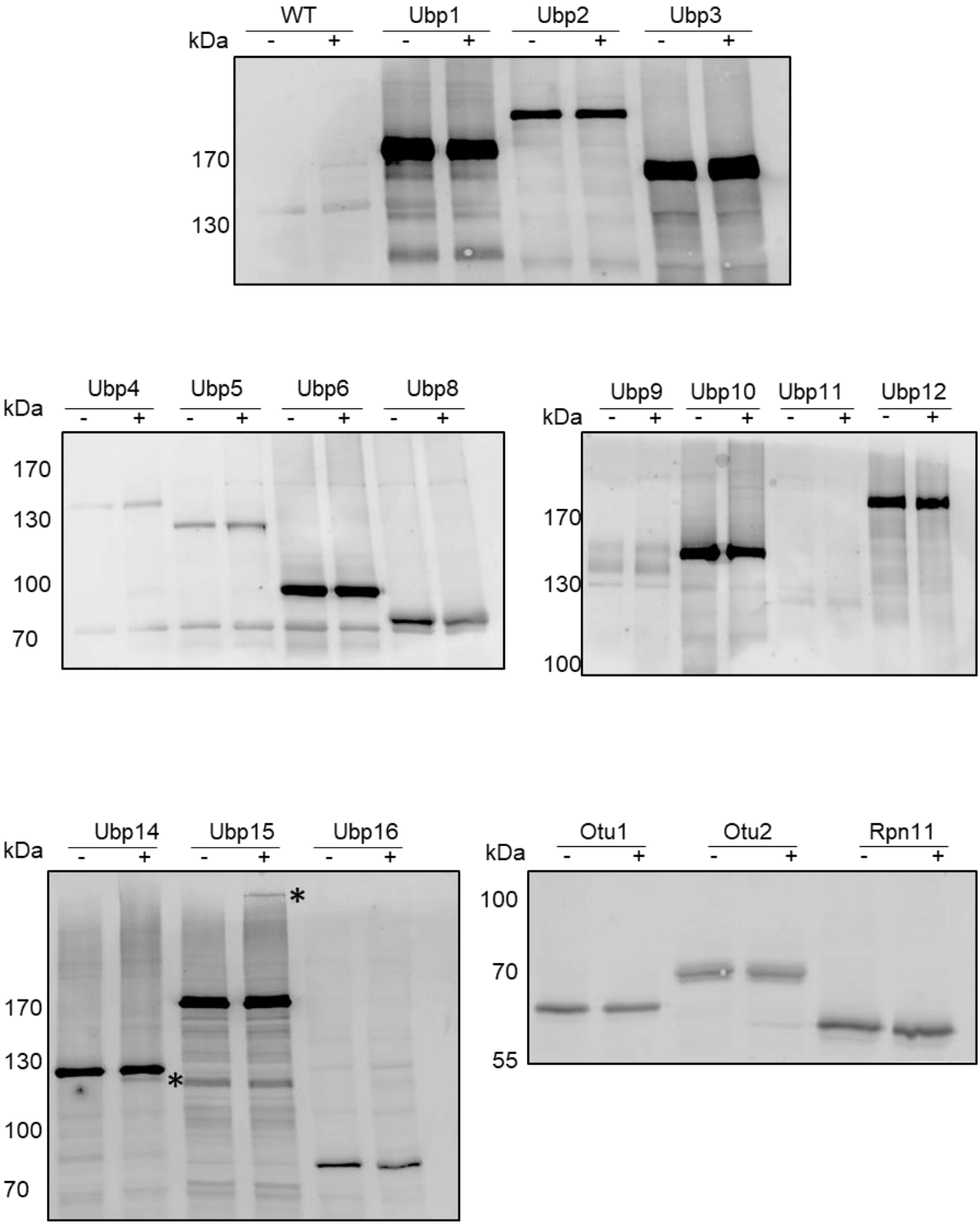


**Figure 3.8: Specific dUbs are modified in response to diamide.** Cells expressing TAP-tagged dUbs (FCC123-FCC125, ELR28-ELR42), and a WT control (FCC23) were incubated with 3 mM diamide for 0 (-) and 10 minutes (+). Protein extracts were prepared in non-reducing conditions and separated by SDS-PAGE. Proteins were visualised using PɑP antibodies. * denotes diamide induced modifications.

Hence it is tempting to speculate that the two HMW complexes are related. In contrast, no smaller HMW band was detected following diamide treatment similar to the smaller HMW band that was induced by $H_2O_2$ in the Ubp15-TAP cells (figures 3.7 and 3.8). Taken together with the experiments with $H_2O_2$, these data suggest different modifications are induced by different oxidising agents and, moreover, demonstrate dUb specificity in the modifications.

*3.2.3.3. Analyses of dUb modification in response to menadione*

We next explored whether any of the dUbs became modified in response to menadione. Cells expressing TAP epitope-tagged dUbs and a wild-type control were grown to mid-log phase and incubated with 0.1 mM menadione. Proteins were extracted in the presence of NEM and analysed via western blot under non-reducing conditions (Figure 3.9). Similar to the effects of $H_2O_2$ and diamide, menadione-specific changes to mobility were detected. In particular, upon menadione treatment the mobility of both Ubp5-TAP and Ubp15-TAP were slightly slower (figure 3.9). It is interesting to note that in this case, and in contrast to $H_2O_2$ and diamide, the entire amount of Ubp5-TAP and Ubp14-TAP appeared to be shifted to the slightly slower mobility forms of each protein (figure 3.9).It is also intriguing to note that the mobility of Ubp5-TAP and Ubp14-TAP was affected by $H_2O_2$ and diamide respectively (Figure 3.7 and 3.8); although in both these cases the mobility change detected appears to be different to that induced by menadione (compare figures 3.7-3.9).

Taken together these results have revealed that the three different oxidising agents induce a range of potential modifications of specific dUbs (summarised in Table 3.2). Furthermore different dUbs are modified by different oxidising agents. Given the range of cellular processes these dUbs influence, these experiments have potentially begun to reveal at a global level some of the aspects of specificity of regulation of deubiquitination that occurs in response to different oxidative stress conditions.

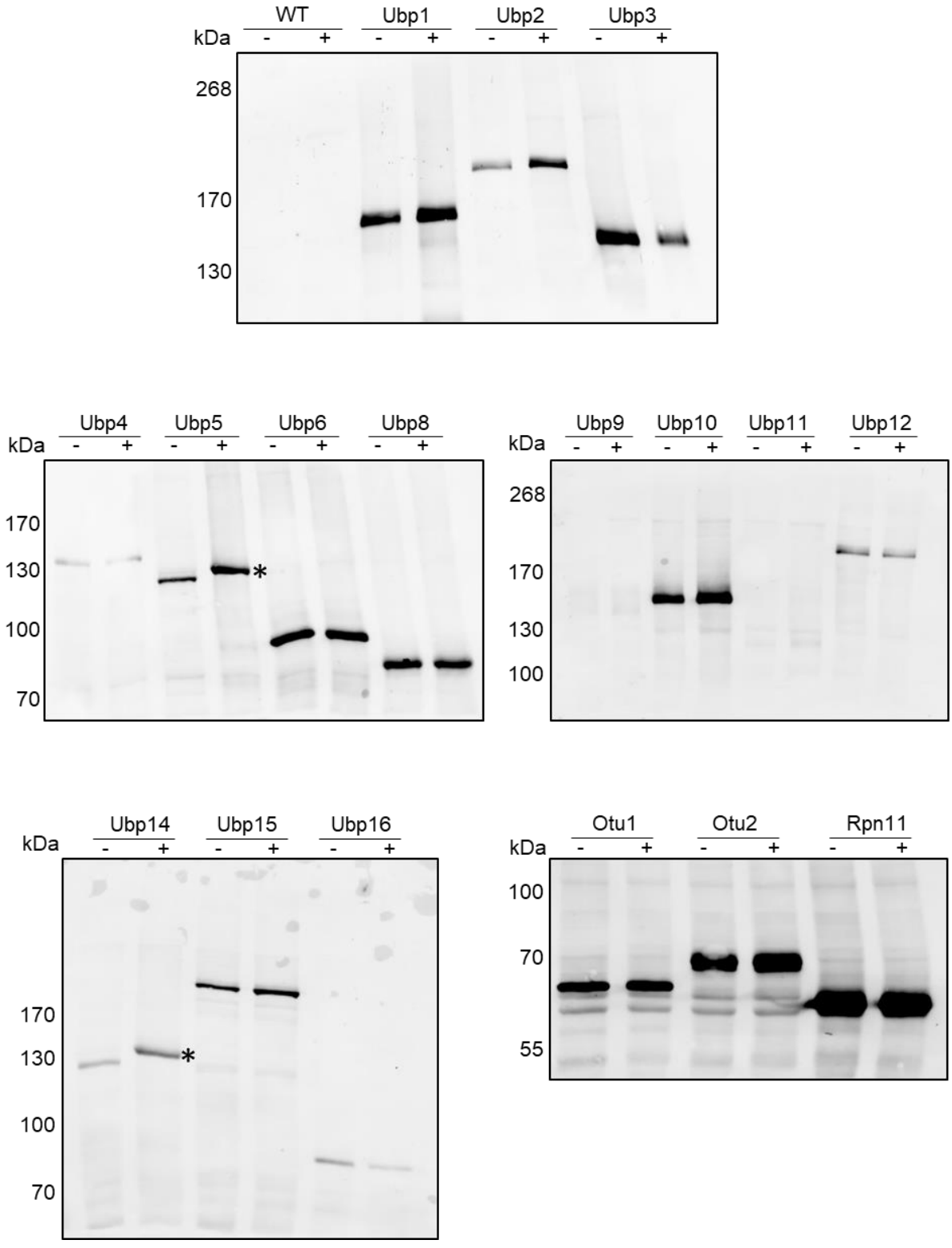


**Figure 3.9: Specific dUbs are modified in response to menadione.** Cells expressing TAP-tagged dUbs (FCC123-FCC125, ELR28-ELR42), and a WT control (FCC23) were incubated with 0.1 mM menadione for 0 (-) and 10 minutes (+). Protein extracts were prepared in non-reducing conditions and separated by SDS-PAGE. Proteins were visualised using PαP antibodies. * denotes menadione induced modifications.

| dUb | Response to oxidising agents | | | Modifications in response to oxidising agents | | |
|---|---|---|---|---|---|---|
| | $H_2O_2$ | diamide | menadione | $H_2O_2$ | diamide | menadione |
| Ubp1 | +++ | WT | WT | | | |
| Ubp2 | - - - - - | + | WT | ? | | |
| Ubp3 | - - - - | - - - | - - - - | | | |
| Ubp4 | N/A | N/A | N/A | | | |
| Ubp5 | ++ | ++ | WT | * | | * |
| Ubp6 | WT | - | WT | * | | |
| Ubp7 | WT | WT | - | N/A | N/A | N/A |
| Ubp8 | WT | + + | - | | | |
| Ubp9 | - - | WT | WT | | | |
| Ubp10 | N/A | N/A | N/A | | | |
| Ubp11 | - - | WT | WT | | | |
| Ubp12 | WT | +++ | - - | * | | |
| Ubp13 | + | WT | - - - | N/A | N/A | N/A |
| Ubp14 | N/A | N/A | N/A | | * | * |
| Ubp15 | WT | - - | - - - - - | ** | * | |
| Ubp16 | - | WT | - | | | |
| Otu1 | - | WT | - - - | | | |
| Otu2 | - - - | - | - | | | |
| Yuh1 | - - | WT | - - - - | N/A | N/A | N/A |
| Rpn11 | N/A | N/A | N/A | | | |

**Table 3.2: Summary of the differential dUb sensitivities and modifications in response to ROS.** Blue columns show a summary of all the relative sensitivities of dUb deletion mutants to the different oxidising agents tested, - indicates level of sensitivity, + indicates level of resistance, and WT indicates the strain responded the same as wild type. Orange columns show a summary of modifications to TAP epitope tagged strains in response to the oxidising agents tested, * indicates modification is present when incubated with each oxidising agent, ** indicates two modifications are seen in the same strain in response to an oxidising agent. ? indicates that a modification was identified occasionally, but not repeatedly. N/A indicates that the strain was either not present in the collections, or was found to be an incorrect strain.

### *3.2.4. Oxidative stress induced HMW modification of Ubp12 and Ubp15 are conserved in different strain backgrounds and with different epitope tags.*

As described earlier two of the dUbs, Ubp12 and Ubp15, form much larger HMW complexes in response to specific oxidising agents. Furthermore, loss of either protein affects the response of cells to various oxidising agents (Table 3.2). However, although none of the other TAP epitope-tagged dUbs displayed such large HMW complexes induced by oxidative stress, it was still possible that one or both complexes might be linked to the presence of the TAP epitope. In addition the TAP epitope-tagged proteins are expressed in the BY4741 strain background. This may also influence the results as previous studies have revealed that the BY4741 behaves differently to another commonly used strain background, W303, in response to different oxidising agents including $H_2O_2$ and diamide (Veal *et al.*, 2003). Hence potential effects of the choice of epitope tag and/or strain background used were investigated next.

#### *3.2.4.1. Analysis of Ubp12 in different strain backgrounds and with different epitope tagging*

As described above, Ubp12-TAP becomes specifically modified in response to $H_2O_2$, forming a HMW complex (Figure 3.7). This specificity to $H_2O_2$ and no other oxidising agent tested suggests that Ubp12 may play a specific role in $H_2O_2$ signalling. However, as described above, Ubp12 modification has only been investigated in the BY4741 strain background, and hence the potential for the epitope tag and/or the strain background to play a role in this response to $H_2O_2$ has not been explored. Indeed the TAP epitope tag is predicted to add ~21 kDa to the expected mobility of the wild type Ubp12 protein (Gloeckner *et al.*, 2007) and yet Ubp12-TAP had a mobility of ~190 kDa instead of the predicted 164 kDa (Ubp12 has a molecular weight of ~143 kDa plus the addition of the 21 kDa TAP epitope tag). This indicates that the TAP epitope tag has an effect on the migration of Ubp12 and perhaps this influences the formation of the HMW complex induced by $H_2O_2$. Hence to address whether the TAP epitope tag was influencing the HMW modification, a strain expressing Ubp12-6HA from the normal chromosomal locus in the BY4741 strain background was obtained

(Gödderz *et al.*, 2017) and checked by PCR (Figure 3.10A). Importantly the PCR analyses of the 6HA epitope-tagged version of Ubp12 identified that the epitope tag was integrated at the correct locus. Next the cells expressing Ubp12-TAP and Ubp12-6HA together with a wild type control were grown to mid log phase and incubated with 2 mM $H_2O_2$. Proteins were extracted in the presence of NEM, and analysed via western blot (Figure 3.10B). As expected, a HMW complex was induced in the cells expressing Ubp12-TAP. Ubp12-6HA also forms a HMW complex following $H_2O_2$ treatment (Figure 3.10B). Interestingly, the mobility of Ubp12-6HA is similar to that observed for Ubp12-TAP. The 6HA epitope tag is predicted to add ~8 kDa to the mobility of the protein (Saiz-Baggetto *et al.*, 2017), thus Ubp12-6HA would be predicted to be ~151 kDa, compared to the observed running size of ~190 kDa. Importantly, although the mobility of Ubp12-TAP and Ubp12-6HA are of similar sizes, the $H_2O_2$ induced HMW complexes are different in size, suggesting that epitope tag may change the size of the $H_2O_2$ induced complex. In both cases ~40% of the Ubp12 protein was in these HMW forms (figure 3.10C). Hence these data suggest the epitope tag does not influence the formation of the HMW complex. Previous analysis of Ubp12-TAP revealed that no HMW complex was formed in response to diamide (figure 3.8). However it was possible that the TAP epitope tag inhibits the formation of a HMW complex. To investigate this possibility, strains expressing Ubp12-TAP or Ubp12-6HA were incubated with 3 mM diamide and proteins were extracted in the presence of NEM and analysed via western blot. As expected, no HMW complex was detected in the Ubp12-TAP extract. Moreover, consistent with the hypothesis that the TAP epitope tag is not inhibiting the formation of a HMW complex, no HMW complexes were detected in the extract from the Ubp12-6HA strain treated with diamide (figure 3.10D).

Next, we explored the potential effect of strain background on Ubp12 modification in response to $H_2O_2$. As described above it has previously been reported that different *S.* cerevisiae strain backgrounds have different responses to oxidative stress and use different signalling pathways (Veal *et al.*, 2003). A 3HA epitope tag cassette, marked with KanMX was introduced to the C-terminus of Ubp12 at the normal chromosomal locus (described in 2.2.3.2). Potential transformants

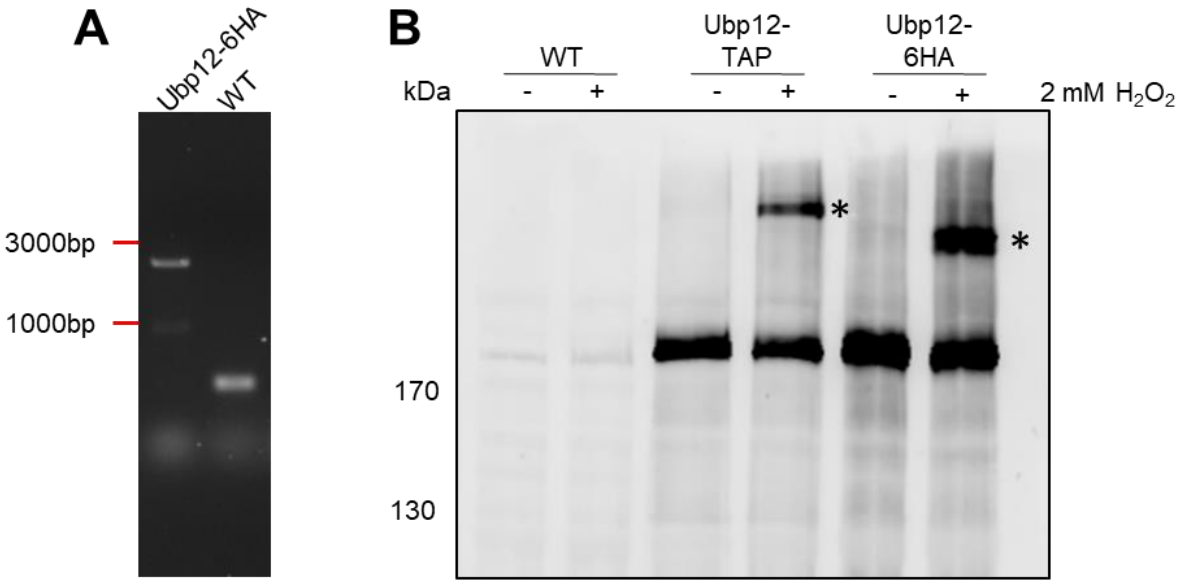
A
Ubp12-6HA
WT
3000bp
1000bp
B
WT
Ubp12-TAP
Ubp12-6HA
kDa
- + - + - +
2 mM H2O2
*
*
170
130

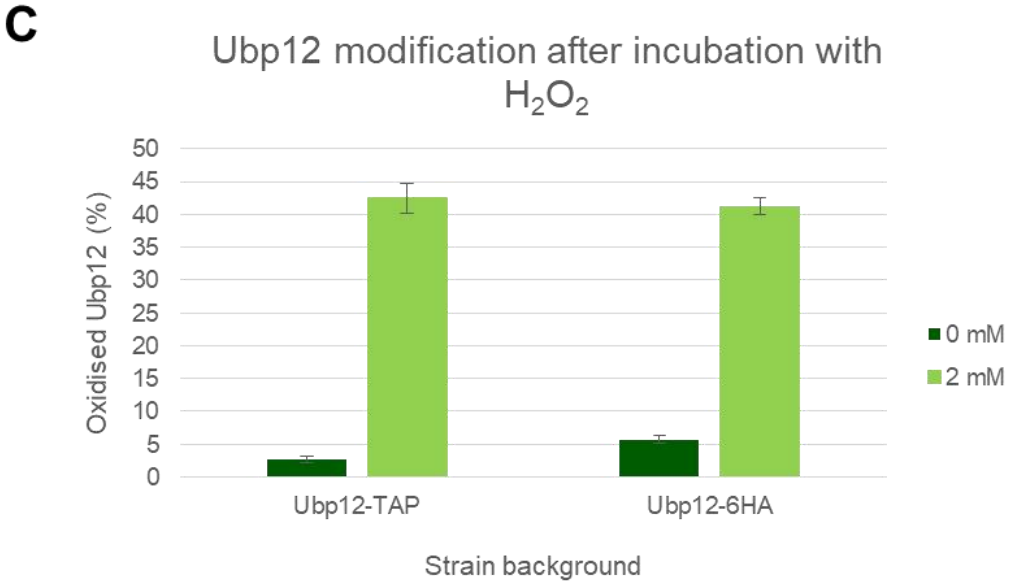
C
Ubp12 modification after incubation with H2O2
Oxidised Ubp12 (%)
50
45
40
35
30
25
20
15
10
5
0
Ubp12-TAP
Ubp12-6HA
Strain background
0 mM
2 mM

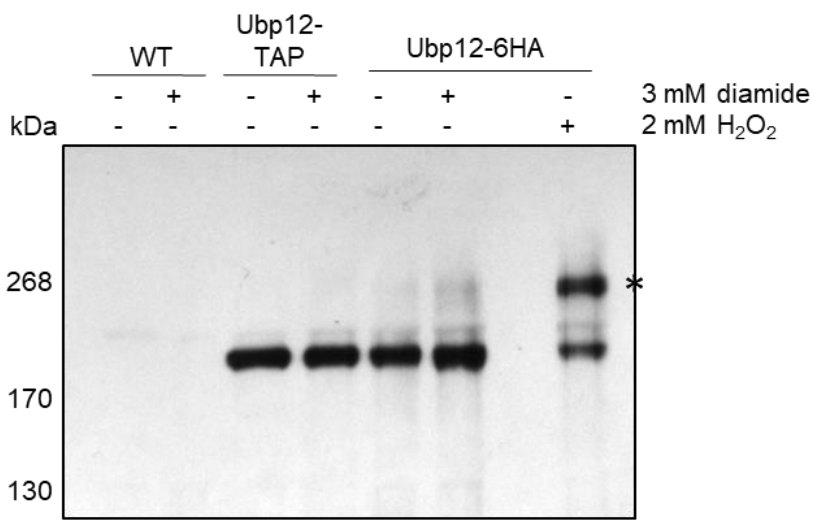
D
WT
Ubp12-TAP
Ubp12-6HA
- + - + - + -
3 mM diamide
kDa - - - - - - +
2 mM H2O2
268
170
130
*

[123]

**Figure 3.10: Different epitope tagged versions of Ubp12 form a HMW modification after $H_2O_2$ treatment.** (A) PCR using Ubp12-specific forward and reverse primers was performed using DNA isolated from Ubp12-6HA (FCC154). Successful integration of the 6HA epitope tag cassette at the Ubp12 gene locus produces a PCR product of ~2300bp. The resulting PCR product was analysed on a 1% agarose gel together with a wild type control using the same primers. (B) Cells in the BY4741 strain background expressing Ubp12-TAP (ELR38) or Ubp12-6HA (FCC154) and a WT control (FCC23) were incubated with 2 mM $H_2O_2$ for 0 (-) and 10 minutes (+). Protein extracts were prepared in non-reducing conditions and separated by SDS-PAGE. Proteins were visualised using PɑP antibodies (Ubp12-TAP) and anti-HA antibodies (Ubp12-6HA). (C) The band intensities of Ubp12-TAP (n=2) and Ubp12-6HA (n=2) with and without $H_2O_2$ (from B) were quantified using ImageQuant. Bars show the percentage of HMW complex with respect to total Ubp12 in each lane, and error bars denote standard error of the mean. (D) Cells in the BY4741 strain background expressing Ubp12-TAP (ELR38) or Ubp12-6HA (FCC154) and a WT control (FCC23) were treated with 3 mM diamide or 2 mM $H_2O_2$ for 10 minutes. Protein extractions were prepared as in (B) and visualised using PɑP antibodies (Ubp12-TAP) and anti-HA antibodies (Ubp12-6HA). * denotes $H_2O_2$ induced modifications

were analysed by PCR to confirm the integration of the 3HA epitope tag (Figure 3.11A) which would show a PCR product of ~2200bp if correctly epitope tagged. After confirmation of the integration of the 3HA epitope tag at the Ubp12 chromosomal locus (Figure 3.11A), W303 cells expressing Ubp12-3HA from the normal chromosomal locus, and Ubp12-6HA control cells were grown to mid-log phase and incubated with 2 mM $H_2O_2$. Proteins were extracted in non-reducing conditions in the presence of NEM and analysed via western blot (Figure 3.11B). Again the 3HA epitope-tagged Ubp12 strain had a slower mobility than predicted. The 3HA epitope tag adds ~3 kDa to the running size of the protein, however Ubp12-3HA runs at ~180 kDa, rather than the predicted 146 kDa. Significantly, Ubp12 forms a HMW complex in response to $H_2O_2$ in protein extracts isolated from both the BY4741 and W303 strain backgrounds. Furthermore, in both cases ~40% of total Ubp12 was detected in the HMW form after incubation with $H_2O_2$. Thus, taken together with these data, it suggests that Ubp12 forms a HMW complex in both a background strain and epitope tag independent manner.

While the epitope tag did not have an effect on the formation of the HMW form of Ubp12 in response to $H_2O_2$, it was unknown whether any of the epitope tags affected the functions and/or the stability of the Ubp12 protein. To obtain some insight into the potential effects of epitope tagging Ubp12, the BY4741 derived strains expressing Ubp12-TAP and Ubp12-6HA, together with *ubp12*Δ and WT strains as controls were grown to mid-log phase and their response to different stress conditions examined (Figure 3.12). Significantly, compared with wild type and *ubp12*Δ cells, it was found that the TAP epitope tag inhibited the normal function of Ubp12 in a variety of stress conditions. This is perhaps not surprising as the TAP epitope tag is large and can potentially affect protein localisation and stability (Gloeckner *et al.*, 2007). Interestingly however, the phenotypes displayed by cells expressing Ubp12-TAP were not consistent with the phenotypes displayed by *ubp12*Δ cells (figure 3.12). The basis of the effects of the epitope tag on Ubp12 are not known but these results suggests that, rather than decreasing the stability of the protein, another aspect of Ubp12 activity is affected such as protein localisation and/or ability to interact with other substrates. In contrast to the TAP epitope tag, epitope tagging Ubp12 with 6HA appeared to result in little effect on Ubp12 function with the possible exception of diamide

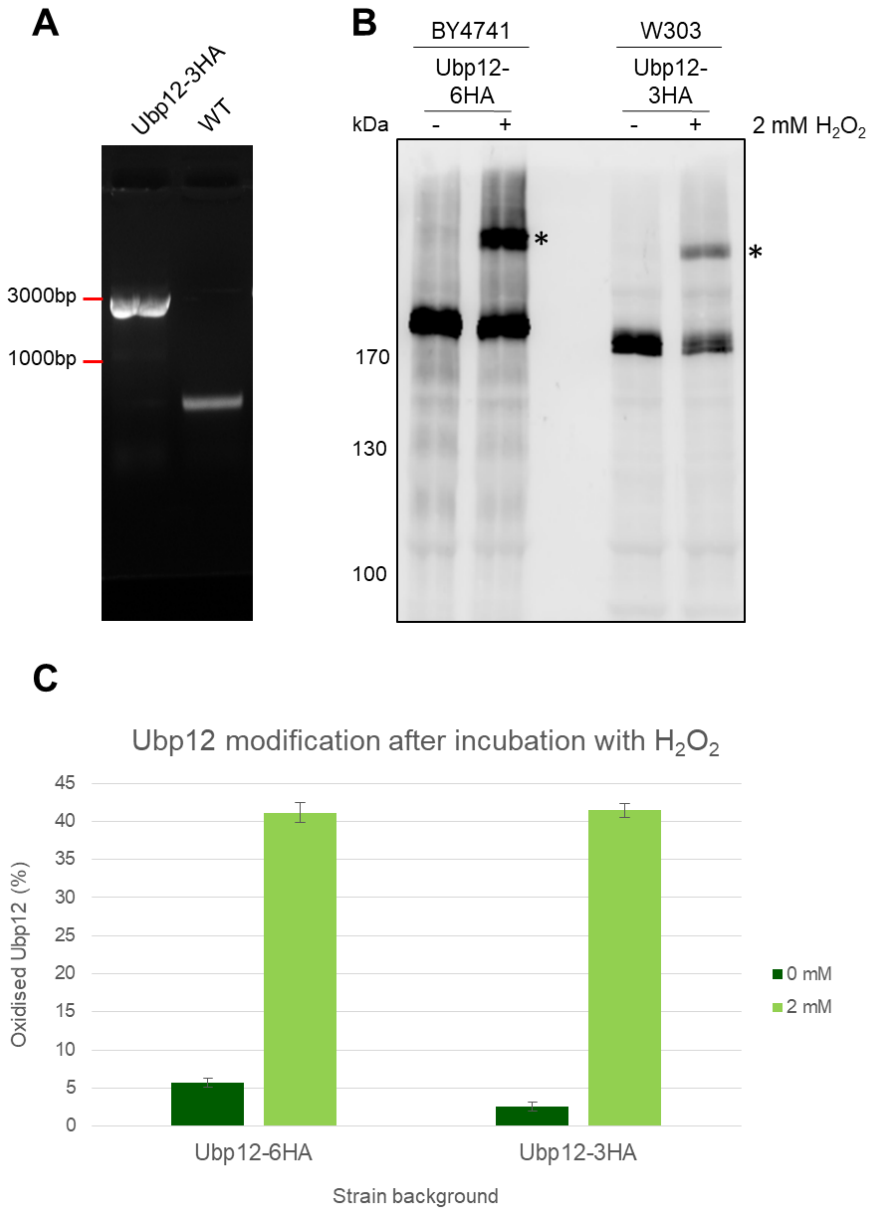


**Figure 3.11: Ubp12 forms a HMW complex after $H_2O_2$ treatment in cells from different strain backgrounds.** (A) PCR using Ubp12-specific forward and reverse primers was performed using DNA isolated from Ubp12-3HA (FCC93). Successful integration of the 3HA epitope tag cassette at the Ubp12 gene locus produces a PCR product of ~2200bp. The resulting PCR product was was analysed on a 1% agarose gel together with a wild type control using the same primers. (B) Cells in the BY4741 strain background expressing Ubp12-6HA (FCC154) and cells in the W303 strain background expressing Ubp12-3HA (FCC93) were treated with 2 mM $H_2O_2$ for 0 (-) and 10 (+) minutes. Protein extracts were prepared in non-reducing conditions and separated by SDS-PAGE. Proteins were visualised using anti-HA antibodies. * denotes HMW modification. (C) The band intensities of Ubp12-6HA (n=2) and Ubp12-3HA (n=3) with and without $H_2O_2$ (from B) were quantified using ImageQuant. Bars show the percentage of HMW complex with respect to total Ubp12 in each lane, and error bars denote standard error of the mean.

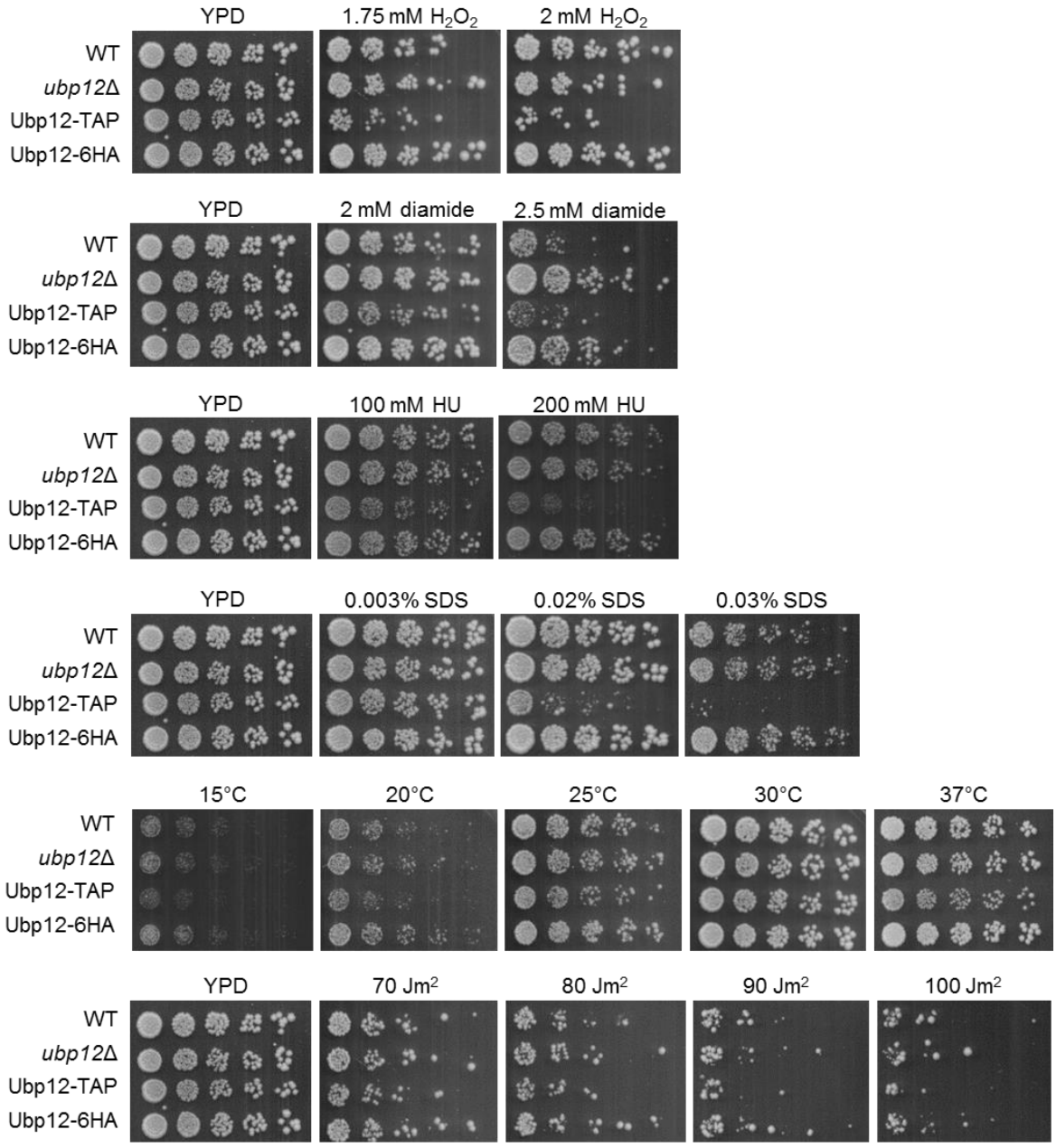


**Figure 3.12: Analyses of the effects of epitope tagging Ubp12.** 5-fold serial dilutions of wild type (FCC23), *ubp12*Δ (FCC75), and strains expressing Ubp12-TAP (ELR38) and Ubp12-6HA (FCC154) from their normal chromosomal locus grown to mid-log phase in YPD, were spotted onto YPD plates containing the indicated concentrations of different stress inducing agents. Plates were incubated at 30°C for 3 days before imaging.

sensitivity where, like the *ubp12*Δ cells, cells expressing Ubp12-6HA appeared slightly more resistant to diamide, although not to the same extent as *ubp12*Δ. Taken together, these results suggest that epitope tags do affect the function of Ubp12, but importantly the 6HA epitope tag has very little impact in protein function. Importantly, neither the epitope tag nor the strain background had an effect on the formation of the $H_2O_2$ induced HMW form of Ubp12.

#### *3.2.4.2. Analysis of Ubp15 in different strain backgrounds and with different epitope tagging*

In contrast to Ubp12, Ubp15 forms a HMW complex in response to both $H_2O_2$ and diamide (see figures 3.7 and 3.8). However, as described above, Ubp15 modifications have only been investigated in the BY4741 strain background, thus the potential for the epitope tag and/or the strain background to play a role in this response to both $H_2O_2$ and diamide has not been explored. As described for Ubp12, the TAP epitope tag is predicted to add ~21 kDa to the mobility of Ubp15, and yet Ubp15-TAP had a mobility of ~180 kDa rather than the expected running size of 165 kDa (Ubp15 has a molecular weight of ~143.5 kDa plus the addition of the 21 kDa TAP epitope tag). This indicates, similar to Ubp12, the TAP epitope tag has an effect on the migration of Ubp15 and may influence the formation of the HMW complexes induced by $H_2O_2$ and diamide. Therefore, to address whether the strain background or the TAP epitope tag was influencing the formation of the HMW form of Ubp15 in response to $H_2O_2$ and diamide, a strain was created expressing Ubp15-3HA at the normal chromosomal locus in the W303 strain background. A 3HA epitope tag, marked with HIS3 was introduced to the C-terminus of Ubp15 at the normal chromosomal locus (described in 2.2.3.2). Potential transformants were analysed by PCR to confirm the integration of the 3HA epitope tag (Figure 3.13A) which would show a PCR product of ~2200bp if correctly epitope tagged. After confirmation of the integration of the 3HA epitope tag at the Ubp15 chromosomal locus (Figure 3.13A), cells expressing Ubp15-TAP and Ubp15-3HA were grown to mid log phase and incubated with 2 mM $H_2O_2$. Proteins were extracted in the presence of NEM, and analysed via western blot (Figure 3.13B). As expected, a HMW complex was induced in the cells expressing Ubp15-TAP. However interestingly, Ubp15-3HA also forms a HMW

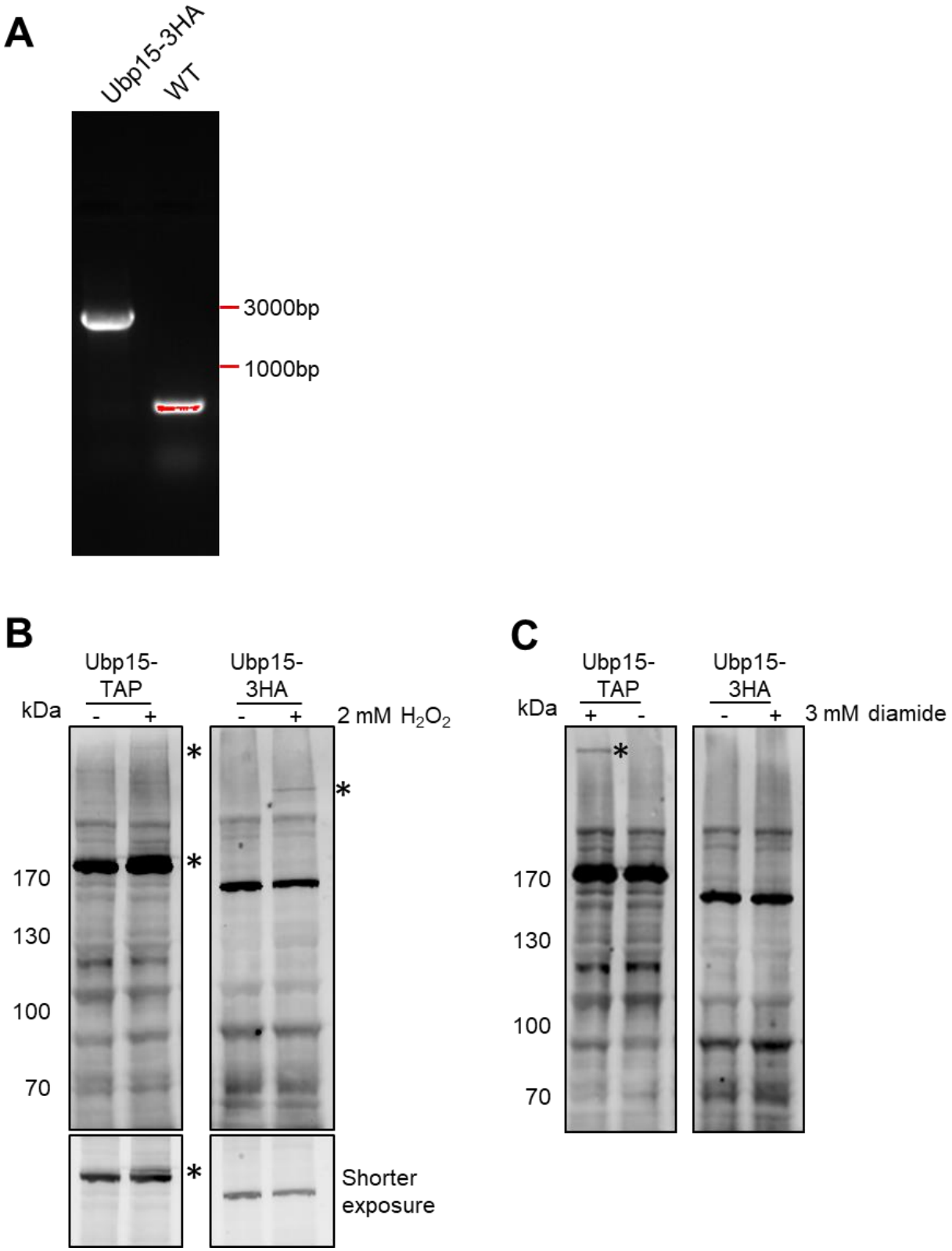
A
Ubp15-3HA
WT
3000bp
1000bp
B
Ubp15-TAP
Ubp15-3HA
kDa
- + - +
2 mM H2O2
170
130
100
70
Shorter exposure
C
Ubp15-TAP
Ubp15-3HA
kDa
+ - - +
3 mM diamide
170
130
100
70

**Figure 3.13: Different epitope tagged versions of Ubp15 form a HMW complex after $H_2O_2$ and diamide treatment in cells from different strain backgrounds.** (A) PCR using Ubp15-specific forward and reverse primers was performed using DNA isolated from Ubp15-3HA (FCC130). Successful integration of the 3HA epitope tag cassette at the Ubp15 gene locus produces a PCR product of ~2200bp. The resulting PCR product was analysed on a 1% agarose gel together with a wild type control using the same primers (A). Cells in the BY4741 strain background expressing Ubp15-TAP (ELR41), and cells in the W303 strain background expressing Ubp15-3HA (FCC130) were treated with 2 mM $H_2O_2$ (B) and 3 mM diamide (C) for 0 (-) and 10 (+) minutes. Protein extracts were prepared in non-reducing conditions and separated by SDS-PAGE. Proteins were visualised using PαP antibodies (Ubp15-TAP) and anti-HA antibodies (Ubp15-3HA). The panel below shows a shorter exposure time for band clarity. *denotes Ubp15 HMW modification

complex of the following $H_2O_2$ treatment (Figure 3.13B). As observed for Ubp12-TAP, Ubp15-3HA had a slower running mobility than expected. Ubp15-3HA had a mobility of ~160 kDa, rather than the predicted 146 kDa. Intriguingly, the HMW complex induced by $H_2O_2$ in the Ubp15-3HA strain background had a faster mobility than the HMW complex formed in the Ubp15-TAP strain. It is also interesting to note that the proportion of HMW induced Ubp15-3HA appears to be different to that induced in the BY4741 strain background. Of note is the formation of the lower HMW band induced in Ubp15-TAP in response to $H_2O_2$, which is not present in the Ubp15-3HA strain. Whether these differences are due to strain background or epitope tag remains unknown. Next, the cells expressing Ubp15-TAP and Ubp15-3HA were grown to mid log phase and incubated with 3 mM diamide. Proteins were extracted in the presence of NEM, and analysed via western blot (Figure 3.13C). As expected, a HMW complex was induced in the cells expressing Ubp15-TAP, however, interestingly, the Ubp15-3HA strain showed no HMW form induced after exposure to diamide. It is possible that Ubp15-3HA would show a modification in response to diamide at different conditions or for different time courses. As both strains are modified in response to $H_2O_2$, and diamide, however differently, it suggests that Ubp15 modification in response to ROS is strain and epitope tag independent.

While the epitope tag did not have an effect on the formation of the HMW form of Ubp15 in response to $H_2O_2$ and diamide, it was unknown whether any of the epitope tags affected the functions and/or the stability of the Ubp15 protein. To obtain some insight into the potential effects of epitope tagging Ubp15, sensitivity analyses were performed on the epitope tagged Ubp15 strain. It was important to be able to compare Ubp15-3HA to an appropriate deletion mutant in the same strain background. Therefore a *ubp15*Δ mutant in the W303 strain background was created. A deletion cassette expressing the *HIS3* gene as a marker was introduced to wild type W303 strains (see Section 2.2.3.1), and potential transformants were checked for correct gene deletion by PCR (Figure 3.14A). PCR analyses using a gene-specific forward primer for Ubp15, and a generic HIS3 reverse primer would show a correct *ubp15*Δ band at approximately 1600bp. In a wild type strain a PCR product would not be produced (Figure 3.14A). After confirmation of a correct *ubp15*Δ deletion mutant, the W303 derived

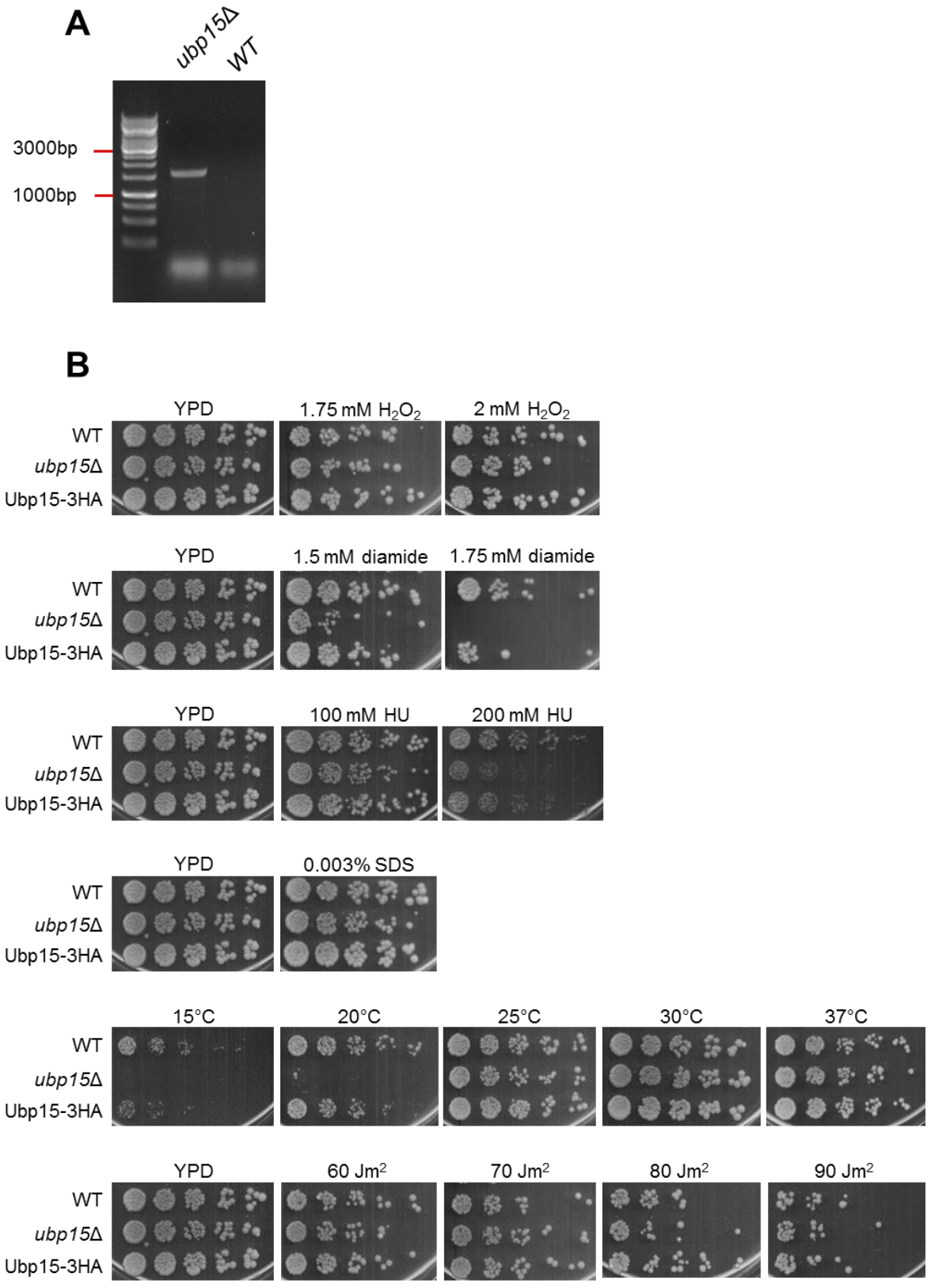
A
ubp15Δ
WT
3000bp
1000bp
B
YPD
1.75 mM H2O2
2 mM H2O2
WT
ubp15Δ
Ubp15-3HA
YPD
1.5 mM diamide
1.75 mM diamide
YPD
100 mM HU
200 mM HU
YPD
0.003% SDS
15°C
20°C
25°C
30°C
37°C
YPD
60 Jm2
70 Jm2
80 Jm2
90 Jm2

**Figure 3.14: Analysis of the effects of epitope tagging Ubp15.** (A) PCR using Ubp15-specific forward and generic His reverse primers was performed using DNA isolated from *ubp15*Δ (FCC60). Successful deletion of the *UBP15* gene produces a PCR product of ~1600bp. The resulting PCR product was analysed on a 1% agarose gel together with a wild type control using the same primers (A). (B) 5-fold serial dilutions of wild type (FCC1), *ubp15*Δ (FCC60), and a strain expressing Ubp15-3HA (FCC130) from the normal chromosomal locus grown to mid-log phase in YPD, were spotted onto YPD plates containing the indicated concentrations of different stress inducing agents. Plates were incubated at 30°C for 3 days before imaging.

strains expressing Ubp15-3HA, together with a *ubp15*Δ strain and wild type control were grown to mid-log phase and their response to different stress conditions examined (Figure 3.14B). Significantly, compared to wild type and *ubp15*Δ it was found that the strain expressing Ubp15-3HA from the normal chromosomal locus had very little effect on protein function, with the possible exception of cold stress, although not to the same extent as *ubp15*Δ. Taken together these results suggest that epitope tags do not affect the function of Ubp15-3HA. Importantly, although the different strain backgrounds show differences in forming HMW complexes in response to stress, the presence of the complexes is independent of strain background and epitope tag.

## 3.3. Discussion

While the detrimental effects of high levels of ROS are well characterised, the beneficial effects of low ROS levels are only recently becoming apparent. The mechanisms underlying how cells distinguish between low and high ROS levels to respond appropriately are not well understood, however oxidation of redox sensitive catalytic cysteines appears to be an important part of this regulation. dUbs have a conserved catalytic cysteine (Amerik *et al.*, 2000) which have the potential to be oxidised by ROS (Clague, 2013). Hence, it was possible that the relative sensitivities of different dUb cysteines to ROS could determine cellular responses to ROS. To investigate this hypothesis we have utilised the genetic tools available to investigate dUbs in response to ROS in *S. cerevisiae*. Using the readily available *S. cerevisiae* gene deletion strain collection (Giaever *et al.*, 2002) and TAP epitope tag strain collection (Ghaemmaghami *et al.*, 2003a) all available dUb-TAPs and dUb deletion strains were exposed to three different types of oxidative stress, $H_2O_2$, diamide (glutathione oxidiser) and menadione (superoxide producer). Interestingly diverse roles and specific sensitivities were observed using the gene deletion strains, and certain dUbs become modified in response to specific oxidising agents (Table 3.2).

Using the strains acquired from the *S. cerevisiae* gene deletion collection, the specific roles of dUbs in response to different oxidising agents was observed.

Importantly, all the dUbs investigated showed some indication of increase in sensitivity or resistance to the different oxidising agents. Certain dUb deletion strains showed a growth phenotype to only one oxidising agent tested. For example *ubp9*Δ and *ubp11*Δ showed increased sensitivity only to $H_2O_2$, and *ubp7*Δ only showed increased sensitivity to menadione, whereas *ubp1*Δ showed an increased resistance to $H_2O_2$ specifically. In contrast to this many dUbs showed sensitivity or resistance to multiple different oxidising agents. For example *yuh1*Δ, *otu1*Δ, and *ubp16*Δ all show increased sensitivity to both $H_2O_2$ and menadione, and *ubp15*Δ has increased sensitivity to diamide and menadione. It is also interesting to note that many of the dUb deletion strains show differences in sensitivity and resistance to different oxidising agents. For example, *ubp2*Δ is extremely sensitive to $H_2O_2$ however shows increased resistance to diamide, and *ubp12*Δ is resistant to diamide but shows increased sensitivity to menadione. The difference in sensitivity and resistance to certain oxidising agents suggests dUbs have specific responses to different oxidising agents. Since this study began, another study has looked at all dUbs in *S. cerevisiae* and their response $H_2O_2$ (Huseinovic *et al.*, 2018). The research confirms many of the phenotypes shown by the dUbs in this screen in response to $H_2O_2$, including increased resistance in *ubp1*Δ strain, and increased sensitivity in *otu2*Δ, *ubp2*Δ, and *ubp3*Δ (Huseinovic *et al.*, 2018), however the authors do not go into detail on the specific sensitivities the dUbs show in response to $H_2O_2$. However it must be remembered that the results gained may not be complete answers about dUb sensitivity to ROS due to the redundancy of dUbs across the cell (Amerik *et al.*, 2000; Kouranti *et al.*, 2010; Ostapenko *et al.*, 2015). While dUbs have specific cellular roles that many research groups are investigating, their similar domain architecture, specifically the similarity in active site, allows dUbs to potentially fulfil roles normally carried out by other dUbs. Hence deletion of a single dUb may show little phenotype in response to stress. Indeed, a strain with 5 dUbs deleted (*ubp1*Δ*, ubp2*Δ*, ubp3*Δ*, ubp7*Δ*,* and *ubp8*Δ) showed the same growth under normal growth conditions to a single *ubp8*Δ deletion strain (Amerik *et al.*, 2000) indicating the large redundancy of the dUbs. A technique that may overcome this problem is to over-express dUbs individually and repeat the spot tests performed, to see if any increased sensitivity or resistance is recovered and to identify which protein inhibit or activate cell resistance. It is also

important to note that not all the dUb deletion mutants were available. Hence, it is possible that Ubp4, Ubp10, and/or Ubp14 may have roles which were not investigated in this thesis. However in other published studies of *S. cerevisiae* dUbs it was found that *ubp4*Δ, *ubp10*Δ, and *ubp14*Δ strains have similar growth phenotypes to wild type in unstressed conditions (Amerik *et al.*, 2000; Huseinovic *et al.*, 2018).

One dUb of note in this screen was *ubp3*Δ, which showed increased sensitivity to all of the oxidising agents tested, suggesting Ubp3 may play a more general role in oxidative stress responses. Importantly, this analysis is consistent with other studies which have been published since work on this thesis began revealing that ubp3Δ is more sensitive to $H_2O_2$ (Jin, 2017; Huseinovic *et al.*, 2018), and diamide (Dodgson *et al.*, 2016). Interestingly *ubp3*Δ sensitivity is not limited to only oxidative stress. Huseinovic *et al* (2018) investigated all *S. cerevisiae* dUbs to many different stresses including rapamycin, ibuprofen, and benomyl among others suggesting Ubp3 is needed for most stress responses. Interestingly, *ubp3*Δ did not show a growth phenotype in response to the DNA damaging agents MMS (which methylates DNA (Hanway *et al.*, 2002)) or HU (which inhibits DNA synthesis and repair (Koc *et al.*, 2004), suggesting Ubp3 is not required for DNA damage responses. Since this thesis work was performed, subsequent work published in 2016 identified that lacking Ubp3 were unable to form stress granules, leading to a decrease in cell survival in stationary phase (Nostramo *et al.*, 2016). While this group only looked at temperature associated stress responses and not oxidative stress responses, it is possible that Ubp3 is important for the response to oxidative stress in a similar mechanism. Ubp3 has also been associated with mitochondrial control as a negative regulator of mitophagy (Müller *et al.*, 2015). Mitophagy is an important cellular response as a mechanism to remove mitochondria damage by ROS (Müller and Reichert, 2011). As mitochondria are intracellular ROS producers, any regulation of Ubp3 by ROS has potentially important stress response roles. The sensitivity of *ubp3*Δ to $H_2O_2$, diamide, and menadione suggests that cells which cannot undergo mitophagy are less resistant to oxidative stress.

When investigating potential modifications to the dUbs in response to the oxidising agents, all experiments were carried out under non-reducing conditions to preserve the potential modifications that would affect mobility. Several dUbs, Ubp2, Ubp5, Ubp6, Ubp12, Ubp14, and Ubp15, showed altered mobility suggesting protein modification. The modifications were not characterised here, but possibilities include oxidation events, phosphorylation, and ubiquitination among others. The nature of the modification to Ubp12 and Ubp15 will be explored in chapters 4 and 5. Similar to the sensitivity data associated with the gene deletion strains, the specificity of the dUb modifications is apparent (Table 3.2). Again a range of responses are seen, however in contrast to the sensitivity data where all of the dUb deletion strains showed some response to ROS, only a small number of dUbs show any modification in response to ROS. However, again it must be noted that, similar to the dUb deletion strain collection, not all the dUbs were available in the epitope tag collection for study. Thus investigations of any potential modifications of Ubp7, Ubp13, and Yuh1 were not performed preventing a complete understanding of dUb modifications in response to different oxidising agents. Of the six TAP epitope-tagged dUbs that showed change in mobility, three showed modifications specific to one type of oxidising agent. Ubp2, Ubp6 and Ubp12 showed modification specific to $H_2O_2$. The specificity of these dUbs to modifications by $H_2O_2$ suggests their potential role in signalling pathways, as $H_2O_2$ is a potent signalling molecule. This nature of certain dUbs being modified in response to specific types of ROS may potentially suggest the tight regulation of downstream deubiquitination is critical for cellular function, although it remains unknown whether the modifications identified in this work enables or inhibits protein activity. The method of detection of modification must also be considered. In this case NEM was added to protein samples after oxidation to preserve the oxidation event. However, using NEM to maintain oxidation states only shows modifications that cause a change in mobility, for example a disulphide in response to oxidation, or phosphorylation. In order to have a wider understanding of dUb modification by oxidative stresses AMS could be used to bind to oxidised cysteines, thus increasing the molecular weight and mobility of oxidised proteins. However chemicals such as AMS only increase protein size by a small shift (0.5 kDa (Rudyk and Eaton, 2014)), which may be hard to detect in proteins as large as the dUbs. As such a dramatic effect was

observed to specific dUbs when using NEM it concluded that these dUbs would be focused upon, however to have a more comprehensive understanding of dUb modification by oxidising agents other methods could also be investigated.

Research published since work on this thesis began has identified that Ubp2 is oxidised in response to $H_2O_2$ but not in response to other stresses (Silva *et al.*, 2015a). Silva *et al* (2015) found that in response to low levels of $H_2O_2$ K63 poly-ubiquitination levels dramatically increased in order to overcome $H_2O_2$ induced stress. They found the K63 poly-ubiquitination to be due to the reversible oxidation and thus inhibition of Ubp2 (Silva *et al.*, 2015a) which normally functioned to remove K63 linked chains. As seen in figure 3.7B, Ubp2 is occasionally modified by $H_2O_2$, however this was not repeatable. However, as the shift is quite faint for Ubp2 after $H_2O_2$ treatment it is possible that in the time frame investigated, or concentration of $H_2O_2$ used, Ubp2 modification may have been missed. It is possible that the modification of Ubp2 observed in the present results may be linked to Ubp2 oxidation and could be important for K63 regulation in response to stress. Although there has been very little research looking into the modification of dUbs, it has been observed that mammalian USP19 forms a HMW complex at ~250 kDa in response to $H_2O_2$ (Lee *et al.*, 2013). Curiously,the HMW disulphide for USP19 is a very similar size to that of Ubp12 modification in response to $H_2O_2$ in the present results, suggesting possible linked events.

It is striking from the results shown, that two particular dUbs showed very large HMW shifts after treatment with specific oxidising agents. Ubp12-TAP formed a HMW shift after only $H_2O_2$ treatment, and Ubp15-TAP showed a HMW shift after $H_2O_2$ and diamide treatment. Interestingly, Ubp12 had a $H_2O_2$ induced HMW modification which contained a large portion of the total protein. Further analyses indicated that ~40% of Ubp12 was modified independent of strain background or epitope tag. Although the closest mammalian homolog to Ubp12 is USP15 (and the related USP11 and USP4), when comparing the mammalian USP19 dUb to the *S. cerevisiae* genome, Ubp12 has the highest similarity. This suggests that Ubp12 may be oxidised similarly to USP19 in mammalian cells. Importantly, Lee *et al* (2013) also identified that USP15 was inactivated by ROS, suggesting Ubp12 has the potential to be oxidised which will be investigated further in

chapter 4. The other dUb found to be modified in response to oxidising agents was Ubp15, which formed HMW forms in response to $H_2O_2$ and diamide. Thus Ubp15 shows less specificity for regulation by oxidation; however it does not show modifications in response to menadione. It is striking that the response by Ubp15 to oxidising agents closely resembles that of Cdc34, which was found to be oxidised in response to $H_2O_2$ and diamide, but not menadione. Importantly, Cdc34 oxidation has been shown to be critical in regulating G1-S phase progression through ubiquitination of Sic1 (see Section 1.3.3). Interestingly, Ubp15 has also been hypothesised to regulate the cell cycle as it is a known physical interactor with the APC/C activator Cdh1 (Bozza and Zhuang, 2011), whereby Ubp15 potentially regulates cell cycle proteins. This raises the exciting possibility that both Ubp15 and Cdc34 are oxidised in response to $H_2O_2$ and diamide in order to regulate cell cycle progression. It must also be noted that although it is known that the HMW Cdc34 complex formed by oxidative stress contains Cdc34 and Uba1, it is possible that the complex also contains other unknown proteins. The potential link between Ubp15 and Cdc34 oxidation and the subsequent cell cycle regulation will be investigated further in chapter 5.

In conclusion we have identified specific dUb requirements for different oxidative stresses, suggesting that dUbs have diverse roles and responses to oxidising agents. We have also identified a novel range of modifications of different dUbs in response to specific oxidising conditions. Ubp12 and Ubp15 will be explored further in this these, but it is clear that dUbs have many roles in cellular response to stress which, although worthy of further study, is outside the scope of this thesis.

# Chapter Four: Analyses of the roles and regulation of the dUb Ubp12 in stress responses.

## 4.1. Introduction

*S. cerevisiae* has 20 identified deubiquitinases, 16 of which form the main cysteine thiol USP group (Finley *et al.*, 2012). USP dUbs have a highly conserved active site containing histidine and aspartic acid residues which deprotonate the catalytic cysteine allowing it to attack the isopeptide bond between the ubiquitin moiety and the substrate (Amerik and Hochstrasser, 2004) (see 1.1.2.2). Deprotonation of the catalytic cysteine reduces the pKa value of the cysteine and as a consequence increases its susceptibility to attack by oxidation (Finkel, 2011). Although Ubp12 is a relatively uncharacterised USP dUb in *S. cerevisiae* a recent study revealed that it can cleave ubiquitin indiscriminately from the ends of longer lysine linked chains (Schaefer and Morgan, 2011). Ubp12 is also known to regulate mitochondrial dynamics through deubiquitination of the mitofusin Fzo1 (Anton *et al.*, 2013), and has been observed to deubiquitinate the G-protein α subunit Gpa1, which changes the localisation from the cellular membrane to the cytoplasm and vacuole (Wang *et al.*, 2005). Excitingly, work presented in the previous chapter revealed that Ubp12 forms a $H_2O_2$-induced HMW complex, independent of epitope tag and strain background. Furthermore, this is very specific as Ubp12 was only modified in response to $H_2O_2$ and no other oxidising agent tested. These data suggest that Ubp12 is specifically regulated by $H_2O_2$. As Ubp12 is a member of the thiol USP group (see above) this raises the exciting possibility that the oxidation of the catalytic cysteine of Ubp12 may be a mechanism by which the protein is regulated, thus affecting downstream targets. In this chapter we aimed to understand the nature of Ubp12 modification in response to $H_2O_2$. Specific objectives were to investigate the possibility that Ubp12 is regulated by oxidation and to elucidate the potential roles and regulation of Ubp12 by oxidative stress.

## 4.2. Results

### *4.2.1. Analysis into the $H_2O_2$-induced HMW form of Ubp12*

When analysing proteins by western blotting, changes to protein mobility can occur for many different reasons including post translation modifications, such as phosphorylation, ubiquitination, and/or oxidation (Carruthers *et al.*, 2015). For example, phosphorylation of proteins by the addition of a phosphate group(s) can cause the phosphorylated protein to change shape and size and therefore affect protein mobility (Peck, 2006). In addition, phosphorylation can influence the interaction with phospho-binding proteins. Similarly, ubiquitination of a protein can increase protein size by either the addition of a single ubiquitin molecule, or of chains of poly-ubiquitin. Proteins can also become oxidised at cysteine residues, which can result in the change of protein structure and potentially initiate disulphide intermolecular or intramolecular interactions with other cysteine residues possibly changing the size of the complex (Cumming *et al.*, 2004; Doris *et al.*, 2012).

To investigate the $H_2O_2$-induced HMW form of Ubp12, the possibility that Ubp12 was becoming oxidised was examined. Hence, cells expressing Ubp12-TAP weres treated with 2 mM $H_2O_2$. Protein extracts were then prepared in either reducing or non-reducing conditions, and analysed by western blot (Figure 4.1). When incubated in the presence of β-mercaptoethanol as a reducing agent, the $H_2O_2$-induced HMW form of Ubp12 was no longer present (Figure 4.1), suggesting that the HMW complex contained disulphide bond(s) and/or a sulphenylamide as a result of oxidation by $H_2O_2$. Although it is unclear whether the $H_2O_2$-induced HMW form of Ubp12 contains disulphide(s) or sulphenylamide(s), the highly reactive and transient nature of sulphenylamides (Rehder and Borges, 2010), and their potential to rapidly form disulphides (Gupta and Carroll, 2014), supports the hypothesis that the $H_2O_2$-induced HMW form of Ubp12 contains at least one disulphide.

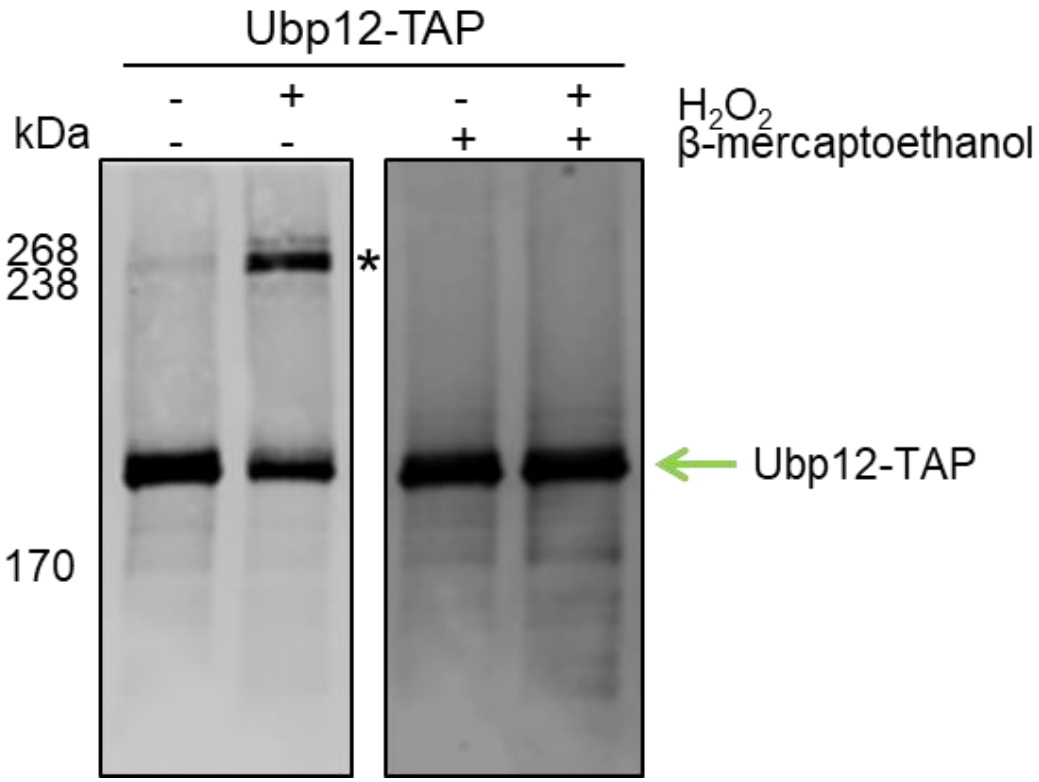


**Figure 4.1: Ubp12 HMW complex is reduced by β-mercaptoethanol.** Cells expressing Ubp12-TAP (ELR38) in the BY4741 strain background were incubated with 2 mM $H_2O_2$ for 0 (-) and 10 (+) minutes. Protein extracts were prepared in reducing (+ 10% v/v β-mercaptoethanol) and non-reducing conditions and separated by SDS-PAGE. Proteins were visualised using PαP antibodies. * denotes $H_2O_2$-induced modification.

#### *4.2.1.1. The oxidation of Ubp12 responds to different concentrations of $H_2O_2$*

As described elsewhere (see Chapter1 Section 1.2.5), it is important for cells to be able to sense the different types and concentrations of ROS. Work described in the previous chapter revealed that Ubp12 was specifically modified in response to $H_2O_2$. Having established that this modification of Ubp12 involves oxidation, the next question was to address how this oxidation responds to a range of concentrations of $H_2O_2$. To investigate this, cells expressing Ubp12-6HA were treated with different concentrations of $H_2O_2$ for 10 minutes and protein extracts were analysed by western blot (Figure 4.2). Interestingly, theUbp12 HMW complex was induced by all the concentrations of $H_2O_2$ investigated. However, interestingly, the oxidation pattern was different depending on the concentration of $H_2O_2$ (Figure 4.2). At low concentrations of $H_2O_2$ (0.2 mM), Ubp12 was mainly in the reduced form, with the HMW complex only becoming apparent after a longer film exposure time. Qualitative analyses suggests that the ratio of HMW Ubp12 to low molecular weight Ubp12 peaks at 1 mM $H_2O_2$ and reduced by 2 mM, after which the ratio is maintained, however further repeats and quantification of band intensity would be beneficial to confirm this. The observed difference in the amounts of Ubp12 HMW complex at different concentrations of $H_2O_2$ raises the possibility that oxidation of Ubp12 is a component of a mechanism by which the concentration of $H_2O_2$ is sensed.

However, since these protein samples were all extracted at 10 minutes, it was possible that lower concentrations of $H_2O_2$ may induce higher levels of oxidation of Ubp12 but over a longer timeframe. It was also unknown whether the oxidation of Ubp12 was irreversible. Indeed dUbs can be either reversibly oxidised into a sulphenic form, or irreversibly oxidised into sulphinic and sulphonic forms which could initiate dUb degradation (Clague, 2013). Hence, next the dynamics of Ubp12 HMW complex formation were investigated. Cells expressing Ubp12-6HA were incubated with either 0.2 mM or 2 mM $H_2O_2$ for 60 minutes. Protein extracts were obtained at the indicated time points and analysed by western blot (Figure 4.3). When incubated with 2 mM $H_2O_2$ Ubp12 is rapidly modified into the HMW form within 30 seconds, and this is sustained over the entire hour of the experiment (Figure 4.3A). Strikingly, 30% of Ubp12 is in the HMW complex by 30

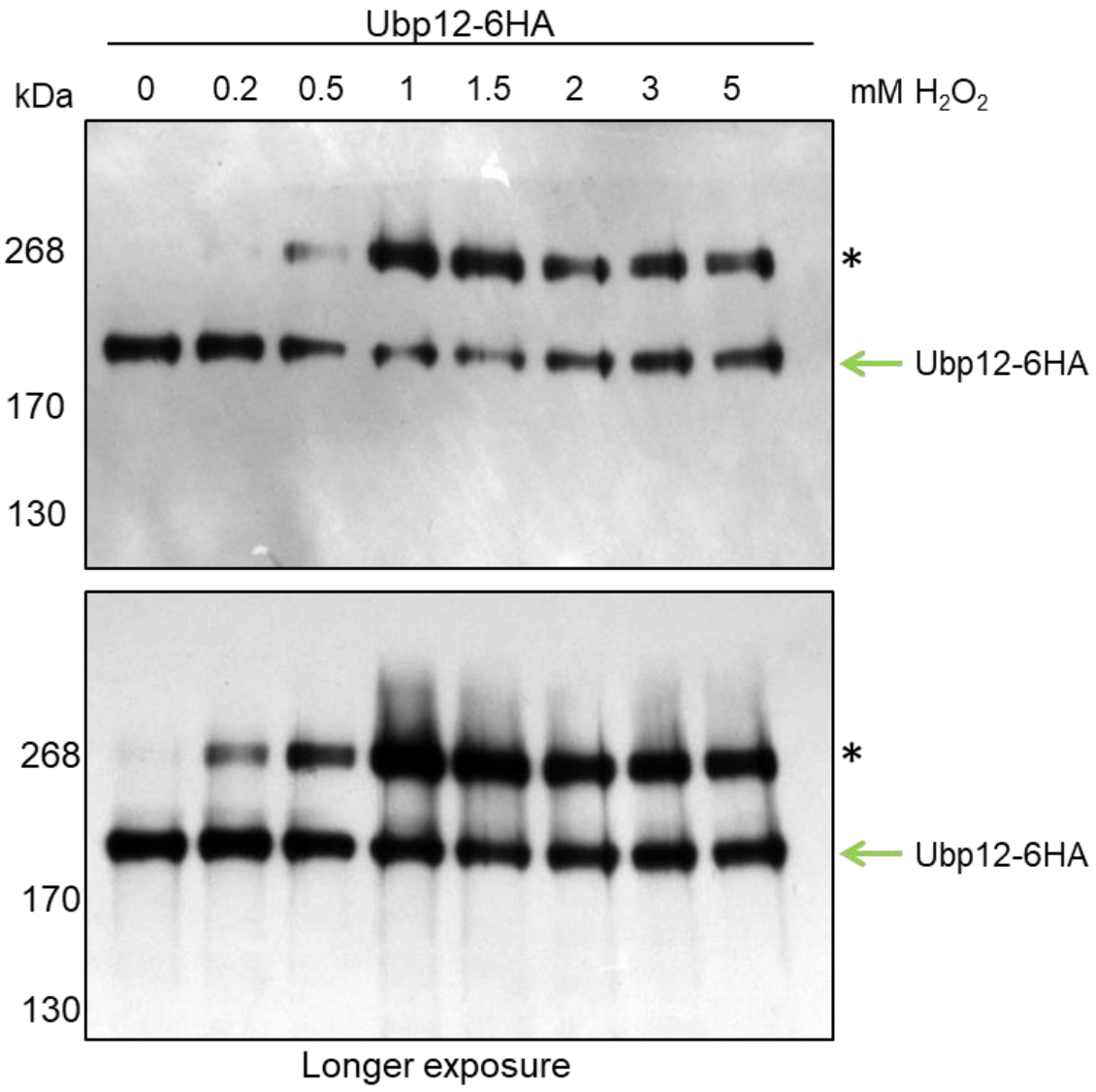


**Figure 4.2: Ubp12 is oxidised by a range of $H_2O_2$ conditions.** Protein extracts from cells expressing Ubp12-6HA (FCC154) in the BY4741 strain background were incubated with a range of concentrations of $H_2O_2$ as indicated for 10 minutes. Protein extracts were prepared in non-reducing conditions and separated by SDS-PAGE. Proteins were visualised using α-HA antibodies. * denotes $H_2O_2$-induced modification. The bottom panel is a longer exposure of the top panel.

**A**

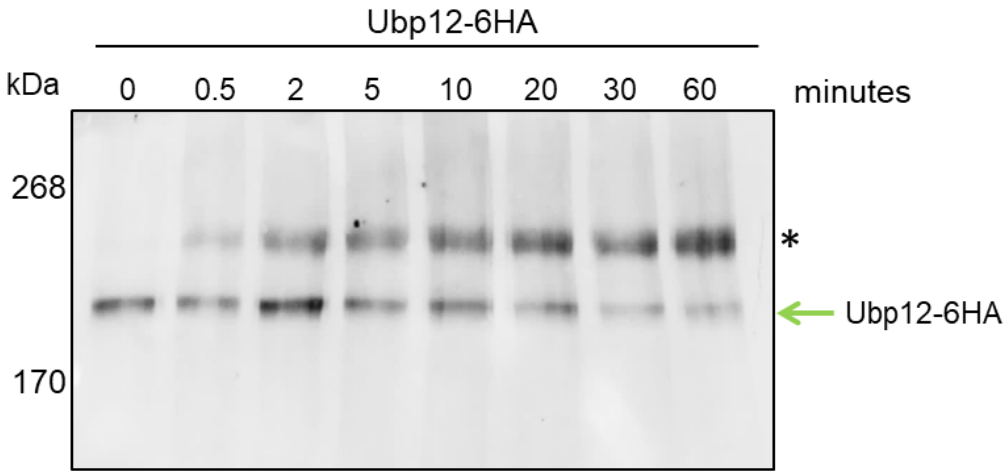
Ubp12-6HA
kDa
0
0.5
2
5
10
20
30
60
minutes
268
170
*
Ubp12-6HA

**B**

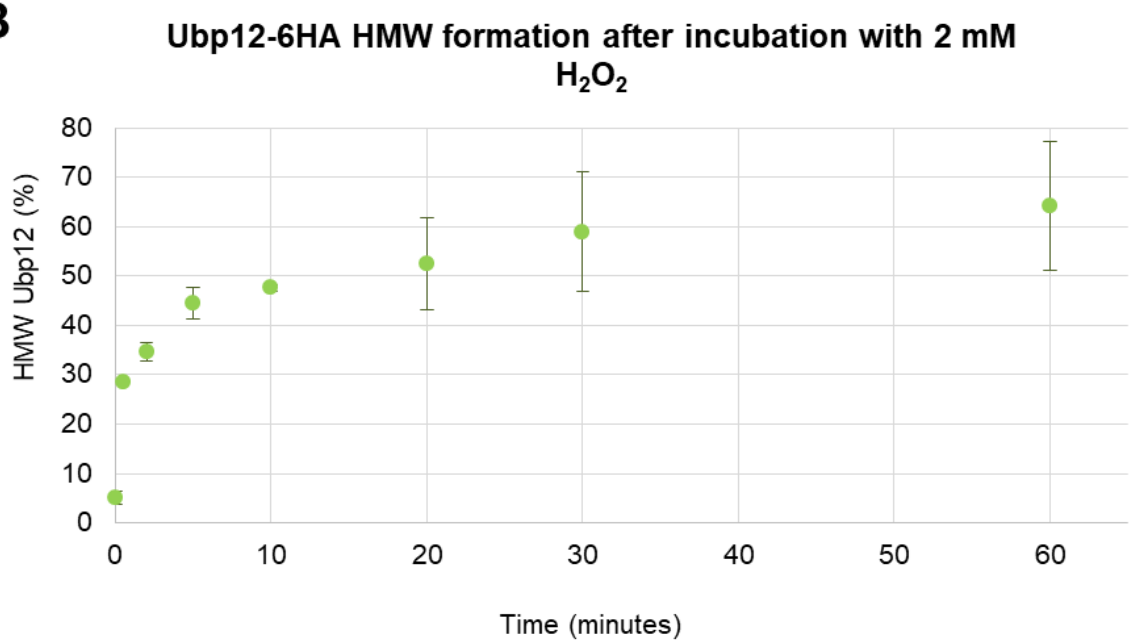
Ubp12-6HA HMW formation after incubation with 2 mM $H_2O_2$
HMW Ubp12 (%)
80
70
60
50
40
30
20
10
0
0
10
20
30
40
50
60
Time (minutes)

**C**

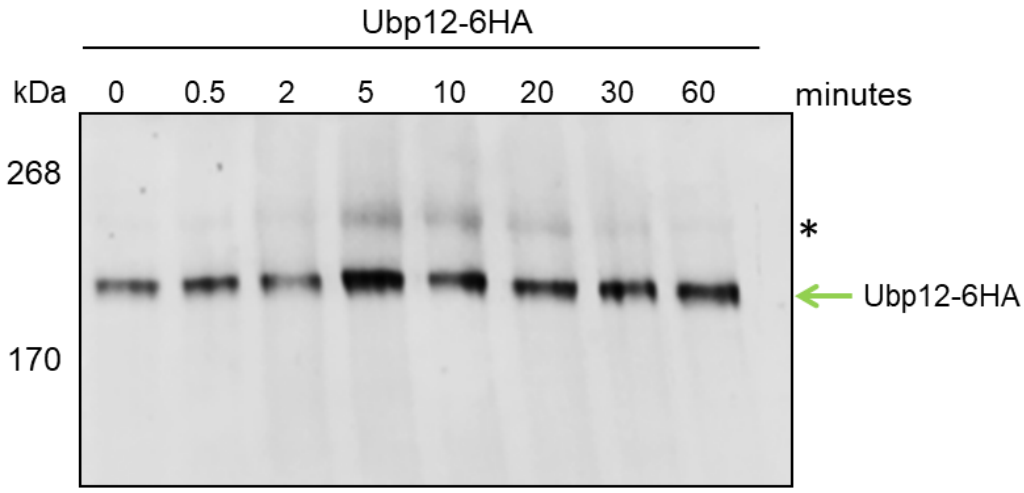
Ubp12-6HA
kDa
0
0.5
2
5
10
20
30
60
minutes
268
170
*
Ubp12-6HA

**D**

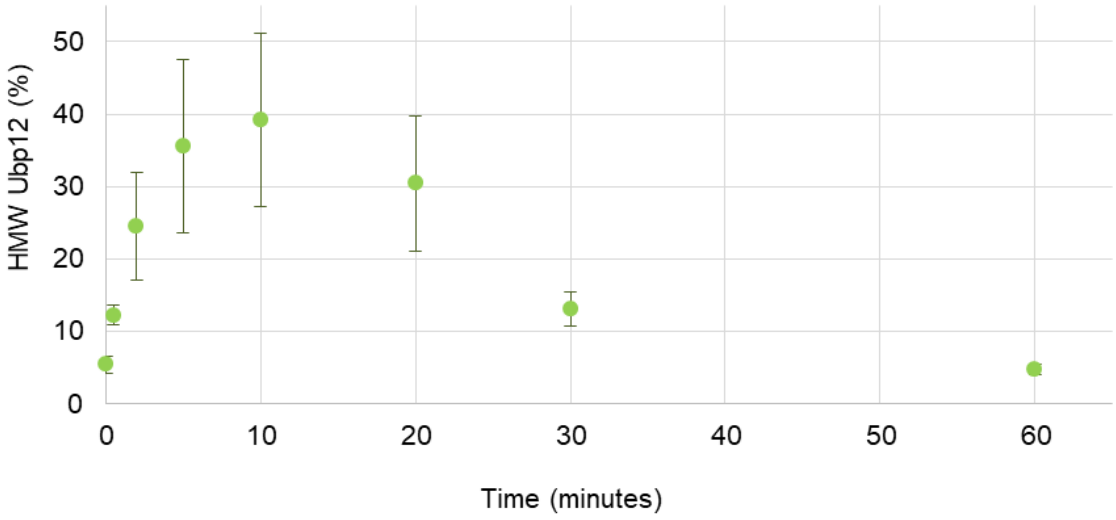
Ubp12-6HA HMW formation after incubation with 0.2 mM H2O2
HMW Ubp12 (%)
50
40
30
20
10
0
0
10
20
30
40
50
60
Time (minutes)

**Figure 4.3: The kinetics of the formation of the HMW form of Ubp12 is $H_2O_2$ concentration-dependent.** (A) Protein extracts from cells expressing Ubp12-6HA (FCC154) in the BY4741 strain background were incubated with 2 mM $H_2O_2$ for 0 – 60 minutes as indicated. Protein extracts were prepared in non-reducing conditions and separated by SDS-PAGE. Proteins were visualised using α-HA antibodies. * denotes $H_2O_2$ induced modification. (B) The band intensities of Ubp12-6HA (n=2) at each time point (from A) were quantified using ImageQuant. Each point shows the percentage of HMW complex with respect to total Ubp12 in each lane, and error bars denote standard error of the mean. (C) Protein extracts from cells expressing Ubp12-6HA were incubated with 0.2 mM $H_2O_2$ for 0 – 60 minutes as indicated. Protein extracts were prepared and visualised as in (A) * denotes $H_2O_2$ induced modification. (D) The band intensities of Ubp12-6HA (n=2) at each time point (from B) were quantified using ImageQuant. Each point shows the percentage of HMW complex with respect to total Ubp12 in each lane, and error bars denote standard error of the mean.

seconds (Figure 4.3B). After this, the amount of Ubp12 present in the HMW complex increases at a much slower rate until 60 minutes when ~65% is in the complex (Figure 4.3B). Interestingly, the pattern of HMW complex formation is different at 0.2 mM and 2 mM $H_2O_2$. In contrast to 2 mM $H_2O_2$, when cells were incubated with 0.2 mM $H_2O_2$ a smaller amount of Ubp12 was in the in both the 30 second and the 2 minute sample (Figure 4.3C and D). After treatment with 0.2 mM $H_2O_2$ only ~12% of total Ubp12 is in the HMW form at 30 seconds, which increases to ~40% after 10 minutes (Figure 4.3D). Furthermore, after 10 minutes the amount of HMW complex begins to fall, and by 60 minutes has returned to basal levels (Figure 4.3D). The pattern of HMW formation at low levels of $H_2O_2$ suggests that Ubp12 becomes oxidised but significantly, is able to recover its reduced state. The differences in HMW formation at low and high levels of $H_2O_2$ could form the basis of a sensing mechanism for $H_2O_2$ levels whereby high levels of $H_2O_2$ cause Ubp12 to remain in the oxidised form for longer. However, these results cannot distinguish whether oxidised Ubp12 is reduced back to the original reduced form, or whether, perhaps, the oxidised form of Ubp12 is degraded and replaced with newly expressed reduced Ubp12. Interestingly, it is also worth noting that ~5% of Ubp12 is in the HMW form in unstressed conditions, suggesting that Ubp12 oxidation may be a cellular mechanism by which Ubp12 activity is regulated in the absence of external stress.

#### *4.2.1.2. Analysis of the regulation of Ubp12 oxidation*

Oxidised proteins are regulated both enzymatically and non-enzymatically to maintain a redox balance within the cell (see Chapter 1 Section 1.2.4). Eukaryotes utilise two key non-enzymatic systems by which oxidised proteins are regulated, the glutaredoxin (Grx) and thioredoxin (Trx) pathways (see Section 1.2.4.2). Glutathione (GSH) is an essential peptide found in the cytosol that can be oxidised by ROS into a GSSG form or protein-bound GSH (see Section 1.2.4.2.1). Importantly, redox cycling of GSH by the glutaredoxin system allows GSH to act as a ROS scavenger to regulate the oxidation of many proteins (see Section 1.2.4.2.2). The chemical BSO inhibits Gsh1, which as a consequence depletes GSH in cells (Drew and Miners, 1984). Hence, BSO can be utilised to investigate whether GSH is required for the regulation of specific oxidised

proteins. Indeed, it has been shown previously that BSO addition triggers the formation of Cdc34 HMW complex similar to that observed after oxidation of Cdc34 by $H_2O_2$ and diamide (Doris *et al.*, 2012). To investigate whether GSH plays a role in the regulation of Ubp12 HMW complex formation, cells expressing Ubp12-6HA were incubated with 5 mM BSO. Cells expressing Cdc34-13Myc were included as a positive control. However, despite multiple repeated attempts, the results obtained were inconclusive as the BSO-induced HMW form of Cdc34-myc was difficult to observe in the positive control (data not shown).

Another major eukaryotic system to regulate oxidised proteins is the thioredoxin system (see Section 1.2.4.2.3). Thioredoxins (Trx) reduce disulphides that are formed by oxidative stress by forming a disulphide with the oxidised cysteine of the substrate. The reduction of the substrate then initiates oxidation of the Trx which in turn is reduced by thioredoxin reductase and NADPH (see Chapter 1 Figure 1.7). It is necessary for thioredoxin reductase to be active to maintain a reduced state within the cell; therefore thioredoxin reductase can be classed as a rate limiting step in the reduction of oxidised thiols by the thioredoxin system (Brown *et al.*, 2013; Tomalin *et al.*, 2016). To investigate whether Ubp12 is regulated by the thioredoxin pathway, a *trr1*Δ mutant expressing Ubp12-3HA from the normal chromosomal locus was created in the W303 strain background. A 3HA epitope tag PCR cassette, containing KanMX, was introduced into the 3' end of the *UBP12* gene at the normal chromosomal locus (described in Section 2.2.3.2) in the *trr1*Δ strain. Potential integrants were analysed by PCR to confirm the integration of the 3HA epitope tag cassette (Figure 4.4A). The presence of a PCR product of ~2300bp indicates correct integration whilst a PCR product of ~400bp indicates the wild type *UBP12* locus. Several positive integrants were identified (Figure 4.4A). Next, three different *trr1*Δ strains containing the Ubp12-3HA cassette were grown to mid-log phase and incubated with 2 mM $H_2O_2$. Proteins were extracted in non-reducing conditions in the presence of NEM and analysed via western blot (Figure 4.4B). As expected, Ubp12-3HA *TRR1* forms the HMW complex after $H_2O_2$ treatment, and quantification suggests ~40% Ubp12 is in the HMW form (Figure 4.4B and C), as seen previously (Figure 3.11). Importantly, there is no Ubp12-3HA observed in the *trr1*Δ control strain, however a non-specific band can still be identified. Interestingly, there is a clear indication

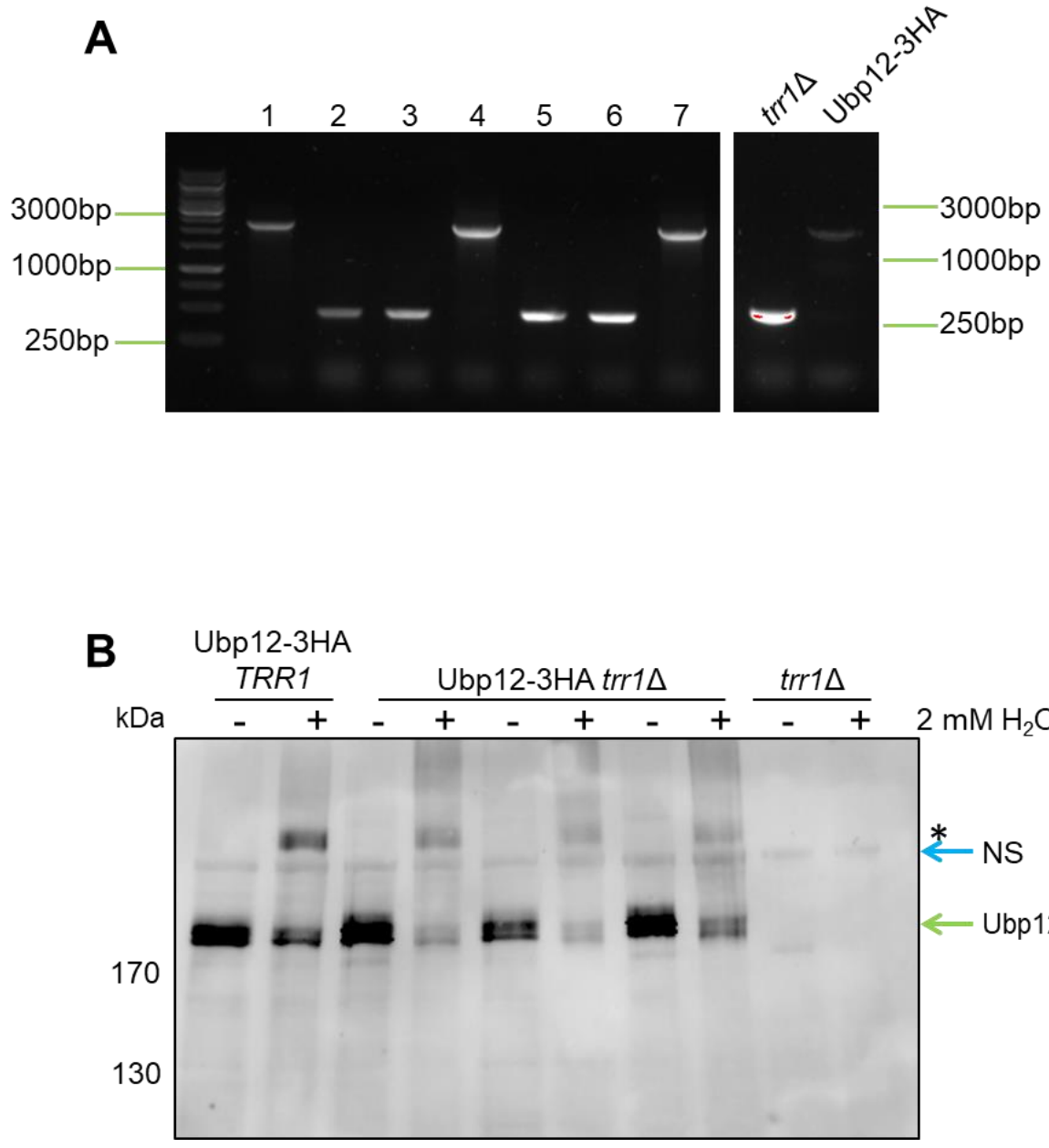
A
1
2
3
4
5
6
7
trr1Δ
Ubp12-3HA
3000bp
1000bp
250bp
3000bp
1000bp
250bp
B
Ubp12-3HA
TRR1
Ubp12-3HA trr1Δ
trr1Δ
kDa
- + - + - + - + - +
2 mM H2O2
*
NS
Ubp12-3HA
170
130

**C**

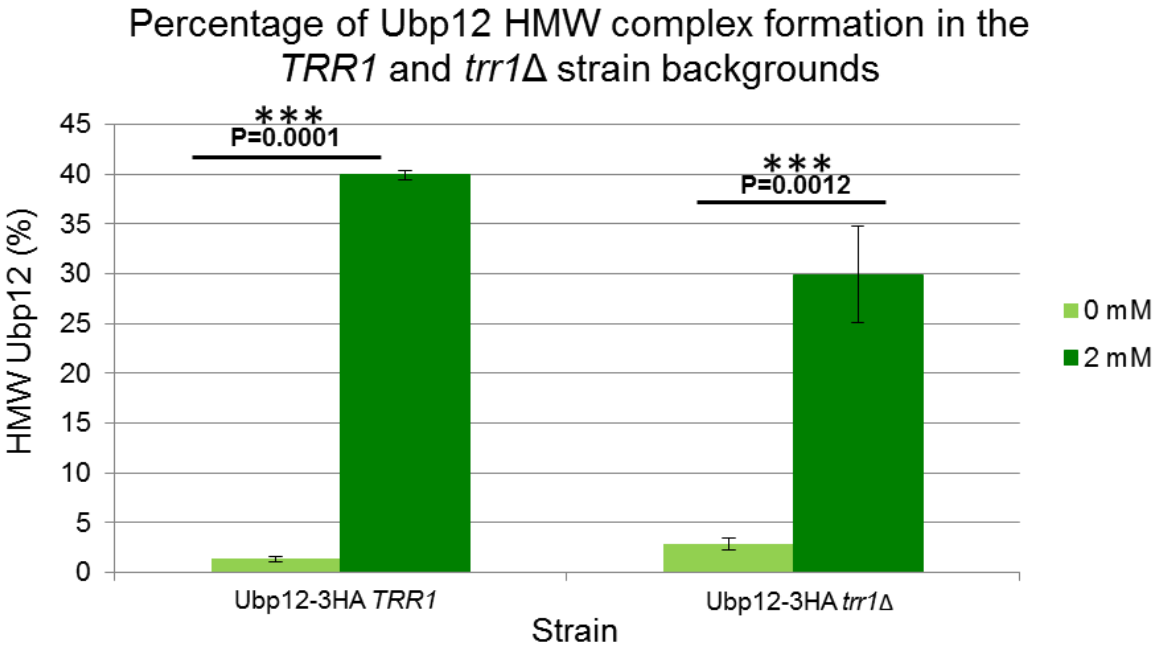
Percentage of Ubp12 HMW complex formation in the TRR1 and trr1Δ strain backgrounds
HMW Ubp12 (%)
45
40
35
30
25
20
15
10
5
0
***
P=0.0001
***
P=0.0012
0 mM
2 mM
Ubp12-3HA TRR1
Ubp12-3HA trr1Δ
Strain

**D**

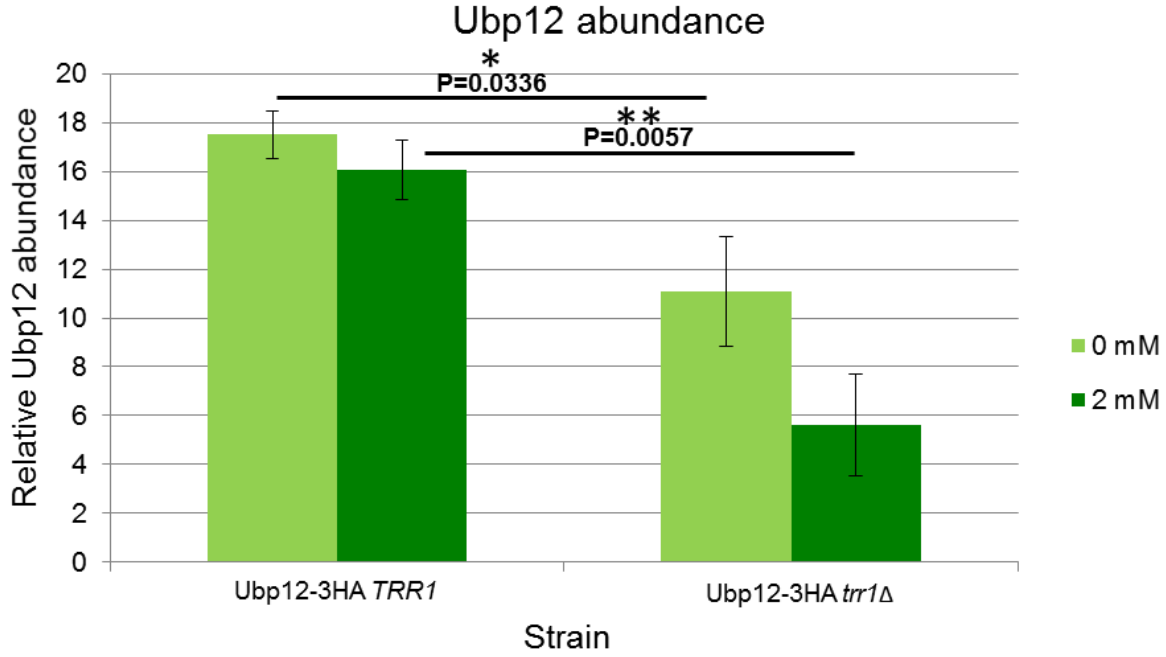
Ubp12 abundance
Relative Ubp12 abundance
20
18
16
14
12
10
8
6
4
2
0
*
P=0.0336
**
P=0.0057
0 mM
2 mM
Ubp12-3HA TRR1
Ubp12-3HA trr1Δ
Strain

**Figure 4.4: Ubp12 oxidation is potentially regulated by the thioredoxin system.** (A) PCR using *UBP12*-specific forward and reverse primers was performed using DNA isolated from 7 potential integrants of the 3HA epitope tag cassette into the *trr1*Δ strain (FCC167). Successful integration of the 3HA epitope tag cassette at the *UBP12* gene locus produces a PCR product of ~2300bp (lanes 1, 4, and 7), whereas the *UBP12* wild type locus produces a PCR product of ~400bp (lanes 2, 3, 5, and 6). The resulting PCR products were analysed on a 1% agarose gel. The right panel shows PCR with an untagged *trr1*Δ negative control (FCC167) and a Ubp12-3HA positive control (FCC93) using the same primers. (B) Cells of a Ubp12-3HA strain (FCC93), a *trr1*Δ strain (FCC167), and three *trr1*Δ Ubp12-3HA strains (FCC171, 172, 175), all W303 strain background, were treated with 2 mM $H_2O_2$ for 0 (-) and 10 (+) minutes. Protein extracts were prepared in non-reducing conditions and separated by SDS-PAGE. Proteins were visualised using α-HA antibodies. NS identified a non-specific band in each lane used as a loading control. (C) The band intensities of Ubp12-3HA *TRR1* (n=4) and Ubp12-3HA *trr1*Δ (n=3) were quantified using ImageQuant. The percentage of HMW complex with respect to total Ubp12 is shown in each lane, and error bars denote standard error of the mean. T-test analysis between 0 and 2 mM $H_2O_2$ for Ubp12-3HA gives a value of P=0.000, and for *trr1*Δ Ubp12-3HA gives a value of P=0.0012. (D) The band intensities of Ubp12-3HA (n=4) *trr1*Δ Ubp12-3HA (n=3) were quantified using ImageQuant. The total protein abundance of Ubp12 in each lane was calculated relative to the non-specific (NS) band (from B) indicated by the arrow. Error bars denote standard error of the mean. T-test analysis between both strains without $H_2O_2$ gives a value of P=0.0336, and T-test analysis between both strains after $H_2O_2$ treatment gives a value of P=0.0057.

of HMW complex formation in the Ubp12-3HA *trr1*Δ cells following $H_2O_2$ treatment (Figure 4.4B). The percentage of Ubp12 HMW complex formation was quantified in relation to the total amount of Ubp12 in the *trr1*Δ strain background (Figure 4.4C). However, the percentage of HMW complex in the *trr1*Δ strain after $H_2O_2$ treatment is 30%, compared to 40% seen in the *TRR1* wild type (Figure 4.4C). Whilst this difference is not quite significant as judged by the P value (P=0.0577), the error bar for the *trr1*Δ mutant strains is quite large (Figure 4.4C). Hence, it is possible that further repeats may reduce the error bars and increase the significance of the observed difference between the *TRR1* and *trr1*Δ strain backgrounds. These data also suggest that basal levels of the HMW form of Ubp12 may be increased in *trr1*Δ cells (Figure 4.4C), however statistical analyses confirm that there is no significant difference between Ubp12-3HA levels in unstressed *TRR1* or *trr1*Δ cells (P=0.0616). Importantly, it was observed that the total amount of Ubp12, both before and after stress, was reduced in the *trr1*Δ mutant compared to the *TRR1* wild type control (Figure 4.4D). In particular, prior to $H_2O_2$ treatment, the amount of Ubp12 present in the *trr1*Δ strain was significantly lower (P=0.036) compared to the wild type strain (Figure 4.4D). Furthermore, following $H_2O_2$ treatment for 10 minutes the relative amount of Ubp12 in the *trr1*Δ mutant strain decreased significantly (P=0.0057) (Figure 4.4D).

Taken together this data suggests that a significant proportion of Ubp12 is oxidised into a HMW complex in response to $H_2O_2$. The data also revealed that the kinetics of complex formation is dependent on the concentration of $H_2O_2$, suggesting that Ubp12 oxidation may be a component of a mechanism that senses and responds to different levels of $H_2O_2$. The results also suggest that the thioredoxin system plays an important role in regulating the levels of Ubp12, both in normal conditions and after $H_2O_2$ stress.

### *4.2.2. Analyses of the Ubp12 HMW complex*

The nature of the $H_2O_2$-induced Ubp12 HMW complex was next examined. One hypothesis to explain the HMW complex is that it consists of a disulphide complex between Ubp12 and on or more other proteins. Hence the first step was to attempt to identify the components of the complex.

*4.2.2.1. Analysis of Ubp12 HMW complex by mass spectrometry*

Oxidised cysteines have the potential to form disulphide bonds with other cysteines. This can be with a cysteine in another protein thus forming an intermolecular dimer or between two cysteines in the same protein, resulting in an intramolecular disulphide bond. Interestingly, it was found that a specific mammalian USP dUb, USP19 forms a HMW disulphide complex which was hypothesised to involve an intermolecular disulphide bond (Lee et al., 2013). Although the closest mammalian homolog of Ubp12 is USP15 (and the related USP11 and USP4), USP19 shares 38% identity with Ubp12, suggesting that the HMW disulphide complex of Ubp12 may also be an intermolecular complex with another protein. Hence, to better understand the Ubp12 HMW complex large scale purification of the Ubp12-TAP protein was performed and the HMW complex analysed by mass spectrometry (University of Aberdeen). Large scale purification of Ubp12-TAP and protein analysis was performed twice. For both analyses, large scale purification was performed using cells expressing using Ubp12-TAP and a wild type control strain, both treated with 2 mM $H_2O_2$ for 10 minutes. However, for the second analysis, large scale purification was also performed using unstressed Ubp12-TAP expressing cells. To isolate the HMW complex, Ubp12-TAP and wild type control cells were incubated with 2 mM $H_2O_2$, soluble proteins were extracted from the lysate (for details see Section 2.1.9), and 1% input of lysate was retained for analysis. Ubp12-TAP was then purified from the lysate using IgG beads (Section 2.1.9), and after conjugation 1% of the lysate was retained to confirm that Ubp12-TAP was bound specifically to the beads and was no longer in the supernatant. Ubp12-TAP was removed from the beads by boiling under non-reducing conditions and samples were separated by SDS-PAGE and stained by Coomassie to visualise the proteins (Section 2.1.9). 1/10 of the sample was retained and visualised by western blot analysis using α-TAP antibodies to confirm the presence of protein at the expected mobility, and to confirm that Ubp12-TAP has been enriched in the purified sample. Importantly, the western blot analyses confirmed Ubp12-TAP in the protein lysate (Figure 4.5A), and that no Ubp12 was present in the supernatant after Ubp12-TAP had been conjugated to the beads. Furthermore, Ubp12-TAP was enriched after removal from the IgG beads (Figure 4.5A). Large smears were observed after

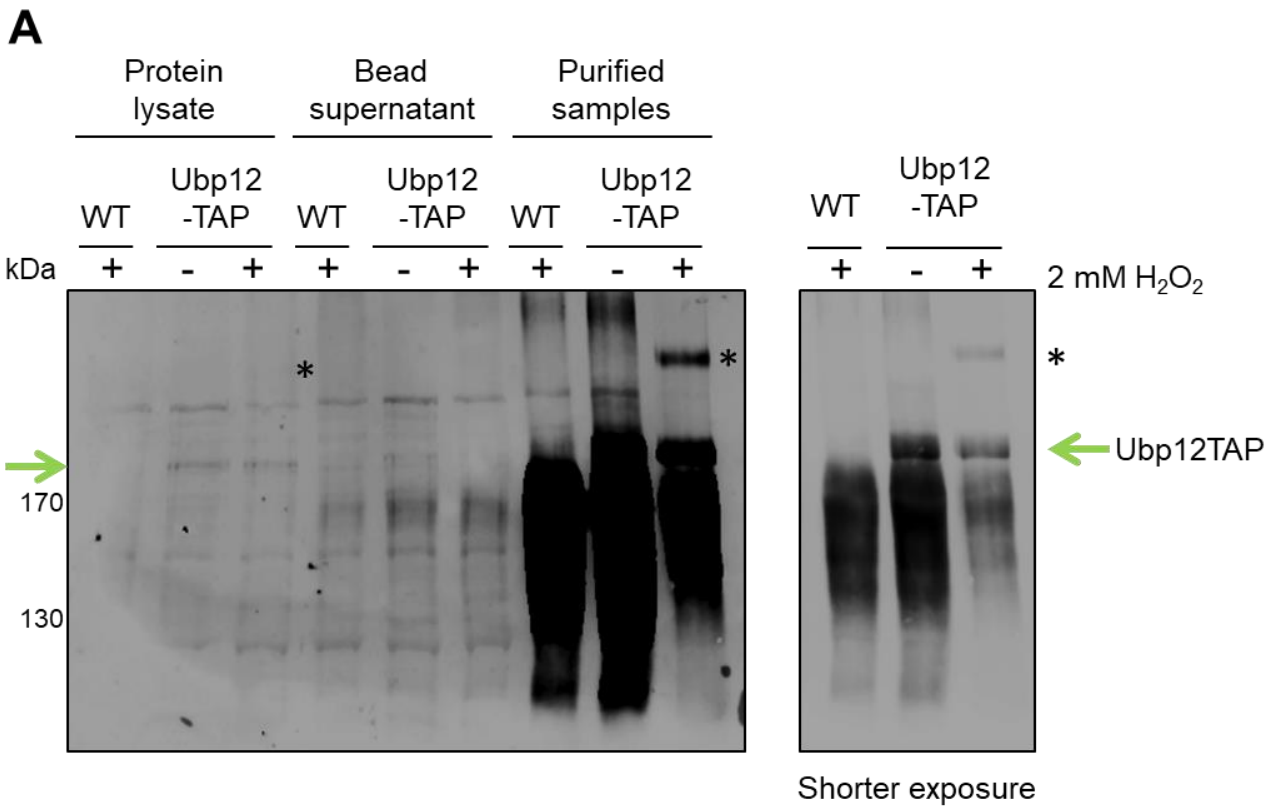
A
Protein lysate
Bead supernatant
Purified samples
WT
Ubp12 -TAP
kDa
+ - + + - + + - +
2 mM $H_2O_2$
170
130
*
Ubp12TAP
Shorter exposure

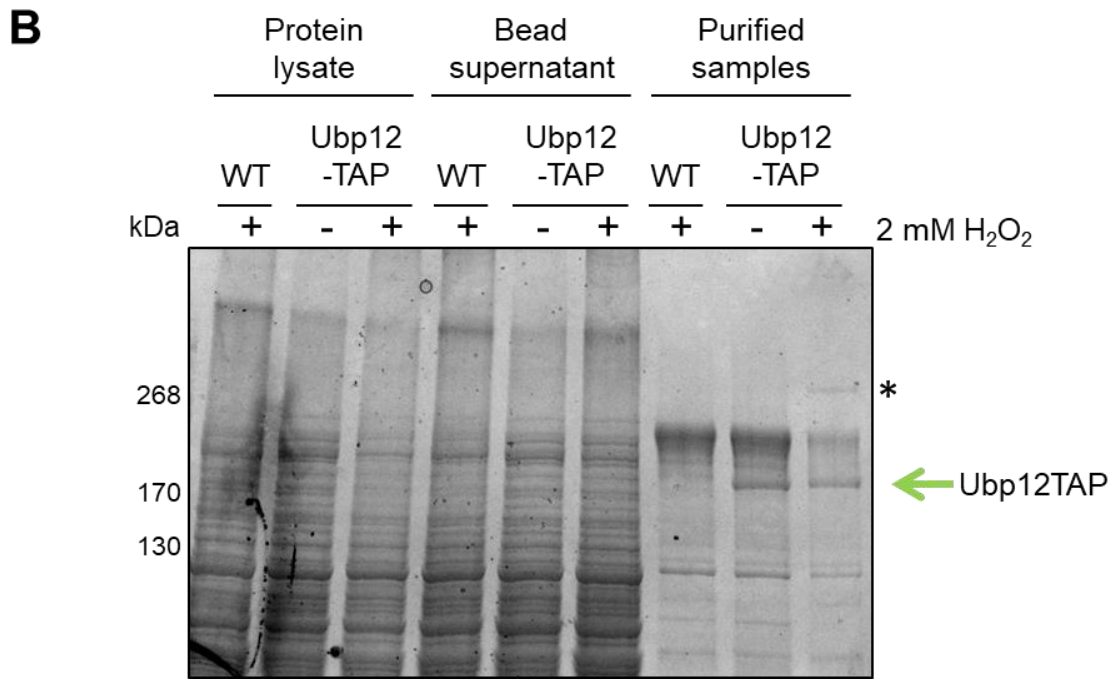
B
Protein lysate
Bead supernatant
Purified samples
WT
Ubp12 -TAP
kDa
+ - + + - + + - +
2 mM $H_2O_2$
268
170
130
*
Ubp12TAP

**Figure 4.5: Sample preparation for mass spectrometry analyses of oxidised Ubp12.** Protein samples were obtained from wild type (WT) (FCC23) and Ubp12-TAP (ELR38) cells in a BY4741 strain background treated with 2 mM $H_2O_2$ for 0 (-) or 10 (+) minutes. Soluble proteins were extracted and prepared in non-reducing conditions. TAP epitope-tagged proteins were purified by binding to IgG beads, washed, and released from the beads by boiling. (A) 1/10 dilutions of protein samples from the whole protein lysate, bead supernatant, and purified samples were separated by SDS-PAGE and visualised using α-TAP antibodies. * denotes $H_2O_2$-induced HMW complex and arrows identify reduced Ubp12-TAP. The right hand panel shows a shorter exposure of the tracks containing purified samples. (B) Protein samples from the whole protein lysate, bead supernatant, and purified samples were separated by SDS-PAGE on a 4-15% gradient gel and stained with InstantBlue. * denotes $H_2O_2$-induced HMW complex and the arrow identifies reduced Ubp12-TAP.

purification (Figure 4.5A), likely from the beads left in the sample which are detected by the secondary antibody. Using Coomassie stain, a band consistent with the mobility of Ubp12-TAP was identified after purification in samples isolated before and after stress. Importantly, $H_2O_2$-induced oxidation of Ubp12 into the HMW disulphide complex was also identified by Coomassie (Figure 4.5B-asterisk).

Next, the $H_2O_2$-induced HMW complex was excised from the Coomassie-stained gel, together with the region of the gel of the corresponding size in the wild type and the unstressed Ubp12-TAP lanes. To identify the proteins present in the excised gel slices, the slices were analysed by mass spectrometry using Q Exactive LC-MS, and potential matches were searched for in the *S. cerevisiae* database (SGD). Mass spectrometry and this computational analysis were performed by David Stead at Aberdeen University. The raw data was analysed and proteins were identified based on the values of score, coverage and peptide number (# peptide). The score indicates the sum of the ion scores of all the distinct peptides, hence a higher score suggests a more confident match. The coverage indicates the percentage of the protein sequence covered by the identified peptides. Finally, the peptide number indicates the total number of distinct peptides identified from a specific protein. Using these analyses, the protein hits were ranked based on their cumulative score (Table 4.1). Importantly, results from both independent purification experiments identified Ubp12-TAP as the major component in the $H_2O_2$-induced HMW complex. However, some other proteins were identified with the potential that they could be part of the HMW complex and hence were investigated further (Table 4.1). For the full lists of mass spectrometry results see Appendix A and B.

In the first mass spectrometry analysis, as expected, Ubp12 was identified in the gel slice of the HMW complex in the Ubp12-TAP lane, with a high score, coverage, and peptide number (Table 4.1A). Moreover, no Ubp12 was identified in the gel slice from the wild type lane at the equivalent mobility. Interestingly, Cex1 was also identified in the Ubp12-TAP sample but not the wild type sample (Table 4.1A). However the score, coverage, and peptide numbers for Cex1 were low, suggesting that Cex1 may be a contaminant of the Ubp12-TAP slice.

**A**

| Gene Name | Protein | MW kDa | WT + $H_2O_2$ | | | Ubp12-TAP + $H_2O_2$ | | |
|---|---|---|---|---|---|---|---|---|
| | | | Score | Coverage | # Peptides | Score | Coverage | # Peptides |
| Ubp12 | Ubiquitin specific protease present in nucleus and cytoplasm | 143.1 | - | - | - | 1491.41 | 40.19 | 37 |
| Cex1 | Component of nuclear aminoacylation-dependent tRNA export pathway | 84.7 | - | - | - | 41.75 | 2.23 | 1 |

**B**

| Gene Name | Protein | MW kDa | WT + $H_2O_2$ | | | Unstressed Ubp12-TAP | | | Ubp12-TAP + $H_2O_2$ | | |
|---|---|---|---|---|---|---|---|---|---|---|---|
| | | | Score | Coverage | # Peptides | Score | Coverage | # Peptides | Score | Coverage | # Peptides |
| Ubp12 | Ubiquitin specific protease present in nucleus and cytoplasm | 143.1 | 292.95 | 12.52 | 11 | 1765.80 | 36.12 | 32 | 4197.79 | 53.99 | 48 |
| His4 | Multifunctional enzyme containing phosphoribosyl-ATP pyrophosphatase; phosphoribosyl-AMP cyclohydrolase, and histidinol dehydrogenase activities | 87.7 | 771.25 | 30.04 | 17 | 581.64 | 23.03 | 13 | 576.24 | 22.03 | 12 |
| Cdc19 | Pyruvate kinase | 54.5 | 399.97 | 36.00 | 11 | 331.71 | 31.60 | 10 | 269.04 | 28.20 | 11 |
| Pdc1 | Major of three pyruvate decarboxylase isozymes | 61.5 | 214.03 | 23.98 | 8 | 376.94 | 28.24 | 9 | 236.64 | 17.76 | 6 |
| Tef2 | Translational elongation factor EF-1 alpha | 50.0 | 202.01 | 17.25 | 4 | 254.17 | 27.29 | 7 | 126.99 | 19.21 | 5 |
| Aco1 | Aconitase; required for TCA cycle and mitochondrial genome maintenance | 85.3 | 97.62 | 5.53 | 3 | 55.06 | 3.21 | 2 | 128.77 | 7.97 | 5 |

**Table 4.1: Potential proteins in the $H_2O_2$-induced HMW complex identified by mass spectrometry.** Proteins identified by mass spectrometry were ranked based on their score, coverage and peptide number from two independent repeats (A and B).

Nevertheless, the presence of Cex1 was investigated further as it was possible that it was a component of the Ubp12 HMW complex.

In the second mass spectrometry analysis a gel slice from the unstressed Ubp12-TAP lane at the equivalent mobility was also included. This control was added in case Ubp12 was detected in the first analysis due to contamination with reduced Ubp12-TAP. Indeed, Ubp12-TAP was detected in the equivalent gel slice from the unstressed sample (Table 4.1B). However, the score, coverage, and peptide numbers were lower than those obtained in the analysis of the stressed Ubp12-TAP lane (Table 4.1B). The detection of Ubp12-TAP in the unstressed sample could be a contaminant of the whole lane, with Ubp12-TAP and/or possible due to the presence of a small amount of the Ubp12 HMW complex in unstressed cells. Ubp12 was also detected in the wild type control; however with such low numbers it is possible that this is contamination from the neighbouring lane. Importantly, the highest scores for Ubp12 were identified in the $H_2O_2$ treated Ubp12-TAP sample (Table 4.1B). As in the first experiment, Ubp12 was the predominant component identified by the analysis (Table 4.1B). However, several other proteins were potentially identified, all be it with much lower scores that may indicate some link to the HMW protein complex. It was observed that the analysis for $H_2O_2$ treated Ubp12-TAP cells did not give as high a value for Ubp12 as expected from the Coomassie stained gel. The overall score for Ubp12-TAP treated with $H_2O_2$ was only 4 times higher than the score for unstressed Ubp12-TAP. However, the Coomassie stained gel suggested that the HMW form of stressed Ubp12-TAP had more than four times the amount of protein. Therefore it was suggested that the analysis for $H_2O_2$ treated Ubp12-TAP may not have worked as well as the other samples. When identifying components of the HMW complex, it was taken into account that it was possible that the scores for suggested proteins in the $H_2O_2$ treated Ubp12-TAP sample were higher than the results suggested. Protein hits that had a similar score for both stressed and unstressed Ubp12-TAP samples, ideally with a score higher than the result for the wild type sample, were identified as possible hits. Based on these criteria, His4, Cdc19, Pdc1, and Tef2 (Table 4.1B) which were selected for further analyses. Of all proteins identified by the second mass spectrometry analysis, only Aco1 displayed higher values for score, coverage, and peptide number in

the stressed Ubp12-TAP lane compared with the unstressed Ubp12-TAP lane (Table 4.1B). Therefore, Aco1 was also selected for further analysis.

Next, to test whether Cex1, His4, Cdc19, Pdc1, Tef2, and/or Aco1 are potentially components of the $H_2O_2$-induced HMW complex with Ubp12, TAP epitope-tagged strains for each protein were obtained from the TAP epitope tag strain collection (Ghaemmaghami *et al.*, 2003a). First, the TAP epitope-tagged strains were checked to confirm the presence of a TAP epitope tag, in frame at the C-terminus of each individual protein. PCR analyses using gene-specific forward primers and a TAP reverse primer were performed (Figure 4.6A). Using these primers, strains containing the TAP epitope tag cassette at the correct location were predicted to produce PCR products of approximately 200-500bp depending on the position of the specific forward primer, whilst the wild type untagged strains would not produce a PCR product (Figure 4.6A). These analyses indicated that all the strains were correct. Next, the various TAP epitope-tagged strains, and cell expressing Ubp12-TAP, were grown to mid log phase and incubated with 2 mM $H_2O_2$. Proteins were extracted in the presence of NEM, and analysed via western blot (Figure 4.6B-C). It was predicted that if any individual TAP epitope-tagged protein forms an intermolecular disulphide complex with Ubp12 after $H_2O_2$ incubation then a HMW complex would be detected in the relevant lane with mobility similar to the Ubp12-TAP HMW complex. Importantly, no HMW form similar to that of Ubp12-TAP was observed using strains expressing any of the TAP epitope-tagged proteins identified by mass spectrometry, although neither Tef2-TAP nor His4-TAP could be observed by western blot analysis (Figure 4.6B and C). Interestingly, Cex1-TAP did actually form a HMW complex in response to $H_2O_2$; however the HMW complex did not appear to have the same mobility or abundance as the HMW Ubp12 complex (Figure 4.6C). Cex1 is an important component of tRNA export from the nucleus (Nozawa *et al.*, 2013) and, although these analyses are preliminary they do suggest that Cex1 may be regulated by oxidation. However further investigation of Cex1 oxidation is outside the scope of this thesis, as there is no evidence of linkage to the Ubp12 HMW complex.

Taken together, the mass spectrometry and western blotting analyses suggest that Ubp12 is the only protein present in the $H_2O_2$ induced HMW complex. This

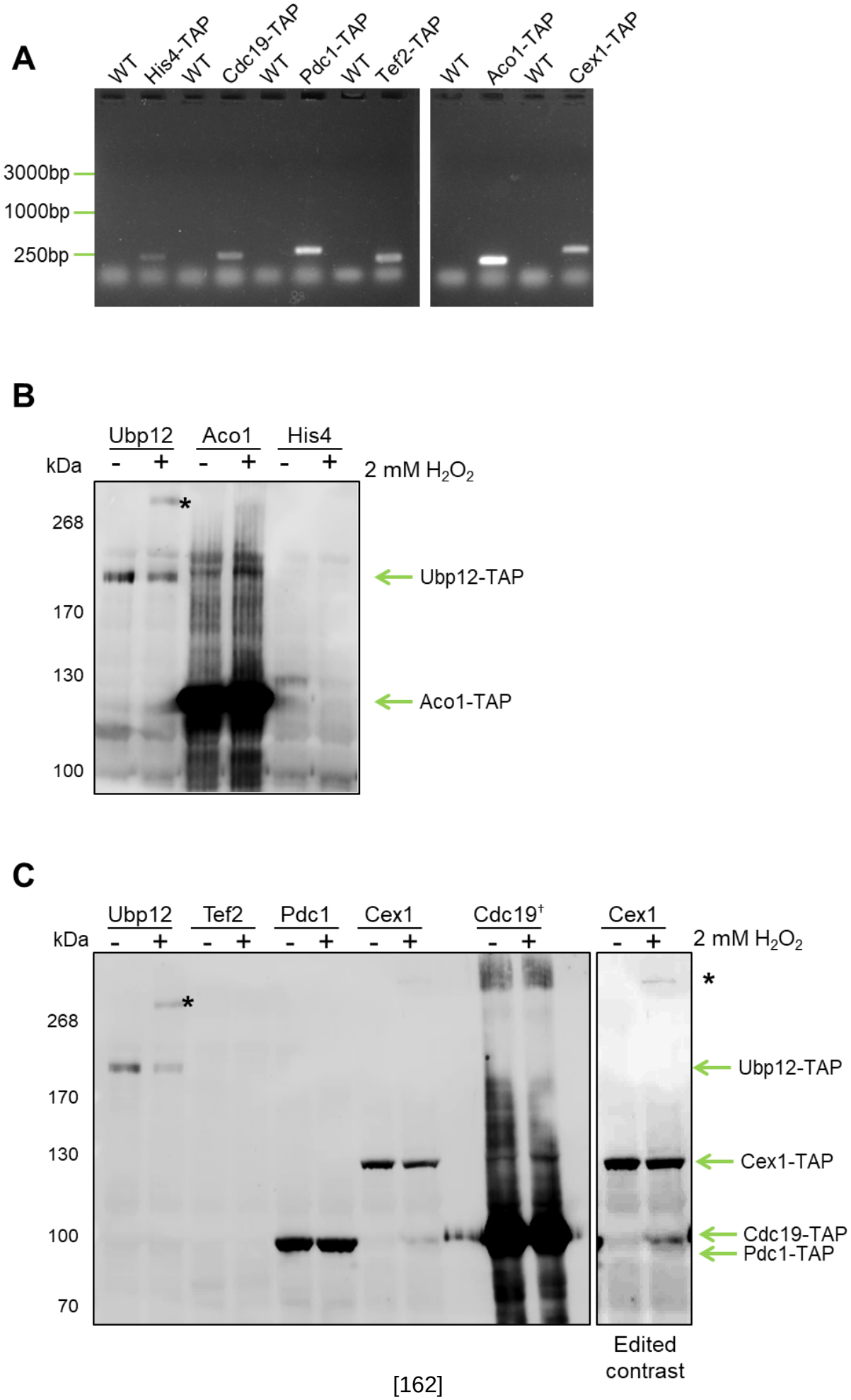
A
WT
His4-TAP
WT
Cdc19-TAP
WT
Pdc1-TAP
WT
Tef2-TAP
WT
Aco1-TAP
WT
Cex1-TAP
3000bp
1000bp
250bp
B
Ubp12
Aco1
His4
kDa
- + - + - +
2 mM H2O2
268
170
130
100
Ubp12-TAP
Aco1-TAP
C
Ubp12
Tef2
Pdc1
Cex1
Cdc19†
Cex1
kDa
- + - + - + - + - + - +
2 mM H2O2
268
170
130
100
70
Ubp12-TAP
Cex1-TAP
Cdc19-TAP
Pdc1-TAP
Edited contrast

**Figure 4.6: The potential hits from mass spectrometry analysis do not form the same HMW complex as Ubp12-TAP.** (A) PCR analyses, using a generic TAP reverse primer and gene specific forward primers, was performed with DNA isolated from each each TAP epitope-tagged strain obtained from the *S. cere*visiae TAP epitope-tag collection; Aco1-TAP (FCC150), His4-TAP (FCC146), Tef2-TAP (FCC149), Pdc1-TAP (FCC148), Cex1-TAP (FCC135), and Cdc19-TAP (FCC147). The PCR products using DNA from each potential TAP epitope-tagged strain were analysed on a 1% agarose gel together with a wild type control (FCC23) using the same primers. (B) and (C) Cells expressing Ubp12-TAP (ELR38), Aco1-TAP (FCC150), His4-TAP (FCC146), Tef2-TAP (FCC149), Pdc1-TAP (FCC148), Cex1-TAP (FCC135), and Cdc19-TAP (FCC147) were incubated with 2 mM $H_2O_2$ for 0 (-) and 10 (+) minutes. Protein extracts were prepared in non-reducing conditions and separated by SDS-PAGE. Proteins were visualised using PαP antibodies. * denotes $H_2O_2$ induced HMW complexes. † denotes protein loaded at 1/5 dilution.

raised the possibility that the HMW complex consists of either a homodimer of two Ubp12 proteins, or perhaps contains one Ubp12 with one or more intramolecular disulphide bonds causing the Ubp12 protein to have a slower mobility. However it is also important to note that the mass spectrometry analyses may have missed potential components of the complex.

*4.2.2.2. Analysis of Ubp12 disulphide complex*

As discussed mass spectrometry analyses suggests that only Ubp12 is present in the $H_2O_2$-induced HMW complex. However, whether this consists of two Ubp12 proteins forming a complex together, or consists of Ubp12 protein with one or more intramolecular disulphides is unclear. Hence, to gain further insight into the $H_2O_2$-induced HMW complex, a diploid strain containing one copy of Ubp12-TAP and one copy of untagged Ubp12 was created by mating the *MATa* Ubp12-TAP strain with the BY4742 *MATα* wild type strain. Potential diploid strains were analysed by PCR to confirm the presence of both wild type *UBP12*, and *UBP12*-TAP genes (Figure 4.7A). Correct diploid strains were predicted to contain a PCR product for wild type *UBP12* gene at approximately 300bp, and a PCR product for *UBP12*-TAP at approximately 2900bp (Figure 4.7A). After confirmation of the construction of the correct Ubp12/Ubp12-TAP diploid strain, diploid cells, haploid cells expressing Ubp12-TAP, and wild type cells were grown to mid-log phase and incubated with 2 mM $H_2O_2$. Proteins were extracted in non-reducing conditions in the presence of NEM and analysed by western blot (Figure 4.7B). As expected, the $H_2O_2$-induced HMW complex was observed in the Ubp12-TAP extracts. Significantly, the extract from the Ubp12/Ubp12-TAP diploid also showed a single $H_2O_2$-inducedHMW complex (Figure 4.7B). It was predicted that if the HMW complex contained two Ubp12 protein then two bands were expected to be detected, one containing two Ubp12-TAP and one containing Ubp12-TAP and untagged Ubp12. This second complex, if formed, would be predicted to have faster mobility than the complex containing two Ubp12-TAP due to loss of one TAP epitope (~21 kDa in size). However, only one HMW complex was detected of the same mobility as the Ubp12-TAP complex in lane 4 suggesting that the HMW complex does not contain two proteins. However, to confirm this, another diploid strain was constructed whereby the two copies of Ubp12 were

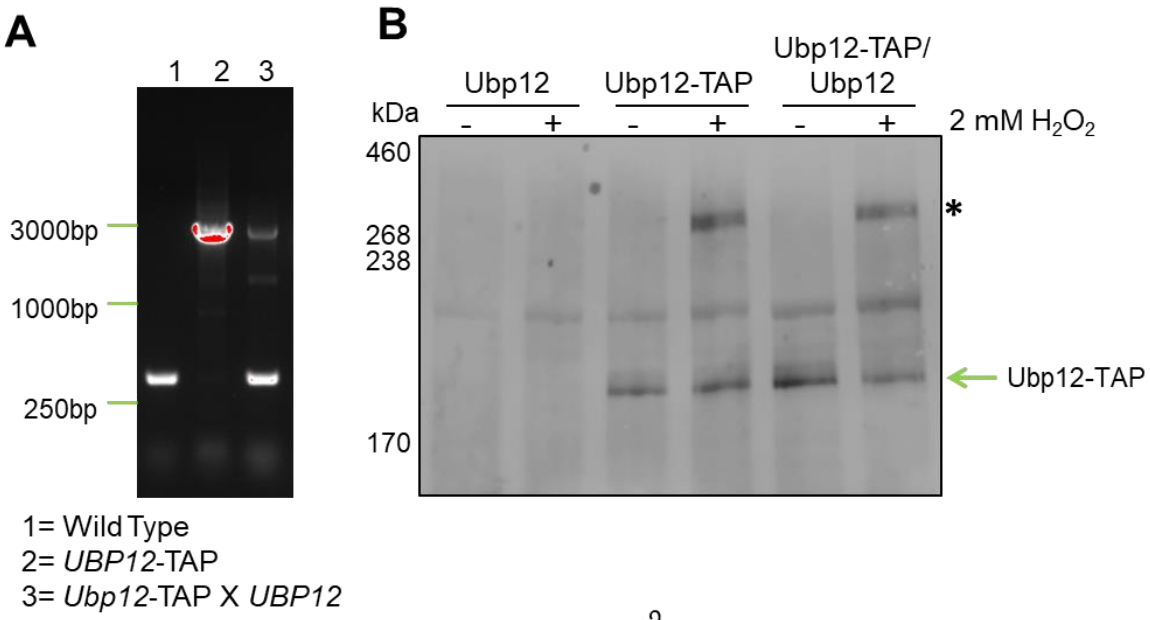
A
1 2 3
3000bp
1000bp
250bp
1= Wild Type
2= UBP12-TAP
3= Ubp12-TAP X UBP12
B
Ubp12
Ubp12-TAP
Ubp12-TAP/ Ubp12
kDa
- + - + - +
2 mM H2O2
460
268
238
170
*
Ubp12-TAP

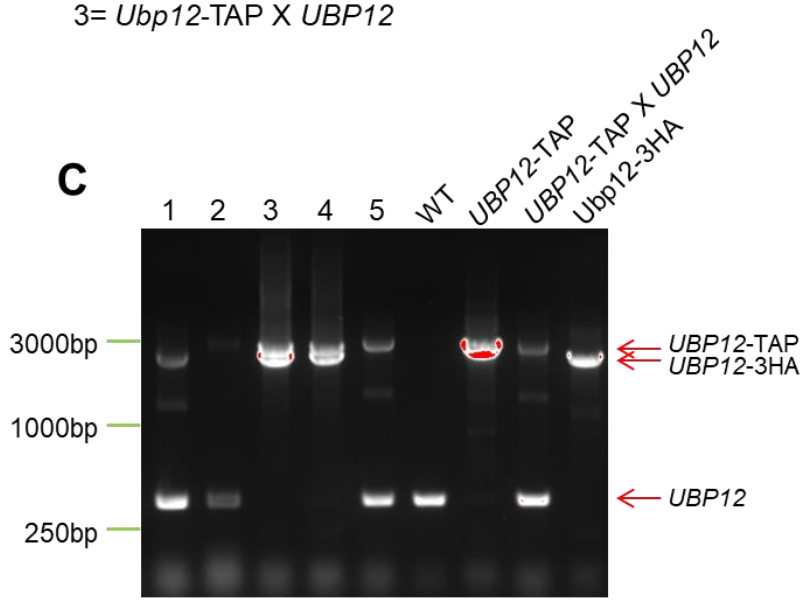
C
1 2 3 4 5 WT UBP12-TAP UBP12-TAP X UBP12 Ubp12-3HA
3000bp
1000bp
250bp
UBP12-TAP
UBP12-3HA
UBP12

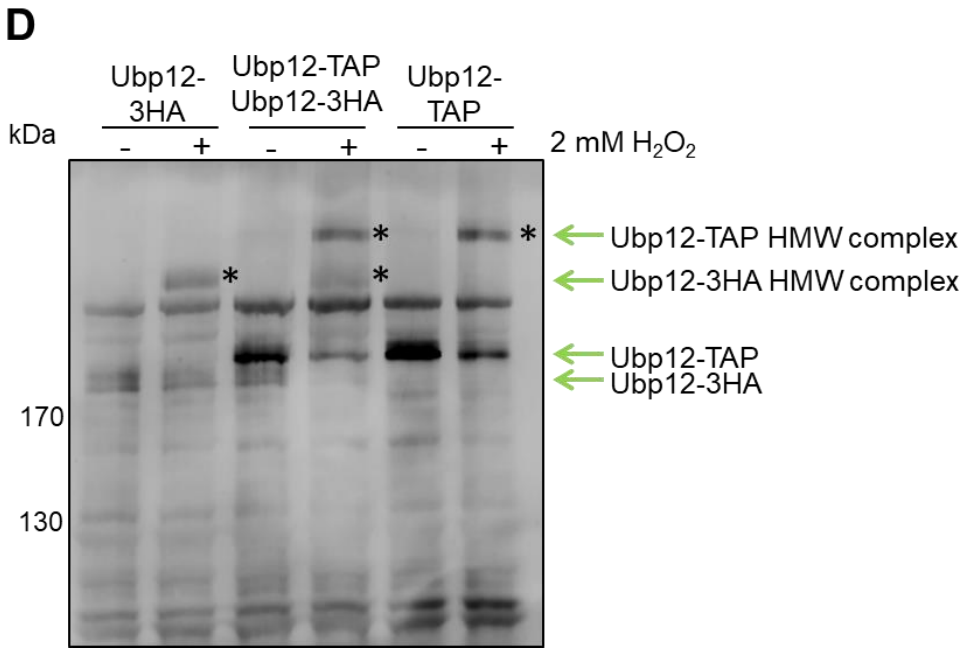
D
Ubp12-3HA
Ubp12-TAP Ubp12-3HA
Ubp12-TAP
kDa
- + - + - +
2 mM H2O2
*
Ubp12-TAP HMW complex
Ubp12-3HA HMW complex
Ubp12-TAP
Ubp12-3HA
170
130

**Figure 4.7: Ubp12 does not form a homodimer in response to $H_2O_2$.** (A) Haploid wild type (FCC63) and Ubp12-TAP (ELR38) were mated and the resulting diploid strain was checked by PCR analysis using specific Ubp12 forward and reverse primers. (B) *UBP12/UBP12*-TAP diploid strain (FCC70), *UBP12*-TAP, and wild type control strains were incubated with 2 mM $H_2O_2$ for 0 (-) and 10 (+) minutes. Protein extracts were prepared in non-reducing conditions and separated by SDS-PAGE. Proteins were visualised using PɑP antibodies. * denotes $H_2O_2$-induced HMW complex. (C) A Ubp12-3HA cassette was transformed into the *UBP12/Ubp12*-TAP diploid strain (FCC70) to produce the *UBP12*-3HA/*UBP12*-TAP diploid strain. Potential integrants were checked by PCR analysis and compared to control strains using specific Ubp12 forward and reverse primers. (D) Cells expressing Ubp12-3HA and Ubp12-TAP (Lane 3 from (C) FCC158), Ubp12-3HA (FCC93), and Ubp12-TAP were incubated with 2 mM $H_2O_2$ for 0 (-) and 10 (+) minutes. Protein extracts were prepared in non-reducing conditions and separated by SDS-PAGE. Proteins were visualised using PɑP antibodies (Ubp12-TAP) and ɑ-HA (Ubp12-3HA) * denotes $H_2O_2$-induced HMW complex.

tagged by two different C-terminal epitope tags. To construct the strain a PCR cassette for a 3HA epitope tag was integrated into the 3' end of the *UBP12* gene in the *UBP12/UBP12*-TAP diploid strain (described in Section 2.2.3.2). Potential integrants were analysed by PCR to confirm the presence of both the Ubp12-TAP epitope tag and Up12-3HA epitope tag in the new strain (Figure 4.7C). Correct diploid strains were predicted to contain a PCR product for *Ubp12*-TAP at approximately 2900bp, and a PCR product for *UBP12*-3HA at approximately 2200bp. In addition, the product for untagged *UBP12* strain at approximately 300bp was predicted to be absent (Figure 4.7C). Positive strains were observed in lanes 3 and 4 (Figure 4.7C). After confirmation of the construction of the correct *UBP12*-3HA/*UBP12*-TAP diploid strain, diploid cells, and haploid cells expressing either Ubp12-TAP or Ubp12-3HA, were grown to mid-log phase and incubated with 2 mM $H_2O_2$. Proteins were extracted in non-reducing conditions in the presence of NEM and analysed by western blot (Figure 4.7D). Again this analysis suggested that the $H_2O_2$-induced HMW Ubp12 complexes only contain one Ubp12 protein (Figure 4.7D). If both epitope tags were present in a HMW complex it was predicted that a third band would appear in protein extracts from the diploid strain. However, the presence of only two $H_2O_2$-induced HMW complexes of the same mobilities as that observed in the Ubp12-3HA and Ubp12-TAP expressing haploid strains suggests that only one epitope-tagged version of Ubp12 is present in the complex.

Taken together, mass spectrometry analyses and the protein analysis of the diploid strains suggest that Ubp12 forms a HMW intramolecular disulphide complex after treatment with $H_2O_2$.

### *4.2.3. Characterisation of the role of Ubp12 catalytic cysteine*

The results obtained from mass spectrometry and western blot analyses suggested that the $H_2O_2$-induced HMW Ubp12 complex may be due to one or more intramolecular disulphide(s) bond. Ubp12 has 19 cysteine residues which may be part of the HMW complex. We next explored the potential cysteine residue(s) which may be involved in the HMW complex formation. Inactive dUb catalytic cysteines are unable to be oxidised due to their higher pKa value. However, after deprotonation, the pKa value is reduced, increasing the

susceptibility of the catalytic cysteine to oxidation (Cotto-Rios *et al.*, 2012). Most cysteines within Ubp12 are non-catalytic, which means they may not have a pKa value low enough to be susceptible to oxidation. The catalytic cysteine, however, is deprotonated to allow cleavage, hence it was hypothesised that one of the cysteines that form the $H_2O_2$-induced HMW intramolecular disulphide Ubp12 complex included the catalytic cysteine. This does not rule out the role of other cysteines within Ubp12 that may have the potential to form a disulphide complex, however as there are 19 cysteines within the protein it was suggested that the catalytic cysteine would be a place to start investigations. To investigate this hypothesis, a catalytic cysteine mutant version of Ubp12 was created whereby the catalytic cysteine residue (C373) was mutated to a serine residue (C373S) which cannot become oxidised into a disulphide complex. To create a plasmid expressing the Ubp12$^{C373S}$ from the *UBP12* promoter and tagged with 3HA epitopes at the C-terminus, overlapping PCR fragments incorporating the cysteine to serine substitution were first created by PCR using wild type *UBP12* DNA as a template (see Section 2.2.4.1). The fragments were transformed into *ubp12*Δ cells, with a pRS426 vector backbone, which would recombine the fragment and plasmid backbone to create a pRS426 plasmid containing Ubp12$^{C373S}$-3HA. Wild type Ubp12-3HA fragments were also recombined into the pRS426 plasmid. Colonies containing the potential recombined plasmids were analysed by PCR using M13 forward and reverse primers which bind on either side of the insertion site in the plasmid (see Section 2.2.4.1). Plasmids which produced a PCR product of the expected size were extracted from *ubp12*Δ strains and transformed into *E. coli*. Plasmids were isolated from *E. coli* and sequenced to confirm the correct mutation of the cysteine 373 codon (TGT) to serine codon (TCT).

Sequencing analysis confirmed the construction of pRS426-Ubp12-3HA, and pRS426-Ubp12$^{C373S}$-3HA plasmids. We next wanted to use the plasmids pRS426-Ubp12-3HA and pRS426-Ubp12$^{C373S}$-3HA to test the oxidative potential of the catalytic cysteine in the Ubp12 HMW complex. Hence, we introduced both plasmids and empty vector into *ubp12*Δ cells. Following successful transformation the different plasmid containing strains were grown in SD minimal media to mid-log phase and incubated with 1 mM $H_2O_2$. Proteins were extracted

in the presence of NEM, and analysed by western blot (Figure 4.8A). Importantly, a band with the expected mobility for Ubp12-HA was observed in cells containing pRS426-Ubp12-3HA and pRS426-Ubp12$^{C373S}$-3HA, suggesting that the plasmid expresses Ubp12 correctly, and the 3HA epitope tag is able to be visualised. In addition, the data indicates expression of wild type and mutant proteins is similar, suggesting that the cysteine mutation does not affect protein stability. Interestingly, in contrast to cells containing pRS426-Ubp12-3HA no $H_2O_2$-induced HMW complex was observed in the cysteine mutant plasmid containing cells, suggesting that the formation of the disulphide complex is dependent on the presence of the catalytic cysteine (Figure 4.8A). It is also interesting to note that the data suggests that a higher proportion of wild type Ubp12-3HA is in the HMW form after $H_2O_2$ treatment than was observed previously (compare Figure 4.8 with Figure 4.4B and Figure 3.11). However, in the case of the experiments presented in figure 4.8 SD minimal media was used to maintain plasmid selection, whereas YPD media was used in the other experiments (Figure 4.4B and 3.11). SD minimal media has less buffering capacity than YPD therefore the effective concentration of $H_2O_2$ used to treat the strains expressing Ubp12 on the pRS426 plasmid is different to YPD media. Hence, to investigate whether the concentration of $H_2O_2$ was having an effect on the formation of the $H_2O_2$-induced HMW complex in SD media, *ubp12*Δ cells containing pRS426, pRS426-Ubp12-3HA and pRS426-Ubp12$^{C373S}$-3HA were grown to mid log phase in SD minimal media and incubated with either 0.2 mM or 1 mM $H_2O_2$. Proteins were extracted in the presence of NEM and analysed by western blot (Figure 4.8B). As expected, Ubp12-3HA, but not Ubp12$^{C373S}$-3HA formed a $H_2O_2$-induced HMW complex after treatment with 1 mM $H_2O_2$. However, after treatment with 0.2 mM $H_2O_2$, there was no observable HMW complex formed (Figure 4.8B) which contrasts with 0.2 mM in YPD media. The basis of this difference in HMW formation is unclear, although it is worth noting that these analyses have only been performed once. Consequently further repeats are necessary to confirm the results observed. Taken together, a key conclusion of this work is that no $H_2O_2$-induced HMW complex was observed in cells expressing Ubp12$^{C373S}$-3HA (Figure 4.8B), suggesting that oxidation of the catalytic cysteine in Ubp12 is essential for formation of the HMW complex.

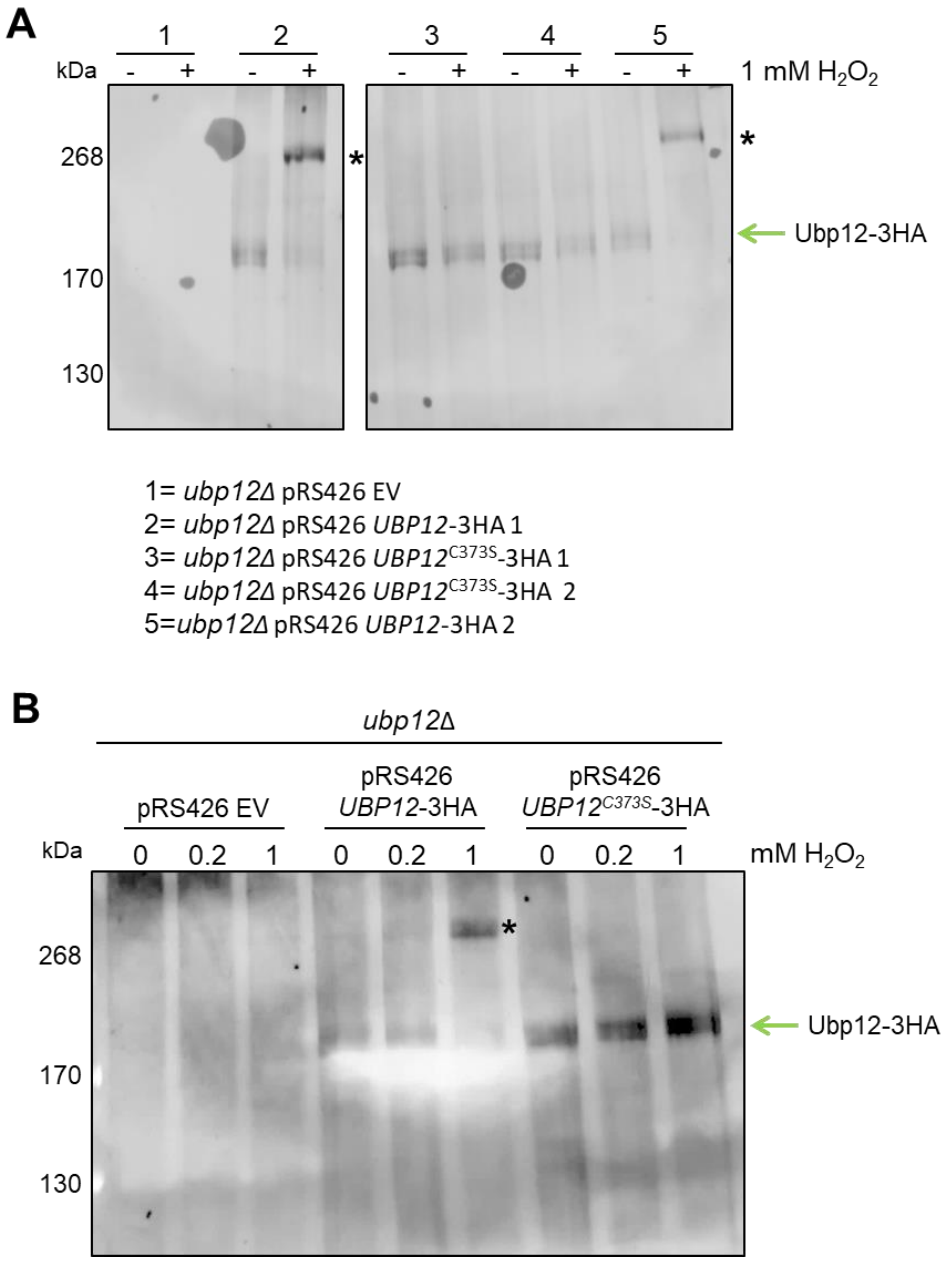


**Figure 4.8: Ubp12 does not form a $H_2O_2$-induced HMW complex in the absence of the catalytic cysteine.** (A) The *ubp12*Δ (FCC73) in BY4741 strain background containing either pRS426 empty vector (EV), *pRS42*6-UBP12-3HA, or *pRS42*6-UBP12$^{C373S}$-3HA, were grown to mid-log phase in minimal media and incubtaed with 1 mM $H_2O_2$ for 0 (-) and 10 (+) minutes. Two replicates of plasmids were used (labelled 1 and 2). Protein extracts were prepared in non-reducing conditions and separated by SDS-PAGE. Proteins were visualised using anti-HA antibodies. * indicates $H_2O_2$-induced HMW complex. (B) The *ubp12*Δ (FCC73) in BY4741 strain background containing either pRS426 empty vector (EV), *pRS42*6-UBP12-3HA, or *pRS42*6-UBP12$^{C373S}$-3HA, were grown to mid-log phase in minimal media and treated with 0.2 or 1 mM $H_2O_2$ as indicated for 10 minutes. Protein extracts were prepared in non-reducing conditions and separated by SDS-PAGE. Proteins were visualised using anti-HA antibodies. * indicates $H_2O_2$-induced HMW complex.

### *4.2.4. Ubp12 functions in responses to oxidative stress*

The results described above suggest that Ubp12 activity is regulated in response to $H_2O_2$ treatment. Although the role of this regulation is unclear it is known that Ubp12 is able to indiscriminately remove chains of ubiquitin from substrates, regardless of chain linkage type (Schaefer and Morgan, 2011), suggesting that Ubp12 oxidation may have a global effect on ubiquitination throughout the cell. Furthermore, there is still much to learn about the specific cellular functions of Ubp12, although some specific pathways and interacting partners have been identified. Hence, this section explores further relationships between Ubp12 and oxidative stress responses.

#### *4.2.4.1. Overexpression of UBP12 affects cell responses to oxidative stress*

To understand potential consequences of Ubp12 oxidation it was important to more fully understand the roles of Ubp12 in oxidative stress responses. As described in Chapter 3, *ubp12*Δ cells display increased resistance to diamide, and increased sensitivity to menadione compared to wild type cells (Figure 3.5 and 3.6). However, in contrast, *ubp12*Δ cells appeared to behave similarly to wild type cells to $H_2O_2$ (Figure 3.4). These data suggest that Ubp12 activity is necessary for resistance to menadione, but that Ubp12 activity inhibits the response to diamide. However, as described previously, dUbs have overlapping roles/functional redundancy (see Section 1.1.3); hence the use of single deletion mutants to investigate specific phenotypes may not allow a full understanding of the role of Ubp12 in response to stress. To gain a better understanding of the functions of Ubp12 in oxidative stress responses it was decided to examine the effects of increasing *UBP12* expression. Hence, pRS426-*UBP12* was constructed which expresses *UBP12* from its own promoter on a multicopy (~20 copies per cell) 2 micron plasmid (Christianson *et al.*, 1992). To obtain pRS426-*UBP12,* the *UBP12* gene including promoter and 3' region was incorporated into the multiple cloning site of pRS426 plasmid using overlapping PCR fragments (described in Section 2.2.4.1) , however the HA C-terminal epitope tag fragment was not included. The overlapping PCR fragments and pRS426 vector backbone were transformed into wild type yeast strains to allow recombination events to create a full pRS426-*UBP12* plasmid (described in Section 2.2.4.1). Plasmids were

isolated from *ura*+ colonies and sequenced to confirm plasmid construction. To examine the effects of overexpression of *UBP12*, wild type and *ubp12*Δ strains were transformed with either pRS426 vector or pRS426-*UBP12*. Next, strains were grown to mid-log phase in SD minimal media to maintain selection for the plasmid, and spotted onto SD minimal media plates containing several oxidising agents (Figure 4.9). Consistent with the previous analyses (Chapter 3), *ubp12*Δ cells with vector displayed increased resistance to diamide compared to wild type cells with vector (Figure 4.9). These results indicate that *ubp12*Δ cells are more resistant to diamide than wild type cells on both YPD media (Figure 3.5) and SD minimal media (Figure 4.9). Interestingly, consistent with the proposal that Ubp12 activity inhibits responses to diamide, *UBP12* overexpression in either wild type or *ubp12*Δ cells caused increased sensitivity to diamide (Figure 4.9). In contrast to the phenotypes observed when *ubp12*Δ cells were grown on YPD media containing $H_2O_2$, when grown on SD minimal media containing $H_2O_2$ *ubp12*Δ cells containing vector display slightly increased resistance (Figure 4.9). The basis for this difference in $H_2O_2$ resistance is not clear, but it is possible it is linked to the fact that SD media does not contain glutathione. Nevertheless, this data suggests that inhibition of Ubp12 may be important for responses to $H_2O_2$. This difference in media use may also explain the differences in increased sensitivity to menadione displayed by the Ubp12 mutant on YPD media (Figure 3.6) versus SD minimal media (Figure 4.9). On SD media, *ubp12*Δ cells containing vector appear to show less increased sensitivity to menadione. When *UBP12* was overexpressed in wild type and *ubp12*Δ cells there is some evidence that this causes increased sensitivity to both $H_2O_2$ and menadione (Figure 4.9). However, these observations are not as clear cut as the effects of *UBP12* overexpression on diamide sensitivity. Taken together with the analyses of the *ubp12*Δ mutant, these data suggest that Ubp12 activity has specific roles in response to oxidative stress.

#### *4.2.4.2. Analyses of the effects of overexpression of Ubp12$^{C373S}$ on responses to oxidative stress*

DUbs cleave the isopeptide bond between ubiquitin molecules and the substrate lysine by utilising the activity of the catalytic cysteine which resides in the active site. The potential of this catalytic cysteine to be oxidised suggests a mechanism

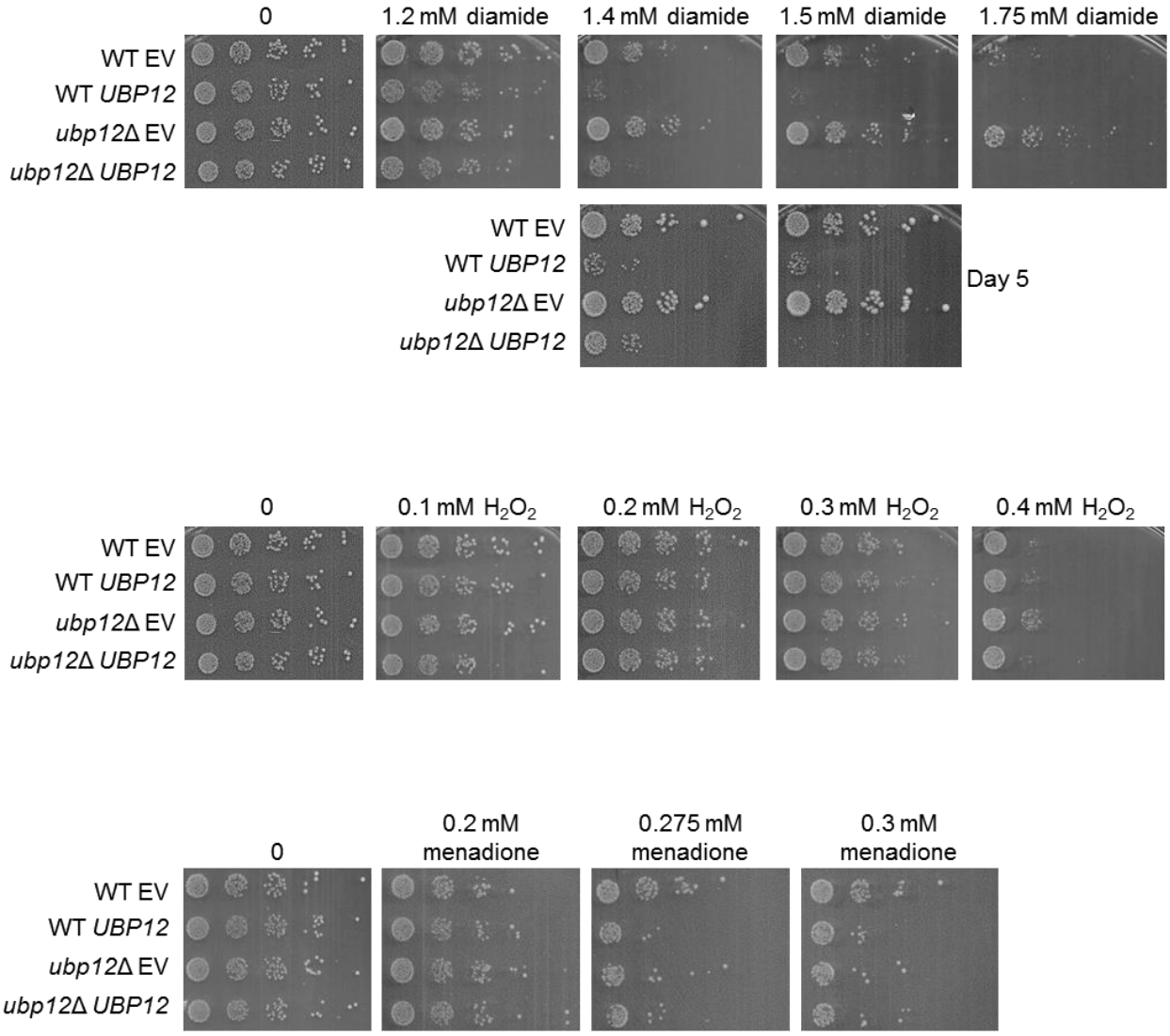


**Figure 4.9: Overexpression of *UBP12* affects responses to oxidative stress.** Wild type (FCC23) and *ubp12*Δ (FCC75) strains in the BY4741 strain background containing either pRS426 empty vector (EV) or pRS426 *UBP12* were grown to mid-log phase, spotted onto SD minimal media containing increasing concentrations of $H_2O_2$, diamide, and menadione, and incubated at 30 °C. Plates were incubated for 3 days, unless otherwise stated, before imaging.

by which the catalytic activity of the dUb enzyme can be regulated. Indeed, when specific mammalian dUbs were incubated with a reducing agent their activity was activated (Lee et al., 2013), suggesting that oxidation inhibited their catalytic activity. However, it is possible that one or more phenotypes associated with deletion and/or overexpression of *UBP12* may be linked to another unidentified activity of Ubp12 unlinked to dUb catalytic activity. To address this possibility pRS426-*UBP12*-3HA and pRS426-*UBP12*$^{C373S}$-3HA were introduced into *ubp12*Δ cells, grown to mid log phase in SD minimal media and spotted onto plates containing different oxidising agents (Figure 4.10). As a further control, wild type and *ubp12*Δ cells containing *UBP12*-3HA or empty vector were included to confirm that the 3HA epitope tags did not affect Ubp12 function. As expected *ubp12*Δ cells containing vector showed increased resistance to diamide compared with the wild type control strain, and moreover, overexpression of *UBP12* in wild type and *ubp12*Δ cells resulted in increased sensitivity to diamide (Figure 4.10). Importantly, *ubp12*Δ cells containing pRS426-*UBP12*-3HA had a similar phenotype to diamide as *ubp12*Δ cells expressing untagged *UBP12* from pRS426-*UBP12* suggesting the 3HA epitope tags do not affect the function of Ubp12 (Figure 4.10). *ubp12*Δ cells containing pRS426-*UBP12*$^{C373S}$-3HA displayed similar increased resistance to diamide as *ubp12*Δ cells containing vector (Figure 4.10). This result suggests that the increased resistance of cells lacking Ubp12 to diamide is due to loss of the catalytic activity of Ubp12. The effects of overexpression of *UBP12* on the resistance/sensitivity of *ubp12*Δ cells to $H_2O_2$ and menadione are smaller than those observed using diamide (Figure 4.9 and 4.10). Nevertheless, the data suggests that *ubp12*Δ cells expressing pRS426-*UBP12*$^{C373S}$-3HA have similar phenotypes in response to $H_2O_2$ and menadione as *ubp12*Δ cells containing vector (Figure 4.10). Taken together, these data suggest that the effects of loss or overexpression of Ubp12 on responses to several oxidising agents is linked to the catalytic activity of the dUb rather than another function of Ubp12. However to further confirm these results it would be useful to examine the effects of expression of *UBP12* and *UBP12*$^{C373S}$ from a CEN plasmid.

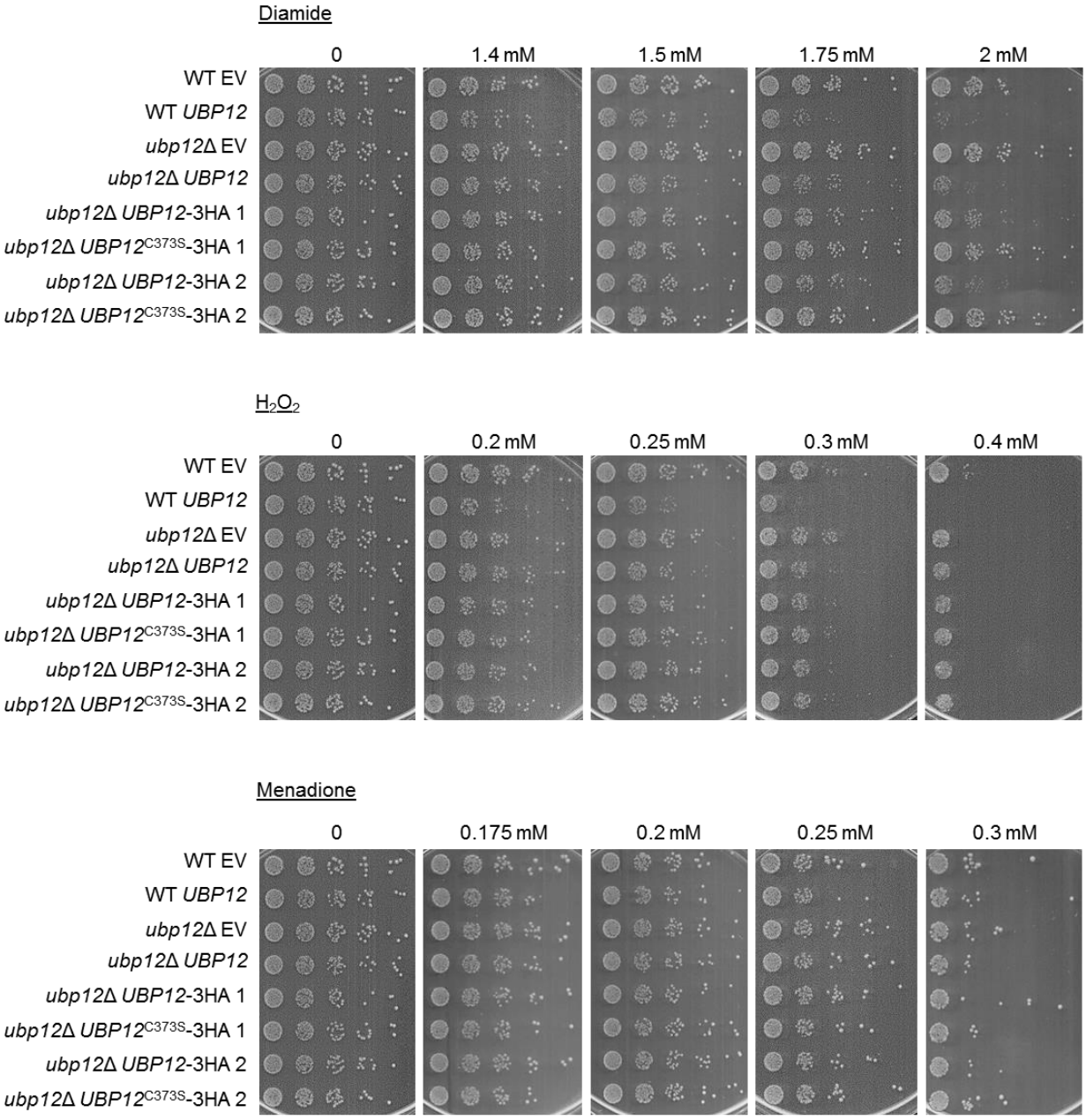


**Figure 4.10: Phenotypes associated with overexpression of wild type *UBP12* require the catalytic cysteine.** Wild type (FCC23) and *ubp12*Δ (FCC75) strains in the BY4741 strain background containing either pRS426 empty vector (EV), pRS426 *UBP12*, *pRS42*6 *UBP12*-3HA, or *pRS42*6 *UBP12*$^{C373S}$-3HA were grown to mid-log phase, spotted onto SD minimal media containing increasing concentrations of $H_2O_2$, diamide, and menadione, and incubated at 30°C. Two replicates of plasmids were used (labelled 1 and 2). Plates were incubated for 3 days before imaging.

*4.2.4.3. Analyses of global ubiquitin levels after oxidative stress*

It has been shown previously that Ubp12 can indiscriminately remove ubiquitin chains from proteins, regardless of the linkage type (Schaefer and Morgan, 2011). It was therefore possible that Ubp12 oxidation regulates global ubiquitination. For example, if oxidised Ubp12 was no longer able to de-conjugate ubiquitin signals, it might be predicted that global ubiquitination would increase after $H_2O_2$ stress in a Ubp12-dependent manner. However, nobody has compared global ubiquitin levels in BY4741 and W303 backgrounds in *S. cerevisiae* before and after $H_2O_2$ and diamide treatment. Therefore, it was important to establish the effects of $H_2O_2$ and diamide stress on global ubiquitination levels in the BY4741 and W303 strain backgrounds. Wild type cells in both strain backgrounds were grown to mid-log phase and incubated with 3 mM diamide or 2 mM $H_2O_2$ for ten minutes. Proteins were extracted in non-reducing conditions in the presence of NEM and analysed by western blot, (Figure 4.11A and B). Given the predicted slow mobility of heavily ubiquitinated substrates, the stacking gel was included in the western analyses.

Significantly, after incubation with diamide no changes in the levels of the HMW substrates or free ubiquitin levels were detected (Figure 4.11A), suggesting that diamide does not induce global ubiquitination changes in either of the W303 and BY4741 strain backgrounds. Interestingly however, after incubation with $H_2O_2$ the levels of HMW ubiquitin conjugated substrates were induced (Figure 4.11B). Furthermore, this induction coincided with a decrease in the levels of free ubiquitin (Figure 4.11B). Hence these results suggest that $H_2O_2$ regulates the global cellular levels of ubiquitination in both strain backgrounds. It is striking that free ubiquitin is differently affected by $H_2O_2$ and diamide. After treatment with diamide the levels of free ubiquitin remain constant; however after incubation with $H_2O_2$ the levels of free ubiquitin are suggested to decrease, however further quantification would be necessary to confirm the precise abundance. It is possible that $H_2O_2$ may inhibit one of the currently unknown dUbs which process immature ubiquitin into free ubiquitin, which results in the loss of free ubiquitin. However the rapid change in protein level suggests that this may not be the case. It has been suggested in mammalian cells that after $H_2O_2$ treatment the levels of

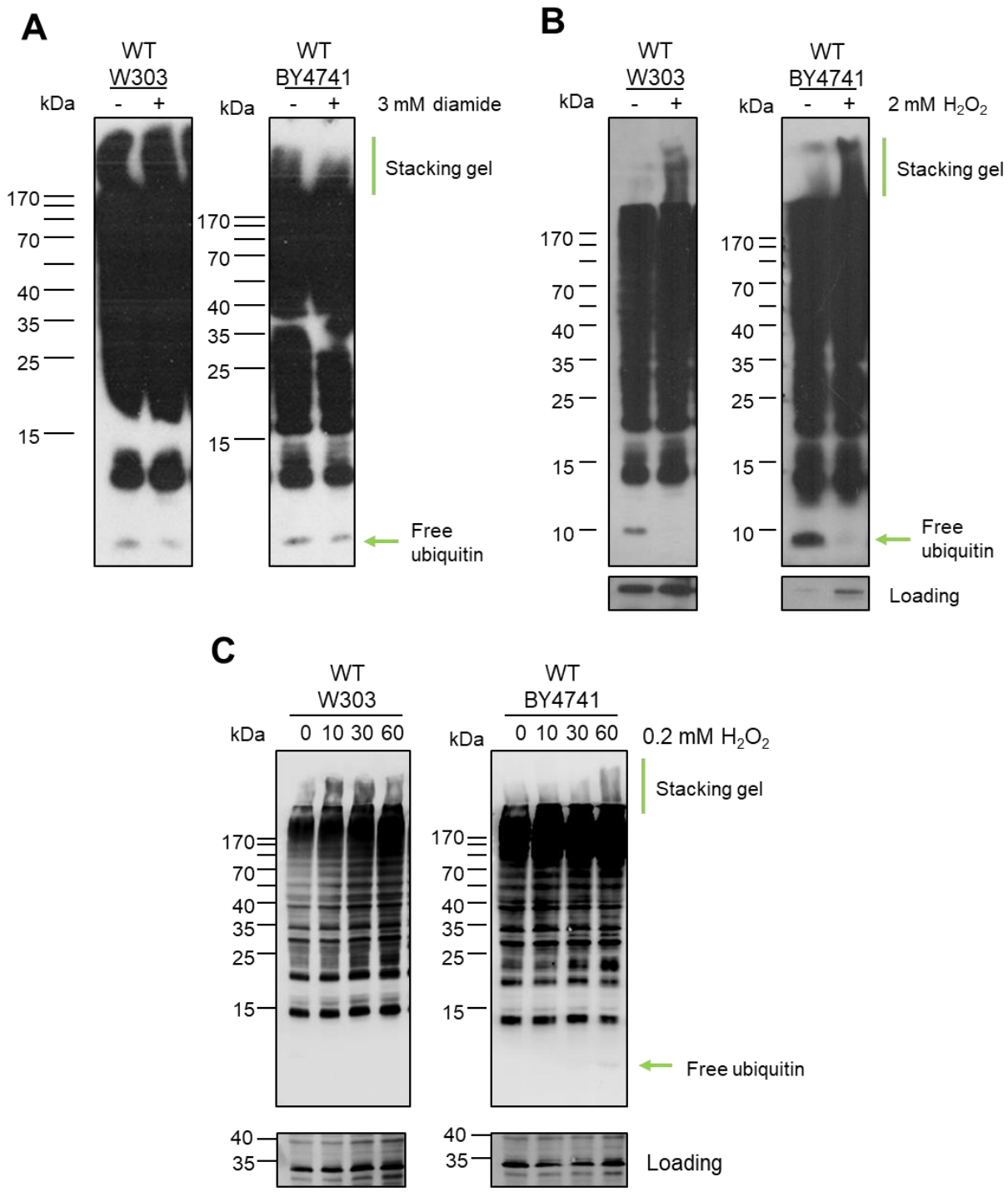


**Figure 4.11: $H_2O_2$, but not diamide, affects global ubiquitination.** Wild type (WT) cells in the BY4741 (FCC23) and W303 (FCC1) strain backgrounds were incubated with (A) 3 mM diamide or (B) 2 mM $H_2O_2$ for 0 (-) and 10 (+) minutes. Protein extracts were prepared in non-reducing conditions and separated by SDS-PAGE. Ubiquitinated proteins were visualised using α-ubiquitin antibodies. As a loading control in (B) Skn7 was visualised using α-Skn7. (C) Wild type (WT) cells in the BY4741 and W303 strain backgrounds were incubated with 0.2 mM $H_2O_2$ for 0-60 minutes and samples were taken as indicated. Protein extracts were prepared and visualised as above (A and B). As a loading control Cdc28 was visualised using α-Cdc28 antibodies.

free ubiquitin reduce (Salazar *et al*, 2009), however the authors do not go into detail about the reasons behind this or the potential mechanisms involved. It is of interest to note that the levels of free SUMO in mammalian cells are observed to increase after incubation with $H_2O_2$ (Bossis and Melchior, 2006), suggesting that the results observed in the present data are specific to ubiquitin, or potentially specific to *S. cerevisiae*. Many papers focus on the change to poly-ubiquitination or HMW forms of ubiquitin after $H_2O_2$ stress, therefore further investigations into the nature of the loss of free ubiquitin would be of high interest. The nature of the decrease in abundance in free ubiquitin after $H_2O_2$ treatment is unclear, but the potential for oxidative stress to regulate the pool of free ubiquitin is of interest for further investigation.

It is intriguing that Ubp12 forms a HMW complex after $H_2O_2$ but not diamide treatment, and that this appears to mimic effects of these oxidising agents on global ubiquitination. This suggests a potential connection between global ubiquitination and Ubp12 oxidation. As described previously (Figure 4.3), Ubp12 was also found to form the HMW complex in response to 0.2 mM $H_2O_2$. Furthermore, Ubp12 HMW complex formation peaked at ten minutes following addition of 0.2 mM $H_2O_2$ and this was reversed back to basal levels by 60 minutes (Figure 4.3D). Hence, it was interesting to next examine the potential effects of 0.2 mM $H_2O_2$ on global ubiquitination over a similar timescale to further explore the relationship between Ubp12 oxidation and global ubiquitination. Wild type cells, in both the BY4741 and W303 strain backgrounds, were incubated with 0.2 mM $H_2O_2$ for 1 hour, with samples taken at 0, 10, 30, and 60 minutes. Proteins were extracted in non-reducing conditions in the presence of NEM and analysed via western blot, including the stacking gel (Figure 4.11C). This experiment was only performed once, and hence the results are preliminary. However, results suggest that the levels of HMW ubiquitin-conjugated substrates increase after incubation with 0.2 mM $H_2O_2$ (Figure 4.11C). Interestingly, the levels do not seem to peak and/or decrease in a manner that mimics Ubp12 oxidation, suggesting the two events may be unlinked. Unfortunately, however, free ubiquitin levels also cannot be observed in this experiment. Hence it will be important to repeat this experiment before further conclusions are made.

Although the pattern of global ubiquitination did not mirror changes in the patterns of Ubp12 oxidation/HMW formation at 0.2 mM $H_2O_2$ this did not rule out the possibility that Ubp12 activity regulates $H_2O_2$ induced changes to ubiquitination. Hence, to further examine the potential role of Ubp12, wild type and *ubp12*Δ strains in both the W303 and BY4741 strain backgrounds were incubated with 2 mM $H_2O_2$. Proteins were then extracted in non-reducing conditions in the presence of NEM and analysed by western blot, including the stacking gel (Figure 4.12). However, in both strain backgrounds the levels of HMW ubiquitin-conjugated substrates and free ubiquitin appeared to show no differences between the wild type and *ubp12*Δ strains, suggesting that Ubp12 activity does not have a major impact on global ubiquitination in response to $H_2O_2$. In contrast to data presented here, a recent paper revealed that *ubp12*Δ strain has an increase in conjugated ubiquitin in unstressed cells, but did not affect free ubiquitin levels (Simões et al., 2018). The reason behind this discrepancy in results is unknown; however differences in strain background, growth conditions, and/or antibodies may play a role. However the present study suggests that Ubp12 is not involved in the regulation of ubiquitination after $H_2O_2$ stress.

#### *4.2.4.4. Analysis of known interacting partners of Ubp12*

Although no specific linkage of changes in global ubiquitination with Ubp12 function was observed in response to $H_2O_2$, it remained possible that specific proteins may be regulated by Ubp12 oxidation. However, unfortunately to date only 10 known physical interactors with Ubp12 have been identified (according to the *Saccharomyces cerevisiae* Genome Database). Hence, as to understand the function of Ubp12 oxidation it will be important to identify all of the potential Ubp12 interactions by large scale analyses. Nevertheless, it was decided to investigate whether a few of the small number of identified interactors are affected by $H_2O_2$. Interestingly, Ubp12 is known to localise to both the nucleus and the cytoplasm, therefore candidate proteins were selected for further investigation from each of these locations. In particular Gcn5 and Fkh1 are nuclear proteins which both function in pathways known to be regulated by ubiquitination. Fkh1 is a forkhead family transcription factor which regulates

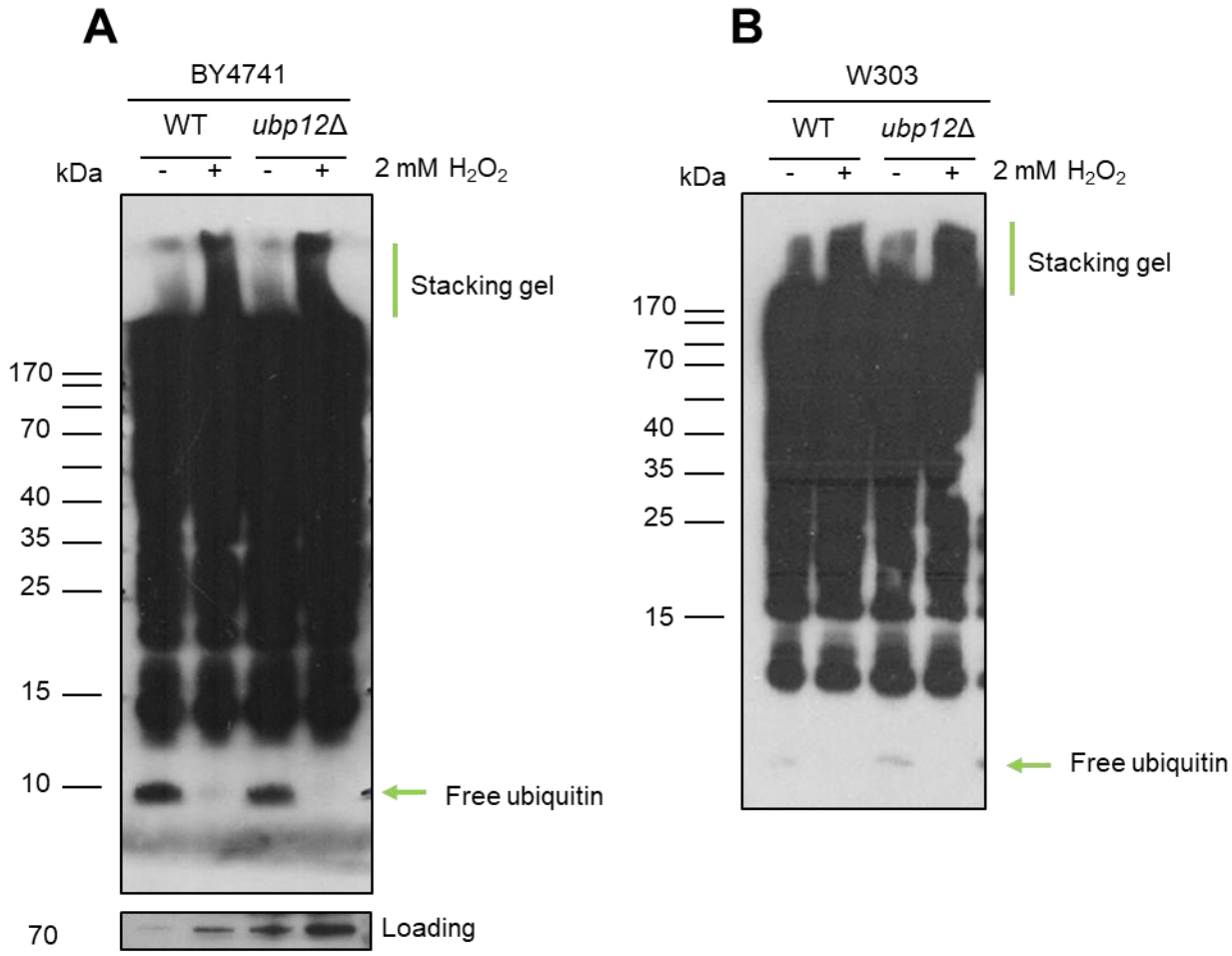


**Figure 4.12: Loss of Ubp12 does not appear to affect global ubiquitination.** Wild type (WT) and *ubp12*Δ cells in the (A) BY4741 (FCC23 and FCC75) and (B) W303 (FCC1 and FCC10) strain backgrounds were grown to mid-log phase and then incubated with 2 mM $H_2O_2$ for 0 (-) and 10 (+) minutes. Protein extracts were prepared in non-reducing conditions and separated by SDS-PAGE. Ubiquitinated proteins were visualised using α-ubiquitin antibodies. As a loading control Skn7 was visualised using α-Skn7 antibodies.

transcriptional elongation (Morillon *et al.*, 2003) and is important for cell cycle progression from G2-M phase (Coïc *et al.*, 2006). Gcn5 is a catalytic subunit of ADA and SAGA histone acetyltransferase complexes which acetylates lysines on H2B and H3 (Grant *et al.*, 1997; Hoke *et al.*, 2008). Interestingly, Gcn5 has also been linked to the Ubl SUMO pathway, however this ubiquitin-like modification does not regulate the enzymatic activity of Gcn5 (Sterner *et al.*, 2006). Puf3 is another protein known to interact with Ubp12 which, in contrast to Gcn5 and Fkh1, localises to the cytoplasmic side of the mitochondrial outer membrane (García-Rodríguez *et al.*, 2007). Puf3 binds to mRNAs and initiates degradation (Gerber *et al.*, 2004), and has also been linked to the Arp2/3 complex during mitochondrial movement (García-Rodríguez *et al.*, 2007). Puf3 has also been observed to regulate mitochondrial morphology and biogenesis (García-Rodríguez *et al.*, 2007). Strains expressing TAP epitope-tagged versions of the selected proteins were obtained from the TAP epitope tag strain collection (Ghaemmaghami *et al.*, 2003a). Next, cells expressing either Ubp12-TAP, Fkh1-TAP, Gcn5-TAP, or Puf3-TAP were grown to mid-log phase, treated with 0.2 mM $H_2O_2$ for 1 hour, and samples taken for protein extracts at 0, 10, and 60 minutes. Proteins were extracted in non-reducing conditions in the presence of NEM and analysed by western blot (Figure 4.13A). As expected, Ubp12-TAP formed a $H_2O_2$-induced HMW complex after 10 minutes, which contained ~55% of total Ubp12, which reduced to ~40% after 60 minutes (Figure 4.13B). Interestingly, the percentage of Ubp12 HMW complex after 60 minutes had not returned to basal levels (Figure 4.13B) in contrast to previous results (Figure 4.3B). The basis of this difference is not clear, but may possibly be linked to the use of different epitope tags. For example, perhaps TAP epitope-tagged Ubp12 is more resistant to reduction of the HMW complex. In addition, it is important to note that these data with Ubp12-TAP are preliminary and require more repeats to confirm the results. In contrast to Ubp12, neither Fkh1, Gcn5, nor Puf3 appear to form $H_2O_2$-induced HMW complexes (Figure 4.13A). Interestingly, however, preliminary quantification (from only one experiment) revealed that the relative abundance of each protein did appear to change after incubation with $H_2O_2$. In particular, the abundance of Fkh1 increased after incubation with $H_2O_2$ for ten minutes, and was maintained at 60 minutes (Figure 4.13C). Furthermore, the levels of Gcn5 also appeared to increase after $H_2O_2$ incubation, but in this case, had decreased

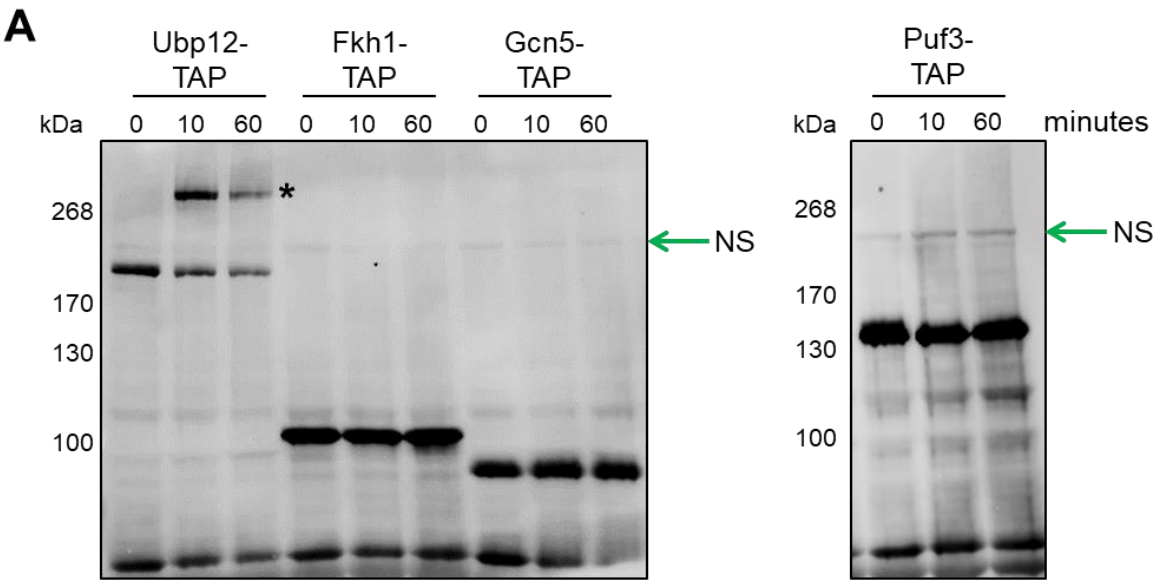
A
Ubp12-TAP
Fkh1-TAP
Gcn5-TAP
Puf3-TAP
kDa
0 10 60 0 10 60 0 10 60
0 10 60
minutes
268
170
130
100
*
NS
NS

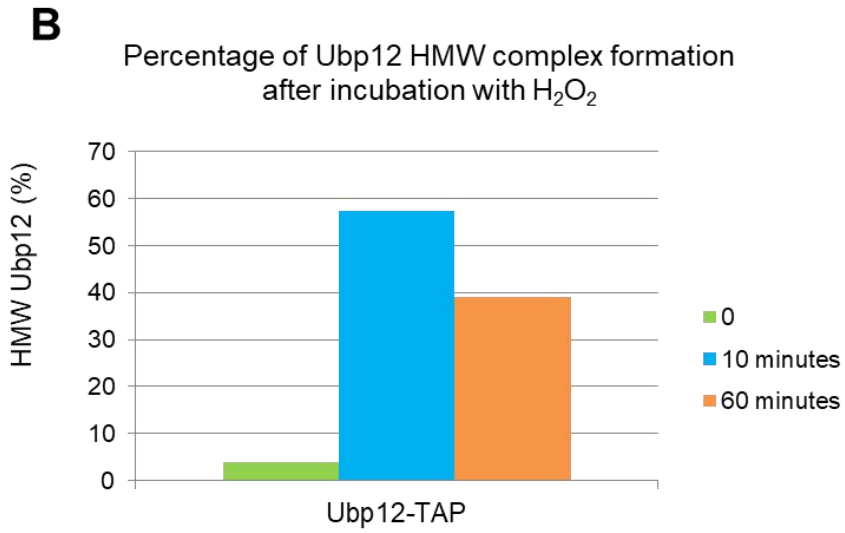
B
Percentage of Ubp12 HMW complex formation after incubation with $H_2O_2$
HMW Ubp12 (%)
70
60
50
40
30
20
10
0
Ubp12-TAP
0
10 minutes
60 minutes

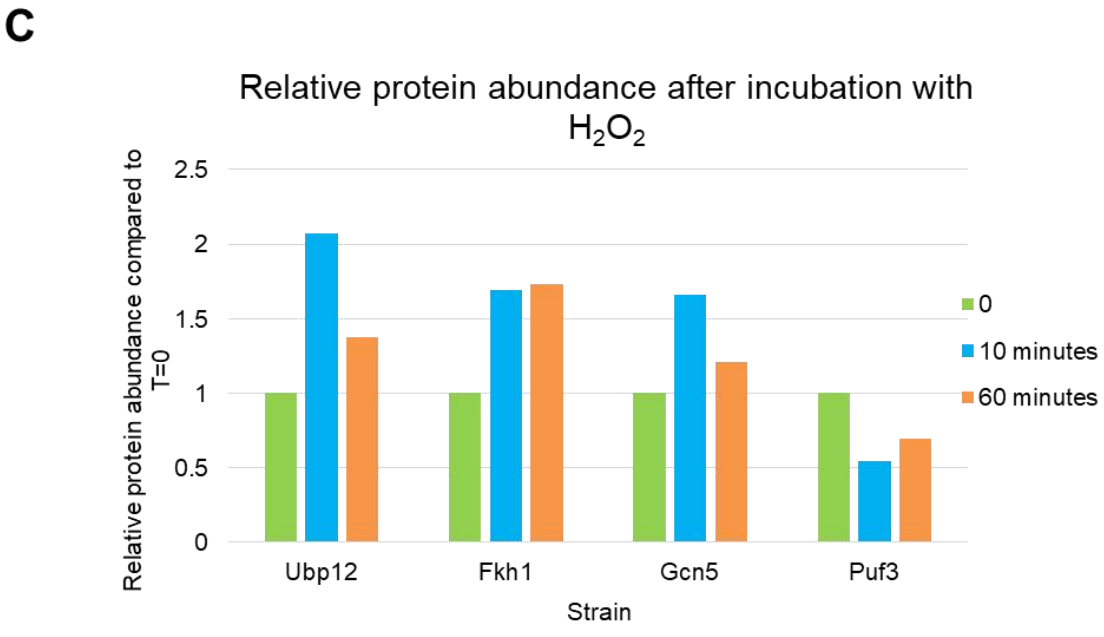
C
Relative protein abundance after incubation with $H_2O_2$
Relative protein abundance compared to T=0
2.5
2
1.5
1
0.5
0
Ubp12
Fkh1
Gcn5
Puf3
Strain
0
10 minutes
60 minutes

**Figure 4.13: The relative abundance of known interacting partners of Ubp12 are affected by $H_2O_2$.** (A) Cells expressing Ubp12-TAP (ELR38), Fkh1-TAP (FCC179), Gcn5-TAP (FCC178), and Puf3-TAP (FCC176) were incubated with 0.2 mM $H_2O_2$ for 0, 10, and 60 minutes as indicated. Protein extracts were prepared in non-reducing conditions and separated by SDS-PAGE. Proteins were visualised using PɑP antibodies. * denotes $H_2O_2$-induced HMW complex of Ubp12. Arrows show a non-specific band used for protein abundance quantification. (B) The band intensities of Ubp12-TAP (from A) were quantified using ImageQuant and the bars show the percentage of HMW complex with respect to total Ubp12 in each lane. (C) The band intensities for TAP epitope-tagged proteins (from A) were quantified using ImageQuant. Bars show total amount of protein at each time point, related to the non-specific band denoted by the arrow (in A), and normalised to 0 minutes for each protein.

from this peak by 60 minutes (Figure 4.13C). At this stage it is not clear whether these changes in abundance are linked in some way to HMW complex formation of Ubp12 but it is intriguing that the preliminary data suggests that the abundance of these nuclear proteins changes with a timing that mimics the formation of the Ubp12 HMW complex. In contrast to Fkh1 and Gcn5, Puf3 levels appeared to decrease following $H_2O_2$ treatment (Figure 4.13C). Hence this preliminary analysis suggests that the abundance of several Ubp12 interacting proteins, (and Ubp12 itself) changes after $H_2O_2$ treatment and hence further experiments will focus on investigating whether there is a relationship between these changes and formation of Ubp12 HMW complex.

Taken together, these data suggest that Ubp12 catalytic activity influences the responses of cells to several oxidising agents. We also observed that the formation of the Ubp12 HMW complex is dependent on the catalytic cysteine, and that Ubp12 likely forms a $H_2O_2$-induced intramolecular disulphide bridge between the catalytic cysteine and another cysteine in Ubp12. Furthermore, global ubiquitination is induced by $H_2O_2$, but at this stage it is unclear if this is linked to inhibition of Ubp12 activity. Interestingly, the abundance of several Ubp12 interacting proteins is affected by $H_2O_2$. Hence, the data suggests that Ubp12 plays key roles in oxidative stress responses.

## 4.3. Discussion

Ubp12 is a relatively uncharacterised *S. cerevisiae* USP dUb, and many specific roles and regulation of Ubp12 are unknown. Work in the Chapter 3 of this thesis revealed that a striking proportion of Ubp12 was specifically modified by $H_2O_2$ into a HMW complex. In this chapter the main objective was to investigate the $H_2O_2$-induced HMW complex of Ubp12, and also begin to investigate the roles and regulation of Ubp12 in response to oxidative stress. Excitingly, here we found Ubp12 to be oxidised by $H_2O_2$, and importantly we found that Ubp12 is oxidised differentially depending on the concentration of $H_2O_2$ and moreover that this oxidation is the result an intramolecular disulphide complex which requires the catalytic cysteine. It was also observed that Ubp12 activity inhibited cellular growth after diamide and $H_2O_2$ stress, potentially suggesting a mechanism by

which Ubp12 was inhibited to allow cellular response to these oxidising agents. Interestingly, it was observed that Ubp12 was regulated by the thioredoxin pathway and preliminary investigations into specific Ubp12 substrates identified that Ubp12 oxidation may regulate the abundance of certain Ubp12 interacting proteins.

As described previously, cells must be able to sense between the different types and levels of oxidising agent in order to elicit the appropriate downstream response (see Section 1.2.5). As described in Chapter 3, Ubp12 was found to form a HMW complex specifically in response to $H_2O_2$ and none of the other oxidising agents that were tested. This raises the possibility that Ubp12 oxidation may be a component of a signal transduction pathway to sense $H_2O_2$ stress. Furthermore, experiments also revealed that Ubp12 forms the HMW complex with kinetics that depend on the concentration of $H_2O_2$. For example, after incubation with high levels of $H_2O_2$, the Ubp12 HMW complex forms very rapidly, and moreover, the amount of Ubp12 contained in the complex continues to increase over the 60 minute time course. In contrast, when cells were exposed to lower levels of $H_2O_2$, the Ubp12 HMW complex formed at a slower rate, and reached a lower peak than that observed using higher concentrations of $H_2O_2$. Interestingly, after treatment with low levels of $H_2O_2$ the Ubp12 HMW complex disappeared over time, returning fully to basal levels by 60 minutes. At this point is unknown whether the HMW complex would also disappear using a longer time course after exposure to higher levels of $H_2O_2$. One likely explanation for this loss of Ubp12 HMW complex is that Ubp12 is reduced as the cells adapt to the levels of $H_2O_2$. However, at this stage another possibility is that the HMW complex is unstable and degraded and thus the loss detected may reflect diminished oxidation of Ubp12 by $H_2O_2$. However, qualitative analysis of the total level of Ubp12 across the time course suggests that protein levels remain constant. Hence, the data is consistent with a model whereby Ubp12 is regulated by oxidation in response to different levels of $H_2O_2$.

To better understand the role of Ubp12 oxidation it was important to attempt to characterise the $H_2O_2$-induced HMW complex and also potentially identify any of the cysteines of Ubp12 involved. Importantly, the data from mass spectrometry

and western blot analyses suggested that the HMW complex likely contains one molecule of Ubp12 and, furthermore, that the increased mobility of Ubp12 was linked to the formation of an intramolecular disulphide(s). It is intriguing that USP19 has previously been shown to form a HMW disulphide complex after incubation with $H_2O_2$ (Lee *et al.*, 2013). Moreover, when USP19 is compared to the *S. cerevisiae* genome, Ubp12 is the dUb with the highest protein similarity. Hence it is tempting to speculate that Ubp12 is forming a HMW complex similar to that observed with USP19, given the similar effects of $H_2O_2$ on the mobility of the dUb. However, in the case of USP19, the authors only proposed the presence of a possible intermolecular disulphide complex, although this was not characterised. Furthermore, no potential cysteine(s) involved in the complex formation were identified. DUbs tend to be cysteine-rich proteins, and indeed Ubp12 contains 19 cysteine residues, any of which have the potential to be oxidised and form an intramolecular disulphide bond(s). The catalytic cysteine in dUbs is deprotonated to allow catalytic activity whereby the cysteine can attack the isopeptide bond between the ubiquitin moiety and target lysine (see Section 1.1.3). Importantly, deprotonation reduces the pKa value raising the possibility that this cysteine may be involved in disulphide bond formation. Excitingly, point mutation of the Ubp12 catalytic cysteine, C373, to serine prevented formation of the $H_2O_2$-induced HMW complex. Hence this suggests that C373 is part of the disulphide. However, it is also possible that the HMW complex may also be another form of oxidation such as a sulphenylamide, which could be confirmed by further mass spectrometry analyses. Interestingly, using software to predict protein structure, no other cysteine residue is predicted to be in close enough proximity to C373 of Ubp12 to be able to form a disulphide bridge. However it is worth noting that certain dUbs have been found to undergo conformational changes after binding to ubiquitin (Turcu *et al.*, 2009). For example, the mammalian dUb USP7 undergoes conformational change to align the catalytic triad to allow hydrolysis (Hu *et al.*, 2002). Furthermore, the active site of another mammalian dUb, USP14, is blocked by a loop which has to be displaced to allow deubiquitination (Hu *et al.*, 2005), and another dUb, USP8 requires movement of a finger domain to allow binding of ubiquitin to the active site (Avvakumov *et al.*, 2006). Interestingly, Ubp12 contains a large insertion between catalytic regions (Turcu *et al.*, 2009), and although conformational changes of Ubp12 have not

been explored, it is possible that under certain structural conditions, that a cysteine in one of the insertion regions may be in close proximity to the catalytic cysteine and thus be able to form a disulphide bridge after $H_2O_2$ stress. As a next step in the investigation of Ubp12 it would be useful to identify which cysteine in Ubp12 is forming an intramolecular disulphide with C373. For example, further mass spectrometry analyses where Ubp12 HMW complex has been treated with an alkylating agent to cap reduced thiols, followed by addition of a reducing agent to reduce disulphide bridges could help to identify the possible target cysteine(s) which forms an intramolecular disulphide with the C373. Importantly, the inclusion of the catalytic cysteine in the disulphide complex suggests that oxidation of Ubp12 by $H_2O_2$ inhibits the deubiquitinating activity of the dUb. One role of this oxidation may be to prevent the further oxidation of the catalytic cysteine to an irreversible modification, in other words acting to protect Ubp12. However, it is also possible that the role of this oxidation is to inhibit dUb activity. Interestingly, support for this hypothesis comes from the observation that overexpression of *UBP12* causes an increase in sensitivity of wild type cells to $H_2O_2$ (Figure 4.10). However, oxidation serves two purposes both protection and regulation. For example, the regulation of mammalian deSUMOylases by $H_2O_2$ forms a sensing mechanism, and subsequent regulation, of the SUMO pathway (Bossis and Melchior, 2006). Further studies will be required to resolve these possibilities for Ubp12 oxidation.

Intracellular protein oxidation must be tightly regulated to maintain redox states. The thioredoxin system consists of multiple enzymes with redox capabilities to allow the reduction of specific substrates (see Section 1.2.4.2.3). Thioredoxin reductase (Trr) has been characterised as a rate limiting step in this system (Brown *et al.*, 2013; Tomalin *et al.*, 2016). As a consequence, *trr1*Δ mutants have fully oxidised thioredoxin, preventing reduction of oxidised thioredoxin substrates. Hence it was hypothesised that if Ubp12 oxidation was regulated by the thioredoxin system, the Ubp12 HMW complex would be dysregulated in a *trr1*Δ mutant. Analyses of the formation of the Ubp12 HMW complex in a *trr1*Δ mutant suggested that Ubp12 was oxidised similarly to a wild type strain background. However surprisingly, the total abundance of Ubp12 was significantly reduced in the *trr1*Δ mutant. In particular the abundance of Ubp12 in the *trr1*Δ strain

background in unstressed conditions was ~63% of that in a wild type background strain. Moreover, this difference in abundance increased after $H_2O_2$ treatment, where the levels of Ubp12 in the *trr1*Δ strain were ~35% of the wild type strain. Taken together, these data suggest that the thioredoxin system is actually crucial in maintaining Ubp12 stability in both stressed and unstressed conditions. The basis of this effect of the thioredoxin system on Ubp12 stability is unclear. However, it is worth noting that thioredoxin peroxidases (peroxiredoxin) and thioredoxin have been linked to molecular chaperone activity (Jang *et al.*, 2004). For example, hyperoxidation of the 2-Cys peroxiredoxin Tsa1 in *S. cerevisiae* by oxidative stress activates molecular chaperone activity and reduces its peroxidatic activity (MacDiarmid *et al.*, 2013). It would therefore be interesting to investigate the potential role of Tsa1 in regulating Ubp12 HMW complex formation and abundance of Ubp12.

Interestingly, only ~50% of Ubp12-3HA is oxidised after treatment with $H_2O_2$. It is possible that only a subset of total cellular Ubp12 is being oxidised. Ubp12 is known to localise to the cytoplasm and the nucleus, therefore it is possible that only Ubp12 in one localisation is regulated by oxidation. To date, only 10 proteins have been identified as binding partners of Ubp12, although interestingly these include cytoplasmic and nuclear located proteins. Hence, to begin to explore the role of oxidation of Ubp12 example proteins were selected from each cellular location for further investigation. The nuclear Fkh1 and Gcn5 proteins were selected due to their links to pathways known to be regulated by ubiquitination. Fkh1, a forkhead family transcription factor, is ubiquitinated by $APC^{Cdc20}$ to initiate Fkh1 degradation and thus promote cell cycle progression through mitosis and G1 phase (Malo *et al.*, 2016). Gcn5 is a sub-unit component of ADA and SAGA histone acetyltransferase complexes. Histone regulation has been linked to ubiquitination previously (Zou and Mallampalli, 2014), and interestingly, Gcn5 is SUMOylated, however this is thought to not regulate Gcn5 histone acetyltransferase function and instead has a role in transcriptional regulation (Sterner *et al.*, 2006). Puf3, a mitochondrial outer membrane protein which faces into the cytoplasm, is an mRNA binding protein which interacts with mRNA transcripts and transports them to the mitochondria. Puf3 has been identified to inhibit mitochondrial biogenesis as Puf3 levels decrease after induction of

respiratory metabolism which promotes mitochondrial biogenesis (García-Rodríguez *et al.*, 2007). Preliminary investigations into the protein levels after treatment with low concentrations of $H_2O_2$ suggested that protein abundance of Fkh1, Gcn5, and Puf3 all changed. Interestingly, the pattern of change to protein abundance mimicked that of Ubp12 oxidation. However after these preliminary investigations it is not clear whether the change in protein abundance is due to Ubp12 oxidation, Ubp12 abundance, or the $H_2O_2$ treatment independent of Ubp12. In addition, since work on this thesis project began, Ubp12 has been identified to physically interact with more proteins and investigations into their regulation by Ubp12 would also be of interest.

It is interesting to note that recent studies have linked Ubp12 to mitochondrial regulation (Anton *et al.*, 2013, Simões *et al.*, 2018). Furthermore, Ubp12 regulated mitochondrial dynamics by working in opposition to another dUb, Ubp2 in *S. cerevisiae* (Figure 4.14). It was demonstrated that Ubp2 and Ubp12 both remove specific ubiquitin signals from the mitofusin Fzo1, regulating Fzo1 levels and resulting in either mitochondrial fission or fusion (Anton *et al.*, 2013). In particular, Ubp2 recognises Fzo1 targeted for destruction and removes these destabilising chains, effectively promoting mitochondrial fusion. On the other hand, Ubp12 removes ubiquitin chains which promote Fzo1 stability and as such promotes mitochondrial fission (Anton *et al.*, 2013) (Figure 4.14) which is vital for mitophagy (Mao and Klionsky, 2013). Ubp12 has more recently been shown to regulate Ubp2 stability, suggesting that the dUbs work in a hierarchy to regulate mitochondrial dynamics (Simões *et al.*, 2018). Interestingly it was observed in the present study that Ubp2 becomes modified in response to $H_2O_2$ (Chapter 3, Figure 3.7). However, the detection of the modification of Ubp2 was inconsistent. As described in Chapter 3, a study published since work on this thesis began revealed that the oxidation of Ubp2 in response to $H_2O_2$ is linked to the regulation of cellular K63 poly-ubiquitin levels (Silva *et al.*, 2015a). However, no specific modification was identified in the 2015 study. Here, it was hypothesised that if the $H_2O_2$-induced Ubp2 modification was oxidation, the HMW shift might be reduced by a reducing agent. Indeed, after incubation of protein extracts with β-mercaptoethanol, the $H_2O_2$-induced HMW form of Ubp2 was no longer detected (Figure 4.15A), suggesting that Ubp2 does become oxidised into a HMW form by

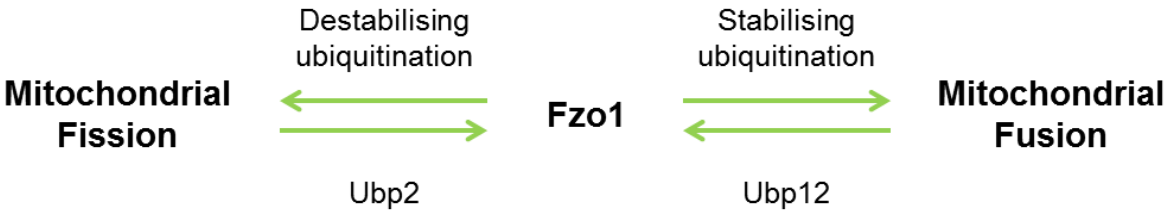


**Figure 4.14: Regulation of mitochondrial morphology by Ubp2 and Ubp12.** Fzo1 can be ubiquitinated differently to promote different mitochondrial morphology. Ubiquitination can either promote degradation of Fzo1 (destabilising chains) or promote Fzo1 stability (stabilising chains). Ubp2 removes the destabilising ubiquitin signals and promotes mitochondrial fusion. In contrast, Ubp12 removes stabilising chains from Fzo1, thus promoting mitochondrial fission. Adapted from (Anton *et al.*, 2013).

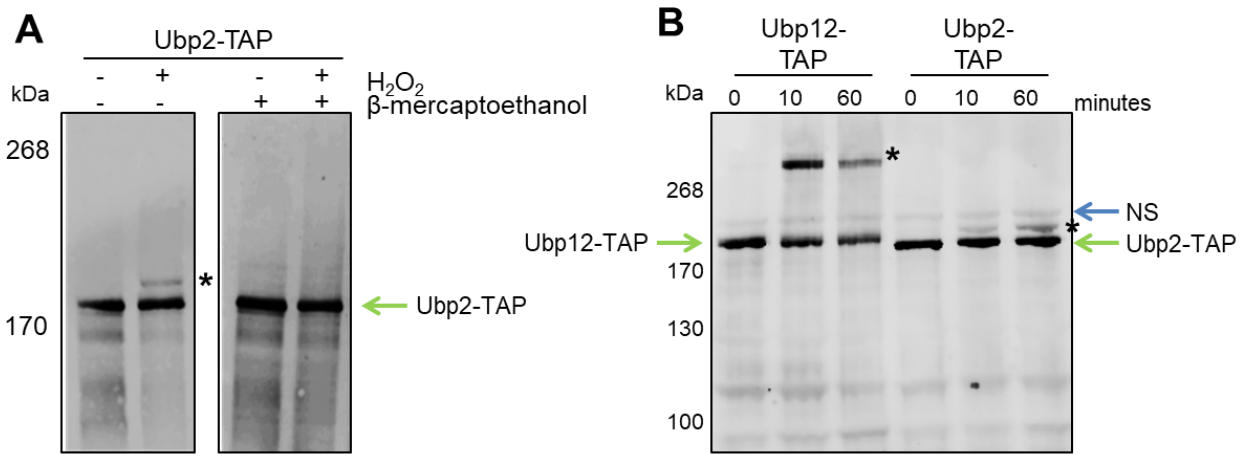
A
Ubp2-TAP
kDa
- + - +
- - + +
H2O2
β-mercaptoethanol
268
170
*
Ubp2-TAP
B
Ubp12-TAP
Ubp2-TAP
kDa
0 10 60 0 10 60
minutes
268
170
130
100
*
NS
Ubp12-TAP
Ubp2-TAP

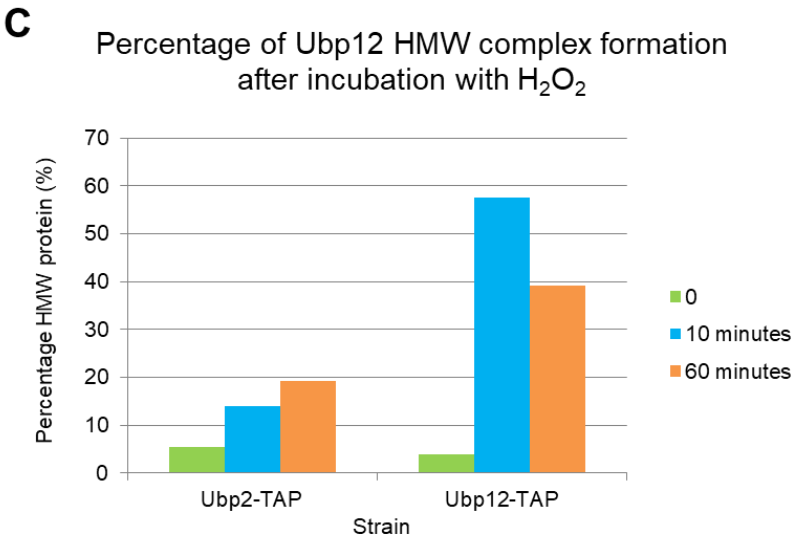
C
Percentage of Ubp12 HMW complex formation after incubation with H2O2
Percentage HMW protein (%)
70
60
50
40
30
20
10
0
Ubp2-TAP
Ubp12-TAP
Strain
0
10 minutes
60 minutes

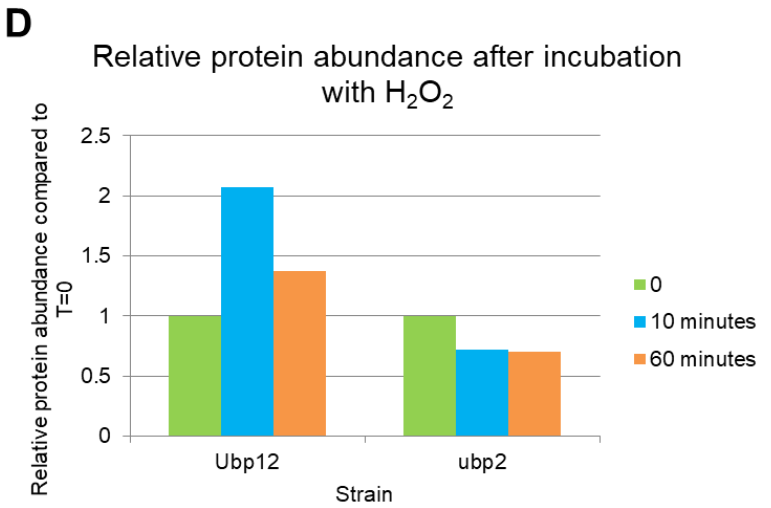
D
Relative protein abundance after incubation with H2O2
Relative protein abundance compared to T=0
2.5
2
1.5
1
0.5
0
Ubp12
ubp2
Strain
0
10 minutes
60 minutes

**Figure 4.15: Ubp2 oxidised in response to $H_2O_2$.** (A) Cells expressing Ubp2-TAP (ELR29) in the BY4741 strain background were incubated with 2 mM $H_2O_2$ for 0 (-) and 10 (+) minutes. Protein extracts were prepared in reducing (+ β-mercaptoethanol) and non-reducing conditions and separated by SDS-PAGE. Proteins were visualised using PαP antibodies. * denotes $H_2O_2$-induced complexes. (B)Cells expressing Ubp12-TAP (ELR38) and Ubp2-TAP (ELR29) were grown to mid-log phase and treated with 0.2 mM $H_2O_2$ for 0, 10, and 60 minutes. Protein extractions were prepared in non-reducing conditions in the presence of NEM. Proteins were separated by SDS-PAGE and visualised by western blotting using peroxidase anti-peroxidase antibodies. * indicates HMW modification. (C) The band intensities of Ubp12-TAP and Ubp2-TAP (from B) were quantified using ImageQuant and the bars show the percentage of HMW complex with respect to either total Ubp12 or total Ubp2 in each lane. (D) The band intensities for Ubp12-TAP and Ubp2-TAP (from B) were quantified using ImageQuant. Bars show total amount of protein at each time point, related to the non-specific band denoted by the blue arrow (in B), and normalised to 0 minutes for each protein.

$H_2O_2$. In the experiments described in Chapter 3, a time point of 10 minutes after $H_2O_2$ addition was chosen to analyse possible modifications of the dUbs. Hence, it was possible that the explanation for the inconsistency of detection of Ubp2 modification was due to the fact that Ubp2 modification, in contrast to Ubp12, was still at the early stages of formation. Therefore, to test this possibility cells expressing Ubp2-TAP were incubated with $H_2O_2$ over a longer time frame to investigate the timing of Ubp2 oxidation. Interestingly, and in contrast to Ubp12 which reached a maximum peak of HMW formation at 10 minutes and decreased in levels by 60 minutes, Ubp2 oxidation was observed to increase over the 60 minutes time course (Figure 4.15C). Thus these results suggest that the kinetics of oxidation of Ubp2 and Ubp12 by $H_2O_2$ is different. It has been described previously that Ubp12 regulates Ubp2 stability (Simões *et al.*, 2018). Hence it was possible that inactivation of a proportion of Ubp12 by oxidation might cause an increase in Ubp2 stability, due to reduced Ubp12 dependent deubiquitination of Ubp2. However, preliminary investigations of Ubp2 levels after oxidation of Ubp12 suggested a small decrease protein abundance (Figure 4.15D). However this result is preliminary and further studies are needed.

Mitochondria are intrinsically linked to ROS levels, and have been shown previously to change their morphology depending on the levels of ROS in the environment (Zemirli *et al.*, 2018). Under mild stress, mitochondria form fused chains, which allows increase of oxidative phosphorylation and ATP production to overcome the cellular stress. However, in contrast, after severe stress, mitochondria undergo fission and become more fragmented to allow damaged mitochondria to undergo mitophagy and be removed from the environment (Zemirli *et al.*, 2018). Importantly mitochondrial homeostasis is a dynamic event which occurs naturally in the cell and readily adapts to the environment. Based on the observations about Ubp2 and Ubp12 oxidation described in this thesis work, together with the previous study demonstrating that Ubp2 and Ubp12 act in opposition to regulate mitochondrial dynamics, we propose a model whereby the relative sensitivities of Ubp2 and Ubp12 to oxidation by $H_2O_2$ stress regulates whether mitochondria undergo fission or fusion. In the model, under mild $H_2O_2$ stress Ubp12 becomes oxidised and inactivated thus promoting fusion. However in more prolonged exposure, Ubp12 oxidation is reversed whist Ubp2 oxidation

increases, potentially inactivating Ubp2. In this case mitochondrial fission would be promoted. It would be interesting to investigate whether mitochondrial dynamics support this model using microscopic analyses. It will also be important to attempt to establish in which cell compartments the Ubp2 and Ubp12 dUbs become oxidised.

In the work described in this chapter, Ubp12 was found to be rapidly oxidised by $H_2O_2$ forming a HMW intramolecular disulphide complex in a concentration dependent manner. Furthermore, the catalytic cysteine was shown to be essential for this complex suggesting that it forms an intramolecular disulphide with another unidentified cysteine residue in Ubp12. It was also revealed that Ubp12 abundance is regulated by the thioredoxin system, under stressed and unstressed conditions. Excitingly, the analysis of Ubp12 and Ubp2 led to the proposal of a model for mitochondrial morphology regulation whereby the differential sensitivities of Ubp12 and Ubp2 may regulate mitochondrial dynamics in response to $H_2O_2$ stress. Importantly, Ubp12 and Ubp2 have mammalian homologs, USP15 and USP28 respectively. Mitochondrial regulation is a key aspect of many diseases as mitochondrial fission is necessary for the removal of damaged organelles by mitophagy, it would therefore be extremely interesting to examine the oxidation, and potential regulation, of these proteins in mammalian cells.

# Chapter 5: Analyses of the roles and regulation of the dUb Ubp15 in stress responses and cell cycle regulation

## 5.1. Introduction

Ubp15 is a member of the *S. cerevisiae* USP dUb family, which function by the activity of an active site catalytic cysteine. Although relatively little is currently known about the activity of Ubp15, previous work has revealed that Ubp15 is a highly active dUb (Bozza and Zhuang, 2011) which localises to the cytoplasm and the peroxisome (Debelyy *et al.*, 2011). Excitingly, work presented in Chapter three in this thesis showed that Ubp15 was modified into HMW complexes after incubation with the oxidising agent's diamide and $H_2O_2$, but not menadione. It is striking that the stress-induced HMW forms of Ubp15 appear similar in mobility to those observed when Cdc34 also forms a HMW complex after treatment with $H_2O_2$ and diamide, but not menadione (Doris *et al.*, 2012). This HMW complex of Cdc34 involves an intermolecular disulphide with the E1 Uba1 and moreover, is linked with oxidative stress-induced cell cycle arrest (see Section 1.3.3). Interestingly, some previous work has also linked Ubp15 with cell cycle regulation through direct physical interaction with Cdh1 (Bozza and Zhuang, 2011), a WD40 repeat containing protein which activates the key cell cycle E3, APC/C (see Section 1.1.1.3.1). Ubp15 interacts with Cdh1 at both N- and C- terminal domains. However, the interaction with Cdh1 does not appear to affect Ubp15 activity, leading to the suggestion that Cdh1 may target Ubp15 to substrates (Bozza and Zhuang, 2011). Interestingly Cdh1 determines substrate specificity for the APC/C complex, whereby Cdh1 initiates the interaction with many cell cycle promoting proteins including the B-type cyclin Clb5 (Nagai and Ushimaru, 2014). It was proposed that the interaction of Ubp15 and Cdh1 may tightly regulate cell cycle linked protein substrates of the APC/C. The potential for Ubp15 to regulate the cell cycle, and the similarity between Ubp15 HMW complexes Cdc34-dependent HMW complexes observed previously raised the exciting possibility that Ubp15 may be modified as a component of a mechanism to regulate cell cycle progression in response to oxidative stress. Hence, this

Chapter aimed to understand the nature of Ubp15 HMW complexes, to investigate the regulation of Ubp15 modification and to explore further the potential regulation of the cell cycle by Ubp15.

## 5.2. Results

### *5.2.1. Analyses of the $H_2O_2$- and diamide-induced HMW forms of Ubp15.*

As described previously, proteins can be modified in multiple ways which result in changes to protein mobility when analysed by western blot (Carruthers *et al.*, 2015). As described in Chapter three, Ubp15 was found to form HMW complexes in response to both diamide and $H_2O_2$. Furthermore, the work revealed that Ubp15 appeared to be modified differently by diamide and $H_2O_2$ in the BY4741 strain background compared with the W303 strain background (Figure 3.13). Interestingly, previous studies revealed that BY4741 strains have a different response to oxidative stresses to W303 (see Section 1.2.4.3). Furthermore, given the similarity of the responses of Ubp15 and Cdc34 to oxidative stress, this raised the possibility that the Ubp15 HMW complexes were due to oxidation induced by $H_2O_2$ and diamide. Hence to investigate whether the HMW modifications of Ubp15 induced by diamide and $H_2O_2$ were oxidation, cells expressing TAP epitope tagged Ubp15 were treated with either 3 mM diamide or 2 mM $H_2O_2$. Protein extracts were prepared in either reducing or non-reducing conditions, and analysed by western blot (Figure 5.1). As a diamide-induced HMW form of Ubp15 was not observed previously in the W303 strain (Figure 3.13), the effects of diamide on Ubp15 were only investigated in the BY4741 TAP-tagged strain background. Importantly, the diamide-induced HMW form of Ubp15 was found to be reduced by β-mercaptoethanol (Figure 5.1A), suggesting that Ubp15 was indeed oxidised by diamide. Interestingly, Ubp15 appears to be modified differently in response to $H_2O_2$ depending on the strain background. In the BY4741 background two HMW modifications of Ubp15 are observed after $H_2O_2$ treatment; a very large HMW form, and another form which has only a slightly slower mobility than in unstressed cells (Figure 5.1B). In contrast, in the W303 strain background only one HMW modification is detected, which appears to have

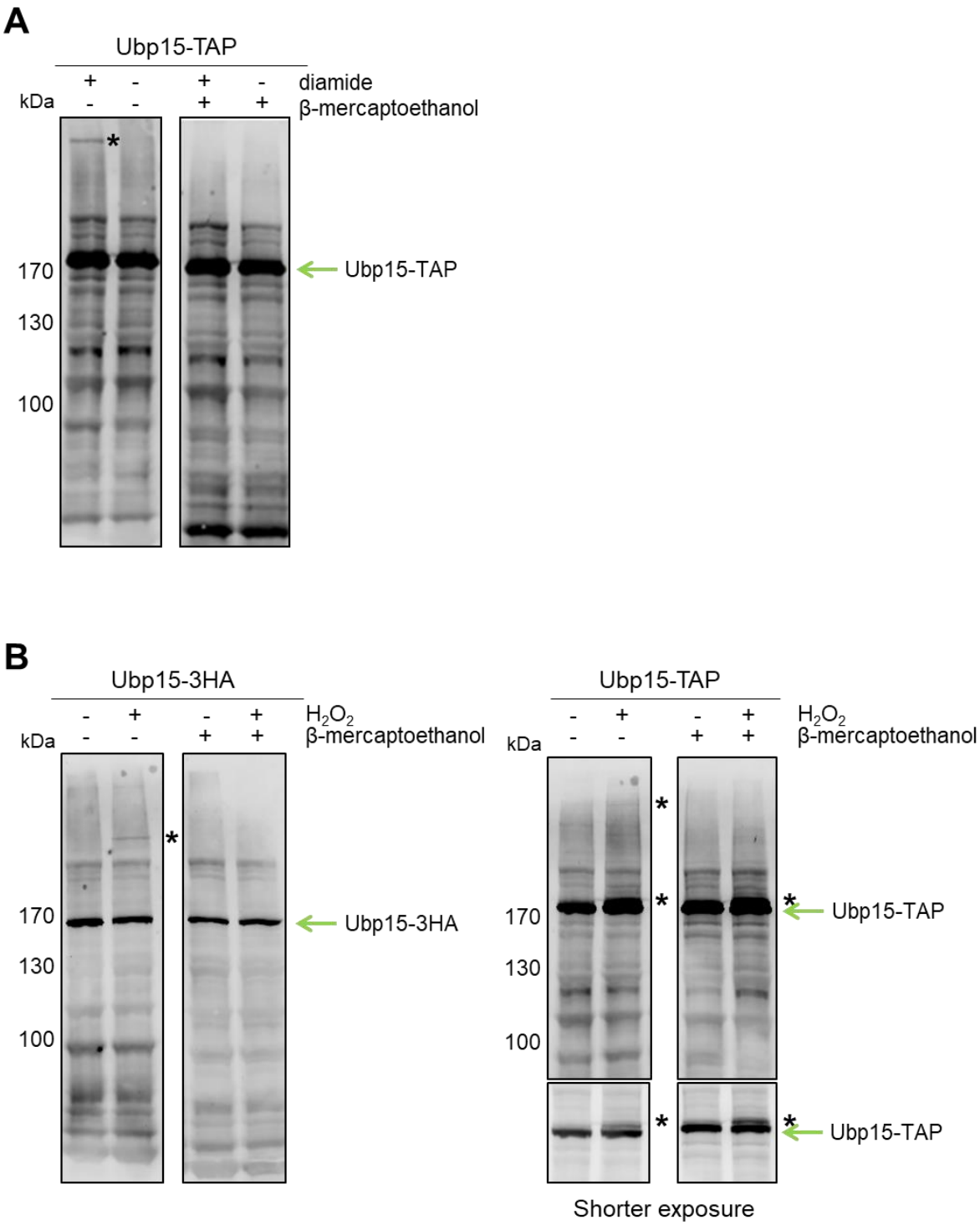


**Figure 5.1: Ubp15 HMW modification is reduced by β-mercaptoethanol.** (A) Cells expressing Ubp15-TAP (ELR41) in the BY4741 strain background were incubated with 3 mM diamide for 0 (-) and 10 (+) minutes. Protein extracts were prepared in reducing (β-mercaptoethanol) and non-reducing conditions and separated by SDS-PAGE. Proteins were visualised using PαP antibodies. * denotes diamide-induced HMW complexes. (B) Cells expressing Ubp15-3HA (FCC130) in the W303 strain background, and cells expressing Ubp15-TAP in the BY4741 strain background, were incubated with 2 mM $H_2O_2$ for 0 (-) and 10 (+) minutes. Protein extracts were prepared as in (A), and visualised using α-HA antibodies. * denotes $H_2O_2$-induced modifications.

a similar mobility as the very large HMW form seen in the BY4741 strain background (Figure 5.1B). Importantly, the large HMW forms of Ubp15 observed in both strain backgrounds were reduced by β-mercaptoethanol, suggesting that these HMW forms involve oxidation of Ubp15. However, in contrast, the relatively smaller modified form of Ubp15 detected in the BY4741 strain background was not reduced by β-mercaptoethanol, suggesting that this modification is not due to oxidation (Figure 5.1B). The basis of this β-mercaptoethanol resistant form of Ubp15 is not known, but it may be due to modifications such as phosphorylation or ubiquitination, which cannot be reduced by a reducing agent. Indeed, Ubp15 has 5 lysine residues which have been observed to be ubiquitinated previously (K303, K508, K771, K1127, and K1163) (Swaney *et al.*, 2013). Taken together these results indicate that, although the smaller mobility shift of Ubp15 in response to $H_2O_2$ in the BY4741 strain background is unlikely to be due to oxidation, the very large HMW forms of Ubp15 are reduced by a reducing agent, suggesting that they are dependent on the oxidation of Ubp15 by $H_2O_2$ and diamide.

#### *5.2.1.1. Analyses of the oxidation of Ubp15 by different concentrations of $H_2O_2$ and diamide*

In order to respond in an appropriate manner cells need to be able to sense the different types and concentrations of oxidising agents (see Section 1.2.5). As described previously, Ubp15 is oxidised by $H_2O_2$ into HMW forms in both the BY4741 and W303 strain backgrounds. However, the initial studies suggested that only Ubp15 in the BY4741 strain background was oxidised by diamide. Previous studies have suggested that Ubp15 potentially regulates the cell cycle through its interaction with Cdh1, and the APC/C complex (Bozza and Zhuang, 2011). For investigations of the cell cycle, the W303 strain background is particularly ideal as the cells can be easily synchronised using α-factor. Therefore, to investigate the oxidation of Ubp15 and the potential links to cell cycle progression in response to oxidative stress it was decided to investigate Ubp15 oxidation in the W303 strain background. One possible explanation of the lack of detection of a diamide-induced HMW Ubp15 complex in the W303 strain background was that the concentration and/or timing of incubation required to

detect the complex is different to the BY4741 strain background. In Chapter 4 it was also shown that the kinetics of Ubp12 HMW complex formation is different depending on the concentration of $H_2O_2$ used. Hence, to explore some of these issues, cells expressing Ubp15-3HA in the W303 strain background were incubated with different concentrations of $H_2O_2$ and diamide for ten minutes and protein extracts were analysed by western blot (Figure 5.2). As observed previously, Ubp15 forms a very HMW complex in response to $H_2O_2$ (Figure 5.2A). However, interestingly, the formation of this complex appears to depend on the different concentrations of $H_2O_2$ used. For example, at low concentrations of $H_2O_2$, only a relatively small amount of Ubp15 can be detected in the HMW form. However, as the concentration of $H_2O_2$ used is increased the relative level of HMW complex is observed to increase, peaking at 2 mM $H_2O_2$. The levels of HMW complex then appear to reduce as the $H_2O_2$ concentration is further increased to 5 mM (Figure 5.2A). This difference in HMW complex formation depending on the concentration of $H_2O_2$ raises the possibility that this is a component of a mechanism that can sense and responds to different concentrations of $H_2O_2$. Interestingly, HMW forms of Ubp15 were also observed in response to diamide treatment (Figure 5.2B), similar to the studies of Ubp15-TAP in the BY4741 strain background (Figure 5.1). However the levels of diamide-induced HMW forms detected in the W303 strain background seems to be much lower than those detected in the BY4741 strain background. It is also interesting to note that, although the western analyses were performed on different gels, in relation to the size marker track there seems to be a difference in the mobilities of the HMW complexes formed after $H_2O_2$ and diamide treatment (Figure 5.2 compare A and B). When comparing the Ubp15 HMW complexes formed in BY4741 strain background in response to $H_2O_2$ and diamide, it is hard to distinguish any obvious differences in mobility (Figure 5.1). However, the TAP epitope tag is large, and as a consequence may mask any differences in mobility. In conclusion, given the low levels of Ubp15 HMW complex formed in response to diamide in the W303 strain background, the next experiments focused on the $H_2O_2$-induced HMW complex. However, it is intriguing that different complexes are detected in response to different oxidising agents.

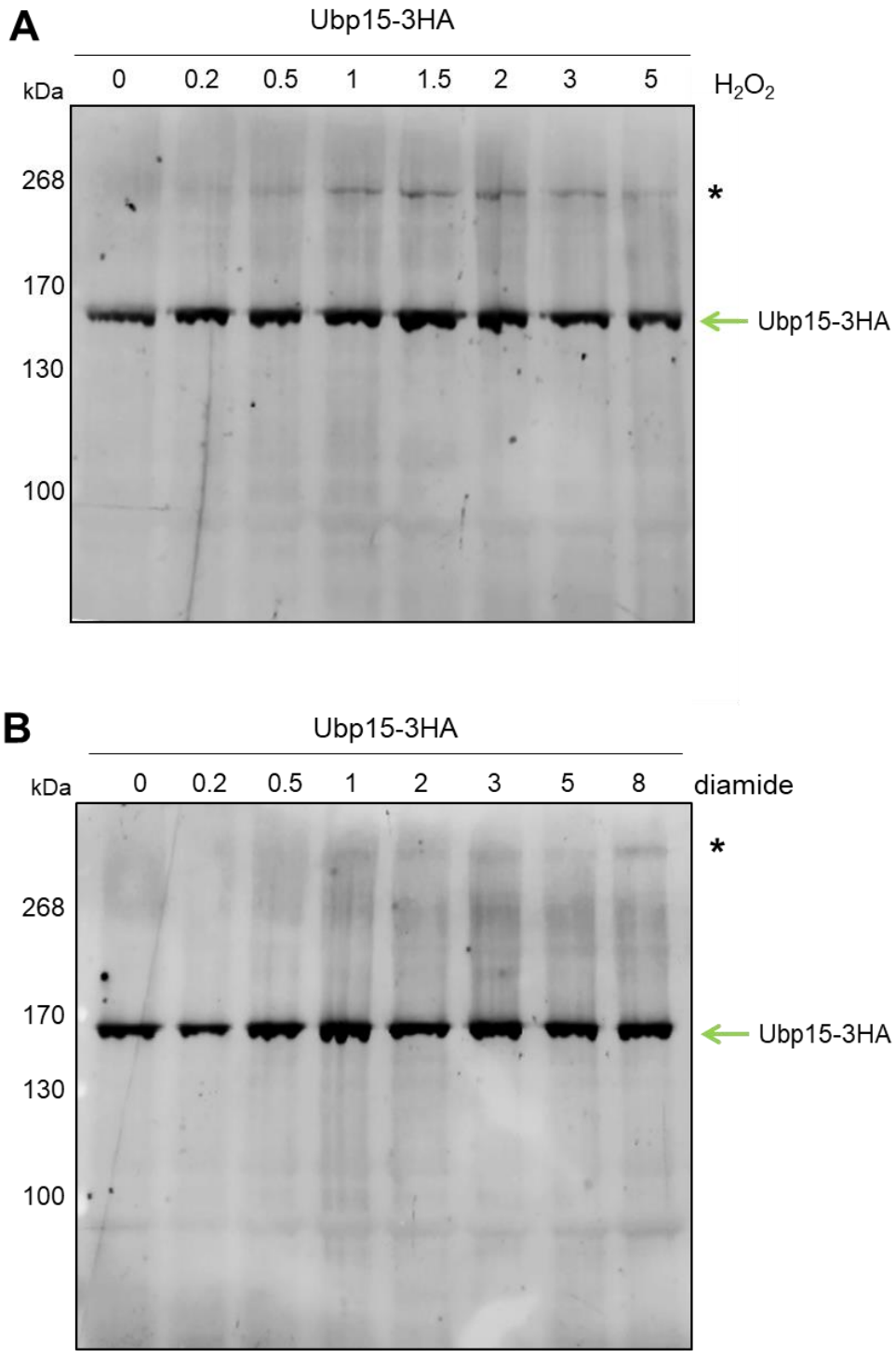


**Figure 5.2: Ubp15 is oxidised by a range of oxidising conditions.** (A) Cells expressing Ubp15-3HA (FCC130) in the W303 strain background were incubated with a range of concentrations of (A) diamide or (B) $H_2O_2$ as indicated for 10 minutes. Protein extracts were prepared in non-reducing conditions and separated by SDS-PAGE. Proteins were visualised using α-HA antibodies. * denotes stress-induced HMW forms.

Next, the dynamics of Ubp15 HMW complex formation were investigated in response to $H_2O_2$. When incubated with different concentrations of $H_2O_2$ it was observed that different amounts of Ubp15 formed a HMW complex (Figure 5.2A) However, as described above, all the samples analysed in Figure 5.2 were collected after 10 minutes exposure of cells to $H_2O_2$. It was possible, for example, that Ubp15 may form equivalent levels of HMW complex at lower concentrations of $H_2O_2$, but at a slower rate. Hence, to examine this possibility, cells expressing Ubp15-3HA was incubated with either 0.5 mM or 2 mM $H_2O_2$ for 60 minutes. Samples were taken at the indicated time points and analysed by western blot (Figure 5.3). When incubated with 2 mM $H_2O_2$ Ubp15 HMW complex forms by 30 seconds, and is sustained over the 60 minutes time course (Figure 5.3A). The amount of Ubp15 in the HMW complex with respect to the total amount of Ubp15 in each lane was calculated from two independent repeats (Figure 5.3B). By 30 seconds, approximately 8% of Ubp15 is found in the HMW complex, which increases to a maximum of ~22% by 20 minutes (Figure 5.3B). Interestingly, the level of Ubp15 HMW complex is maintained at approximately the same amount as the maximum over the time course. Interestingly, the pattern of HMW complex at 0.5 mM $H_2O_2$ is different to that observed with 2 mM $H_2O_2$. When cells were incubated with 0.5 mM $H_2O_2$ no HMW complex was detectable until ~5 minutes (Figure 5.3C). The amount of Ubp15 HMW complex with respect to total Ubp15 was calculated from two independent repeats and confirmed this observation (Figure 5.3D). Strikingly, Ubp15 HMW formation with 0.5 mM $H_2O_2$ reached a maximum peak of only ~9% by ten minutes, after which the relative amount of HMW complex decreased over the time course (Figure 5.3D). It was also interesting to note that the relative amount of HMW complex was lower than basal levels at 30 and 60 minutes. However it is important to note that the basal level calculated is quite high and has a large error bar, therefore it is suggested that the actual basal level of Ubp15 oxidation is much lower, as per Figure 5.3B. Over both time courses the error bars are large, suggesting that basal and induced levels of HMW complex are difficult to quantify. This is potentially due to the low level of $H_2O_2$-induced HMW complex formation observed for Ubp15, as the signal is quite low it is hard to detect therefore the error bars are increased. However, taken together, these data indicate that Ubp15 HMW complex forms differentially depending on the concentration of $H_2O_2$. Thus it is possible that this

**A**

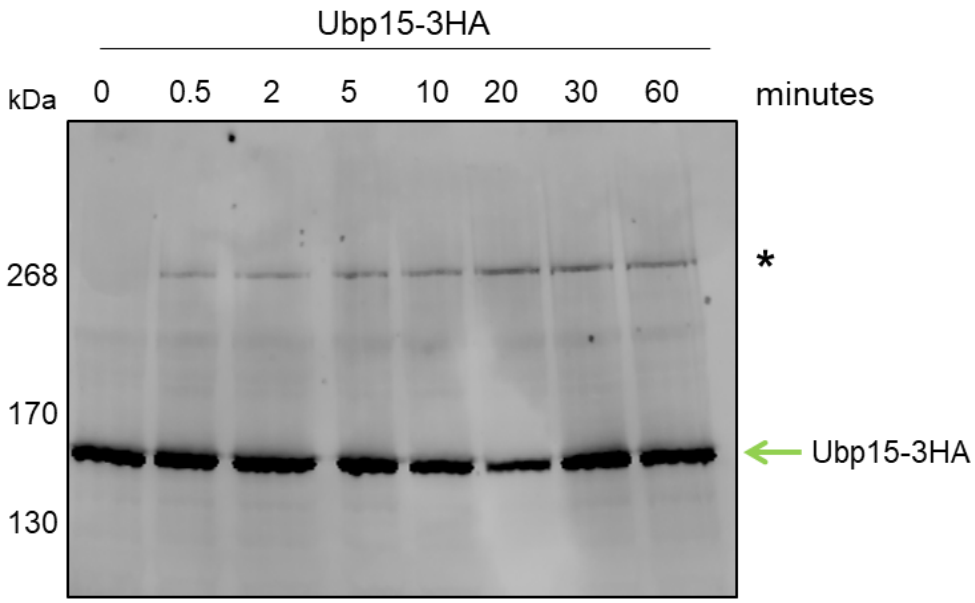
Ubp15-3HA
kDa
0
0.5
2
5
10
20
30
60
minutes
268
170
130
*
Ubp15-3HA

**B**

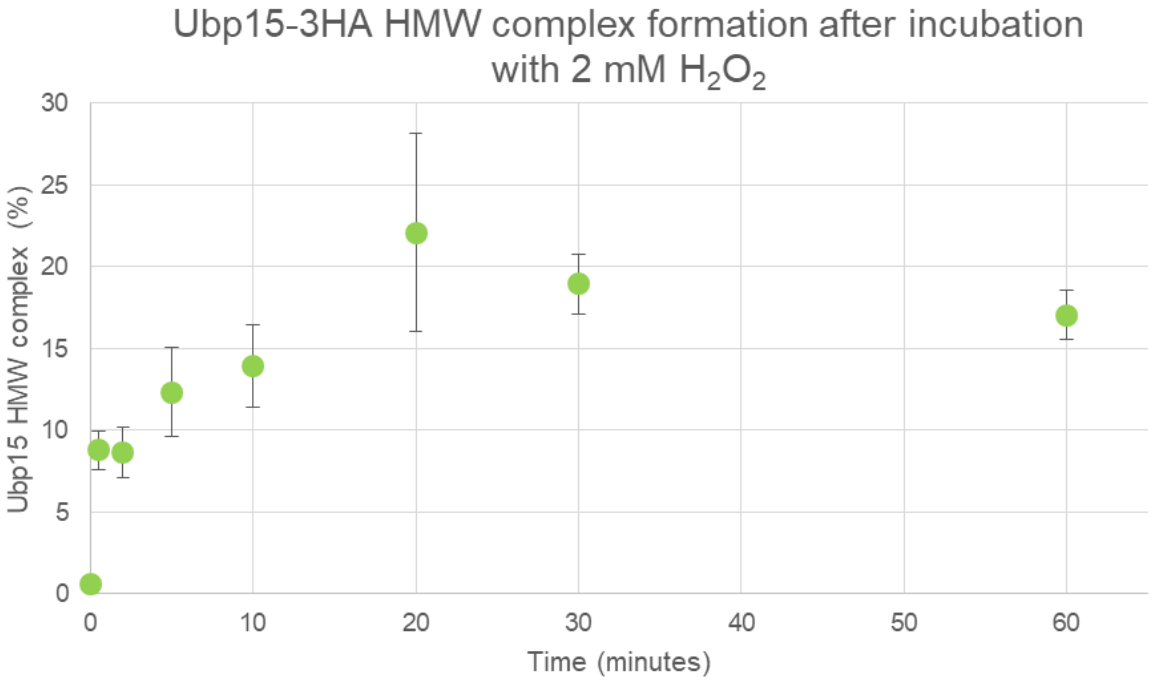
Ubp15-3HA HMW complex formation after incubation with 2 mM $H_2O_2$
Ubp15 HMW complex (%)
30
25
20
15
10
5
0
0
10
20
30
40
50
60
Time (minutes)

C

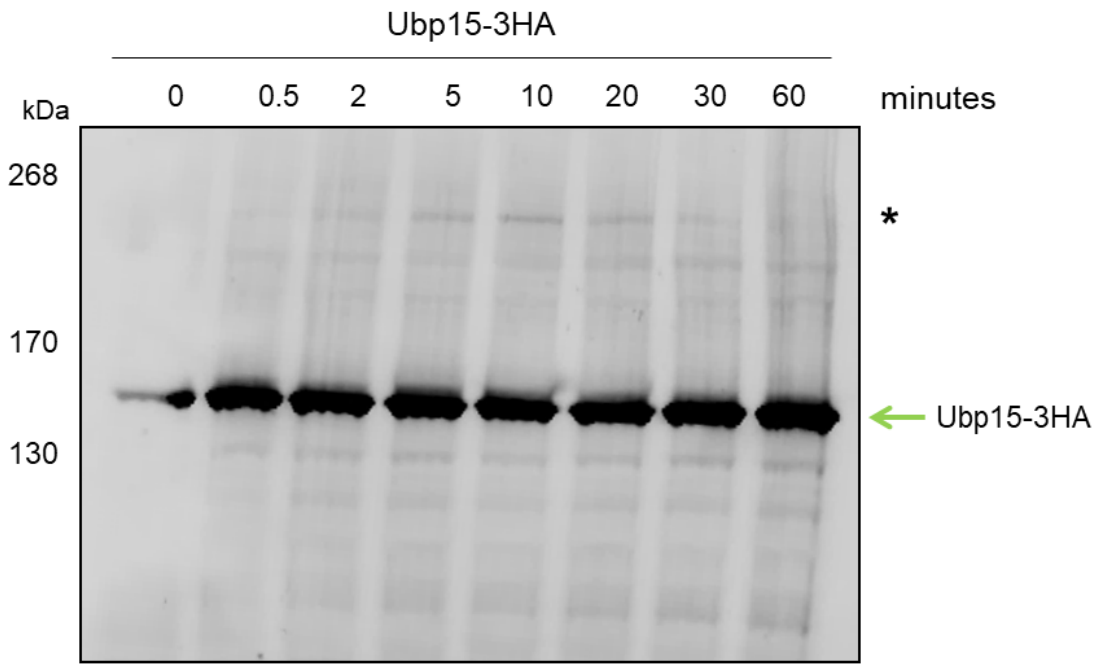
Ubp15-3HA
0
0.5
2
5
10
20
30
60
minutes
kDa
268
170
130
*
Ubp15-3HA

D

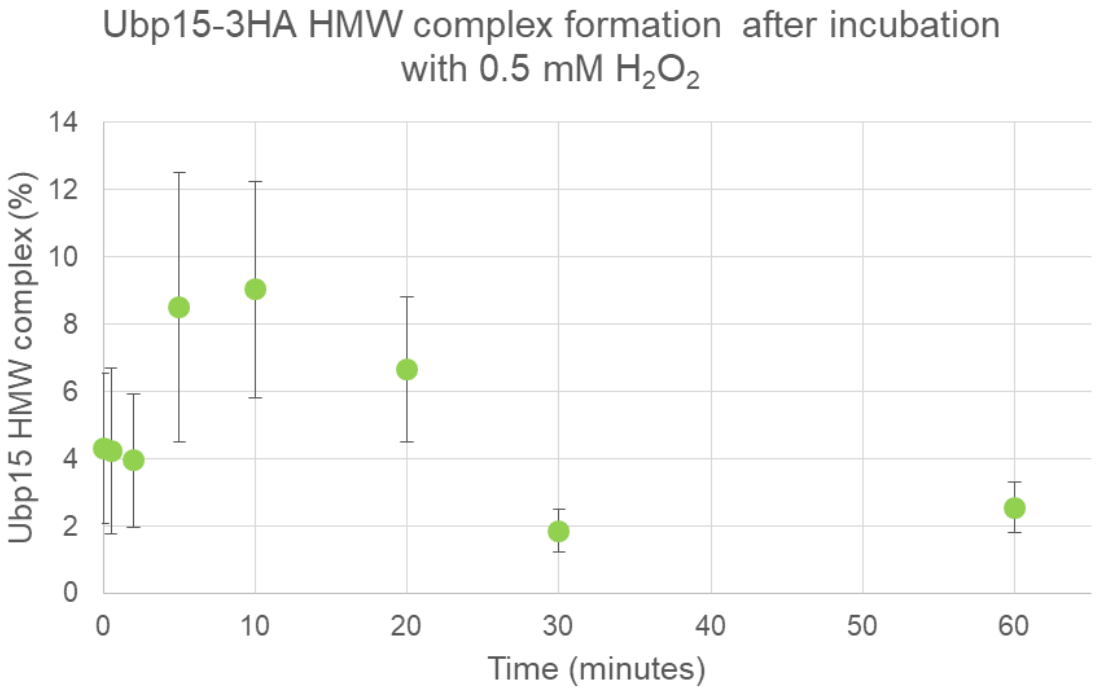
Ubp15-3HA HMW complex formation after incubation with 0.5 mM $H_2O_2$
Ubp15 HMW complex (%)
0
2
4
6
8
10
12
14
0
10
20
30
40
50
60
Time (minutes)

**Figure 5.3: The kinetics of Ubp15 HMW complex formation is $H_2O_2$ concentration-dependent.** (A) Cells expressing Ubp15-3HA (FCC130) in the W303 strain background were incubated with 2 mM $H_2O_2$ for 0 – 60 minutes as indicated. Protein extracts were prepared in non-reducing conditions and separated by SDS-PAGE. Proteins were visualised using α-HA antibodies. * denotes $H_2O_2$-induced HMW complex. (B) The band intensities of Ubp15-3HA (n=2) at each time point (from A) were quantified using ImageQuant. Points show the percentage of HMW complex with respect to total Ubp15 in each lane, and error bars denote the standard error of the mean. (C) Cells expressing Ubp15-3HA in the W303 strain background were incubated with 0.5mM $H_2O_2$ for 0 – 60 minutes as indicated. Protein extracts were prepared and visualised as in (A) * denotes $H_2O_2$-induced HMW complex. (D) The band intensities of Ubp15-3HA (n=2) at each time point (from C) were quantified using ImageQuant. Points show the percentage of HMW complex with respect to total Ubp15 in each lane, and error bars denote the standard error of the mean.

difference in complex formation is part of a mechanism that allows the cell to respond to the detected $H_2O_2$ concentration in an appropriate manner.

### *5.2.1.2. Analyses into the regulation of Ubp15 oxidation*

Oxidised proteins are tightly regulated to maintain a redox balance within the cell (see Sections 1.2.4 and 4.2.1.2). It was observed in Chapter 4 that Ubp12 protein abundance is potentially regulated by the Trx system. However, it was unknown if the Trx, or indeed the Grx, pathway, would play a role in the regulation of the formation of Ubp15 HMW complex formation. The regulation of Ubp15 oxidation by the Grx system was investigated using the chemical BSO which inhibits Gsh1 thus reducing cellular GSH levels. As described in the previous chapter (see Section 4.2.1.4) the chemical BSO inhibits Gsh1, which as a consequence depletes GSH in cells (Drew and Miners, 1984). Hence, BSO can be utilised to investigate whether GSH is required for the regulation of specific oxidised proteins. To investigate whether GSH plays a role in the regulation of Ubp15 HMW complex formation, cells expressing Ubp15-3HA were incubated with 5 mM BSO. Cells expressing Cdc34-13Myc were included as a positive control. However, despite multiple repeated attempts, the results obtained were inconclusive as the BSO-induced HMW form of Cdc34-myc was difficult to observe in the positive control (data not shown).

Next, the potential regulation of Ubp15 by the Trx system was investigated. As described previously, Trr1 acts as a rate limiting step in the thioredoxin system and deletion of Trr1 inhibits the ability of the thioredoxin system to reduce proteins (see Sections 1.2.4.2.3, and 4.2.1.2). Hence, the first step in the investigation was to construct a *trr1*Δ strain that expresses Ubp15 tagged with 3HA epitopes at the C-terminus from its normal locus. To obtain this strain a *trr1*Δ haploid was mated with a strain expressing Ubp15-3HA from its normal locus. The resulting diploid was sporulated and resulting haploids tested by PCR analyses to identify the required strain (*trr1*Δ expressing Ubp15-3HA) (Figure 5.4A and B). The potential strains were checked with gene specific primers to confirm the presence of the 3HA epitope tag cassette at the *UBP15* gene locus

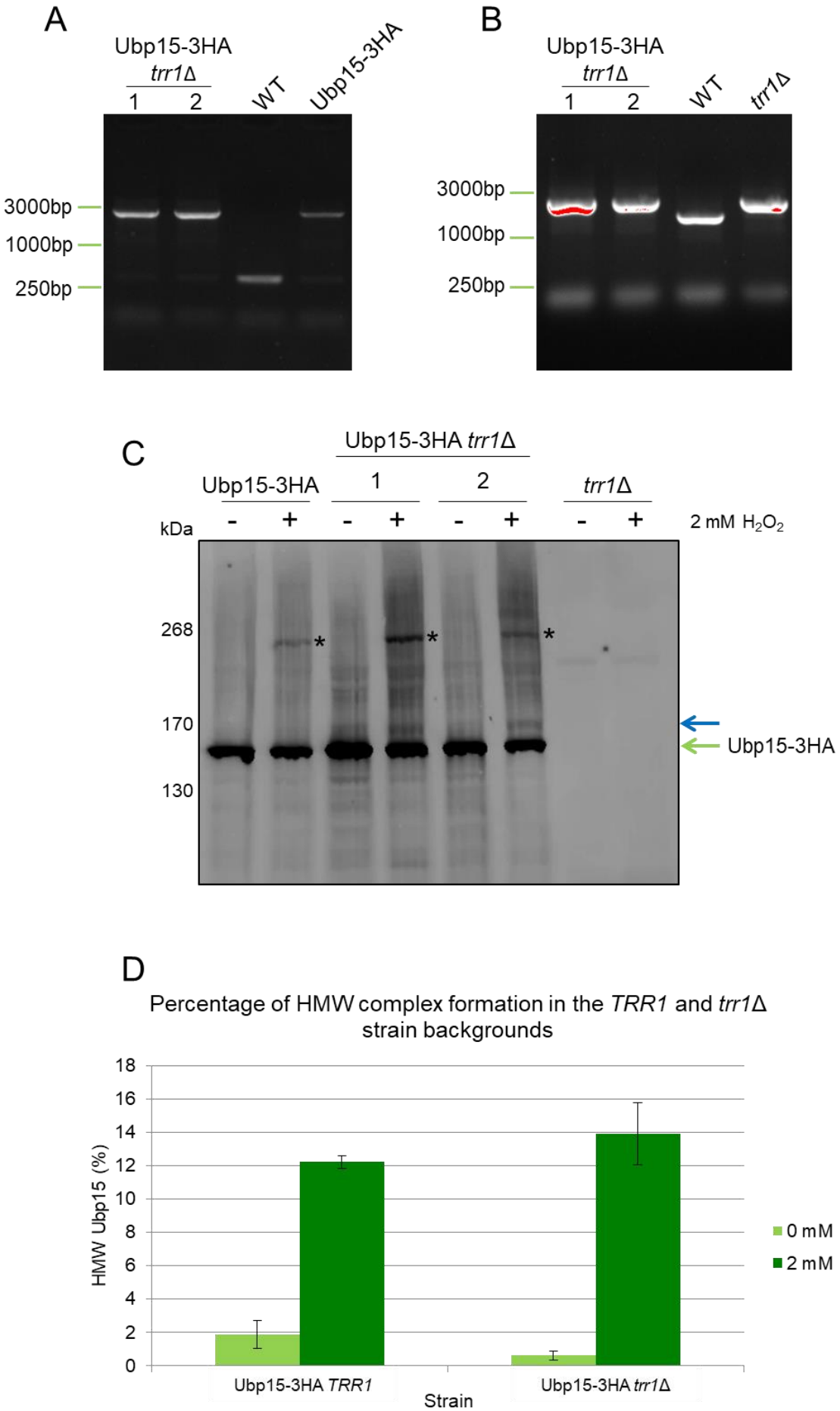
A
Ubp15-3HA
trr1Δ
1
2
WT
Ubp15-3HA
3000bp
1000bp
250bp
B
Ubp15-3HA
trr1Δ
1
2
WT
trr1Δ
3000bp
1000bp
250bp
C
Ubp15-3HA trr1Δ
Ubp15-3HA
1
2
trr1Δ
kDa
- + - + - + - +
2 mM H2O2
268
170
130
*
*
*
Ubp15-3HA
D
Percentage of HMW complex formation in the TRR1 and trr1Δ strain backgrounds
HMW Ubp15 (%)
18
16
14
12
10
8
6
4
2
0
Ubp15-3HA TRR1
Ubp15-3HA trr1Δ
Strain
0 mM
2 mM

[206]

**Figure 5.4: Ubp15 oxidation is not regulated by the thioredoxin system.** (A) PCR using *UBP15*-specific forward and reverse primers, and (B) *TRR1*-specific forward and reverse primers was performed using DNA isolated from the haploids isolated from the dissection of the sporulated diploid cells. The resulting PCR products were analysed on a 1% agarose gel. Strains with the 3HA epitope tag cassette at the *UBP15* gene locus produce a PCR product of approximately 2900 bp whereas the wild type (WT) *UBP15* gene locus produces a PCR product of ~300 bp. Strains with the deletion of the *TRR1* gene (*trr1*Δ) produce a PCR product of approximately 2000 bp whereas the wild type *TRR1* gene locus produces a PCR product of ~1600 bp. DNA from WT (FCC1), Ubp15-3HA (FCC130), and *trr1*Δ (FCC167) were included as controls in the PCR analyses. (C) Cells of a Ubp15-3HA strain, a *trr1*Δ strain, and two Ubp15-3HA *trr1*Δ strains (1 (FCC162) and 2 (FCC163)) all W303 strain background, were treated with 2 mM for 0 (-) and 10 (+) minutes. Protein extracts were prepared in non-reducing conditions and separated by SDS-PAGE. Proteins were visualised using α-HA antibodies. * denotes $H_2O_2$-induced HMW complexes. The blue arrow identifies *trr1*Δ specific HMW modification of Ubp15. (D) The band intensities of Ubp15-3HA (n=2) and *trr1*Δ Ubp15-3HA (n=2) (from C) were quantified using ImageQuant. The percentage of HMW complex with respect to total Ubp15 is shown in each lane, and error bars denote standard error of the mean.

(Figure 5.4A). The presence of the cassette would give a PCR product of ~2900 bp. Wild type *UBP15*, and Ubp15-3HA expressing strains were analysed as control with the same primers which should yield PCR products of ~300bp or ~2900 bp respectively (Figure 5.4A). Potential haploids were also checked with gene specific *TRR1* primers, (Figure 5.4B), which were predicted to give a PCR product of ~2000 bp if the *TRR1* gene was correctly deleted from the chromosome. Wild type *TRR1* and *trr1*Δ mutant strains were analysed as controls with the same primers which should yield PCR products of ~1600 bp and 2000 bp respectively. Two *trr1*Δ *UBP15*-3HA strains were confirmed (Figure 5.4A and B). Next, the two *trr1*Δ *UBP15*-3HA strains, the *trr1*Δ *UBP15* strain, and the *TRR1 UBP15*-3HA strains were grown to mid-log phase and incubated with 2 mM $H_2O_2$. Proteins were extracted in non-reducing conditions in the presence of NEM and analysed by western blot (Figure 5.4C). As expected, the $H_2O_2$ induced HMW complex was detected in the *TRR1 UBP15*-3HA cells (Figure 5.4C). Interestingly, a $H_2O_2$-induced HMW complex was also observed in the *trr1*Δ *UBP15* extracts (Figure 5.4C). Moreover, quantification of the percentage HMW complex in relation to the total amount of Ubp15-3HA in both strain backgrounds was very similar, suggesting that approximately the same proportion of Ubp15 is oxidised in response to $H_2O_2$ independent of the Trx system (Figure 5.4D). However, it is worth noting that the error bar for complex formation in the *trr1*Δ strain is large. Hence, it is possible that further repeats may reduce the error bars and perhaps reveal a significant difference in the amounts of Ubp15 oxidised in the *TRR1* versus *trr1*Δ strain backgrounds.

Interestingly, previously undetected, smaller HMW forms of Ubp15 were present in extracts from the *trr1*Δ *UBP15*-3HA strain, in both stressed and unstressed conditions (Figure 4.4C-blue arrow). The underlying basis of this mobility shift is unclear, but suggests that it is linked to the loss of Trr1 function. It is also interesting that this new HMW form has a similar mobility to the small HMW form of Ubp15 observed in the BY4741 strain background when treated with $H_2O_2$ (Figure 5.1B). In this case the smaller HMW form of Ubp15 in the BY4741 strain background was found to be resistant to reduction by a reducing agent (Figure 5.1B). Hence, to investigate whether the new HMW form of Ubp15 detected in *trr1*Δ cells was also resistant to reduction a *trr1*Δ *UBP15*-3HA strain, and a

*UBP15*-3HA control strain were grown to mid-log phase and treated with 2 mM $H_2O_2$, prepared in either reducing or non-reducing conditions, and analysed by western blot (Figure 5.5). As expected, the large HMW $H_2O_2$-induced complex of Ubp15-3HA was reduced by β-mercaptoethanol. Interestingly, the *trr1*Δ-specific smaller HMW form of Ubp15 was also reduced by β-mercaptoethanol, suggesting that Ubp15 is oxidised in the absence of Trr1 function. However the small HMW form did not appear in the presence of wild type *TRR1*, or was indeed induced by $H_2O_2$ in the *trr1*Δ strain background. Hence, it is not clear at this stage whether the smaller oxidised HMW complex is relevant to the regulation of Ubp15. Thus, taken together, the results reveal that the large $H_2O_2$-induced HMW form of Ubp15 appears to form independent of the Trx system. However, Ubp15 HMW complex formation in the *trr1*Δ strain background was only investigated after 10 minutes incubation with $H_2O_2$, the kinetics of Ubp15 HMW complex formation were not investigated. Therefore, it remains possible that the Trx system (and indeed the GSH system) may be involved in reversing Ubp15 oxidation at a later time point.

### *5.2.2. Comparison of the Ubp15 and Cdc34 HMW complexes*

Previous work from our lab revealed that an E2 enzyme in the ubiquitin conjugation cycle, Cdc34, forms a HMW intermolecular disulphide complex with Uba1 in response to specific oxidising agents (Doris *et al.*, 2012) (see Section 1.3.3). Furthermore, the formation of this Cdc34-Uba1 complex was linked to increased stability of the cyclin dependent kinase inhibitor Sic1 and delay of cell cycle progression from G1 to S phase (Doris *et al.*, 2012) (see Section 1.3.3). Interestingly a key function of Sic1 is to inhibit Cdc28-Clb5 and thus delays actovation of DNA replication. However, despite these studies all the precise components of the Cdc34-Uba1 complex were not completely clear given the very large size of the complex. As revealed earlier, Ubp15 is also oxidised by $H_2O_2$ and diamide, but not menadione, forming large HMW complexes. Strikingly, the mobility of these complexes, and the proportion of oxidised Ubp15 appears quite similar to Cdc34 oxidation. Hence, our hypothesis to explain these observations is that Ubp15 is also a component of the Cdc34-Uba1 complex and vice versa. To investigate whether Ubp15 and Cdc34 are present in the same

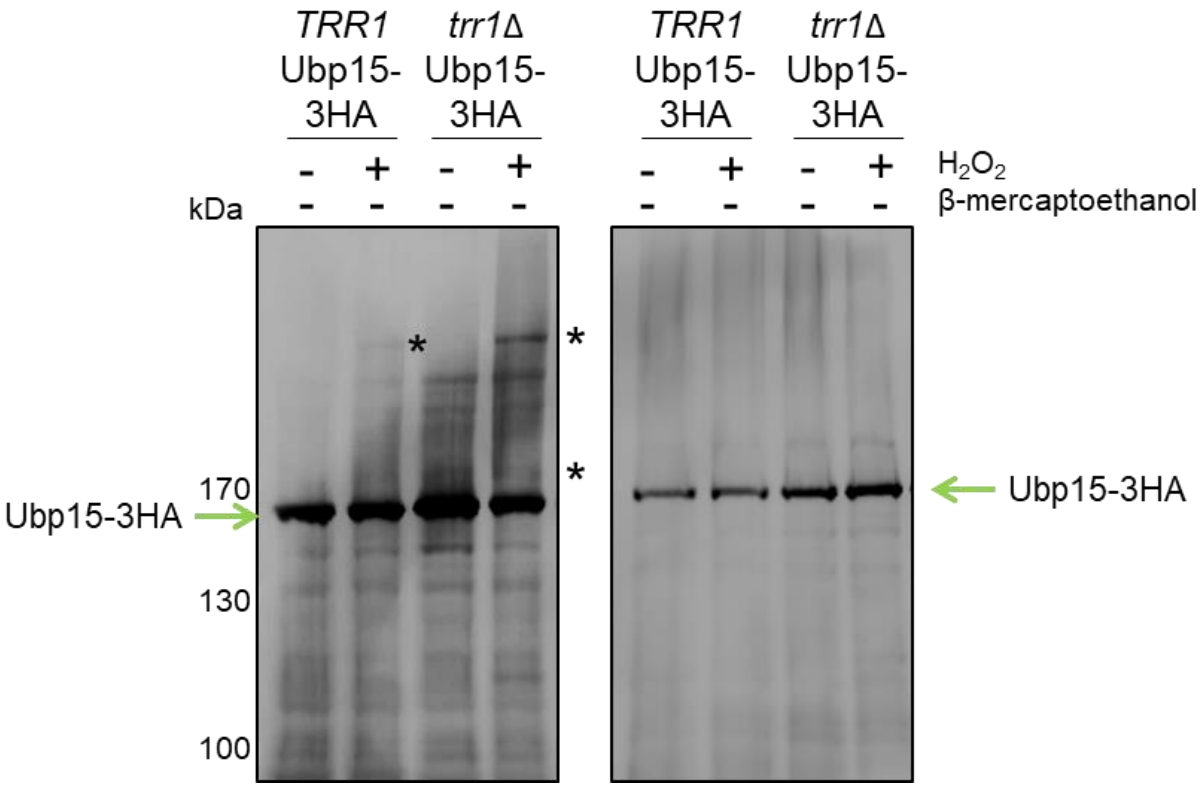


**Figure 5.5: HMW modifications of Ubp15 in the *TRR1* and *trr1*Δ strains are due to oxidation.** *TRR1* Ubp15-3HA (FCC130) and *trr1*Δ Ubp15-3HA (FCC162) cells in the W303 strain background were incubated with 2 mM $H_2O_2$ for 0 (-) and 10 (+) minutes. Protein extracts were prepared in reducing (+ β-mercaptoethanol) and non-reducing conditions and separated by SDS-PAGE. Proteins were visualised using PαP antibodies. * denotes $H_2O_2$-induced modifications.

HMW complex, cells expressing TAP epitope tagged versions of Ubp15 and Cdc34 in the BY4741 strain background were incubated with $H_2O_2$ and diamide. Proteins were extracted in non-reducing conditions in the presence of NEM and analysed by western blot (Figure 5.6). It was proposed that if Ubp15 was in the same HMW complex as Cdc34 the HMW oxidised forms of Cdc34-TAP and Ubp15-TAP would have similar mobilities. However, when exposed to the different oxidising agents the HMW complexes of Cdc34-TAP and Ubp15-TAP were not observed to have the same mobility (Figure 5.6). However it is important to note that epitope tags may affect the proteins differently resulting in differences in protein mobility. In addition, proteins with a mobility of this size often migrate through the gel differently to expectations. Hence, due to these potential problems in interpretation, a *ubp15*Δ strain was constructed expressing Cdc34-13Myc from its normal chromosomal locus. A *ubp15*Δ haploid was mated with a haploid expressing Cdc34-13Myc and the resulting diploid sporulated. Haploid spores were then analysed by PCR to confirm the presence of the *ubp15*Δ locus and the 13Myc tag cassette at the *CDC34* locus. To check the presence of the 13Myc tag cassette gene-specific *CDC34* forward and reverse primers were used. The detection of a PCR product of ~3000 bp signifies a positive result whereas the detection of a band of ~300bp signifies no cassette present (Figure 5.7A). To check for the presence of the *ubp15*Δ locus gene-specific *UBP15* forward primers and generic *HIS* reverse primers were used. A PCR product of ~2000 bp signifies the presence of the *ubp15*Δ allele, whereas no band present indicates the *UBP15* wild type gene (Figure 5.7B). After confirmation of strain construction, the Cdc34-13Myc *ubp15*Δ strain, together with Cdc34-13Myc *UBP15* were grown to mid-log phase and incubated with 2 mM $H_2O_2$. Proteins were extracted in non-reducing conditions in the presence of NEM and analysed by western blot (Figure 5.7C). It was predicted that if Ubp15 was normally a part of the Cdc34-Uba1 complex, the $H_2O_2$-induced HMW form of Cdc34 would not be present and/or would display a change in mobility. As expected, Cdc34 formed a $H_2O_2$-induced HMW complex in *UBP15* cells (Figure 5.7C). However, a HMW complex of a very similar mobility was formed in the absence of *UBP15.* Collectively, these data suggest that Cdc34 and Ubp15 are not components of the same HMW complex in responses to $H_2O_2$ and diamide.

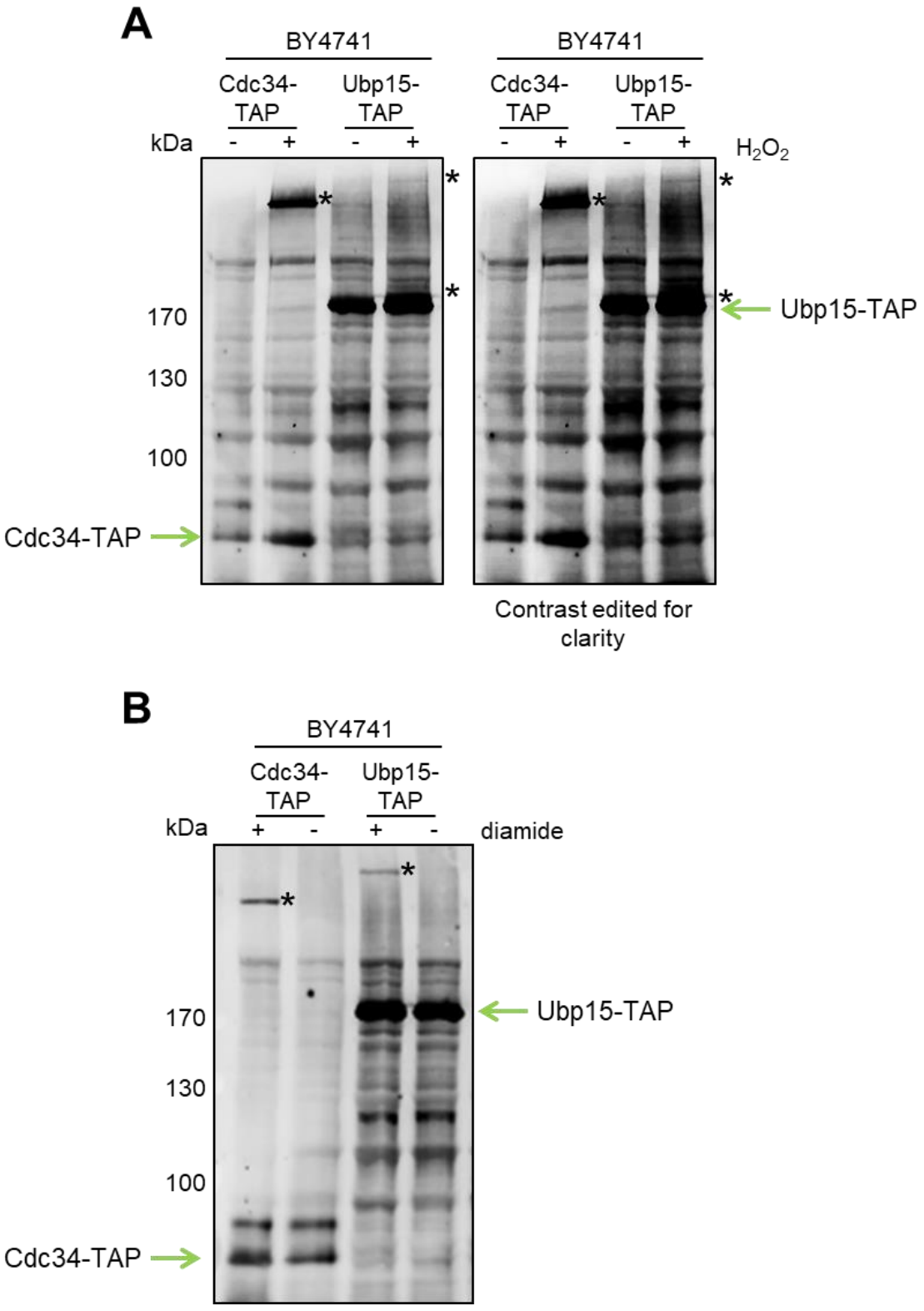


**Figure 5.6: Ubp15 and Cdc34 HMW complexes have different mobilities.** Cells expressing Ubp15-TAP (ELR41) and Cdc34-TAP (FCC145) in the BY4741 strain background were incubated with (A) 2 mM $H_2O_2$ or (B) 3 mM diamide for 0 (-) and 10 (+) minutes. Protein extracts were prepared in non-reducing conditions and separated by SDS-PAGE. Proteins were visualised using PɑP antibodies * denotes $H_2O_2$- and diamide-induced HMW complexes.

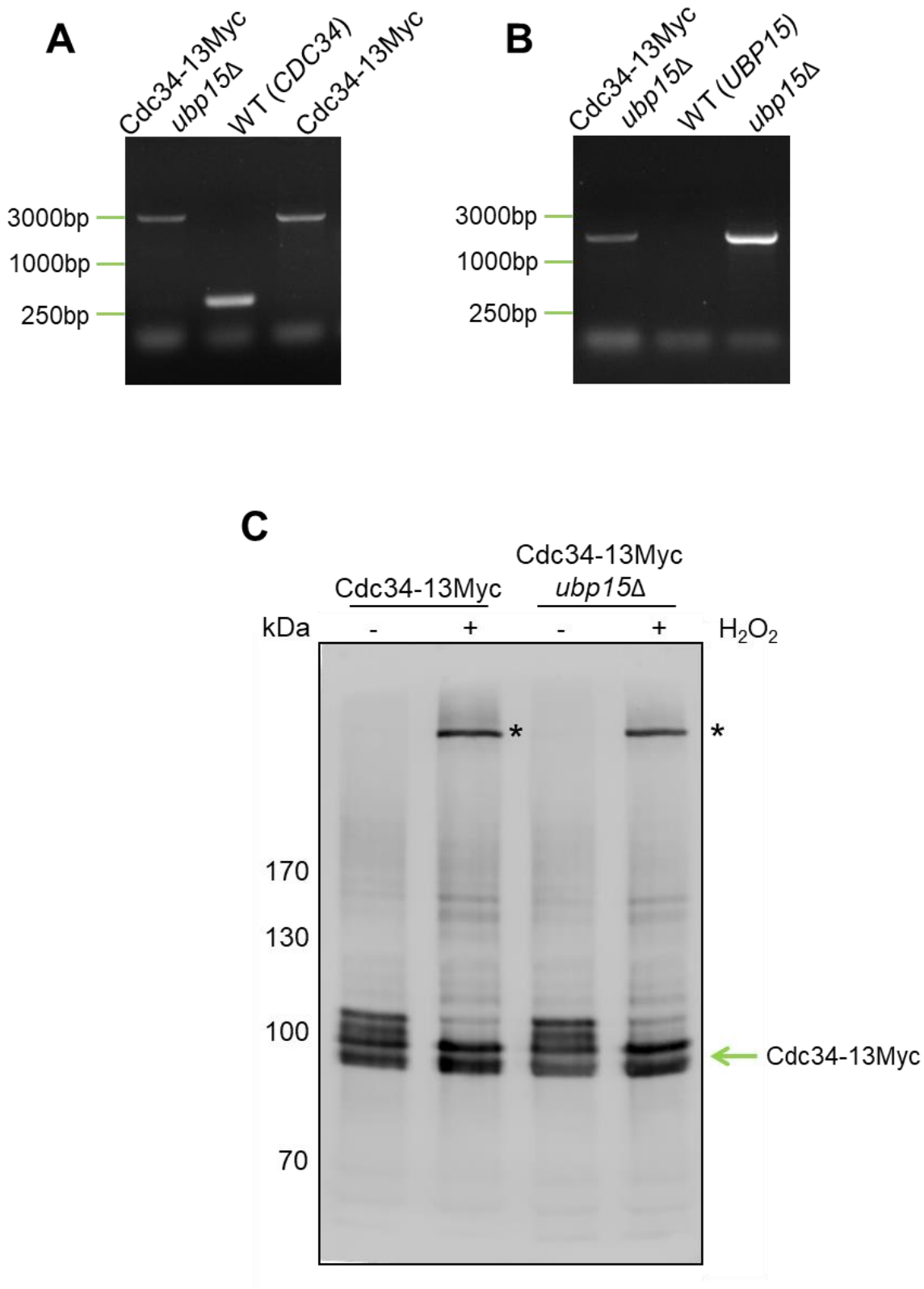
A
Cdc34-13Myc
ubp15Δ
WT (CDC34)
Cdc34-13Myc
3000bp
1000bp
250bp
B
Cdc34-13Myc
ubp15Δ
WT (UBP15)
ubp15Δ
3000bp
1000bp
250bp
C
Cdc34-13Myc
Cdc34-13Myc
ubp15Δ
kDa
-
+
-
+
H2O2
*
*
170
130
100
70
Cdc34-13Myc

**Figure 5.7: Ubp15 is not oxidised into the same HMW complex as Cdc34.** PCR using (A) *CDC34*-specific forward and reverse primers, and (B) *UBP15* gene-specific forward primers and generic *HIS* reverse primers was performed using DNA isolated from a possible *ubp15*Δ haploid expressing Cdc34-13Myc from sporulated cells. The resulting PCR products were analysed on a 1% agarose gel. The presence of a 13Myc tag cassette at the *CDC34* locus produces a PCR product of ~3000bp, whereas the wild type *CDC34* produces a PCR product of ~300 bp. The presence of the *ubp15*Δ allele at the *UBP15* locus produces a PCR product of ~2000 bp. Control strains in (A) were wild type (WT) (FCC1) and Cdc34-13Myc expressing cells (FCC156). In (B) the control strains were WT (FCC1) and *ubp15*Δ (FCC60). (C) *UBP15* and *ubp15*Δ cells expressing Cdc34-13Myc (FCC156, *UBP15*; FCC161, *ubp15*Δ) in the W303 strain background were treated with 2 mM $H_2O_2$ for 0 (-) and 10 (+) minutes. Protein extracts were prepared in non-reducing conditions and separated by SDS-PAGE. Proteins were visualised using α-Myc antibodies and α-HA. * denotes $H_2O_2$-induced HMW complexes.

### *5.2.3. Characterisation of the potential role of the Ubp15 catalytic cysteine in the HMW complex formation*

As described previously, USP dUbs catalyse the isopetide bond between the ubiquitin moiety and the substrate lysine by the activity of a catalytic cysteine which resides within the active site (Amerik and Hochstrasser, 2004). After deprotonation the pKa value is reduced which results in the cysteine being susceptible to oxidation (Cotto-Rios *et al.*, 2012). As described in Chapter 4, the catalytic cysteine of Ubp12 is essential for HMW complex formation, suggesting that this cysteine becomes oxidised in response to $H_2O_2$. Hence, it was possible that the catalytic cysteine of Ubp15 might also be involved in $H_2O_2$- and diamide-induced HMW complex formation. To investigate this possibility, a mutant version of Ubp15 was created whereby the catalytic cysteine residue (C214) was mutated to a serine residue (C214S). To allow visualisation by western blot analysis the mutation was introduced into a version of Ubp15 tagged with 3HA epitopes and expressed from a plasmid (see Section 2.2.4.1). To create a plasmid expressing the Ubp15$^{C214S}$ from the *UBP15* promoter and tagged with 3HA epitopes at the C-terminus, overlapping PCR fragments incorporating the cysteine to serine substitution were first created by PCR using wild type *UBP15* DNA as a template (see Section 2.2.4.1). The fragments were transformed into *ubp15*Δ cells, with a pRS316 vector backbone, which would recombine the fragment and plasmid backbone to create a pRS316 plasmid containing *UBP15*$^{C214S}$-3HA. The creation of a wild type version of *UBP15*-3HA in the pRS316 plasmid was attempted; however construction of the control plasmid of pRS316-*UBP15*-3HA was not completed. Colonies containing the potential recombined pRS316-*UBP15*$^{C214S}$-3HA plasmids were analysed by PCR using M13 forward and reverse primers which bind on either side of the insertion site in the plasmid (see Section 2.2.4.1). Plasmids which produced a PCR product of the expected size were extracted from *ubp15*Δ strains and transformed into *E. coli*. Plasmids were isolated from *E. coli* and sequenced to confirm the correct mutation of the cysteine 214 codon (TGC) to serine codon (TCT).

After confirmation of successful construction of pRS316-*UBP15*$^{C214S}$-3HA the plasmid was transformed into *ubp15*Δ cells. Because attempts to construct a wild

type version of this plasmid were unsuccessful the pRS316 vector was transformed into cells expressing Ubp15-3HA at the normal locus and also into *UBP15* wild type cells. Strains were then grown in SD minimal media to mid-log phase and incubated with 1 mM $H_2O_2$. Proteins were extracted in the presence of NEM, and analysed via western blot (Figure 5.8). As expected, cells expressing Ubp15-3HA from the normal locus containing empty vector pRS316 formed a $H_2O_2$-induced HMW complex (Figure 5.8). However, importantly, in the *ubp15*Δ cells containing pRS316-*UBP15*$^{C214S}$-3HA no HMW complex can be detected, suggesting that the catalytic cysteine is essential for oxidation of Ubp15 by $H_2O_2$. As described above (See section 5.2.2), Ubp15 does not form a HMW complex with Cdc34 after treatment with $H_2O_2$. However, it is possible that Ubp15 forms a disulphide complex with another protein(s), perhaps even with another Ubp15 protein. It is also possible that, similar to Ubp12, Ubp15 forms an intramolecular disulphide involving the catalytic cysteine residue, which affects mobility. Indeed Ubp15 contains another 6 cysteine residues in addition to the catalytic cysteine which may form part of the complex. It is also noteworthy that Ubp15 appears to form a different HMW complex after incubation with diamide compared to $H_2O_2$, and hence it would be important to investigate the role of the catalytic cysteine in the response of Ubp15 to diamide.

### *5.2.4. Ubp15 functions in responses to oxidative stress*

Although Ubp15 activity is relatively uncharacterised, the results described above suggest that Ubp15 may have roles in responses to oxidative stress. Previous studies revealed that Ubp15 cleaves mono-ubiquitin from substrates (Schaefer and Morgan, 2011), therefore it is possible that oxidation of Ubp15 may regulate this process. Ubp15 has also been proposed to be linked to regulation of the cell cycle through interaction with Cdh1 (Bozza and Zhuang, 2011), where it was suggested that Ubp15 may counteract the activity of the APC/C complex. Hence, perhaps oxidation of Ubp15 influences cell cycle progression. Indeed, oxidation of specific proteins is a well characterised mechanism by which cell cycle progression is regulated (for reviews see (Shackelford *et al.*, 2000; Chiu and Dawes, 2012; Diaz-Moralli *et al.*, 2013)).

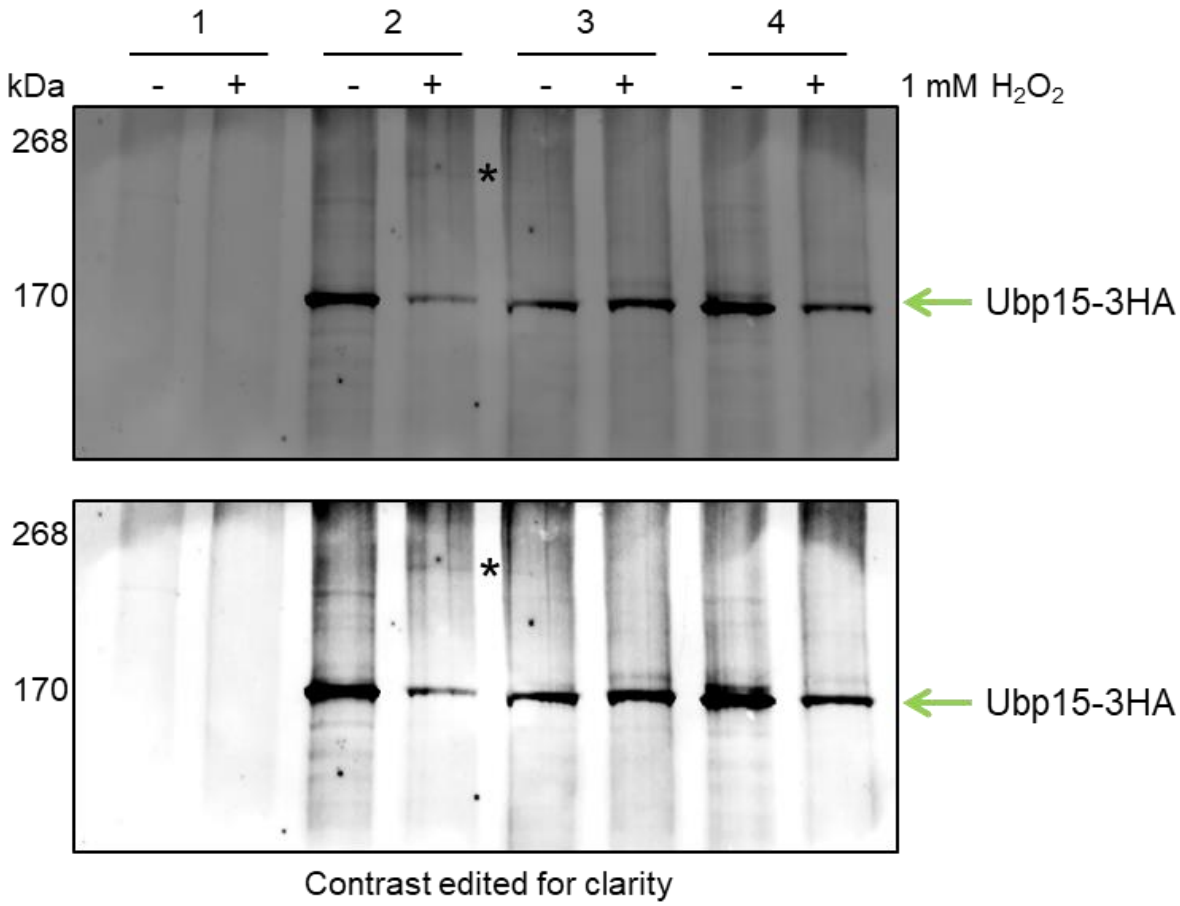


1= *UBP15* pRS316 EV
2= *UBP15*-3HA pRS316 EV
3= *ubp15Δ* pRS316-*UBP15* $^{C214S}$-3HA 1
4= *ubp15Δ* pRS316-*UBP15* $^{C214S}$-3HA 2

**Figure 5.8: The catalytic cysteine of Ubp15 is required for $H_2O_2$-induced HMW complex formation.** Wild type (*UBP15*) (FCC1) and *UBP15*-3HA (FCC130) cells containing pRS316 empty vector (EV) and *ubp15*Δ (FCC60) cells containing two different pRS316-*UBP15*$^{C214S}$-3HA plasmids in the W303 strain background were grown to mid-log phase in SD media and incubated with 1 mM $H_2O_2$ for 0 (-) and 10 (+) minutes. Protein extracts were prepared in non-reducing conditions and separated by SDS-PAGE. Proteins were visualised using anti-HA antibodies. * indicates $H_2O_2$-induced HMW complex.

*5.2.4.1. Global phenotypic analyses of Ubp15*

To begin to understand potential roles and regulation of Ubp15 in responses to oxidative stress it was decided to investigate global effects on ubiquitination. As described previously (see Chapter 3), *ubp15*Δ strains display increased sensitivity to menadione and diamide, but similar sensitivity to $H_2O_2$ as wild type cells. Interestingly, it was also found that *ubp15*Δ cells showed increased sensitivity to cold temperature (see Section 3.2.4.2). Hence, these data suggest that Ubp15 is necessary for cell responses to diamide, menadione and cold stress. However, as described previously, deletion of any specific dUb may not show severe phenotypes, due to overlapping roles with other dUbs (see Section 1.1.3). Therefore it is difficult to make firm conclusions about specific dUb roles in response to stress based on analyses of single mutants. In attempt to overcome these limitations, a plasmid overexpressing *UBP15* was constructed. If Ubp15 is involved in different stress responses it was hoped that overexpression might reveal roles for Ubp15 and confirm connections with stress responses identified in *ubp15*Δ cells. Hence, *UBP15* was overexpressed using a pRS426 2micron plasmid (pRS426-*UBP15*). To obtain pRS426-*UBP15,* the *UBP15* gene including promoter and 3' region was incorporated into the multiple cloning site of pRS426 plasmid using overlapping PCR fragments (described in Section 2.2.4.1). The overlapping PCR fragments, and pRS426 vector backbone were transformed into wild type yeast strains to allow recombination events to create a full pRS426-*UBP15* plasmid (described in Section 2.2.4.1). Plasmids were isolated from *ura*+ colonies and sequenced to confirm plasmid construction. To examine the effects of overexpression of *UBP15*, wild type and *ubp15*Δ strains were transformed with either pRS426 vector or pRS426-*UBP15*. Next, strains were grown to mid-log phase in SD minimal media to maintain selection for the plasmid, and spotted onto SD minimal media plates containing several oxidising agents (Figure 5.9). To further investigate whether Ubp15 was required for responses to different temperatures, plates were incubated at different temperatures, as indicated (Figure 5.9). Consistent with previous experiments (Figure 3.4), *ubp15*Δ containing vector display similar sensitivity to $H_2O_2$ as wild type cells (Figure 5.9). However interestingly, wild type cells containing pRS426-*UBP15* display a small increase in sensitivity to $H_2O_2$ compared to the same cells containing vector

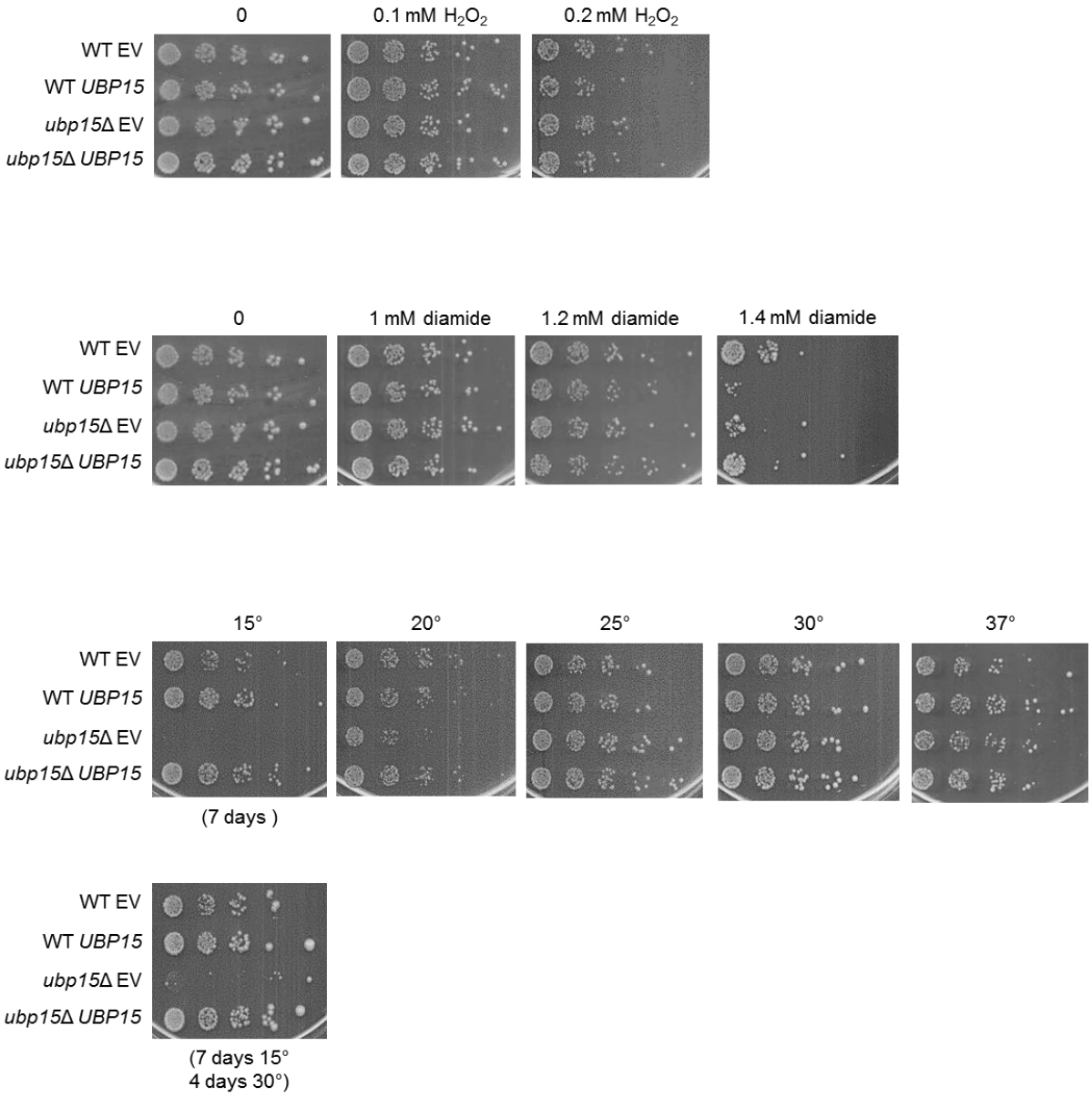


**Figure 5.9: Over expression of *UBP15* affects responses to oxidative stresses.** Wild type (WT) (FCC1) and *ubp15*Δ (FCC60) strains containing either pRS426 empty vector (EV) or pRS426-*UBP15* were grown to mid-log phase in SD media, spotted onto SD media containing increasing concentrations of the indicated oxidising agent, and then incubated at 30 °C. To investigate the potential links with temperature strains were spotted onto SD minimal plates and incubated at the temperatures indicated. Plates were incubated for 3 days, unless otherwise stated, before imaging.

(Figure 5.9), suggesting that Ubp15 may mildly inhibit cellular growth in response to $H_2O_2$ stress. It was also interesting to note that *ubp15*Δ containing vector and wild type cells containing pRS426-*UBP15* displayed increased sensitivity to diamide compared to wild type cells containing vector (Figure 5.9). Studies of the *ubp15*Δ strain using YPD media also indicated increased sensitivity to diamide (Figure 3.5). The explanation of why both deletion and overexpression of *UBP15* increases sensitivity to diamide is not clear at this stage but suggests that the activity of this dUb must be finely balanced to allow cells to respond to the oxidising agent in an appropriate manner. Attempts were made to examine the effect of pRS426-*UBP15* on menadione sensitivity; however the results were inconclusive and would need to be repeated. As described in Chapter 3 (see Section 3.4.2.4) *ubp15*Δ strains display decreased growth at cold temperature compared to wild type cells. Consistent with these observations, cells containing empty vector also showed inhibited growth at cold temperatures (15°C) compared to wild type strains (Figure5.9). Moreover, this growth inhibition was complemented by pRS426-*UBP15* (Figure 5.9), suggesting that Ubp15 is required for cell growth at these temperatures. Previous work has also reported that Ubp15 is required for cold temperatures, confirming the present results (Amerik *et al.*, 2000). Interestingly, the study by Amerik *et al* (2000) also found that the growth of *ubp15*Δ strains were more sensitive to high temperatures (37°C). However in the present results this result was not observed. The basis for this inconsistency is not clear but perhaps it is linked to the strain background used in the studies. Nevertheless, these studies suggest that Ubp15 is required for the response of cells to cold temperature. To explore the response to cold temperature further, *ubp15*Δ cells incubated at 15°C were placed at 30°C after 7 days to test whether the lack of growth at 15°C was due to growth inhibition or cell death (Figure 5.9). Interestingly, the growth of the *ubp15*Δ strains containing empty vector was not recovered at 30°C, suggesting that cell death had occurred at 15°C in the absence of *UBP15*. Taken together with the analyses of the *ubp15*Δ mutant, these data suggest that Ubp15 activity has specific roles in responses to oxidative and temperature stresses. It would be of interest to understand whether the catalytic activity of Ubp15 was required for the response to oxidising agents tested. Using the catalytic cysteine mutant strains created previously (see Section 5.2.3), would enable investigations into the necessity of

the catalytic cysteine in response to the different oxidising agents. If the cysteine mutant strain has the same phenotype as the deletion mutant it could be hypothesised that the catalytic cysteine mutant is required for growth in response to the different oxidative stress inducing agents, and temperature.

#### *5.2.4.2. Investigation of the potential role of Ubp15 in the regulation of global ubiquitin levels*

To investigate whether Ubp15 influences the ubiquitination of many substrates the global ubiquitin pattern was investigated in both wild type and *ubp15*Δ cells in stressed and unstressed conditions. Previous work revealed that Ubp15 has a high affinity for mono-ubiquitinated substrates, and that K48 linkages are more resistant to Ubp15 activity (Schaefer and Morgan, 2011). However, the breakdown of other poly-ubiquitin chains might also be catalysed by Ubp15, and consistent with this proposal it has been observed that Ubp15 removes both mono- and poly-ubiquitin from the substrate Pex5 (Debelyy *et al.*, 2011). It was therefore possible that Ubp15 may regulate global ubiquitin levels. In Chapter 4 global ubiquitination was examined in wild type cells after treatment with both $H_2O_2$ and diamide and significantly ubiquitination only changed in response to $H_2O_2$ (Figure 4.11). Therefore, here the potential role of ubp15 was investigated after $H_2O_2$ treatment. Wild type and *ubp15*Δ strains in both the W303 and BY4741 strain backgrounds were incubated with 2 mM $H_2O_2$. Proteins were extracted in non-reducing conditions in the presence of NEM and analysed by western blot, including the stacking gel (Figure 5.10). Consistent with the previous analysis in Chapter 4, incubation with $H_2O_2$ resulted in the increase in HMW ubiquitin conjugates in wild type cells and a corresponding decrease in free ubiquitin levels (compare Figure 4.11 and Figure 5.10). Interestingly, free ubiquitin also decreased after incubation with $H_2O_2$ in *ubp15*Δ in both strain backgrounds, suggesting that Ubp15 does not affect free levels of ubiquitin after $H_2O_2$ stress. However, in contrast, the pattern of HMW ubiquitin conjugates observed in extracts from *ubp15*Δ cells from different strain backgrounds displayed differences. In particular, in the W303 background *ubp15*Δ cells the HMW ubiquitin conjugates are not observed to increase similarly to wild type cells

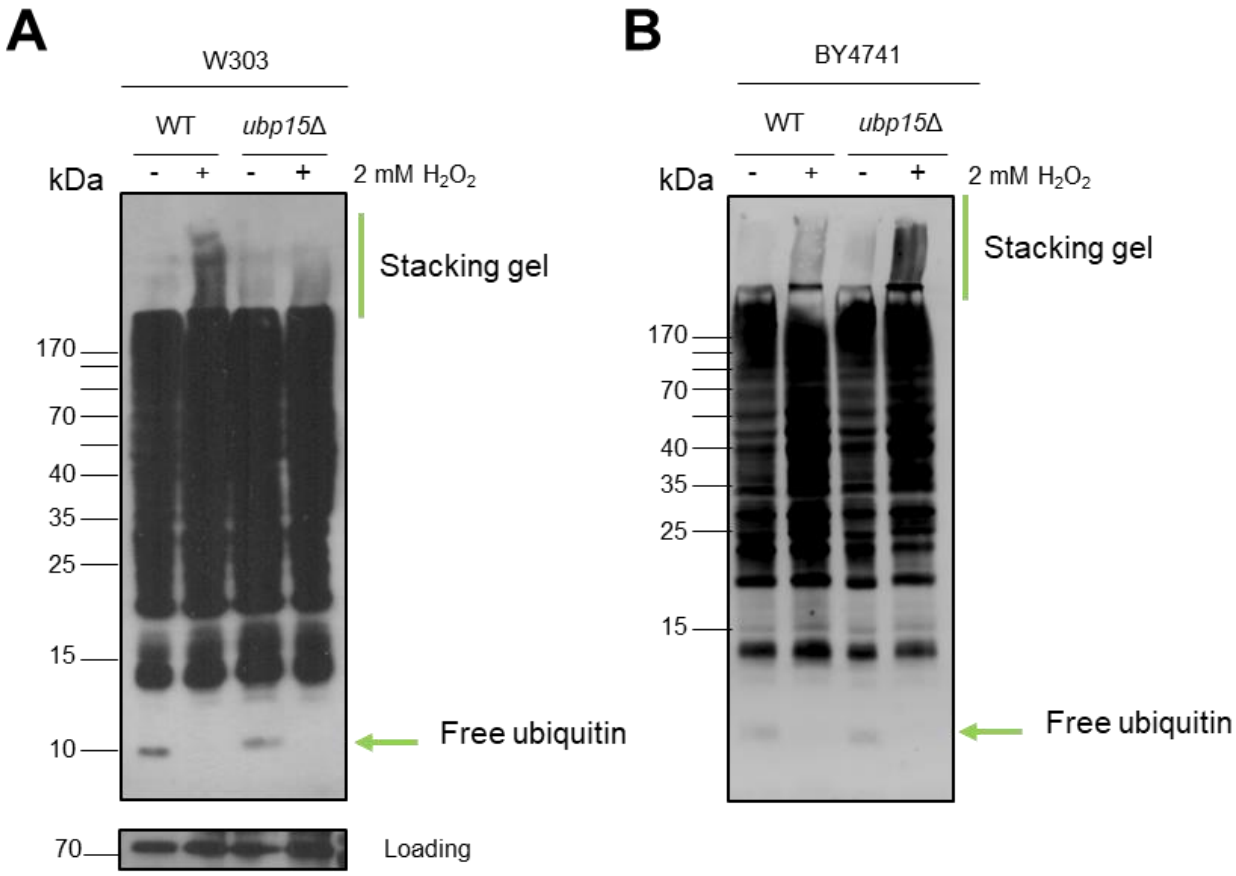


**Figure 5.10: Ubp15 regulates global ubiquitination.** Wild type (WT) and *ubp15*Δ cells in the (A) W303 (FCC1 and FCC60) and (B) BY4741 (FCC23 and FCC106) strain backgrounds were incubated with 2 mM $H_2O_2$ for 0 (-) and 10 (+) minutes. Protein extracts were prepared in non-reducing conditions and separated by SDS-PAGE. Ubiquitinated proteins were visualised using α-ubiquitin antibodies. Skn7 was visualised using α-Skn7 antibodies as a loading control.

following $H_2O_2$ treatment (Figure 5.10A). It is not clear whether this reflects the fact that Ubp15 is critical in maintaining the level of either poly-ubiquitination and/or HMW mono-ubiquitination or perhaps alternatively that these ubiquitinated substrates are more unstable in the absence of Ubp15. Indeed, loss of a dUb would be predicted to increase substrate ubiquitination, potentially increasing instability. In contrast to the results with the W303 background, global ubiquitination appeared to be induced to a greater extent in the *ubp15*Δ cells in the BY4741 strain background compared to the wild type control cells (Figure 5.10B). These data suggest that in the BY4741 strain background Ubp15 inhibits ubiquitination (or reverses ubiquitination) of substrates after $H_2O_2$ treatment. It will be interesting to investigate the specific type of ubiquitin linkage which is regulated by Ubp15 in response to $H_2O_2$ stress in the different strain backgrounds using linkage specific antibodies. Collectively, these results suggest that Ubp15 activity is important for global ubiquitination following $H_2O_2$ stress, and, moreover that Ubp15 plays different roles in this response in different strain backgrounds.

*5.2.4.3. Investigation of the relationship between Ubp15 and the cell cycle*

Ubp15 has been suggested to play a role in the regulation of cell cycle progression through its interaction with Cdh1 (Bozza and Zhuang, 2011), an activator subunit of the APC/C complex (Krek, 1998). Cdh1 is important for activating the APC/C and also for substrate specificity (Visintin *et al.*, 1997), and thus Cdh1 is critical for the ubiquitination of many cell-cycle related proteins. As Ubp15 interacts with Cdh1 (Bozza and Zhuang, 2011), it was suggested that Ubp15 may play a role in deubiquitinating APC/C substrates. Taken together with these studies, and based on the observation that Ubp15 is oxidised following $H_2O_2$ and diamide treatment, this led to the hypothesis that oxidation of Ubp15 may influence the ubiquitination of certain cell cycle-related proteins. Indeed, it has been shown previously that oxidative stress influences cell cycle progression. For example $H_2O_2$ has been observed to cause G2 phase arrest in *S. cerevisiae* in a Rad9-dependent manner (Flattery-O'Brien and Dawes, 1998). Moreover, previous work from our lab and by others has identified a G1 phase arrest in *S. cerevisiae* in response to $H_2O_2$, although the underlying mechanism remains unknown (Leroy *et al.*, 2001; O'Callaghan, 2004). As described previously, our

lab also linked oxidation of Cdc34 to cell cycle inhibition in G1 phase via the stabilisation of the CDK inhibitor Sic1 (see Section 1.3.3) (Doris *et al.*, 2012). As described above, the $H_2O_2$-induced HMW complex of Ubp15 does not appear to include Cdc34 (see Section 5.2.2), suggesting that if oxidation of Ubp15 does regulate the cell cycle it is not by the same mechanism as that observed for Cdc34 and Sic1. However it seemed possible that perhaps Ubp15 oxidation is critical for the regulation of the cell cycle by influencing Ubp15 activity towards APC/C substrates. Hence, to investigate the potential link between the Ubp15 oxidation and the cell cycle, asynchronous cultures of mid-log phase growing wild type and *ubp15*Δ strains were incubated with 2 mM $H_2O_2$ for 60 minutes and DNA content analysis was performed (Figure 5.11A). Gating analysis also identified the proportion of the cell population with 1C (G1), 2C (G2/M), and 1-2C (S) DNA content (Figure 5.11B). Interestingly, after incubation with 2 mM $H_2O_2$ the percentage of wild type and *ubp15*Δ cells in G1 phase increased, suggesting a $H_2O_2$-induced G1 phase delay, similar to that described previously by other studies (Leroy *et al.*, 2001; O'Callaghan, 2004). Furthermore, this increase in G1 phase cells corresponded in both wild type and *ubp15*Δ cell population with a decrease in the proportion of cells with 2C content (Figure 5.11B). However, it is important to note that growth analyses were not performed on these samples so it is not clear whether the cells have arrested or are just progressing through the cell cycle at a slower rate. It is also interesting to note that a similar proportion of G1 phase cells were detected in wild type and *ubp15*Δ cell populations in unstressed conditions (Figure 5.11B). This contrasts with a recent paper published after the thesis work was initiated suggesting that *ubp15*Δ cells had a larger proportion of G1 phase cells than normal (Ostapenko *et al.*, 2015). The differences in conclusion between this paper and the present analyses is not clear but it is possible that issues such as strain background and/or cell clumping may influence the interpretation of the published study. It is also interesting to note that a higher proportion of G1 cells was observed following $H_2O_2$ treatment in the *ubp15*Δ cell population versus the wild type cell population (Figure 5.11B). The basis for this apparent increase in *ubp15*Δ cells is unknown but suggests Ubp15 activity influences the effects of oxidative stress on cell cycle progression.

**A**

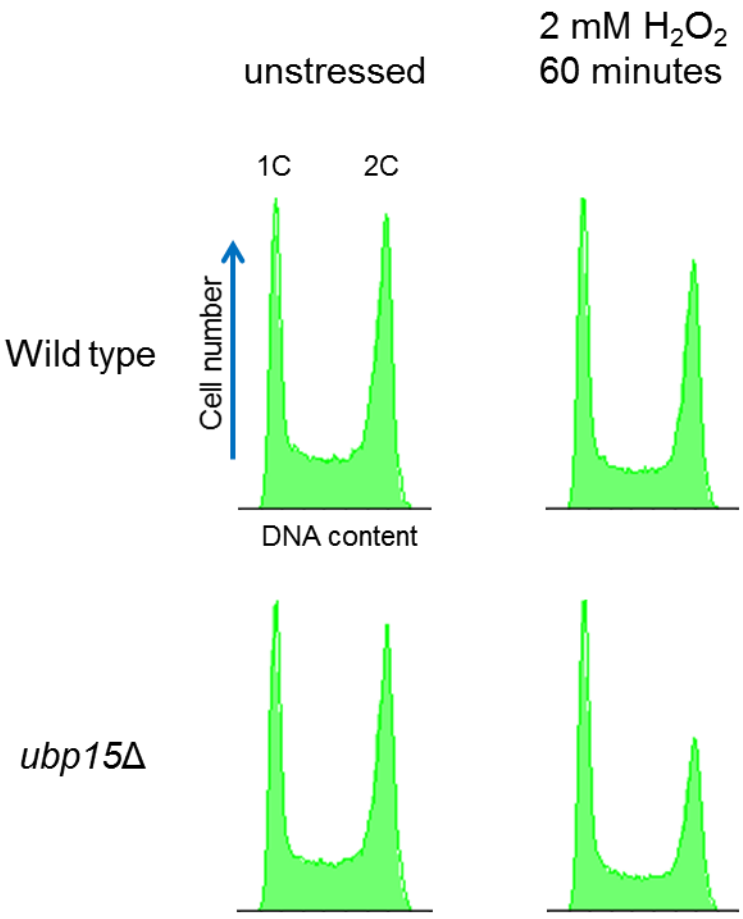
unstressed
2 mM $H_2O_2$
60 minutes
1C
2C
Wild type
Cell number
DNA content
*ubp15*Δ

**B**

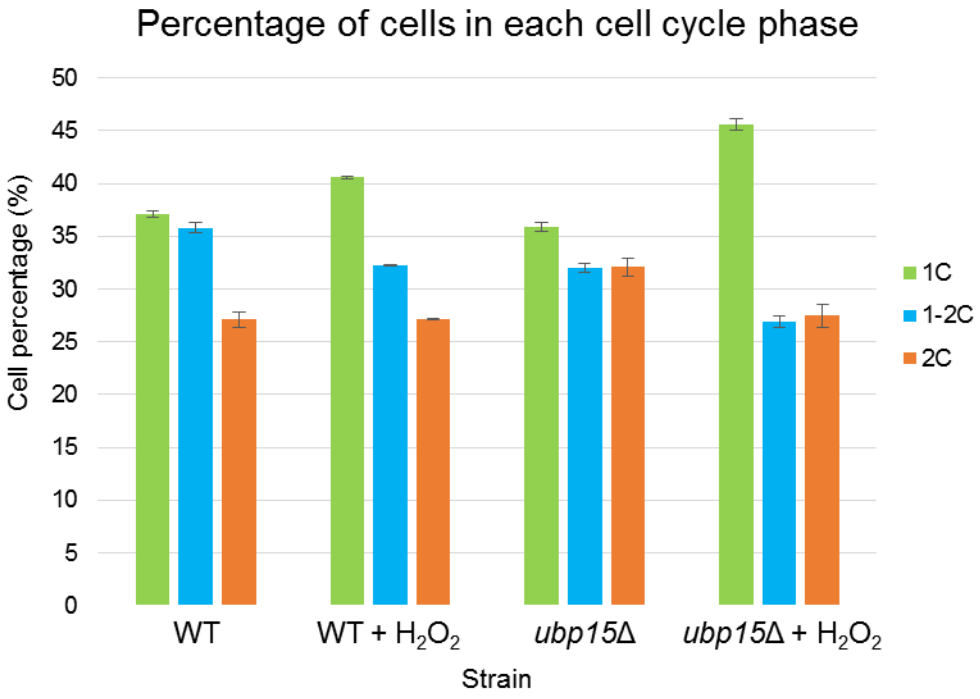
Percentage of cells in each cell cycle phase
Cell percentage (%)
50
45
40
35
30
25
20
15
10
5
0
WT
WT + $H_2O_2$
*ubp15*Δ
*ubp15*Δ + $H_2O_2$
Strain
1C
1-2C
2C

**Figure 5.11: DNA content analyses of wild type and *ubp15*Δ cells in response to 2 mM $H_2O_2$ treatment.** Mid-log phase growing wild type (WT) (FCC1) and (FCC60) cells were incubated with 2 mM $H_2O_2$ for 60 minutes. The cells were fixed, DNA was stained with SYTOX green, and DNA content was analysed by flow cytometry. (A) DNA content histogram of the data from WT and *ubp15*Δ cells either unstressed or treated with $H_2O_2$ shows cell number plotted against relative fluorescence. (B) Graph shows gating analysis to determine the proportion of cells with 1C, 1-2C, or 2C DNA in $H_2O_2$ treated and unstressed WT and *ubp15*Δ cells. Error bars show the standard error of the mean where n=2.

It was possible that the results obtained above were influenced by the high $H_2O_2$ concentration. Hence further analyses were performed using a lower concentration of $H_2O_2$. Previous studies from our lab and others revealed that low concentrations of $H_2O_2$ induced multiple cell cycle arrest points, including in G2 phase in a Rad9 dependent manner (Flattery-O'Brien and Dawes, 1998), and in G1 phase (Leroy *et al.*, 2001; O'Callaghan, 2004). For example, treatment with 0.5 mM $H_2O_2$ triggers cell cycle arrest (Doris *et al.*, 2012). Hence 0.5 mM $H_2O_2$ was chosen as a lower concentration to investigate Ubp15 links to cell cycle control. To confirm that treatment of cells with 0.5 mM $H_2O_2$ induced cell cycle arrest, wild type and *ubp15*Δ cells were treated with this concentration of $H_2O_2$ and growth analysed (Figure 5.12A). In the absence of $H_2O_2$ wild type and *ubp15*Δ cultures displayed exponential growth over the time course and their respective doubling times were 82.4 minutes (wild type, SE 0.58, n=2), compared to 75.5 minutes (*ubp15*Δ, SE 0.74, n=2). In contrast, after addition of $H_2O_2$ to a concentration of 0.5 mM the growth of cultures was inhibited greatly (Figure 5.12A). However, some growth of both cultures was still apparent albeit with an extremely low doubling time (Figure 5.12A and B). After 300 minutes wild type cells have a fold growth of ~1.75, and *ubp15*Δ cells have a fold growth of ~2.5. The basis for these slower growth rates is not clear as the experiment has only been carried out once. It is possible that they reflect leaky arrest at several checkpoints which allows the cells to divide eventually. However it is also possible that the slow growth rates reflect a small proportion of the population that are dividing relatively quickly whilst the other cells in the population are completely arrested or perhaps even dying. Nevertheless, these data indicate that 0.5 mM $H_2O_2$ triggers cell cycle arrest in both wild type and *ubp15*Δ cells.

Next, in an attempt to understand the effects of 0.5 mM $H_2O_2$ on the cell cycle profiles of the wild type and *ubp15*Δ cells, the DNA content of each strain was analysed (Figure 5.12C). From visual analyses of the asynchronous unstressed cultures of wild type and *ubp15*Δ cells it is apparent that there is some variability in the DNA content analyses at different time points (Figure 5.12C). Using gating analyses to find the number of cells with either 1C, 1-2C, or 2C DNA content, the relative timing of each phase in the cell cycle can be estimated using the doubling time calculated previously and the average number of cells in each phase of the

**A**

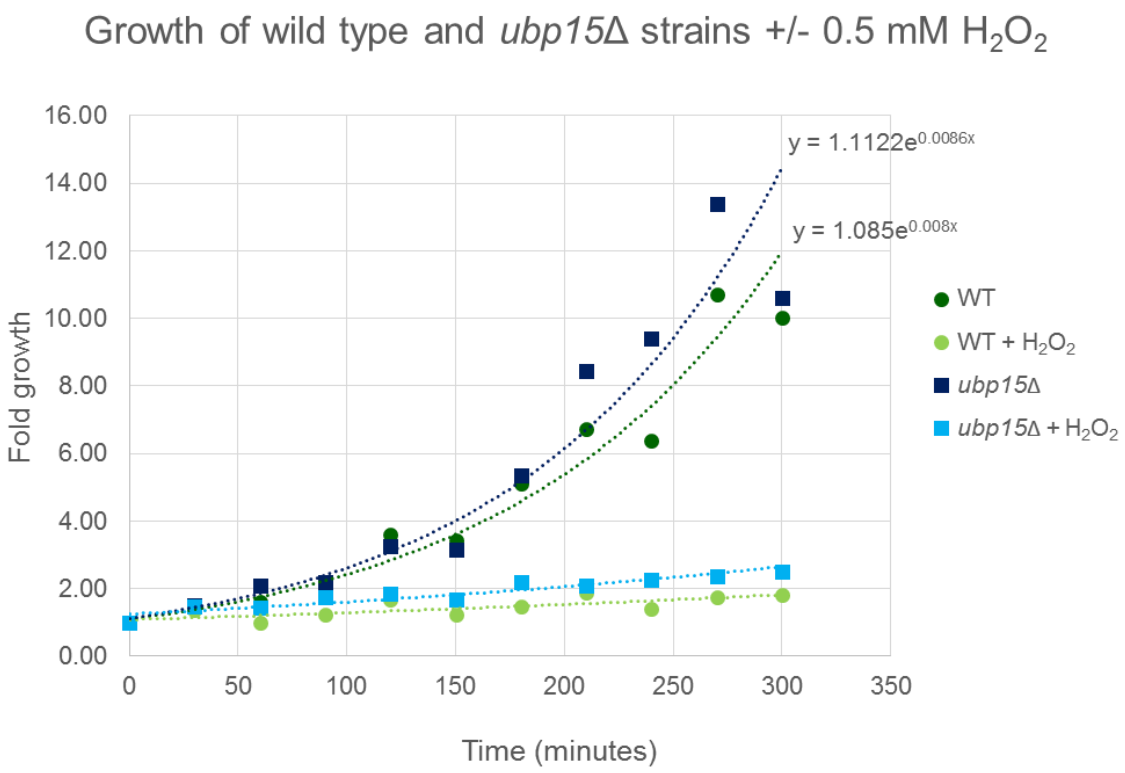
Growth of wild type and ubp15Δ strains +/- 0.5 mM H2O2
Fold growth
Time (minutes)
y = 1.1122e0.0086x
y = 1.085e0.008x
WT
WT + H2O2
ubp15Δ
ubp15Δ + H2O2

**B**

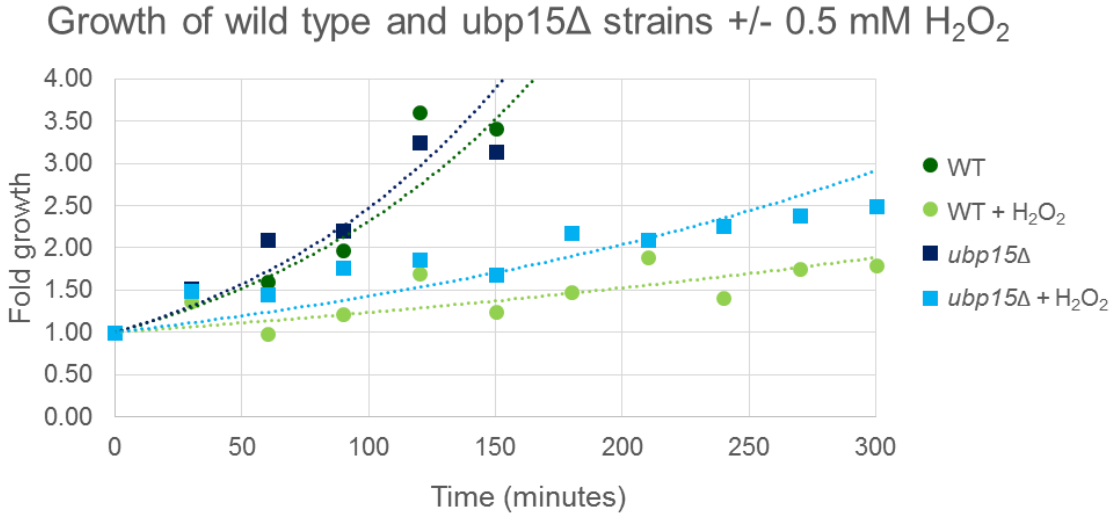
Growth of wild type and ubp15Δ strains +/- 0.5 mM H2O2
Fold growth
Time (minutes)
WT
WT + H2O2
ubp15Δ
ubp15Δ + H2O2

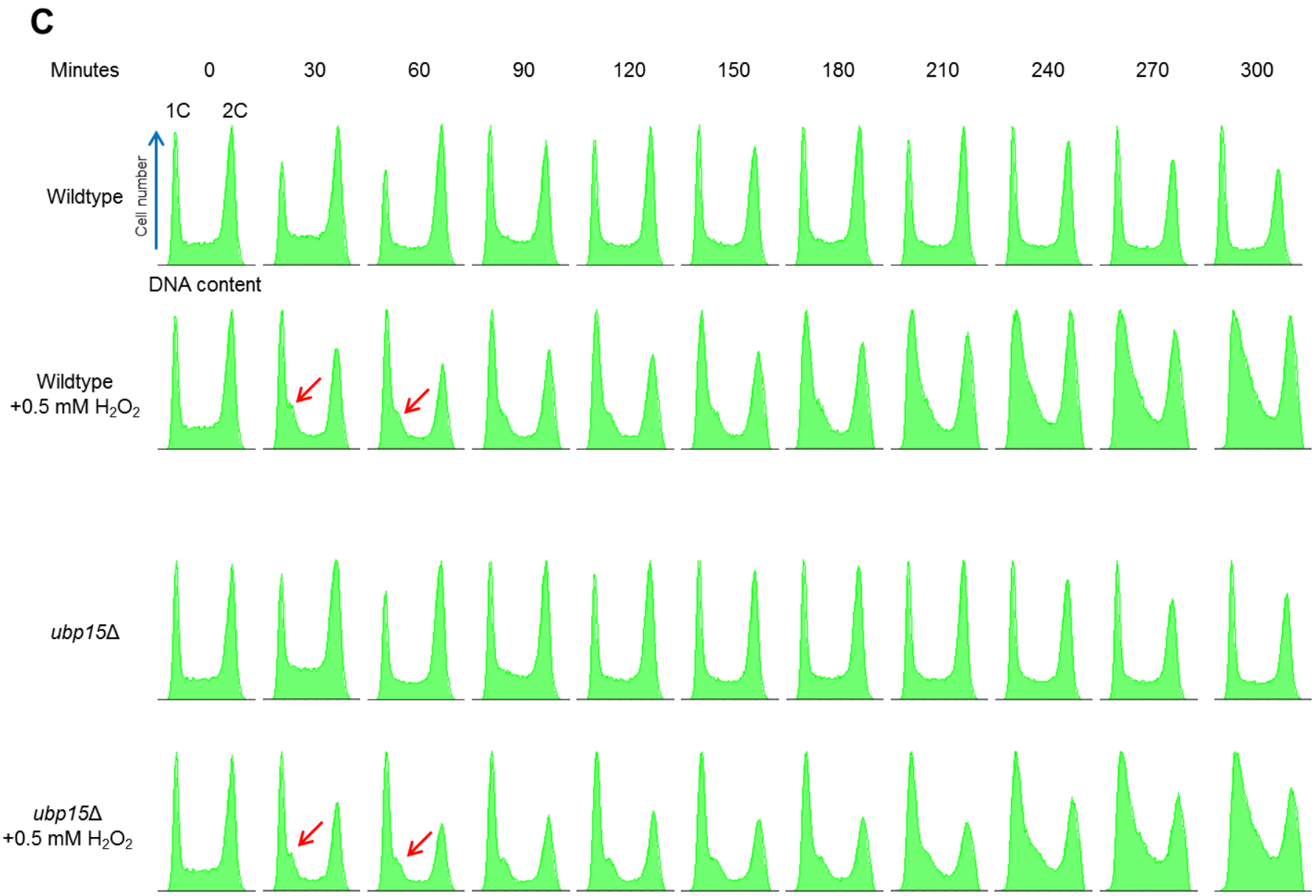
C
Minutes
0
30
60
90
120
150
180
210
240
270
300
1C
2C
Cell number
DNA content
Wildtype
Wildtype
+0.5 mM H2O2
ubp15Δ
ubp15Δ
+0.5 mM H2O2

**Figure 5.12: Regulation of the cell cycle after 0.5 mM $H_2O_2$ treatment in wild type and *ubp15*Δ strains.** (A) Mid log phase growing wild type (FCC1) and *ubp15*Δ (FCC60) cells in the W303 strain background were diluted to an $OD_{660}$ of 0.05, and either left untreated or treated with 0.5 mM $H_2O_2$. Samples were taken every 30 minutes and the cells were counted using a CASY® Model TT Cell Counter. Fold growth was calculated using the cell number at the time points relative to the cell number at time 0. Fold growth was calculated from one repeat. (B) The y-axis from the graph in (A) was modified to illuminate the fold growth of cells treated with 0.5 mM $H_2O_2$. (C) DNA content histogram from WT and *ubp15*Δ cells either unstressed or treated with $H_2O_2$ over the time course of 300 minutes shows cell number plotted against relative fluorescence. Histograms are representative of one repeat.

cell cycle in wild type and *ubp15*Δ strains (Table 5.1). It is interesting to note that *ubp15*Δ cells have a slightly shorter S phase when compared to wild type cells. However, the amount of time for each strain spent in G1 phase is similar. This result is in agreement with that observed previously (Figure 5.11B) where wild type and *ubp15*Δ cells have a similar G1 phase in unstressed conditions. It also seems to contradict the published results observed by Ostapenko *et al.*, (2015) where unstressed *ubp15*Δ strains have a G1 arrest/growth delay.

Given the extremely slow doubling rate following addition of 0.5 mM $H_2O_2$ to the wild type and *ubp15*Δ cultures, the DNA content profiles of both strains suggests that $H_2O_2$ causes cells to arrest at various points in the cell cycle (Figure 5.12C). It is also clear that cells do not arrest at one point in the cell cycle, in agreement with earlier studies (Flattery-O'Brien and Dawes, 1998; Leroy *et al.*, 2001; O'Callaghan, 2004; Doris *et al.*, 2012). It has been described previously that *S. cerevisiae* cells in the W303 strain background have $H_2O_2$-induced cell cycle arrest points at G1 and G2 phase (Flattery-O'Brien and Dawes, 1998) and the present analysis of wild type cells is consistent with these conclusions (Figure 5.12C). However, excitingly, the analyses presented here also revealed a potential cell cycle arrest in early S phase (Figure 5.12C red arrows). However it is important to note that these analyses have only been carried out once, therefore conclusions are preliminary. In addition, it is also important to consider that some cells may possibly indicate arrest suggesting a cell cycle checkpoint but in fact be ‘arrested’ due to killing by $H_2O_2$. With these points in mind, gating analysis was utilised to investigate how the cell cycle profiles of wild type and *ubp15*Δ cells were affected by $H_2O_2$. The data from one experiment were analysed in several ways (Figures 5.13). In particular, the percentage of cells in each phase of the cell cycle was plotted against time following the addition of $H_2O_2$ for both wild type (Figure 5.13A) and *ubp15*Δ (Figure 5.13B) strains. Interestingly, the percentage of cells with 2C content (indicative of G2/M phases) were quite similar and remained relatively constant for both the wild type and *ubp15*Δ cells over the time course, suggesting that there is at least one arrest point located later in the cell cycle. In contrast analyses of the 1C DNA content (indicative of G1 phase) suggested that wild type and *ubp15*Δ cells behave differently when treated with $H_2O_2$. In the wild type culture, the cells were

| Strain | Doubling time (minutes) | G1 phase (minutes) | S phase (minutes) | G2/M phase (minutes) |
|---|---|---|---|---|
| Wild type | 82.4 (SE 0.58) | 28.6 | 27.2 | 26.6 |
| *ubp15*Δ | 75.5 (SE 0.74) | 28.8 | 22.1 | 24.6 |

**Table 5.1: Growth and cell cycle analyses of wild type and *ubp15*Δ cells.** The time taken in G1, S, and G2 phase was predicted using the doubling time calculated from the fold growth of each strain (growth curves from Figure 5.12). Gating analysis of the DNA content histogram gave the percentage of cells with either 1C (G1), 2C (G2/M), or 1-2C (S). The cell percentage was used to calculate the approximate predicted time spent in each phase of the cell cycle using the doubling rate. Data is representative of one repeat.

**A**

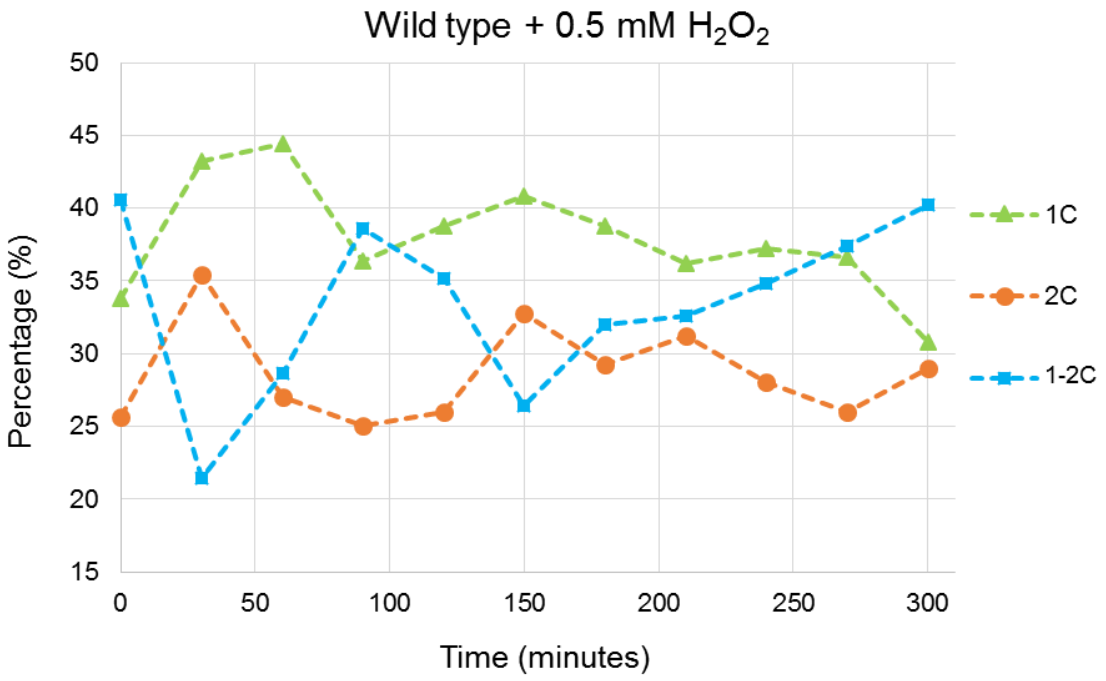
Wild type + 0.5 mM $H_2O_2$
Percentage (%)
50
45
40
35
30
25
20
15
0
50
100
150
200
250
300
Time (minutes)
1C
2C
1-2C

**B**

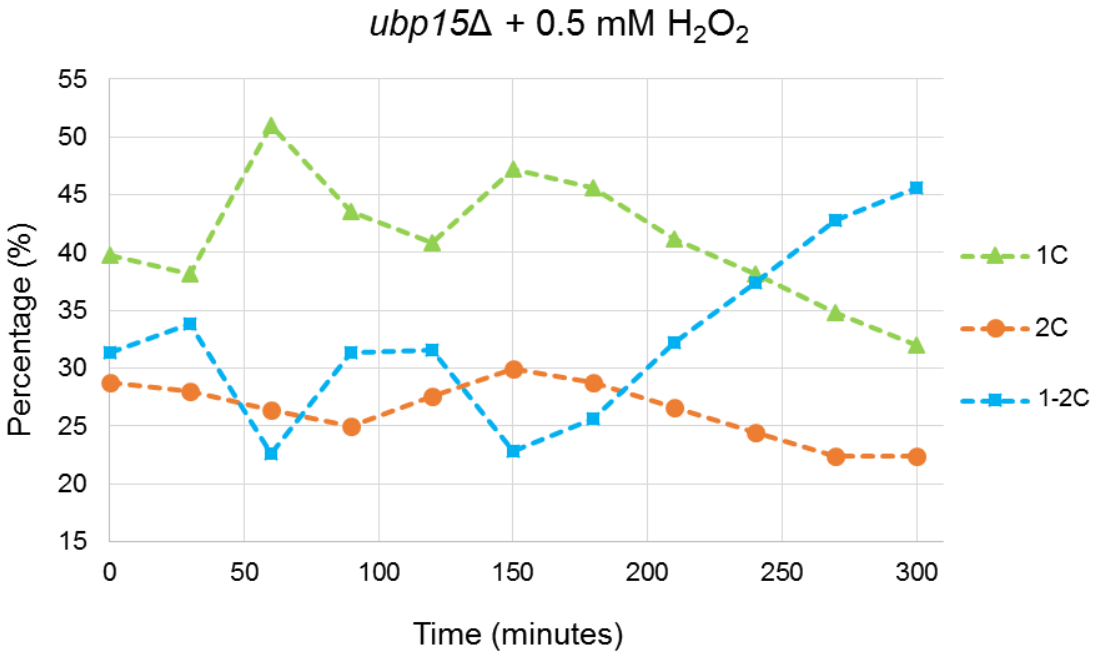
*ubp15*Δ + 0.5 mM $H_2O_2$
Percentage (%)
55
50
45
40
35
30
25
20
15
0
50
100
150
200
250
300
Time (minutes)
1C
2C
1-2C

**C**

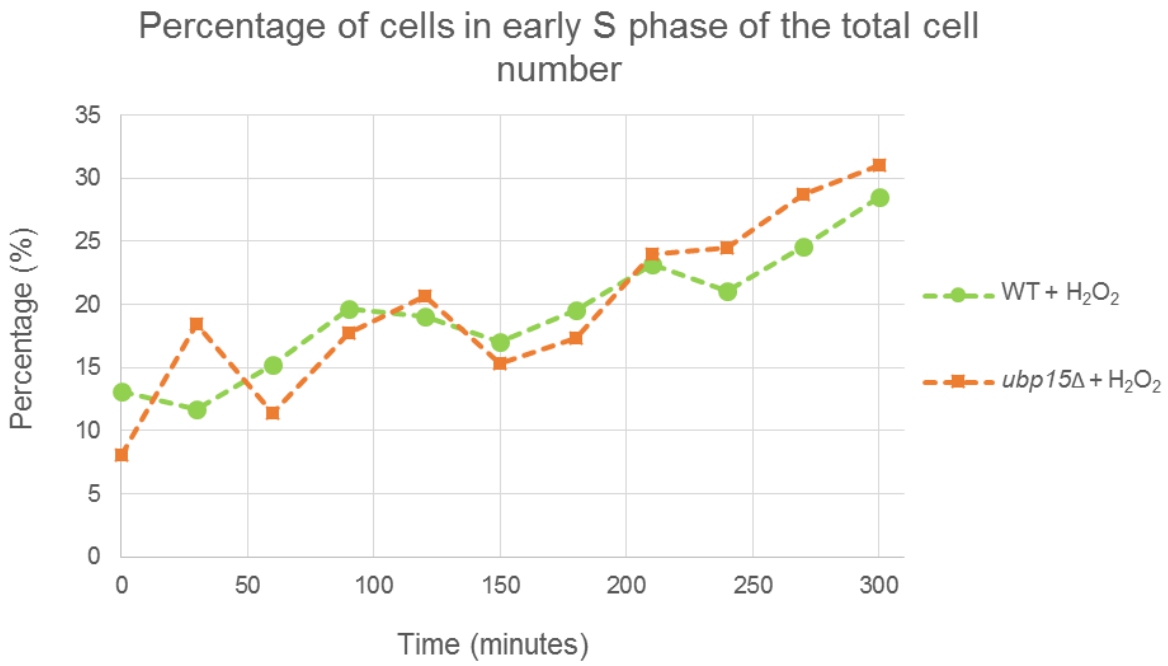


**Figure 5.13: Analyses of DNA content after exposure of cells to 0.5 mM $H_2O_2$.** Gating analysis of the DNA content histogram (Figure 5.12C) gave the percentage of cells with 1C, 2C, or 1-2C DNA content. The percentage of cells with particular DNA content for (A) wild type (FCC1) and (B) *ubp15*Δ (FCC60) strains was plotted against time. The graphs represent data from one experiment. (C) Gating analysis of the DNA content histogram (Figure 5.12C) gave the percentage of cells with DNA in the early S phase region (red arrow in Figure 5.12C) relative to the total number of cells for Wild type (WT) and *ubp15*Δ strains.

observed to rapidly build up in G1 phase peaking by 60 minutes (Figure 5.13A), consistent with previous work that there is at least one cell cycle arrest point in G1 phase. In contrast, there is a possible delay in the initial increase in G1 phase cells of the *ubp15*Δ culture, although the peak also occurs at 60 minutes (Figure 5.13B). Interestingly, there is some indication that a greater proportion of cells from the *ubp15*Δ culture are arrested in G1 phase compared to the wild type control (Figure 5.13 A and B). At later time points (from ~150 minutes) there is evidence in the DNA content profiles from both the wild type and *ubp15*Δ $H_2O_2$ treated cultures that the cells delayed in G1 phase move into S phase (compare 1C and 1-2C in Figure 5.13A and B). However, it appears that *ubp15*Δ cells may be entering S phase faster that the wild type cells (compare the slopes in Figure 5.13A and B). Further analyses of the S phase profiles of both cultures (Figure 5.13C) suggest that the percentage of cells in early S phase after 150 minutes is higher in the *ubp15*Δ versus wild type cell populations although in both cases the amount of cells in early S phase increases (Figure 5.13C). This may reflect the fact that in both cultures cells delayed in G1 phase are beginning to move into early S phase where they pile up due to the presence of a further checkpoint. Furthermore, the possible indication that more cells from the *ubp15*Δ culture than the wild type culture are present in early S phase at these later time points may simply reflect the fact that more cells were delayed initially in G1 phase in the *ubp15*Δ culture versus the wild type culture (Figure 5.13C). Although this data needs to be repeated there is some indication that the loss of Ubp15 function affects the cell cycle arrest profiles of cells, particularly in G1 phase initially and at the early S phase arrest point in the later time points following addition of $H_2O_2$. It is also interesting to note that the 2C content analyses (G2/M phases) of both cultures appears to change relatively little and similarly in both wild type and *ubp15*Δ cultures over the time course of the $H_2O_2$ treatment, despite the detected increases in cell numbers entering S phase after ~150 minutes (Figure 5.13A-C). Hence, taken together with the growth analyses (Figure 5.12A and B) these data suggest that the G2/M phase checkpoint remains active even after 300 minutes and that may be independent of Ubp15 activity. Taken together, investigations of the growth rate and DNA content of wild type and *ubp15*Δ cells suggests that $H_2O_2$ induces cell cycle arrest/delay in at least three places within the cell cycle; G1 phase, early S phase, and G2/M phase. Preliminary data also suggests that

Ubp15 function is important for the G1 arrest point, as indicated by the DNA profiles of *ubp15*Δ cells. There is also some evidence that Ubp15 affects the release of cells from G1 phase into early S phase at later time points following $H_2O_2$ addition. However, those cells that move into S phase don not appear to move quickly into G2/M phases suggesting S phase delay/arrest is still active. Analyses of the S phase profiles suggest that this late increase in S phase cells corresponds to a block in early S phase.

Taken together, the data presented in this Chapter suggest that Ubp15 influences the responses of cells to several oxidising agents. We also observed that Ubp15 forms a HMW complex in response to both diamide and $H_2O_2$, and interestingly it was suggested that the HMW complex formed was different for the different oxidising agents. Furthermore, we observed that the formation of the $H_2O_2$-induced Ubp15 HMW complex was dependent on the catalytic cysteine, and that the HMW complex formation is dependent on the concentration of $H_2O_2$. In addition, we also observed that Ubp15 activity is important for global ubiquitination following $H_2O_2$ stress. Preliminary investigations into the cell cycle regulation by Ubp15 suggest that Ubp15 activity may be important for cell cycle arrest in G1 and entry into S phase.

## 5.3. Discussion

Ubp15 is a relatively uncharacterised *S. cerevisiae* USP dUb, which has been identified to be highly active against mono-ubiquitin signals (Schaefer and Morgan, 2011) and has also been identified to interact with Cdh1 (Bozza and Zhuang, 2011), suggesting possible links with cell cycle regulation. Work presented in Chapter 3 in this thesis revealed that Ubp15 is modified into a HMW complex after incubation with both $H_2O_2$ and diamide. In this chapter the HMW modifications of Ubp15 were further investigated. Excitingly, it was found that Ubp15 is oxidised into HMW forms in response to $H_2O_2$ and diamide and, importantly, that Ubp15 is oxidised differentially by $H_2O_2$ depending on the concentration. Further investigations suggested that Ubp15 oxidation occurred at the catalytic cysteine, and that formation of the HMW complex was independent

of Cdc34 oxidation. Interestingly, it was suggested that Ubp15 activity important for both oxidative and temperature stresses and, additionally, is important for global ubiquitination after $H_2O_2$ stress, and that Ubp15 may play an important role in G1 phase delay/arrest and release in response to $H_2O_2$.

As described previously, cells need to be able to sense the difference between the types and levels of different oxidising agents (see Section 1.2.5). In Chapter three it was found that Ubp15 is modified into a HMW complex by diamide and $H_2O_2$. Interestingly, further investigations of this complex described in this chapter revealed that Ubp15 was oxidised by both oxidising agents, but also suggested that Ubp15 forms different complexes depending on the specific oxidising agent. The underlying explanation for this apparent alteration on complex formation is not clear, but it is tempting to speculate that these different complexes are components of mechanisms that allow cells to tailor the specific response to the oxidising agent detected. It is also interesting to note that the kinetics of Ubp15 oxidation is affected by the concentration of $H_2O_2$. Similar to Ubp12 oxidation, lower concentrations of $H_2O_2$ induced slower oxidation of Ubp15, and importantly the oxidation was reduced over the hour time course. In contrast, with higher concentrations of $H_2O_2$ the HMW complex formed faster and to a greater extent and, moreover, was maintained over the time course. It is possible that the different kinetics of Ubp15 oxidation may allow cells to sense and respond differently to different levels of $H_2O_2$.

Interestingly, it was observed in the present study that Ubp15 may respond differently to types of oxidative stresses depending on the specific strain background used in the experiment. In both W303 and BY4741 strain backgrounds, Ubp15 formed large HMW complexes after treatment with both diamide and $H_2O_2$. Interestingly, after $H_2O_2$ treatment of Ubp15 in the BY4741 strain background another, smaller, HMW complex was detected. This complex was resistant to a reducing agent, suggesting that this form is not due to oxidation. However, the larger HMW form of Ubp15 induced by both diamide and $H_2O_2$ in both strain backgrounds was sensitive to a reducing agent, suggesting that they are dependent on oxidation of Ubp15. It was observed that the strength of the oxidised HMW forms of Ubp15 varied depending on the strain background

used. When oxidised by diamide, the signal detected in the BY4741 strain was stronger compared to the signal detected in the W303 strain. Conversely, after oxidation with $H_2O_2$, the signal for the Ubp15 HMW complex was stronger in the W303 strain background. The basis for the differences of Ubp15 oxidation in the different strain backgrounds are unknown, however it is well characterised that W303 and BY4741 strains respond differently to oxidative stress. W303 strains have a mutated version of Ybp1, which is subsequently unable to form a disulphide complex with Yap1 to allow Yap1 nuclear accumulation (Veal *et al.*, 2003) (see Section 1.2.4.3). This results in W303 strain backgrounds having an increased sensitivity to $H_2O_2$ stress (Veal *et al.*, 2003; Tachibana *et al.*, 2009). It is possible that the differences in response to $H_2O_2$ by the strain backgrounds influence the formation of the Ubp15 HMW complex. It is also interesting to note that differences in strain background are apparent when investigating the regulation of global ubiquitination by Ubp15. It was observed that in W303 stain backgrounds, the amount of HMW ubiquitinated substrates decreased in the *ubp15*Δ strain when compared to wild type cells, suggesting that Ubp15 is important for maintaining HMW ubiquitin conjugates after $H_2O_2$ stress. Indeed, this suggests that loss of Ubp15 results in increased ubiquitination of substrates and subsequent degradation. However in contrast, after $H_2O_2$ treatment of *ubp15*Δ cells in the BY4741 strain, global HMW ubiquitination increased, suggesting that in this case, Ubp15 may inhibit, or reverse ubiquitination after $H_2O_2$ stress. It would be interesting to understand the specific type of ubiquitin linkage which may be cleaved by Ubp15 in the BY4741 strain background after $H_2O_2$ stress, and the use of specific ubiquitin linkage antibodies may help understand this further. The basis behind the differences in the regulation of HMW ubiquitin conjugates by Ubp15 in different strain backgrounds, and the differences in the formation of the HMW complexes is unclear. However these results suggest that Ubp15 oxidation may play different roles depending on the specific *S. cerevisiae* strain background.

Interestingly, spot test analyses of *ubp15*Δ cells suggested that Ubp15 activity has specific roles in responses to oxidative and temperature stresses as Ubp15 is required for cellular growth on plates containing different redox stresses and on plates incubated at 15°C. It remains unknown whether the response of *ubp15*Δ

mutants to cold stress and oxidative stress is through the same pathway, or through different roles of Ubp15. However, these types of stresses have been linked previously. In mammalian cells the heat shock protein *Hsf1* is reversibly activated by both heat shock and $H_2O_2$ by oxidation at the catalytic cysteine (Ahn and Thiele, 2003). Similarly, the heat shock proteins Hsp90 and Hsp70 are also induced by both heat and oxidative stress (Fedoroff, 2006). However the precise nature of the link between heat shock and oxidative stress remains unclear. It is possible that Ubp15 may be important for mediating the response to both types of stress, however whether this is through the same mechanism of oxidation of Ubp15, or through independent mechanisms is unclear. Further investigations into the necessity of the catalytic cysteine of Ubp15 in response to redox stress and heat stress could help gain a better understanding of this.

Analysis of the catalytic cysteine of Ubp15 revealed that it is essential for the formation of the $H_2O_2$-induced HMW complex. However it remains unknown whether Ubp15 forms an intermolecular disulphide complex with another protein(s), or whether oxidation by $H_2O_2$ forms an intramolecular disulphide bond(s) similar to that hypothesised for Ubp12 oxidation. Indeed, Ubp15 has 7 cysteine residues, all of which may potentially form an intramolecular disulphide with the catalytic cysteine. Interestingly, Ubp15 contains an extended N-terminal TRAF domain (Bozza and Zhuang, 2011) which is crucial for recruitment of target substrates (Bozza and Zhuang, 2011; Kim *et al.*, 2016). The TRAF domain is unique to Ubp15, and actually contains two cysteine residues (C111 and C112). Perhaps one of these cysteines forms a disulphide complex with the catalytic cysteine (C214). It also remains possible that oxidation of Ubp15 initiates a homodimer complex whereby the binding of two Ubp15 molecules, perhaps involving the catalytic cysteine of both proteins, acts as a protective mechanism to prevent further oxidation of Ubp15. However, although the HMW complex of Ubp15 is similar in mobility to the Cdc34-Uba disulphide complex, all the experiments reported here suggest that the Ubp15 and Cdc34-Uba1 complexes are unrelated. However, it remains possible that Ubp15 forms a disulphide complex with another, unidentified protein(s). Indeed, it is noteworthy that Ubp15 has 71 known physical interactors (according to the *Saccharomyces cerevisiae* Genome Database), any one of which may form a complex with Ubp15.

It is interesting that, compared to Ubp12, only a small proportion of Ubp15 appears to be oxidised by $H_2O_2$ and diamide into HMW complexes. It is possible that only Ubp15 at a specific subcellular location is oxidised in response to $H_2O_2$ and diamide, whereas Ubp15 at other cellular locations does not form a HMW complex. Interestingly, although Ubp15 is known to localise to the cytoplasm, it has also been found that a small portion of Ubp15 localises to the peroxisome (Debelyy *et al.*, 2011). This is intriguing as peroxisomes are important for both ROS scavenging and ROS production (particularly $H_2O_2$) (Schrader and Fahimi, 2006). Furthermore, Ubp15 has been suggested to be critical for peroxisomal biogenesis after $H_2O_2$-induced stress by supporting the import of proteins into the peroxisome (Debelyy *et al.*, 2011). Interestingly, Ubp15 has been shown to physically interact with the AAA peroxin Pex6 (Debelyy *et al.*, 2011) which is important for the release of ubiquitinated Pex5 from the peroxisome membrane (Platta *et al.*, 2005). In addition Pex6 has also been observed to be important for the deubiquitination of Pex5 by Ubp15 (Debelyy *et al.*, 2011). Therefore, it is possible that a Ubp15 interaction with Pex6 regulates the deubiquitination of Pex5 after oxidative stress. In the present study the link between Ubp15 oxidation and peroxisome regulation was not investigated, but is an interesting avenue for future investigation.

As stated above, Ubp15 is found throughout the cytoplasm, suggesting that Ubp15 has other cytoplasmic roles. Interestingly, previous work suggested that Ubp15 may be important for cell cycle regulation via direct interaction with the APC/C activator subunit Cdh1 (Bozza and Zhuang, 2011). Although the interaction between Ubp15 and Cdh1 did not activate Ubp15, it was suggested that interaction with Cdh1 may target Ubp15 to specific substrates (Bozza and Zhuang, 2011). The APC/C complex is an important E3 enzyme that regulates the cell cycle (Qiao *et al.*, 2010), hence it was hypothesised that Ubp15 may play important roles in cell cycle regulation due to the interaction with Cdh1. Thus, in this regard, it is tempting to speculate that oxidation with Cdh1 interaction potentially influences cell cycle progression. Indeed the very fact that the catalytic cysteine of Ubp15 is required for HMW complex formation may interfere with the deubiquitinating activity of Ubp15 towards cell cycle regulators. However, DNA content analysis suggested that cells lacking Ubp15 did not display any major cell

cycle defects in unstressed conditions. This result appears to contradict a recent publication which suggested *ubp15*Δ cells had a delayed progression through S phase, hypothesised to be due to a decrease in the B-type cyclin Clb5 (Ostapenko *et al.*, 2015). However there is some indication in the analyses presented in the paper that clumped cells were present, which would affect the interpretation. However, it is also possible that the difference in conclusions with our data could be linked to differences in strain construction as different markers were used which may affect the phenotype observed.

Previous work has shown that $H_2O_2$ causes arrest points in the cell cycle at both G1 and G2 checkpoints (Flattery-O'Brien and Dawes, 1998; Leroy *et al.*, 2001; O'Callaghan, 2004; Doris *et al.*, 2012). Indeed, in the present study when wild type cells were treated with 0.5 mM $H_2O_2$ they arrested in G1 phase and G2 phase consistent with this previous data. However, the present data also suggested an early S phase arrest as no build up in any specific phase in the cell cycle was observed. Interestingly, when *ubp15*Δ cells were examined, it was suggested that Ubp15 function may influence the G1 arrest as it was observed that more cells accumulated in G1 phase in the *ubp15*Δ cells. Additionally Ubp15 activity is suggested to affect the release into S phase. It is interesting that after 150 minutes at 0.5 mM $H_2O_2$ there seems to be entry into S phase initiated in wild type and *ubp15*Δ. However there is some indication that cells are moving more efficiently into S phase in the *ubp15*Δ strain. The number of cells with 1C content after ~150 minutes in the *ubp15*Δ strain declines more rapidly than wild type, suggesting cells are able to move into S phase faster. This is particularly interesting as previous studies of Ubp15 suggested that Ubp15 regulated Clb5 ubiquitination (Ostapenko *et al.*, 2015), hence since Cdc28-Clb5 is important for S phase entry it might have been expected to have weaker induction into S phase in *ubp15*Δ cells, not more. However these analyses have only been carried out once, therefore further repeats are necessary before any conclusions are made. It would also be helpful to use synchronised cells to explore the function of Ubp15 in the G1 arrest and for progression into S phase. Previous studies of Cdc34-Uba1 oxidation at 0.5 mM $H_2O_2$ revealed that ~150 minutes after $H_2O_2$ addition the HMW Cdc34-Uba1 complex is reduced and this corresponds with decreased stability of Sic1 and entry into S phase (Doris *et al.*,

2012). Hence, this raises the possibility that Sic1 ubiquitination is also a target of the dUb activity of Ubp15 and this is more unstable in *ubp15*Δ cells, allowing for a more robust release into S phase at ~150 minutes. To test this possibility it would be interesting to use synchronised cells repeating the Cdc34 experiment and investigating Sic1 stability and activity in *ubp15*Δ and wild type cells. However it is also important to note that the entry of cells into S phase may have little to do with the oxidation of Ubp15, as at 0.5 mM $H_2O_2$ the HMW form of Ubp15 is not present. It is possible that oxidation of Ubp15 may be possible for establishing G1 arrest, or even that the formation of the HMW Ubp15 complex is a protective mechanism which prevents Ubp15 degradation in response to oxidative stress and ensures Ubp15 is available once the stress has been overcome. However, it is also possible that the oxidation of Ubp15 may regulate another role of Ubp15, for example peroxisome regulation, after $H_2O_2$ stress.

In the work described in this chapter, Ubp15 was found to be oxidised by both $H_2O_2$ and diamide into HMW complexes. Interestingly, the HMW complex formed by the different oxidising agents is potentially different, suggesting a possible mechanism whereby Ubp15 forms complexes with different substrates depending on the specific oxidising agent. Furthermore, the catalytic cysteine was observed to be critical for the formation of $H_2O_2$-induced HMW complex, and interestingly, the formation of this HMW complex was found to be formed in a concentration dependent manner. It was also revealed that Ubp15 activity was important for the response to oxidative and cold temperature stresses, and also, in addition. It was observed that Ubp15 activity was important for global ubiquitination following $H_2O_2$ stress. Preliminary data also suggested that Ubp15 may be important for regulating G1 phase growth arrest/delay and that also Ubp15 may be important for the timing of release into S phase after $H_2O_2$ stress. Importantly, Ubp15 is conserved in mammalian cells, and the homolog USP7 has been observed to have import roles in disease progression, including many cancers. It would therefore be of great interest to examine the oxidation and potential regulation, of USP7 in mammalian cells.

# Chapter 6: Final discussion

Ubiquitination is highly conserved in eukaryotes and has historically been associated with targeting proteins for degradation by the proteasome system. Recently, however, ubiquitination has been observed to have other intracellular signalling roles. Ubiquitination is a reversible modification, and ubiquitin is removed from substrates by the activity of dUbs. DUbs are highly conserved in eukaryotes and remove ubiquitin from substrates by cleaving the isopeptide bond between the substrate lysine and the ubiquitin moiety by the activity of an active site catalytic cysteine. Interestingly, recent studies have shown that the conjugation/deconjugation of the ubiquitin-like modifications SUMO and NEDD8, and specific ubiquitin conjugation/deconjugation machinery can be regulated by ROS. Furthermore, the presence of catalytic cysteine residues in many dUbs suggest that oxidation of dUbs may be a potential mechanism by which deconjugation of ubiquitin is regulated. Indeed, initial studies of specific mammalian dUbs suggested that oxidation may regulate their activity. However, in depth investigations of all the dUbs was not performed due to the large number present. Thus, the overall aim of this project was to utilise *S. cerevisiae* as a model eukaryote in an attempt to examine the potential roles and regulation of most of the dUbs in response to oxidative stress.

## 6.1. Summary and discussion of key findings from this study

Prior to this study, it was unknown whether any *S. cerevisiae* dUbs are regulated by different types of oxidising agents. DUbs (especially the USP dUbs) have similar active site architecture, therefore often exhibit functional redundancy. Consistent with these suggestions, in unstressed conditions it was observed that single dUb deletion mutants showed no obvious change in growth phenotypes when compared to wild type cells. Excitingly, and in contrast to the results obtained with unstressed conditions, all the dUbs investigated showed diverse roles and specific sensitivities in response to the range of oxidising agents tested. This observation suggests that while dUbs may have overlapping roles in unstressed conditions, they may have specific roles in response to oxidative

stress. We also investigated whether any dUbs were modified in response to oxidative stress. Excitingly, it was observed that certain dUbs were indeed modified in response to specific oxidising agents. Interestingly, since work in this thesis began a further subgroup of thiol protease dUbs has been identified, termed MINDY dUbs (Abdul Rehman *et al.*, 2016). These dUbs are found in all eukaryotes and have a high affinity for cleaving K48 linked ubiquitin chains (Abdul Rehman *et al.*, 2016). *S. cerevisiae* expresses two MINDY dUbs, *MIY1* and its paralog encoded by *YGL082W* (Huseinovic *et al.*, 2018), and hence it will be interesting to investigate whether either of these dUbs play a role in, or are modified by, responses to oxidising agents.

Excitingly, it was observed that Ubp12 is oxidised into a HMW complex in response to $H_2O_2$, and moreover, that Ubp12 is modified differently depending on the concentration of $H_2O_2$. Furthermore, analyses of the $H_2O_2$-induced complex suggested that Ubp12 forms an intramolecular disulphide(s) between the catalytic cysteine and an unknown cysteine in Ubp12 after $H_2O_2$ treatment. It is interesting to note that the mammalian dUb USP19, which when compared to the *S. cerevisiae* genome suggests Ubp12 as the highest homology, also forms a HMW complex after treatment with $H_2O_2$ (Lee *et al.*, 2013) with similar mobility as that observed for Ubp12. When aligned, USP19 and Ubp12 have 11 conserved cysteines, and it is tempting to speculate that one of these cysteines forms an intramolecular disulphide with the catalytic cysteine in both Ubp12 and USP19. Excitingly, it was observed that Ubp12 abundance was regulated by Trr1, suggesting that the thioredoxin system is crucial for maintaining Ubp12 stability. However, it is possible that Trr1 may be regulating the gene expression of *UBP12*, rather than protein stability. Interestingly it was also observed that Ubp12 and Ubp2, are oxidised differently by $H_2O_2$. This is intriguing as Ubp2 and Ubp12 function in opposition to one another to regulate mitochondrial morphology homeostasis (Anton *et al.*, 2013). Mitochondria promote fission or fusion depending on the level of oxidative stress. For example, low concentrations of stress induce mitochondrial fission which increases oxidative phosphorylation to overcome the cellular stress (Zemirli *et al.*, 2018), whereas severe stress induces mitochondrial fission to enable mitophagy and remove damaged mitochondria from the environment (Zemirli *et al.*, 2018). Thus the potential for Ubp12 and

Ubp2 to promote either mitochondrial fission or mitochondrial fusion depending on the concentration of $H_2O_2$ and the relative oxidation of each dUb, may suggest a mechanism by which mitochondrial dynamics are regulated. It has recently been observed that Cdc48, a conserved AAA ATPase, may regulate Ubp12 for multiple downstream functions (Gödderz *et al.*, 2017; Chowdhury *et al.*, 2018; Simões *et al.*, 2018). For example, a recent publication revealed that Cdc48 and a Ubp3 cofactor regulates Ubp12 stability in order to promote mitochondrial fission (Chowdhury *et al.*, 2018). In this regard, in the present study it was found that Ubp3 is actually critical for cellular responses to all the oxidising agents, suggesting that the regulation of dUbs by oxidative stress may be a mechanism by which mitochondrial dynamics are regulated.

The roles and regulation of another dUb, Ubp15 was also explored. Ubp15 was found to be oxidised in response to diamide and $H_2O_2$. However results suggested that the HMW Ubp15 complexes formed in response to $H_2O_2$ or diamide were different. It was also demonstrated that Ubp15 oxidation was more responsive to higher concentrations of $H_2O_2$. Taken together these results suggest that Ubp15 oxidation may be depend on the concentration of $H_2O_2$, and also the type of oxidising agent used may regulate the formation of Ubp15 HMW complex. Furthermore although the data suggest that Ubp15 forms a HMW disulphide complex via the catalytic cysteine, it currently remains unknown whether Ubp15 forms a complex with another protein, including another Ubp15, or whether Ubp15 forms an intramolecular disulphide(s). However, despite having similar mobility to Cdc34 HMW complexes, the Ubp15 $H_2O_2$-induced HMW complex does not include Cdc34. Interestingly, preliminary cell cycle analyses of unstressed *ubp15*Δ cells presented in this study suggested that Ubp15 may be important for regulating G1 phase growth arrest/delay, and that Ubp15 may be important for the timing of release into S phase after $H_2O_2$ stress. It is interesting to note that in the fission yeast *S. pombe*, Ubp15 (the homolog of Ubp15 in *S. cerevisiae*) has also been linked to regulating S phase, in this case by deubiquitination of PCNA (Alvarez *et al.*, 2016). In the case of *S. pombe* Ubp15, it was found to regulate PCNA together with other dUbs, Ubp2, Ubp12, and Ubp16, equivalent to Ubp2, Ubp12 and Ubp8 respectively in *S. cerevisiae*. The authors propose that the coordinated activity of these four dUbs remove

specific ubiquitin signals from PCNA at K164, thus allowing cell cycle progression and response to DNA damage/ replication blocks (Alvarez *et al.*, 2016). Ubiquitination of PCNA at K164 is conserved in *S. cerevisiae* (Gallego-Sanchez et al., 2012), however Ubp10 has been observed to remove the K164 ubiquitin signals from *S. cerevisiae* PCNA (Gallego-Sanchez et al., 2012). Interestingly the present study has suggested that *S. cerevisiae* Ubp2, Ubp12 and Ubp15 are all regulated by oxidative stress, although in different ways. It would be of interest to investigate whether oxidation of *S. pombe* Ubp2, Ubp12 and Ubp15 are also regulated by oxidative stress, which could pose a potential mechanism for regulating cell cycle progression via PCNA ubiquitination.

Collectively, this project has revealed that dUbs play a range of specific roles in the responses to oxidative stress, and that under certain oxidising conditions specific dUbs become modified. Furthermore we observed that the dUbs Ubp12 and Ubp15 were modified into HMW complexes by specific oxidising agents, however the relative sensitivity of these dUbs to the oxidising agent was different. It would be interesting in the future to understand the localisation of these dUbs and how this affects modifications by oxidative stress. It would also be interesting to investigate why specific dUbs are more sensitive than others to oxidising agents and to understand what determines the response and modifications to specific oxidising agents.

## 6.2. Implications for mammalian cells

Interestingly, although *S. cerevisiae* expresses only 20 dUbs, in comparison to ~100 dUbs in mammalian cells, many *S. cerevisiae* dUbs are conserved in mammalian cells, both functionally and structurally. Studies in mammalian cells revealed that certain dUbs can be activated by a reducing agent, suggesting oxidation inhibits dUb activity (Lee *et al.*, 2013). Other studies of the regulation of mammalian dUbs by oxidative stress showed that mouse USP18 was upregulated at the transcriptional level after $H_2O_2$ treatment, which had a protective role after oxidative stress and prevented cellular apoptosis, possibly via the upregulation of p53 (Lai *et al.*, 2017). Importantly it was observed that the dysregulation of USP18 in response to oxidative stress could be reduced,

suggesting that USP18 was reversibly oxidised (Lai *et al.*, 2017). Another dUb observed to be regulated by oxidative stress is USP9X. A previous study demonstrated that in response to high levels of $H_2O_2$, USP9X deubiquitinates, and thus stabilises ASK1 which results in cell death in a p38-dependent manner (Nagai *et al.*, 2009). However a recent study revealed that treatment with lower concentrations of $H_2O_2$ causes USP9X levels to increase which results in the stabilisation of the methyl-CpG-binding transcriptional regulator, ZBTB38 (Miotto *et al.*, 2018), which subsequently leads to cell survival after oxidative stress (Miotto *et al.*, 2018). It is possible that these different studies provide evidence for mechanisms by which different concentrations of $H_2O_2$ affects the ability of USP9X to interact with different targets. Hence, it is possible that the differential sensitivity of dUbs to oxidation may be a key mechanism by which specific cellular outcomes are regulated, tailoring the response to both the oxidising agent present and its concentration.

In the present study the roles and regulation of Ubp12 and Ubp15 in response to different oxidising agents were investigated. Interestingly, when the *S. cerevisiae* dUb is compared to the mammalian genome, both Ubp12 and Ubp15 have mammalian homologs, USP15 and USP7 respectively. The potential for these mammalian dUbs to be regulated by oxidative stress similar are discussed below.

### *6.2.1. USP15*

The mammalian homolog to Ubp12, USP15, was observed to be activated by a reducing agent (Lee *et al.*, 2013), suggesting that oxidation inhibits USP15 activity. This is particularly interesting as dysregulation of USP15 has been implicated in many cancers (Chou *et al.*, 2017). Indeed, USP15 has been linked to stabilising many proto-oncogenes, and moreover, upregulation of USP15 has been linked to ovarian and breast cancers and glioblastoma (Zou *et al.*, 2014; Chou *et al.*, 2017). In contrast, USP15 has also been linked to tumour-suppressor substrates, including p53 (Padmanabhan *et al.*, 2018). In addition to cancer, USP15 has also been implicated with Parkinson's disease (Cornelissen *et al.*, 2014). Parkin, an E3 ubiquitin ligase, normally localises to the cytoplasm, but translocates to the mitochondria to initiate mitophagy (Cornelissen *et al.*, 2014). A major cause of Parkinson's disease is the loss of function of Parkin. Interestingly,

USP15 has been observed to counteract Parkin mediated-ubiquitination, as inhibition of USP15 can rescue the defect in Parkin mediated-mitophagy that is observed in severe Parkinson's disease cases (Cornelissen *et al.*, 2014; Chou *et al.*, 2017). It is interesting to note that Ubp12 in *S. cerevisiae* is important for promoting mitochondrial fission, a key element for mitophagy, and we propose that the oxidation of Ubp12 may regulate mitochondrial fission. Thus it would be of interest to investigate the potential links to mitophagy associated with USP15 oxidation. However, it is also relevant that there are more dUbs present in mammalian cells, and hence it is possible that multiple mammalian dUbs may be important for mitochondrial regulation. For example USP30 (Bingol *et al.*, 2014), USP35 (Wang *et al.*, 2015), and USP8 (Durcan and Fon, 2015) have all been linked to mitochondrial morphology regulation in mammalian cells.

### *6.2.2. USP7*

The mammalian homolog of Ubp15 is USP7. USP7 is often dysregulated in cancers (Yeasmin Khusbu *et al.*, 2018), but it is also involved in other diseases including neurological disorders and immune dysfunction (Jackson *et al.*, 2000). USP7 has been linked to many types of cancer, for example brain, prostate, and breast cancers, and also leukaemia (Jackson *et al.*, 2000). USP7 was initially identified as a tumour suppressor by its ability to deubiquitnate p53, however it has also been observed to have oncogenic properties, for example by stabilising MDM2 (Bhattacharya *et al.*, 2018). Indeed to date no USP7 mutations have been found to inhibit cancer progression, suggesting that neither loss, nor gain of function is advantageous (Bhattacharya *et al.*, 2018). USP7 function has also been linked to oxidation. For example when incubated with a reducing agent, USP7 was found to have enhanced activity (Lee *et al.*, 2013), suggesting that USP7 may be regulated by oxidation. Furthermore, USP7 was demonstrated to be reversibly oxidised by $H_2O_2$, and that this oxidation is inversely correlated with ubiquitination of USP7 substrates (Cotto-Rios *et al.*, 2012). Analysis of this oxidation revealed that the catalytic cysteine in USP7 was oxidised to a sulphenic acid, but that activity was recovered after two hours. Interestingly it was also observed that other cysteines in USP7 were oxidised, and the authors hypothesised that USP7 sulphenic oxidation may be converted to a sulphenylamide or disulphide bond, potentially as a protective mechanism (Cotto-

Rios *et al.*, 2012). Hence, given the results presented in this thesis it would be extremely interesting to investigate whether mammalian USP7 forms a $H_2O_2$-induced HMW complex similar to that observed for Ubp15.

### 6.3. Potential implications for drug therapies

In the clinic, several drug therapies have been used successfully that target the ubiquitin-proteasome system (including bortezomib and lenalidomide) (Pal *et al.*, 2014). However these treatments are limited to certain tumour types. As dUbs have a wide range of substrates, and have been observed to be dysregulated in many cancers, they pose an attractive target for therapeutic strategies. In addition, by targeting dUbs the remaining ubiquitin-proteasome system remains functioning, hopefully minimising potential deleterious side effects (Pal *et al.*, 2014). Consequently, many drugs have been developed which target specific mammalian dUbs. For example, the compound ML323 inhibits USP1 activity and therefore regulates PCNA deubiquitination (Liang *et al.*, 2014). The chemicals HBX 41,108 (Colland *et al.*, 2009) and P22077 (Altun *et al.*, 2011) have both been identified to inhibit USP7 activity, and thus may have potential applications for cancer treatment. Interestingly, a recent drug Curcusone D, induces intracellular ROS levels, and thus has been observed to inhibit dUb activity (Cao *et al.*, 2014). Consequently, apoptosis is induced in multiple myeloma cells, and thus Curcusone D has been suggested to be an effective combination therapy with other ubiquitin-proteasome inhibitory drugs to treat cancers (Cao *et al.*, 2014). The suggestion that drug therapies may be able to produce ROS which inactivate specific dUbs highlights the importance of understanding dUb regulation by oxidation. The data presented in this thesis suggests that certain dUbs are regulated differently by oxidative stress. Which highlights the question of why certain dUbs are oxidised by certain oxidising agents while others are not. Understanding this question may prove very beneficial to allow targeting of ROS-producing drug therapies to certain dUbs in specific pathways.

## 6.4. Outstanding questions based on this study

This study has increased our knowledge of the regulation of specific *S. cerevisiae* dUbs in response to different oxidative stresses. However, outstanding questions remain to be addressed in addition to repeating any data that was only obtained from a small number of experiments. For example, although results obtained from this study indicate that Ubp12 forms a $H_2O_2$-induced intramolecular disulphide complex at the catalytic cysteine, further mass spectrometry analyses would hopefully be able to pinpoint the other cysteine(s) involved in the complex. Furthermore, a model was proposed that suggested that the sensitivity of Ubp12 and Ubp2 to oxidation may be important for regulating the dynamics of mitochondrial morphology. In this case, microscopy-based analyses of mitochondrial morphology should shed further light on the regulation of mitochondrial dynamics by oxidative stress. Other work has proposed that Ubp12 may regulate the stability of Ubp2 (Simões *et al.*, 2018), therefore in depth analyses of Ubp2 stability and its relationship with Ubp12 function after incubation with $H_2O_2$ would be of interest. It has also recently been observed that Ubp3 may regulate Ubp12 stability (Chowdhury *et al.*, 2018). Hence further investigations into the relationships between these two dUbs could prove interesting. Furthermore, the mammalian homolog of Ubp12, USP15, has many roles in cancer progression and is a potential drug target. Hence, it would be of interest to investigate whether oxidation of Ubp12 was conserved in USP15 as a potential route to identifying drugs that specifically target this dUb.

Results obtained from the present study have suggested that diamide and $H_2O_2$ potentially modify Ubp15 differently. The basis of these differences in not understood and hence these studies should be expanded to confirm the data and identify the cysteines and proteins involved. In addition, although the catalytic cysteine of Ubp15 is involved in the $H_2O_2$-induced HMW complex, other aspects of this complex are not currently understood. Similar to the Ubp12 studies mass spectrometry analyses could be utilised to investigate this complex. Interestingly, preliminary investigations of the potential connections between Ubp15 function, oxidative stress responses, and cell cycle regulation of several potential cell cycle arrest/delay checkpoints in response to $H_2O_2$, revealed that Ubp15 may influence G1 phase arrest and/or entry into S phase. Indeed from the initial studies a model

was proposed whereby Ubp15 regulates Sic1 levels and consequently regulates timing of S phase entry. Future work to examine whether Ubp15 regulates Sic1 would test this model. It is interesting to note that the mammalian homolog of Cdc34 (Cdc34) also regulates the mammalian of Sic1 (p27Kip1). Furthermore, Cdc28/Clb5 is also conserved in mammalian cells (CDK2, Cyclin E), thus it would be interesting to investigate whether USP7 is involved in regulating progression into S phase in mammalian cells, in a similar fashion as proposed for Ubp15 in *S. cerevisiae*.

Finally, this study has only performed the essential first steps regarding dUb functions and regulation by oxidising agents. Indeed, Ubp5 and Ubp14 were observed to be modified by menadione, a superoxide generating oxidising agent which has not been further investigated in this thesis. Also the method of oxidation detection utilised in this study only shows certain modifications in response to oxidative stress. Other dUbs, indeed including Ubp12 and Ubp15, may also be oxidised in other ways and hence other techniques should be applied in future studies to expand the work in this thesis.

## 6.5. Concluding remarks

While many studies into the regulation of ubiquitin and ubiquitin-like modifications are emerging, detailed investigations of the regulation of many specific pathway enzymes, including the dUbs, involved in these systems remains limited. Work presented here, and also by other groups working with mammalian cell models, has suggested that dUbs are regulated by ROS signalling. As described above, dUbs are often dysregulated in common diseases. Therefore, improving our understanding of dUb regulation by ROS signalling may potentially lead to novel therapies which utilise the differential sensitivity of dUbs to ROS as a clinical approach to benefit human health.

# Appendix A

Total mass spectrometry results from the first mass spectrometry analysis, completed by David Stead at Aberdeen University. The raw data was analysed and proteins were identified based on the values of score, coverage and peptide number (# peptide). The score indicates the sum of the ion scores of all the distinct peptides, hence a higher score suggests a more confident match. The coverage indicates the percentage of the protein sequence covered by the identified peptides. Finally, the peptide number indicates the total number of distinct peptides identified from a specific protein. Also included is #PSM which is the total number of peptide spectrum matches for each protein. Using these analyses, the protein hits were ranked based on their cumulative score.

| Gene | Score Ubp12-TAP | Coverage Ubp12-TAP | # Peptides Ubp12-TAP | # PSM Ubp12-TAP | Score WT | Coverage WT | # Peptides WT | # PSM WT |
|---|---|---|---|---|---|---|---|---|
| UBP12 | 1491.41 | 40.19 | 37 | 63 | | | | |
| URA2 | 1649.41 | 33.20 | 60 | 71 | 2709.07 | 48.87 | 89 | 110 |
| ACC1 | 1690.31 | 34.12 | 52 | 59 | 2685.90 | 48.05 | 77 | 93 |
| HIS4 | 571.21 | 25.03 | 17 | 19 | 985.36 | 37.67 | 26 | 34 |
| GCN1 | 676.56 | 13.96 | 25 | 25 | 460.18 | 8.83 | 18 | 18 |
| POL2 | 197.63 | 6.30 | 10 | 10 | 216.66 | 6.53 | 11 | 11 |
| UBR1 | 42.17 | 1.03 | 2 | 2 | 102.84 | 3.95 | 6 | 6 |
| RPS3S | 46.44 | 7.08 | 1 | 1 | 36.64 | 7.08 | 1 | 1 |
| CEX1 | 41.75 | 2.23 | 1 | 1 | | | | |
| SEC7 | 72.39 | 2.04 | 3 | 3 | 119.07 | 3.14 | 4 | 5 |
| CDC19 | 68.24 | 7.40 | 3 | 3 | 39.73 | 4.80 | 2 | 2 |
| ADH2 | 32.12 | 5.75 | 2 | 2 | 97.48 | 6.90 | 3 | 3 |
| FAS1 | 61.48 | 2.44 | 3 | 3 | 224.04 | 7.26 | 10 | 10 |
| YEF3 | 33.54 | 1.15 | 1 | 1 | 59.84 | 2.49 | 2 | 2 |
| TAO3 | 56.85 | 1.22 | 2 | 2 | 58.85 | 1.73 | 3 | 3 |
| CHC1 | | | | | 23.29 | 0.97 | 1 | 1 |
| ECM33 | | | | | 29.71 | 2.33 | 1 | 1 |
| TEF2 | | | | | 47.59 | 2.40 | 1 | 1 |
| FAS2 | | | | | 21.07 | 0.90 | 1 | 1 |
| FKS1 | | | | | 54.27 | 2.56 | 3 | 3 |
| GLT1 | | | | | 50.42 | 1.96 | 3 | 3 |
| HSC82 | | | | | 83.64 | 9.22 | 5 | 5 |
| SSA2 | | | | | 89.89 | 9.86 | 4 | 4 |
| SSC1 | | | | | 32.09 | 3.82 | 2 | 2 |
| PGK1 | | | | | 39.08 | 3.37 | 1 | 1 |
| PMA1 | | | | | 48.60 | 1.42 | 1 | 1 |
| RPO21 | | | | | 38.37 | 0.92 | 1 | 1 |

# Appendix B

Total mass spectrometry results from the second mass spectrometry analysis, completed by David Stead at Aberdeen University. The raw data was analysed and proteins were identified based on the values of score, coverage and peptide number (# peptide). The score indicates the sum of the ion scores of all the distinct peptides, hence a higher score suggests a more confident match. The coverage indicates the percentage of the protein sequence covered by the identified peptides. Finally, the peptide number indicates the total number of distinct peptides identified from a specific protein. Also included is #PSM which is the total number of peptide spectrum matches for each protein. Using these analyses, the protein hits were ranked based on their cumulative score.

| Gene | Score Ubp12-TAP | Coverage Ubp12-TAP | # Peptides Ubp12-TAP | # PSM Ubp12-TAP | Score Ubp12-TAP + H2O2 | Coverage Ubp12-TAP + H2O2 | # Peptides Ubp12-TAP + H2O2 | # PSM Ubp12-TAP + H2O2 | Score WT + H2O2 | Coverage WT + H2O2 | # Peptides WT + H2O2 | # PSM WT + H2O2 |
|---|---|---|---|---|---|---|---|---|---|---|---|---|
| UBP12 | 1765.80 | 36.12 | 32 | 50 | 4197.79 | 53.99 | 48 | 121 | 292.95 | 12.52 | 11 | 11 |
| VPS13 | 2872.34 | 30.50 | 65 | 77 | 450.93 | 8.14 | 18 | 19 | 2454.24 | 27.51 | 60 | 73 |
| URA2 | 980.15 | 18.25 | 30 | 31 | 283.48 | 6.59 | 12 | 12 | 1021.10 | 16.94 | 29 | 30 |
| HIS4 | 581.64 | 23.03 | 13 | 16 | 576.24 | 22.03 | 12 | 16 | 771.25 | 30.04 | 17 | 23 |
| CDC19 | 331.71 | 31.60 | 10 | 11 | 269.04 | 28.20 | 11 | 13 | 399.97 | 36.00 | 11 | 13 |
| ACC1 | 404.73 | 11.29 | 18 | 18 | 68.88 | 2.28 | 4 | 4 | 290.30 | 7.84 | 12 | 12 |
| FAS1 | 478.69 | 11.65 | 15 | 15 | 33.65 | 0.98 | 1 | 1 | 408.98 | 14.43 | 18 | 18 |
| GCN1 | 332.75 | 6.96 | 15 | 15 | 86.64 | 1.50 | 3 | 3 | 412.92 | 7.30 | 15 | 15 |
| PDC1 | 376.94 | 28.24 | 9 | 12 | 236.64 | 17.76 | 6 | 7 | 214.03 | 23.98 | 8 | 9 |
| FAS2 | 210.24 | 6.84 | 9 | 9 | 28.74 | 1.32 | 2 | 2 | 451.90 | 9.96 | 13 | 13 |
| TOM1 | 542.14 | 7.07 | 19 | 20 | | | | | 54.78 | 1.59 | 4 | 4 |
| TEF2 | 254.17 | 27.29 | 7 | 10 | 126.99 | 19.21 | 5 | 7 | 202.01 | 17.25 | 4 | 6 |
| YEF3 | 294.02 | 15.90 | 11 | 12 | 75.83 | 2.68 | 3 | 3 | 158.75 | 9.00 | 7 | 7 |
| NUM1 | 325.30 | 16.34 | 9 | 11 | 127.82 | 11.97 | 5 | 5 | 127.64 | 11.97 | 5 | 5 |
| TRA1 | 310.55 | 4.11 | 12 | 12 | | | | | 278.38 | 2.48 | 8 | 8 |
| SSA2 | 261.47 | 16.90 | 7 | 7 | 117.01 | 7.36 | 4 | 4 | 162.12 | 15.34 | 6 | 6 |
| ADH1 | 216.69 | 25.00 | 6 | 6 | 147.93 | 15.52 | 4 | 4 | 187.94 | 17.82 | 6 | 6 |
| EFT2 | 141.76 | 10.57 | 6 | 6 | 26.23 | 2.14 | 1 | 1 | 111.26 | 8.19 | 5 | 5 |
| MDN1 | 177.95 | 2.73 | 9 | 9 | | | | | 39.96 | 0.59 | 2 | 2 |
| KRS1 | 118.95 | 14.04 | 7 | 8 | 30.32 | 3.89 | 2 | 2 | 29.60 | 2.03 | 1 | 1 |
| VMA1 | 173.52 | 11.02 | 8 | 8 | 51.43 | 1.40 | 1 | 1 | 59.38 | 2.61 | 2 | 2 |
| ACO1 | 55.06 | 3.21 | 2 | 2 | 128.77 | 7.97 | 5 | 5 | 97.62 | 5.53 | 3 | 3 |
| ECM33 S | 108.85 | 9.32 | 3 | 3 | 89.86 | 5.83 | 2 | 2 | 121.21 | 9.32 | 3 | 3 |
| FKS1 | 73.26 | 2.19 | 2 | 2 | | | | | 81.47 | 5.44 | 6 | 6 |
| PMA1 | 117.55 | 7.63 | 4 | 4 | | | | | 120.08 | 4.47 | 3 | 4 |
| VMA2 | 190.48 | 11.41 | 4 | 4 | 28.67 | 2.90 | 1 | 1 | 94.77 | 4.45 | 2 | 2 |
| SSB1 | 61.68 | 9.62 | 3 | 3 | 25.60 | 2.28 | 1 | 1 | 56.27 | 6.36 | 2 | 2 |
| CDC60 | 65.66 | 5.60 | 3 | 3 | | | | | 80.55 | 4.13 | 3 | 3 |
| CHC1 | 84.70 | 1.63 | 2 | 2 | | | | | 66.09 | 2.36 | 3 | 3 |
| EDE1 | 88.94 | 3.69 | 3 | 3 | | | | | 42.19 | 2.10 | 2 | 2 |
| ILS1 | 43.41 | 1.96 | 2 | 2 | 32.88 | 1.03 | 1 | 1 | 42.75 | 1.96 | 2 | 2 |
| ACT1 | 33.96 | 7.73 | 2 | 2 | | | | | 46.85 | 4.80 | 1 | 2 |
| CYS4 | 93.23 | 5.72 | 2 | 2 | 43.03 | 3.35 | 1 | 1 | 44.21 | 3.55 | 1 | 1 |
| TDH3 | 162.80 | 15.66 | 3 | 3 | 41.85 | 4.22 | 1 | 1 | | | | |

| | | | | | | | | | | | | |
|---|---|---|---|---|---|---|---|---|---|---|---|---|
| S | | | | | | | | | | | | |
| PYK2 | 74.35 | 6.92 | 2 | 2 | 53.56 | 1.98 | 1 | 1 | 68.93 | 1.98 | 1 | 1 |
| RPL27B | 72.82 | 10.29 | 1 | 1 | 37.07 | 10.29 | 1 | 1 | 104.10 | 20.59 | 2 | 2 |
| SEC16 | 45.80 | 1.82 | 3 | 3 | | | | | 48.01 | 0.82 | 1 | 1 |
| UBI4 | 107.34 | 21.00 | 1 | 1 | 93.16 | 32.81 | 2 | 2 | 77.99 | 21.00 | 1 | 1 |
| SAM1 | 175.96 | 12.30 | 3 | 3 | | | | | | | | |
| PHO3 | 68.50 | 3.43 | 1 | 1 | | | | | 41.57 | 6.85 | 2 | 2 |
| RPL3 | 25.71 | 4.13 | 1 | 1 | | | | | 51.44 | 7.49 | 2 | 2 |
| UTP8 | 37.88 | 1.26 | 1 | 1 | 22.85 | 1.26 | 1 | 1 | 23.67 | 1.26 | 1 | 1 |
| HSC82 | | | | | | | | | 51.56 | 4.68 | 3 | 3 |
| ASN1 | 41.92 | 3.85 | 2 | 2 | | | | | | | | |
| ASN2 | 28.84 | 3.85 | 2 | 2 | | | | | | | | |
| SEC7 | 25.43 | 0.40 | 1 | 1 | | | | | 21.36 | 0.50 | 1 | 1 |
| RPA190 | | | | | | | | | 26.58 | 1.62 | 2 | 2 |
| INA1 | | | | | | | | | 39.63 | 4.30 | 2 | 2 |
| GND1 | 62.32 | 3.48 | 1 | 1 | | | | | | | | |
| ATP1 | 44.95 | 2.39 | 1 | 1 | | | | | | | | |
| UTR2 | 20.46 | 3.21 | 1 | 1 | | | | | | | | |
| CYC1 | 35.68 | 10.09 | 1 | 1 | | | | | | | | |
| GUA1 | 38.93 | 2.29 | 1 | 1 | | | | | | | | |
| NSR1 | 21.64 | 3.86 | 1 | 1 | | | | | | | | |
| SAH1 | 36.30 | 3.12 | 1 | 1 | | | | | | | | |
| MES1 | 27.52 | 2.13 | 1 | 1 | | | | | | | | |
| DED81 | 40.63 | 2.53 | 1 | 1 | | | | | | | | |
| TSA1 | 29.15 | 7.14 | 1 | 1 | | | | | | | | |
| YLR035C-A | 21.25 | 1.30 | 1 | 1 | | | | | | | | |
| GLT1 | | | | | | | | | 37.11 | 0.70 | 1 | 1 |
| KAP123 | | | | | | | | | 21.59 | 1.17 | 1 | 1 |
| FAA4 | | | | | | | | | 20.41 | 2.31 | 1 | 1 |
| PFK2 | | | | | | | | | 22.15 | 2.50 | 1 | 1 |
| RRP5 | | | | | | | | | 21.00 | 0.52 | 1 | 1 |
| SMT3 | | | | | | | | | 85.31 | 21.78 | 1 | 1 |

# References


Abdul Rehman, Syed A., Kristariyanto, Yosua A., Choi, S.-Y., Nkosi, P.J., Weidlich, S., Labib, K., Hofmann, K. and Kulathu, Y. (2016) 'MINDY-1 Is a Member of an Evolutionarily Conserved and Structurally Distinct New Family of Deubiquitinating Enzymes', *Molecular Cell*, 63(1), pp. 146-155.

Adorno, M., Sikandar, S., Mitra, S.S., Kuo, A., Nicolis Di Robilant, B., Haro-Acosta, V., Ouadah, Y., Quarta, M., Rodriguez, J., Qian, D., Reddy, V.M., Cheshier, S., Garner, C.C. and Clarke, M.F. (2013) 'Usp16 contributes to somatic stem-cell defects in Down's syndrome', *Nature*, 501(7467), pp. 380-4.

Aguiar, P.H., Furtado, C., Repoles, B.M., Ribeiro, G.A., Mendes, I.C., Peloso, E.F., Gadelha, F.R., Macedo, A.M., Franco, G.R., Pena, S.D., Teixeira, S.M., Vieira, L.Q., Guarneri, A.A., Andrade, L.O. and Machado, C.R. (2013) 'Oxidative stress and DNA lesions: the role of 8-oxoguanine lesions in Trypanosoma cruzi cell viability', *PLoS Negl Trop Dis*, 7(6), p. e2279.

Ahmed, W. and Lingner, J. (2018) 'PRDX1 and MTH1 cooperate to prevent ROS-mediated inhibition of telomerase', *Genes Dev*, 32(9-10), pp. 658-669.

Ahn SG and Thiele DJ (2003) ‘Redox regulation of mammalian heat shock factor 1 is essential for Hsp gene activation and protection from stress’ *Genes Dev*, 17(4) pp. 516-528

Albuquerque, C.P., Smolka, M.B., Payne, S.H., Bafna, V., Eng, J. and Zhou, H. (2008) 'A multidimensional chromatography technology for in-depth phosphoproteome analysis', *Mol Cell Proteomics*, 7(7), pp. 1389-96.

Altun, M., Kramer, H.B., Willems, L.I., McDermott, J.L., Leach, C.A., Goldenberg, S.J., Kumar, K.G., Konietzny, R., Fischer, R., Kogan, E., Mackeen, M.M., McGouran, J., Khoronenkova, S.V., Parsons, J.L., Dianov, G.L., Nicholson, B. and Kessler, B.M. (2011) 'Activity-based chemical proteomics accelerates inhibitor development for deubiquitylating enzymes', *Chem Biol*, 18(11), pp. 1401-12.

Alvarez, V., Vinas, L., Gallego-Sanchez, A., Andres, S., Sacristan, M.P. and Bueno, A. (2016) 'Orderly progression through S-phase requires dynamic ubiquitylation and deubiquitylation of PCNA', *Sci Rep*, 6, p. 25513.

Amerik, A., Swaminathan, S., Krantz, B.A., Wilkinson, K.D. and Hochstrasser, M. (1997) 'In vivo disassembly of free polyubiquitin chains by yeast Ubp14 modulates rates of protein degradation by the proteasome', *Embo j*, 16(16), pp. 4826-38.

Amerik, A.Y. and Hochstrasser, M. (2004) 'Mechanism and function of deubiquitinating enzymes', *Biochimica et Biophysica Acta (BBA) - Molecular Cell Research*, 1695(1), pp. 189-207.

Amerik, A.Y., Li, S.J. and Hochstrasser, M. (2000) 'Analysis of the deubiquitinating enzymes of the yeast Saccharomyces cerevisiae', *Biol Chem*, 381(9-10), pp. 981-92.

Andreini, C., Cavallaro, G., Lorenzini, S. and Rosato, A. (2013) 'MetalPDB: a database of metal sites in biological macromolecular structures', *Nucleic Acids Res*, 41(Database issue), pp. D312-9.

Angelucci, F., Saccoccia, F., Ardini, M., Boumis, G., Brunori, M., Di Leandro, L., Ippoliti, R., Miele, A.E., Natoli, G., Scotti, S. and Bellelli, A. (2013) 'Switching between the Alternative Structures and Functions of a 2-Cys Peroxiredoxin, by Site-Directed Mutagenesis', *Journal of Molecular Biology*, 425(22), pp. 4556-4568.

Ansenberger-Fricano, K., Ganini, D., Mao, M., Chatterjee, S., Dallas, S., Mason, R.P., Stadler, K., Santos, J.H. and Bonini, M.G. (2013) 'The peroxidase activity of mitochondrial superoxide dismutase', *Free Radic Biol Med*, 54, pp. 116-24.

Anton, F., Dittmar, G., Langer, T. and Escobar-Henriques, M. (2013) 'Two deubiquitylases act on mitofusin and regulate mitochondrial fusion along independent pathways', *Mol Cell*, 49(3), pp. 487-98.

Avery, A.M. and Avery, S.V. (2001) 'Saccharomyces cerevisiae expresses three phospholipid hydroperoxide glutathione peroxidases', *J Biol Chem*, 276(36), pp. 33730-5.

Avery, A.M., Willetts, S.A. and Avery, S.V. (2004) 'Genetic dissection of the phospholipid hydroperoxidase activity of yeast gpx3 reveals its functional importance', *J Biol Chem*, 279(45), pp. 46652-8.

Avvakumov, G.V., Walker, J.R., Xue, S., Finerty, P.J., Jr., Mackenzie, F., Newman, E.M. and Dhe-Paganon, S. (2006) 'Amino-terminal dimerization, NRDP1-rhodanese interaction, and inhibited catalytic domain conformation of the ubiquitin-specific protease 8 (USP8)', *J Biol Chem*, 281(49), pp. 38061-70.

Azevedo, D., Tacnet, F., Delaunay, A., Rodrigues-Pousada, C. and Toledano, M.B. (2003) 'Two redox centers within Yap1 for H2O2 and thiol-reactive chemicals signaling', *Free Radical Biology and Medicine*, 35(8), pp. 889-900.

Baker, R.T., Tobias, J.W. and Varshavsky, A. (1992) 'Ubiquitin-specific proteases of Saccharomyces cerevisiae. Cloning of UBP2 and UBP3, and functional analysis of the UBP gene family', *J Biol Chem*, 267(32), pp. 23364-75.

Bakker, B.M., Overkamp, K.M., van Maris, A.J., Kotter, P., Luttik, M.A., van Dijken, J.P. and Pronk, J.T. (2001) 'Stoichiometry and compartmentation of NADH metabolism in Saccharomyces cerevisiae', *FEMS Microbiol Rev*, 25(1), pp. 15-37.

Balak, C.D., Hunter, J.M., Ahearn, M.E., Wiley, D., D'Urso, G. and Baumbach-Reardon, L. (2017) 'Functional characterizations of rare UBA1 variants in X-linked Spinal Muscular Atrophy', *F1000Research*, 6, p. 1636.

Bassermann, F., Eichner, R. and Pagano, M. (2014) 'The ubiquitin proteasome system - implications for cell cycle control and the targeted treatment of cancer', *Biochim Biophys Acta*, 1843(1), pp. 150-62.

Beck J, Maerki S, Posch M, Metzger T, Persaud A, Scheel H, Hofmann K, Rotin D, Pedrioli P, Swedlow JR, Peter M, and Sumara I (2013) ‘Ubiquitylation-dependent localization of PLK1 in mitosis’, *Nat Cell Biol*, 15(4) pp. 430-439

Bedford, L., Lowe, J., Dick, L.R., Mayer, R.J. and Brownell, J.E. (2010) 'Ubiquitin-like protein conjugation and the ubiquitin–proteasome system as drug targets', *Nature Reviews Drug Discovery*, 10, p. 29.

Benschop, J.J., Brabers, N., van Leenen, D., Bakker, L.V., van Deutekom, H.W.M., van Berkum, N.L., Apweiler, E., Lijnzaad, P., Holstege, F.C.P. and Kemmeren, P. (2010) 'A Consensus of Core Protein Complex Compositions for Saccharomyces cerevisiae', *Molecular Cell*, 38(6), pp. 916-928.

Berben, G., Dumont, J., Gilliquet, V., Bolle, P.A. and Hilger, F. (1991) 'The YDp plasmids: a uniform set of vectors bearing versatile gene disruption cassettes for Saccharomyces cerevisiae', *Yeast*, 7(5), pp. 475-7.

Berlett, B.S. and Stadtman, E.R. (1997) 'Protein oxidation in aging, disease, and oxidative stress', *J Biol Chem*, 272(33), pp. 20313-6.

Bersweiler A, D'Autréaux B, Mazon H, Kriznik A, Belli G, Delaunay-Moisan A, Toledano MB, Rahuel-Clermont S., (2017) 'A scaffold protein that chaperones a cysteine-sulfenic acid in H2O2 signaling', *Nat Chem Biol*, 13(8) pp. 909-915

Bertaux, A., Cabon, L., Brunelle-Navas, M.-N., Bouchet, S., Nemazanyy, I. and Susin, S.A. (2018) 'Mitochondrial OXPHOS influences immune cell fate: lessons from hematopoietic AIF-deficient and NDUFS4-deficient mouse models', *Cell Death & Disease*, 9(6), p. 581.

Bhattacharya, S., Chakraborty, D., Basu, M. and Ghosh, M.K. (2018) 'Emerging insights into HAUSP (USP7) in physiology, cancer and other diseases', *Signal Transduction and Targeted Therapy*, 3, p. 17.

Bhattacharya, S. and Ghosh, M.K. (2014) 'HAUSP, a novel deubiquitinase for Rb - MDM2 the critical regulator', *Febs j*, 281(13), pp. 3061-78.

Bienert, G.P., Schjoerring, J.K. and Jahn, T.P. (2006) 'Membrane transport of hydrogen peroxide', *Biochim Biophys Acta*, 1758(8), pp. 994-1003.

Bignell, G.R., Warren, W., Seal, S., Takahashi, M., Rapley, E., Barfoot, R., Green, H., Brown, C., Biggs, P.J., Lakhani, S.R., Jones, C., Hansen, J., Blair, E., Hofmann, B., Siebert, R., Turner, G., Evans, D.G., Schrander-Stumpel, C., Beemer, F.A., van Den Ouweland, A., Halley, D., Delpech, B., Cleveland, M.G., Leigh, I., Leisti, J. and Rasmussen, S. (2000) 'Identification of the familial cylindromatosis tumour-suppressor gene', *Nat Genet*, 25(2), pp. 160-5.

Bingol, B., Tea, J.S., Phu, L., Reichelt, M., Bakalarski, C.E., Song, Q., Foreman, O., Kirkpatrick, D.S. and Sheng, M. (2014) 'The mitochondrial deubiquitinase USP30 opposes parkin-mediated mitophagy', *Nature*, 510(7505), pp. 370-5.

Biteau, B., Labarre, J. and Toledano, M.B. (2003) 'ATP-dependent reduction of cysteine-sulphinic acid by S. cerevisiae sulphiredoxin', *Nature*, 425(6961), pp. 980-4.

Boase, N.A. and Kumar, S. (2015) 'NEDD4: The founding member of a family of ubiquitin-protein ligases', *Gene*, 557(2), pp. 113-22.

Bolton, J.L., Trush, M.A., Penning, T.M., Dryhurst, G. and Monks, T.J. (2000) 'Role of quinones in toxicology', *Chem Res Toxicol*, 13(3), pp. 135-60.

Bossis, G. and Melchior, F. (2006) 'Regulation of SUMOylation by reversible oxidation of SUMO conjugating enzymes', *Mol Cell*, 21(3), pp. 349-57.

Bozza, W.P. and Zhuang, Z. (2011) 'Biochemical characterization of a multidomain deubiquitinating enzyme Ubp15 and the regulatory role of its terminal domains', *Biochemistry*, 50(29), pp. 6423-32.

Bremm, A. and Komander, D. (2011) 'Emerging roles for Lys11-linked polyubiquitin in cellular regulation', *Trends in Biochemical Sciences*, 36(7), pp. 355-363.

Bridge, G., Rashid, S. and Martin, S.A. (2014) 'DNA mismatch repair and oxidative DNA damage: implications for cancer biology and treatment', *Cancers (Basel)*, 6(3), pp. 1597-614.

Brown, Jonathon D., Day, Alison M., Taylor, Sarah R., Tomalin, Lewis E., Morgan, Brian A. and Veal, Elizabeth A. (2013) 'A Peroxiredoxin Promotes H(2)O(2) Signaling and Oxidative Stress Resistance by Oxidizing a Thioredoxin Family Protein', *Cell Reports*, 5(5), pp. 1425-1435.

Buettner, G.R. (1993) 'The pecking order of free radicals and antioxidants: lipid peroxidation, alpha-tocopherol, and ascorbate', *Arch Biochem Biophys*, 300(2), pp. 535-43.

Buhrman, G., Parker, B., Sohn, J., Rudolph, J. and Mattos, C. (2005) 'Structural mechanism of oxidative regulation of the phosphatase Cdc25B via an intramolecular disulfide bond', *Biochemistry*, 44(14), pp. 5307-16.

Cadet, J. and Wagner, J.R. (2013) 'DNA base damage by reactive oxygen species, oxidizing agents, and UV radiation', *Cold Spring Harb Perspect Biol*, 5(2).

Cao, M.-N., Zhou, Y.-B., Gao, A.-H., Cao, J.-Y., Gao, L.-X., Sheng, L., Xu, L., Su, M.-B., Cao, X.-C., Han, M.-m., Wang, M.-K. and Li, J. (2014) 'Curcusone D, a novel ubiquitin–proteasome pathway inhibitor via ROS-induced DUB inhibition, is synergistic with bortezomib against multiple myeloma cell growth', *Biochimica et Biophysica Acta (BBA) - General Subjects*, 1840(6), pp. 2004-2013.

Carruthers, N.J., Parker, G.C., Gratsch, T., Caruso, J.A. and Stemmer, P.M. (2015) 'Protein Mobility Shifts Contribute to Gel Electrophoresis Liquid Chromatography Analysis', *Journal of Biomolecular Techniques : JBT*, 26(3), pp. 103-112.

Catalá, A. (2010) 'A synopsis of the process of lipid peroxidation since the discovery of the essential fatty acids', *Biochemical and Biophysical Research Communications*, 399(3), pp. 318-323.

Chen, Z.J. and Sun, L.J. (2009) 'Nonproteolytic functions of ubiquitin in cell signaling', *Mol Cell*, 33(3), pp. 275-86.

Chiu, J. and Dawes, I.W. (2012) 'Redox control of cell proliferation', *Trends in Cell Biology*, 22(11), pp. 592-601.

Cho, S.J., Roman, G., Yeboah, F. and Konishi, Y. (2007) 'The road to advanced glycation end products: a mechanistic perspective', *Curr Med Chem*, 14(15), pp. 1653-71.

Chondrogianni, N., Petropoulos, I., Grimm, S., Georgila, K., Catalgol, B., Friguet, B., Grune, T. and Gonos, E.S. (2014) 'Protein damage, repair and proteolysis', *Molecular Aspects of Medicine*, 35, pp. 1-71.

Chou, C.-K., Chang, Y.-T., Korinek, M., Chen, Y.-T., Yang, Y.-T., Leu, S., Lin, I.L., Tang, C.-J. and Chiu, C.-C. (2017) 'The Regulations of Deubiquitinase

USP15 and Its Pathophysiological Mechanisms in Diseases', *International Journal of Molecular Sciences*, 18(3), p. 483.

Chowdhury, A., Ogura, T. and Esaki, M. (2018) 'Two Cdc48 cofactors Ubp3 and Ubx2 regulate mitochondrial morphology and protein turnover', *J Biochem*.

Christianson, T.W., Sikorski, R.S., Dante, M., Shero, J.H. and Hieter, P. (1992) 'Multifunctional yeast high-copy-number shuttle vectors', *Gene*, 110(1), pp. 119-122.

Chuang, Y.Y., Chen, Y., Gadisetti, Chandramouli, V.R., Cook, J.A., Coffin, D., Tsai, M.H., DeGraff, W., Yan, H., Zhao, S., Russo, A., Liu, E.T. and Mitchell, J.B. (2002) 'Gene expression after treatment with hydrogen peroxide, menadione, or t-butyl hydroperoxide in breast cancer cells', *Cancer Res*, 62(21), pp. 6246-54.

Chung, W.H. (2017) 'Unraveling new functions of superoxide dismutase using yeast model system: Beyond its conventional role in superoxide radical scavenging', *J Microbiol*, 55(6), pp. 409-416.

Ciechanover, A. (2015) 'The unravelling of the ubiquitin system', *Nat Rev Mol Cell Biol*, 16(5), pp. 322-4.

Ciehanover, A., Hod, Y. and Hershko, A. (1978) 'A heat-stable polypeptide component of an ATP-dependent proteolytic system from reticulocytes', *Biochemical and Biophysical Research Communications*, 81(4), pp. 1100-1105.

Clague, M.J. (2013) 'Biochemistry: Oxidation controls the DUB step', *Nature*, 497(7447), pp. 49-50.

Cohen, M., Stutz, F., Belgareh, N., Haguenauer-Tsapis, R. and Dargemont, C. (2003) 'Ubp3 requires a cofactor, Bre5, to specifically de-ubiquitinate the COPII protein, Sec23', *Nat Cell Biol*, 5(7), pp. 661-7.

Coïc, E., Sun, K., Wu, C. and Haber, J.E. (2006) 'Cell Cycle-Dependent Regulation of Saccharomyces cerevisiae Donor Preference during Mating-Type Switching by SBF (Swi4/Swi6) and Fkh1', *Molecular and Cellular Biology*, 26(14), pp. 5470-5480.

Colland, F., Formstecher, E., Jacq, X., Reverdy, C., Planquette, C., Conrath, S., Trouplin, V., Bianchi, J., Aushev, V.N., Camonis, J., Calabrese, A., Borg-Capra, C., Sippl, W., Collura, V., Boissy, G., Rain, J.-C., Guedat, P., Delansorne, R. and Daviet, L. (2009) 'Small-molecule inhibitor of USP7/HAUSP ubiquitin protease stabilizes and activates p53 in cells', *Molecular Cancer Therapeutics*, 8(8), p. 2286.

Cornelissen, T., Haddad, D., Wauters, F., Van Humbeeck, C., Mandemakers, W., Koentjoro, B., Sue, C., Gevaert, K., De Strooper, B., Verstreken, P. and Vandenberghe, W. (2014) 'The deubiquitinase USP15 antagonizes Parkin-mediated mitochondrial ubiquitination and mitophagy', *Hum Mol Genet*, 23(19), pp. 5227-42.

Cotto-Rios, Xiomaris M., Békés, M., Chapman, J., Ueberheide, B. and Huang, Tony T. (2012) 'Deubiquitinases as a Signaling Target of Oxidative Stress', *Cell Reports*, 2(6), pp. 1475-1484.

Couto, N., Wood, J. and Barber, J. (2016) 'The role of glutathione reductase and related enzymes on cellular redox homoeostasis network', *Free Radical Biology and Medicine*, 95, pp. 27-42.

Cross, F.R., Schroeder, L. and Bean, J.M. (2007) 'Phosphorylation of the Sic1 Inhibitor of B-Type Cyclins in <em>Saccharomyces cerevisiae</em> Is Not Essential but Contributes to Cell Cycle Robustness', *Genetics*, 176(3), p. 1541.

Cumming, R.C., Andon, N.L., Haynes, P.A., Park, M., Fischer, W.H. and Schubert, D. (2004) 'Protein disulfide bond formation in the cytoplasm during oxidative stress', *J Biol Chem*, 279(21), pp. 21749-58.

Dalle-Donne, I., Rossi, R., Giustarini, D., Milzani, A. and Colombo, R. (2003) 'Protein carbonyl groups as biomarkers of oxidative stress', *Clinica Chimica Acta*, 329(1), pp. 23-38.

David, S.S., O'Shea, V.L. and Kundu, S. (2007) 'Base-excision repair of oxidative DNA damage', *Nature*, 447(7147), pp. 941-50.

Day, Alison M., Brown, Jonathon D., Taylor, Sarah R., Rand, Jonathan D., Morgan, Brian A. and Veal, Elizabeth A. (2012) 'Inactivation of a Peroxiredoxin by Hydrogen Peroxide Is Critical for Thioredoxin-Mediated Repair of Oxidized Proteins and Cell Survival', *Molecular Cell*, 45(3), pp. 398-408.

Debelyy, M.O., Platta, H.W., Saffian, D., Hensel, A., Thoms, S., Meyer, H.E., Warscheid, B., Girzalsky, W. and Erdmann, R. (2011) 'Ubp15p, a ubiquitin hydrolase associated with the peroxisomal export machinery', *J Biol Chem*, 286(32), pp. 28223-34.

Delaunay, A., Isnard, A.-D. and Toledano, M.B. (2000) 'H(2)O(2) sensing through oxidation of the Yap1 transcription factor', *The EMBO Journal*, 19(19), pp. 5157-5166.

Delaunay, A., Pflieger, D., Barrault, M.B., Vinh, J. and Toledano, M.B. (2002) 'A thiol peroxidase is an H2O2 receptor and redox-transducer in gene activation', *Cell*, 111(4), pp. 471-81.

Deshaies, R.J., Emberley, E.D. and Saha, A. (2010) 'Control of cullin-ring ubiquitin ligase activity by nedd8', *Subcell Biochem*, 54, pp. 41-56.

Deshaies, R.J. and Joazeiro, C.A.P. (2009) 'RING Domain E3 Ubiquitin Ligases', *Annual Review of Biochemistry*, 78(1), pp. 399-434.

Diaz-Moralli, S., Tarrado-Castellarnau, M., Miranda, A. and Cascante, M. (2013) 'Targeting cell cycle regulation in cancer therapy', *Pharmacology & Therapeutics*, 138(2), pp. 255-271.

Dodgson, S.E., Santaguida, S., Kim, S., Sheltzer, J. and Amon, A. (2016) 'The pleiotropic deubiquitinase Ubp3 confers aneuploidy tolerance', *Genes & Development*, 30(20), pp. 2259-2271.

Doris, K.S., Rumsby, E.L. and Morgan, B.A. (2012) 'Oxidative stress responses involve oxidation of a conserved ubiquitin pathway enzyme', *Mol Cell Biol*, 32(21), pp. 4472-81.

Drag, M. and Salvesen, G.S. (2008) 'DeSUMOylating enzymes--SENPs', *IUBMB Life*, 60(11), pp. 734-42.

Drazic, A. and Winter, J. (2014) 'The physiological role of reversible methionine oxidation', *Biochimica et Biophysica Acta (BBA) - Proteins and Proteomics*, 1844(8), pp. 1367-1382.

Drew, R. and Miners, J.O. (1984) 'The effects of buthionine sulphoximine (BSO) on glutathione depletion and xenobiotic biotransformation', *Biochem Pharmacol*, 33(19), pp. 2989-94.

Duchen, M.R. (2000) 'Mitochondria and calcium: from cell signalling to cell death', *The Journal of physiology*, 529(1), pp. 57-68.

Dupré-Crochet, S., Erard, M. and Nüβe, O. (2013) 'ROS production in phagocytes: why, when, and where?', *Journal of Leukocyte Biology*, 94(4), pp. 657-670.

Durcan, T.M. and Fon, E.A. (2015) 'USP8 and PARK2/parkin-mediated mitophagy', *Autophagy*, 11(2), pp. 428-9.

Eckers, E., Bien, M., Stroobant, V., Herrmann, J.M. and Deponte, M. (2009) 'Biochemical Characterization of Dithiol Glutaredoxin 8 from Saccharomyces cerevisiae: The Catalytic Redox Mechanism Redux', *Biochemistry*, 48(6), pp. 1410-1423.

Eddins, M.J., Carlile, C.M., Gomez, K.M., Pickart, C.M. and Wolberger, C. (2006) 'Mms2-Ubc13 covalently bound to ubiquitin reveals the structural basis of linkage-specific polyubiquitin chain formation', *Nat Struct Mol Biol*, 13(10), pp. 915-20.

Edelmann, M.J. and Kessler, B.M. (2008) 'Ubiquitin and ubiquitin-like specific proteases targeted by infectious pathogens: Emerging patterns and molecular principles', *Biochimica et Biophysica Acta (BBA) - Molecular Basis of Disease*, 1782(12), pp. 809-816.

Ehrentraut, S.F., Curtis, V.F., Wang, R.X., Saeedi, B.J., Ehrentraut, H., Onyiah, J.C., Kelly, C.J., Campbell, E.L., Glover, L.E., Kominsky, D.J. and Colgan, S.P. (2016) 'Perturbation of neddylation-dependent NF-κB responses in the intestinal epithelium drives apoptosis and inhibits resolution of mucosal inflammation', *Molecular Biology of the Cell*, 27(23), pp. 3687-3694.

Eichhorn, P.J.A., Rodón, L., Gonzàlez-Juncà, A., Dirac, A., Gili, M., Martínez-Sáez, E., Aura, C., Barba, I., Peg, V., Prat, A., Cuartas, I., Jimenez, J., García-Dorado, D., Sahuquillo, J., Bernards, R., Baselga, J. and Seoane, J. (2012) 'USP15 stabilizes TGF-β receptor I and promotes oncogenesis through the activation of TGF-β signaling in glioblastoma', *Nature Medicine*, 18, p. 429.

Eletr, Z.M., Huang, D.T., Duda, D.M., Schulman, B.A. and Kuhlman, B. (2005) 'E2 conjugating enzymes must disengage from their E1 enzymes before E3-dependent ubiquitin and ubiquitin-like transfer', *Nature Structural &Amp; Molecular Biology*, 12, p. 933.

Erpapazoglou, Z., Dhaoui, M., Pantazopoulou, M., Giordano, F., Mari, M., Leon, S., Raposo, G., Reggiori, F. and Haguenauer-Tsapis, R. (2012) 'A dual role for K63-linked ubiquitin chains in multivesicular body biogenesis and cargo sorting', *Mol Biol Cell*, 23(11), pp. 2170-83.

Fan, L. and Xiao, W. (2016) 'The Pol30-K196 residue plays a critical role in budding yeast DNA postreplication repair through interaction with Rad18', *DNA Repair*, 47, pp. 42-48.

Fan, Y.H., Cheng, J., Vasudevan, S.A., Dou, J., Zhang, H., Patel, R.H., Ma, I.T., Rojas, Y., Zhao, Y., Yu, Y., Zhang, H., Shohet, J.M., Nuchtern, J.G., Kim, E.S. and Yang, J. (2013) 'USP7 inhibitor P22077 inhibits neuroblastoma growth via inducing p53-mediated apoptosis', *Cell Death Dis*, 4, p. e867.

Fang, J. and Beattie, D.S. (2003) 'External alternative NADH dehydrogenase of Saccharomyces cerevisiae: a potential source of superoxide', *Free Radic Biol Med*, 34(4), pp. 478-88.

Federoff N, (2006) 'Redox Regulatory Mechanisms in Cellular Stress Responses', *Ann Bot*, 98(2) pp. 289–300

Fernandes, A.P. and Holmgren, A. (2004) 'Glutaredoxins: glutathione-dependent redox enzymes with functions far beyond a simple thioredoxin backup system', *Antioxid Redox Signal*, 6(1), pp. 63-74.

Ferreira, J.V., Soares, A.R., Ramalho, J.S., Pereira, P. and Girao, H. (2015) 'K63 linked ubiquitin chain formation is a signal for HIF1A degradation by Chaperone-Mediated Autophagy', *Sci Rep*, 5, p. 10210.

Finkel, T. (2011) 'Signal transduction by reactive oxygen species', *The Journal of Cell Biology*, 194(1), pp. 7-15.

Finley, D., Bartel, B. and Varshavsky, A. (1989) 'The tails of ubiquitin precursors are ribosomal proteins whose fusion to ubiquitin facilitates ribosome biogenesis', *Nature*, 338, p. 394.

Finley, D., Ozkaynak, E. and Varshavsky, A. (1987) 'The yeast polyubiquitin gene is essential for resistance to high temperatures, starvation, and other stresses', *Cell*, 48(6), pp. 1035-46.

Finley, D., Ulrich, H.D., Sommer, T. and Kaiser, P. (2012) 'The Ubiquitin–Proteasome System of Saccharomyces cerevisiae', *Genetics*, 192(2), pp. 319-360.

Flattery-O'Brien, J.A. and Dawes, I.W. (1998) 'Hydrogen peroxide causes RAD9-dependent cell cycle arrest in G2 in Saccharomyces cerevisiae whereas menadione causes G1 arrest independent of RAD9 function', *J Biol Chem*, 273(15), pp. 8564-71.

Fleury, C., Mignotte, B. and Vayssière, J.-L. (2002) 'Mitochondrial reactive oxygen species in cell death signaling', *Biochimie*, 84(2), pp. 131-141.

Forman, H.J. and Torres, M. (2002) 'Reactive oxygen species and cell signaling: respiratory burst in macrophage signaling', *Am J Respir Crit Care Med*, 166(12 Pt 2), pp. S4-8.

Fridovich, I. (1986) 'Biological effects of the superoxide radical', *Archives of Biochemistry and Biophysics*, 247(1), pp. 1-11.

Fritz, S., Weinbach, N. and Westermann, B. (2003) 'Mdm30 Is an F-Box Protein Required for Maintenance of Fusion-competent Mitochondria in Yeast', *Molecular Biology of the Cell*, 14(6), pp. 2303-2313.

Fuchs, A.C.D., Maldoner, L., Wojtynek, M., Hartmann, M.D. and Martin, J. (2018) 'Rpn11-mediated ubiquitin processing in an ancestral archaeal ubiquitination system', *Nature Communications*, 9(1), p. 2696.

Fukai, T. and Ushio-Fukai, M. (2011) 'Superoxide Dismutases: Role in Redox Signaling, Vascular Function, and Diseases', *Antioxidants & Redox Signaling*, 15(6), pp. 1583-1606.

Fukui, M., Choi, H.J. and Zhu, B.T. (2012) 'Rapid generation of mitochondrial superoxide induces mitochondrion-dependent but caspase-independent cell death in hippocampal neuronal cells that morphologically resembles necroptosis()', *Toxicology and applied pharmacology*, 262(2), pp. 156-166.

Furukawa, Y., Torres, A.S. and O'Halloran, T.V. (2004) 'Oxygen-induced maturation of SOD1: a key role for disulfide formation by the copper chaperone CCS', *The EMBO Journal*, 23(14), pp. 2872-2881.

Gallego-Sanchez, A., Andres, S., Conde, F., San-Segundo, P.A. and Bueno, A. (2012) 'Reversal of PCNA ubiquitylation by Ubp10 in Saccharomyces cerevisiae', *PLoS Genet*, 8(7), p. e1002826.

Gallery, M., Blank, J.L., Lin, Y., Gutierrez, J.A., Pulido, J.C., Rappoli, D., Badola, S., Rolfe, M. and Macbeth, K.J. (2007) 'The JAMM motif of human deubiquitinase Poh1 is essential for cell viability', *Mol Cancer Ther*, 6(1), pp. 262-8.

García-Rodríguez, L.J., Gay, A.C. and Pon, L.A. (2007) 'Puf3p, a Pumilio family RNA binding protein, localizes to mitochondria and regulates mitochondrial biogenesis and motility in budding yeast', *The Journal of Cell Biology*, 176(2), pp. 197-207.

García-Ruiz, C., Colell, A., Morales, A., Kaplowitz, N. and Fernández-Checa, J.C. (1995) 'Role of oxidative stress generated from the mitochondrial electron transport chain and mitochondrial glutathione status in loss of mitochondrial function and activation of transcription factor nuclear factor-kappa B: studies with isolated mitochondria and rat hepatocytes', *Molecular Pharmacology*, 48(5), pp. 825-834.

Garrido, E.O. and Grant, C.M. (2002) 'Role of thioredoxins in the response of Saccharomyces cerevisiae to oxidative stress induced by hydroperoxides', *Mol Microbiol*, 43(4), pp. 993-1003.

Gasch, A.P., Spellman, P.T., Kao, C.M., Carmel-Harel, O., Eisen, M.B., Storz, G., Botstein, D. and Brown, P.O. (2000) 'Genomic Expression Programs in the Response of Yeast Cells to Environmental Changes', *Molecular Biology of the Cell*, 11(12), pp. 4241-4257.

Gemayel, R., Yang, Y., Dzialo, M.C., Kominek, J., Vowinckel, J., Saels, V., Van Huffel, L., van der Zande, E., Ralser, M., Steensels, J., Voordeckers, K. and Verstrepen, K.J. (2017) 'Variable repeats in the eukaryotic polyubiquitin gene ubi4 modulate proteostasis and stress survival', *Nature Communications*, 8(1), p. 397.

Gerber, A.P., Herschlag, D. and Brown, P.O. (2004) 'Extensive association of functionally and cytotopically related mRNAs with Puf family RNA-binding proteins in yeast', *PLoS Biol*, 2(3), p. E79.

Ghaemmaghami, S., Huh, W.-K., Bower, K., Howson, R.W., Belle, A., Dephoure, N., O'Shea, E.K. and Weissman, J.S. (2003a) 'Global analysis of protein expression in yeast', *Nature*, 425(6959), pp. 737-741.

Ghaemmaghami, S., Huh, W.K., Bower, K., Howson, R.W., Belle, A., Dephoure, N., O'Shea, E.K. and Weissman, J.S. (2003b) 'Global analysis of protein expression in yeast', *Nature*, 425(6959), pp. 737-41.

Giaever, G., Chu, A.M., Ni, L., Connelly, C., Riles, L., Veronneau, S., Dow, S., Lucau-Danila, A., Anderson, K., Andre, B., Arkin, A.P., Astromoff, A., El Bakkoury, M., Bangham, R., Benito, R., Brachat, S., Campanaro, S., Curtiss, M., Davis, K., Deutschbauer, A., Entian, K.-D., Flaherty, P., Foury, F., Garfinkel, D.J., Gerstein, M., Gotte, D., Guldener, U., Hegemann, J.H., Hempel, S., Herman, Z., Jaramillo, D.F., Kelly, D.E., Kelly, S.L., Kotter, P., LaBonte, D., Lamb, D.C., Lan, N., Liang, H., Liao, H., Liu, L., Luo, C., Lussier, M., Mao, R., Menard, P., Ooi, S.L., Revuelta, J.L., Roberts, C.J., Rose, M., Ross-Macdonald, P., Scherens, B., Schimmack, G., Shafer, B., Shoemaker, D.D., Sookhai-Mahadeo, S., Storms, R.K., Strathern, J.N., Valle, G., Voet, M., Volckaert, G., Wang, C.-y., Ward, T.R., Wilhelmy, J., Winzeler, E.A., Yang, Y., Yen, G., Youngman, E., Yu, K., Bussey, H., Boeke, J.D., Snyder, M., Philippsen, P., Davis, R.W. and Johnston, M. (2002) 'Functional profiling of the Saccharomyces cerevisiae genome', *Nature*, 418(6896), pp. 387-391.

Gloeckner, C.J., Boldt, K., Schumacher, A., Roepman, R. and Ueffing, M. (2007) 'A novel tandem affinity purification strategy for the efficient isolation and characterisation of native protein complexes', *Proteomics*, 7(23), pp. 4228-34.

Gödderz, D., Giovannucci, T.A., Laláková, J., Menéndez-Benito, V. and Dantuma, N.P. (2017) 'The deubiquitylating enzyme Ubp12 regulates Rad23-dependent proteasomal degradation', *Journal of Cell Science*, 130(19), pp. 3336-3346.

Goldknopf, I.L., French, M.F., Musso, R. and Busch, H. (1977) 'Presence of protein A24 in rat liver nucleosomes', *Proceedings of the National Academy of Sciences of the United States of America*, 74(12), pp. 5492-5495.

Gong, L., Kamitani, T., Millas, S. and Yeh, E.T. (2000) 'Identification of a novel isopeptidase with dual specificity for ubiquitin- and NEDD8-conjugated proteins', *J Biol Chem*, 275(19), pp. 14212-6.

Gong, X., Gutala, R. and Jaiswal, A.K. (2008) 'Quinone Oxidoreductases and Vitamin K Metabolism', in *Vitamins & Hormones*. Academic Press, pp. 85-101.

Grant, C.M. (2001) 'Role of the glutathione/glutaredoxin and thioredoxin systems in yeast growth and response to stress conditions', *Mol Microbiol*, 39(3), pp. 533-41.

Grant, C.M., Collinson, L.P., Roe, J.H. and Dawes, I.W. (1996a) 'Yeast glutathione reductase is required for protection against oxidative stress and is a target gene for yAP-1 transcriptional regulation', *Mol Microbiol*, 21(1), pp. 171-9.

Grant, C.M., MacIver, F.H. and Dawes, I.W. (1996b) 'Glutathione is an essential metabolite required for resistance to oxidative stress in the yeast Saccharomyces cerevisiae', *Curr Genet*, 29(6), pp. 511-5.

Grant, P.A., Duggan, L., Cote, J., Roberts, S.M., Brownell, J.E., Candau, R., Ohba, R., Owen-Hughes, T., Allis, C.D., Winston, F., Berger, S.L. and Workman, J.L. (1997) 'Yeast Gcn5 functions in two multisubunit complexes to acetylate nucleosomal histones: characterization of an Ada complex and the SAGA (Spt/Ada) complex', *Genes Dev*, 11(13), pp. 1640-50.

Greetham, D. and Grant, C.M. (2009) 'Antioxidant Activity of the Yeast Mitochondrial One-Cys Peroxiredoxin Is Dependent on Thioredoxin Reductase and Glutathione In Vivo', *Molecular and Cellular Biology*, 29(11), pp. 3229-3240.

Groen, E.J.N. and Gillingwater, T.H. (2015) 'UBA1: At the Crossroads of Ubiquitin Homeostasis and Neurodegeneration', *Trends in Molecular Medicine*, 21(10), pp. 622-632.

Grou, C.P., Pinto, M.P., Mendes, A.V., Domingues, P. and Azevedo, J.E. (2015) 'The de novo synthesis of ubiquitin: identification of deubiquitinases acting on ubiquitin precursors', *Sci Rep*, 5, p. 12836.

Guo, Y.-c., Zhang, S.-w. and Yuan, Q. (2018) 'Deubiquitinating Enzymes and Bone Remodeling', *Stem Cells International*, 2018, p. 3712083.

Gupta, V. and Carroll, K.S. (2014) 'Sulfenic acid chemistry, detection and cellular lifetime', *Biochimica et Biophysica Acta (BBA) - General Subjects*, 1840(2), pp. 847-875.

Guterman, A. and Glickman, M.H. (2004) 'Complementary roles for Rpn11 and Ubp6 in deubiquitination and proteolysis by the proteasome', *J Biol Chem*, 279(3), pp. 1729-38.

Guzzo, C.M. and Matunis, M.J. (2013) 'Expanding SUMO and ubiquitin-mediated signaling through hybrid SUMO-ubiquitin chains and their receptors', *Cell Cycle*, 12(7), pp. 1015-7.

Haas, A.L., Warms, J.V., Hershko, A. and Rose, I.A. (1982) 'Ubiquitin-activating enzyme. Mechanism and role in protein-ubiquitin conjugation', *Journal of Biological Chemistry*, 257(5), pp. 2543-2548.

Haglund, K., Sigismund, S., Polo, S., Szymkiewicz, I., Di Fiore, P.P. and Dikic, I. (2003) 'Multiple monoubiquitination of RTKs is sufficient for their endocytosis and degradation', *Nat Cell Biol*, 5(5), pp. 461-6.

Halliwell, B. (2006) 'Reactive species and antioxidants. Redox biology is a fundamental theme of aerobic life', *Plant Physiol*, 141(2), pp. 312-22.

Hancock, J., Desikan, R. and Neill, S. (2001) 'Role of reactive oxygen species in cell signalling pathways', *Biochemical Society Transactions*, 29(2), pp. 345-349.

Hancock, J.T. (2009) 'The Role of Redox Mechanisms in Cell Signalling', *Molecular Biotechnology*, 43(2), pp. 162-166.

Hanna, J., Hathaway, N.A., Tone, Y., Crosas, B., Elsasser, S., Kirkpatrick, D.S., Leggett, D.S., Gygi, S.P., King, R.W. and Finley, D. (2006) 'Deubiquitinating enzyme Ubp6 functions noncatalytically to delay proteasomal degradation', *Cell*, 127(1), pp. 99-111.

Hanpude, P., Bhattacharya, S., Dey, A.K. and Maiti, T.K. (2015) 'Deubiquitinating enzymes in cellular signaling and disease regulation', *IUBMB Life*, 67(7), pp. 544-555.

Hanschmann, E.-M., Godoy, J.R., Berndt, C., Hudemann, C. and Lillig, C.H. (2013) 'Thioredoxins, Glutaredoxins, and Peroxiredoxins—Molecular Mechanisms and Health Significance: from Cofactors to Antioxidants to Redox Signaling', *Antioxidants & Redox Signaling*, 19(13), pp. 1539-1605.

Hanway, D., Chin, J.K., Xia, G., Oshiro, G., Winzeler, E.A. and Romesberg, F.E. (2002) 'Previously uncharacterized genes in the UV- and MMS-induced DNA damage response in yeast', *Proc Natl Acad Sci U S A*, 99(16), pp. 10605-10.

Harman, D. (1956) 'Aging: a theory based on free radical and radiation chemistry', *J Gerontol*, 11(3), pp. 298-300.

Hay, R.T. (2005) 'SUMO: a history of modification', *Mol Cell*, 18(1), pp. 1-12.

He, M., Zhou, Z., Shah, A.A., Zou, H., Tao, J., Chen, Q. and Wan, Y. (2016) 'The emerging role of deubiquitinating enzymes in genomic integrity, diseases, and therapeutics', *Cell & Bioscience*, 6(1), p. 62.

Heideker, J. and Wertz, Ingrid E. (2015) 'DUBs, the regulation of cell identity and disease', *Biochemical Journal*, 465(1), p. 1.

Hendriks, I.A., D'Souza, R.C., Yang, B., Verlaan-de Vries, M., Mann, M. and Vertegaal, A.C. (2014) 'Uncovering global SUMOylation signaling networks in a site-specific manner', *Nat Struct Mol Biol*, 21(10), pp. 927-36.

Henry, K.W., Wyce, A., Lo, W.S., Duggan, L.J., Emre, N.C., Kao, C.F., Pillus, L., Shilatifard, A., Osley, M.A. and Berger, S.L. (2003) 'Transcriptional activation via sequential histone H2B ubiquitylation and deubiquitylation, mediated by SAGA-associated Ubp8', *Genes Dev*, 17(21), pp. 2648-63.

Heo, J.-M. and Rutter, J. (2011) 'Ubiquitin-dependent mitochondrial protein degradation', *The International Journal of Biochemistry & Cell Biology*, 43(10), pp. 1422-1426.

Heride, C., Urbé, S. and Clague, M.J. (2014) 'Ubiquitin code assembly and disassembly', *Current Biology*, 24(6), pp. R215-R220.

Hernandez-Lopez, M.J., Garcia-Marques, S., Randez-Gil, F. and Prieto, J.A. (2011) 'Multicopy suppression screening of Saccharomyces cerevisiae Identifies the ubiquitination machinery as a main target for improving growth at low temperatures', *Appl Environ Microbiol*, 77(21), pp. 7517-25.

Herrero, E., Ros, J., Bellí, G. and Cabiscol, E. (2008) 'Redox control and oxidative stress in yeast cells', *Biochimica et Biophysica Acta (BBA) - General Subjects*, 1780(11), pp. 1217-1235.

Hershko, A. and Ciechanover, A. (1998) 'The ubiquitin system', *Annu Rev Biochem*, 67, pp. 425-79.

Hicke, L. (2001) 'Protein regulation by monoubiquitin', *Nature Reviews Molecular Cell Biology*, 2, p. 195.

Hickey, C.M., Wilson, N.R. and Hochstrasser, M. (2012) 'Function and regulation of SUMO proteases', *Nat Rev Mol Cell Biol*, 13(12), pp. 755-66.

Hirst, J. (2013) 'Mitochondrial Complex I', *Annual Review of Biochemistry*, 82(1), pp. 551-575.

Hochstrasser, M. (2009) 'Origin and Function of Ubiquitin-like Protein Conjugation', *Nature*, 458(7237), p. 422.

Hoffman, C.S. and Winston, F. (1987) 'A ten-minute DNA preparation from yeast efficiently releases autonomous plasmids for transformation of Escherichia coli', *Gene*, 57(2-3), pp. 267-72.

Hoffman, S.M., Nolin, J.D., McMillan, D.H., Wouters, E.F.M., Janssen-Heininger, Y.M.W. and Reynaert, N.L. (2015) 'Thiol redox chemistry: role of protein cysteine oxidation and altered redox homeostasis in allergic inflammation and asthma', *Journal of cellular biochemistry*, 116(6), pp. 884-892.

Hoke, S.M.T., Genereaux, J., Liang, G. and Brandl, C.J. (2008) 'A Conserved Central Region of Yeast Ada2 Regulates the Histone Acetyltransferase Activity of Gcn5 and Interacts with Phospholipids', *Journal of Molecular Biology*, 384(4), pp. 743-755.

Hoppe, T. (2005) 'Multiubiquitylation by E4 enzymes: 'one size' doesn't fit all', *Trends in Biochemical Sciences*, 30(4), pp. 183-187.

Hu, M., Gu, L., Li, M., Jeffrey, P.D., Gu, W. and Shi, Y. (2006) 'Structural basis of competitive recognition of p53 and MDM2 by HAUSP/USP7: implications for the regulation of the p53-MDM2 pathway', *PLoS Biol*, 4(2), p. e27.

Hu, M., Li, P., Li, M., Li, W., Yao, T., Wu, J.W., Gu, W., Cohen, R.E. and Shi, Y. (2002) 'Crystal structure of a UBP-family deubiquitinating enzyme in isolation and in complex with ubiquitin aldehyde', *Cell*, 111(7), pp. 1041-54.

Hu, M., Li, P., Song, L., Jeffrey, P.D., Chenova, T.A., Wilkinson, K.D., Cohen, R.E. and Shi, Y. (2005) 'Structure and mechanisms of the proteasome-associated deubiquitinating enzyme USP14', *Embo j*, 24(21), pp. 3747-56.

Huang, W.-J., Zhang, X.I.A. and Chen, W.-W. (2016) 'Role of oxidative stress in Alzheimer's disease', *Biomedical Reports*, 4(5), pp. 519-522.

Huguenin-Dezot, N., De Cesare, V., Peltier, J., Knebel, A., Kristaryianto, Y.A., Rogerson, D.T., Kulathu, Y., Trost, M. and Chin, J.W. (2016) 'Synthesis of Isomeric Phosphoubiquitin Chains Reveals that Phosphorylation Controls Deubiquitinase Activity and Specificity', *Cell Rep*, 16(4), pp. 1180-1193.

Huseinovic, A., van Dijk, M., Vermeulen, N.P.E., van Leeuwen, F., Kooter, J.M. and Vos, J.C. (2018) 'Drug toxicity profiling of a Saccharomyces cerevisiae deubiquitinase deletion panel shows that acetaminophen mimics tyrosine', *Toxicology in Vitro*, 47, pp. 259-268.

Hwang, C., Sinskey, A.J. and Lodish, H.F. (1992) 'Oxidized redox state of glutathione in the endoplasmic reticulum', *Science*, 257(5076), pp. 1496-502.

Inoue, Y., Matsuda, T., Sugiyama, K., Izawa, S. and Kimura, A. (1999) 'Genetic analysis of glutathione peroxidase in oxidative stress response of Saccharomyces cerevisiae', *J Biol Chem*, 274(38), pp. 27002-9.

Iwai, K., Fujita, H. and Sasaki, Y. (2014) 'Linear ubiquitin chains: NF-κB signalling, cell death and beyond', *Nature Reviews Molecular Cell Biology*, 15, p. 503.

Izquierdo, A., Casas, C., Mühlenhoff, U., Lillig, C.H. and Herrero, E. (2008) 'Saccharomyces cerevisiae Grx6 and Grx7 Are Monothiol Glutaredoxins Associated with the Early Secretory Pathway', *Eukaryotic Cell*, 7(8), pp. 1415-1426.

Jackson, P.K., Eldridge, A.G., Freed, E., Furstenthal, L., Hsu, J.Y., Kaiser, B.K. and Reimann, J.D.R. (2000) 'The lore of the RINGs: substrate recognition and catalysis by ubiquitin ligases', *Trends in Cell Biology*, 10(10), pp. 429-439.

Jackson, Stephen P. and Durocher, D. (2013) 'Regulation of DNA Damage Responses by Ubiquitin and SUMO', *Molecular Cell*, 49(5), pp. 795-807.

Jadhav, T. and Wooten, M.W. (2009) 'Defining an Embedded Code for Protein Ubiquitination', *Journal of proteomics & bioinformatics*, 2, pp. 316-316.

Jalal, D., Chalissery, J. and Hassan, A.H. (2017) 'Genome maintenance in Saccharomyces cerevisiae: the role of SUMO and SUMO-targeted ubiquitin ligases', *Nucleic Acids Research*, 45(5), pp. 2242-2261.

Jang, H.H., Lee, K.O., Chi, Y.H., Jung, B.G., Park, S.K., Park, J.H., Lee, J.R., Lee, S.S., Moon, J.C., Yun, J.W., Choi, Y.O., Kim, W.Y., Kang, J.S., Cheong, G.-W., Yun, D.-J., Rhee, S.G., Cho, M.J. and Lee, S.Y. (2004) 'Two Enzymes in One: Two Yeast Peroxiredoxins Display Oxidative Stress-Dependent Switching from a Peroxidase to a Molecular Chaperone Function', *Cell*, 117(5), pp. 625-635.

Jastroch, M., Divakaruni, A.S., Mookerjee, S., Treberg, J.R. and Brand, M.D. (2010) 'Mitochondrial proton and electron leaks', *Essays Biochem*, 47, pp. 53-67.

Jena, N.R. (2012) 'DNA damage by reactive species: Mechanisms, mutation and repair', *J Biosci*, 37(3), pp. 503-17.

Jentsch, S., McGrath, J.P. and Varshavsky, A. (1987) 'The yeast DNA repair gene RAD6 encodes a ubiquitin-conjugating enzyme', *Nature*, 329(6135), pp. 131-4.

Jentsch, S. and Pyrowolakis, G. (2000) 'Ubiquitin and its kin: how close are the family ties?', *Trends in Cell Biology*, 10(8), pp. 335-342.

Jeong, W., Bae, S.H., Toledano, M.B. and Rhee, S.G. (2012) 'Role of sulfiredoxin as a regulator of peroxiredoxin function and regulation of its expression', *Free Radical Biology and Medicine*, 53(3), pp. 447-456.

Jin, J., Li, X., Gygi, S.P. and Harper, J.W. (2007) 'Dual E1 activation systems for ubiquitin differentially regulate E2 enzyme charging', *Nature*, 447, p. 1135.

Jin, X. (2017) 'A role of deubiquitinating enzyme Ubp3 in coping with oxidative stress', *The FASEB Journal*, 31(1 Supplement), p. 916.1.

Johnson, E.S. and Blobel, G. (1997) 'Ubc9p is the conjugating enzyme for the ubiquitin-like protein Smt3p', *J Biol Chem*, 272(43), pp. 26799-802.

Kaliszewski, P. and Zoladek, T. (2008) 'The role of Rsp5 ubiquitin ligase in regulation of diverse processes in yeast cells', *Acta Biochim Pol*, 55(4), pp. 649-62.

Kanga, S., Bernard, D., Mager-Heckel, A.M., Erpapazoglou, Z., Mattiroli, F., Sixma, T.K., Leon, S., Urban-Grimal, D., Tarassov, I. and Haguenauer-Tsapis, R. (2012) 'A deubiquitylating complex required for neosynthesis of a yeast mitochondrial ATP synthase subunit', *PLoS One*, 7(6), p. e38071.

Kehrer, J.P. (2000) 'The Haber–Weiss reaction and mechanisms of toxicity', *Toxicology*, 149(1), pp. 43-50.

Kerscher, O., Felberbaum, R. and Hochstrasser, M. (2006) 'Modification of Proteins by Ubiquitin and Ubiquitin-Like Proteins', *Annual Review of Cell and Developmental Biology*, 22(1), pp. 159-180.

Kim, G., Weiss, S.J. and Levine, R.L. (2014) 'Methionine Oxidation and Reduction in Proteins', *Biochimica et biophysica acta*, 1840(2), p. 10.1016/j.bbagen.2013.04.038.

Kim, G.H., Kim, J.E., Rhie, S.J. and Yoon, S. (2015) 'The Role of Oxidative Stress in Neurodegenerative Diseases', *Experimental Neurobiology*, 24(4), pp. 325-340.

Kim, R.Q., van Dijk, W.J. and Sixma, T.K. (2016) 'Structure of USP7 catalytic domain and three Ubl-domains reveals a connector α-helix with regulatory role', *Journal of Structural Biology*, 195(1), pp. 11-18.

Kinner, A. and Kolling, R. (2003) 'The yeast deubiquitinating enzyme Ubp16 is anchored to the outer mitochondrial membrane', *FEBS Lett*, 549(1-3), pp. 135-40.

Kirisako, T., Kamei, K., Murata, S., Kato, M., Fukumoto, H., Kanie, M., Sano, S., Tokunaga, F., Tanaka, K. and Iwai, K. (2006) 'A ubiquitin ligase complex assembles linear polyubiquitin chains', *Embo j*, 25(20), pp. 4877-87.

Kirkman, H.N. and Gaetani, G.F. (1984) 'Catalase: a tetrameric enzyme with four tightly bound molecules of NADPH', *Proc Natl Acad Sci U S A*, 81(14), pp. 4343-7.

Klebanoff, S.J. (2005) 'Myeloperoxidase: friend and foe', *Journal of Leukocyte Biology*, 77(5), pp. 598-625.

Klein, T., Viner, R.I. and Overall, C.M. (2016) 'Quantitative proteomics and terminomics to elucidate the role of ubiquitination and proteolysis in adaptive immunity', *Philosophical Transactions of the Royal Society A: Mathematical, Physical and Engineering Sciences*, 374(2079).

Klotz, L.O. and Steinbrenner, H. (2017) 'Cellular adaptation to xenobiotics: Interplay between xenosensors, reactive oxygen species and FOXO transcription factors', *Redox Biol*, 13, pp. 646-654.

Kobayashi, M., Oshima, S., Maeyashiki, C., Nibe, Y., Otsubo, K., Matsuzawa, Y., Nemoto, Y., Nagaishi, T., Okamoto, R., Tsuchiya, K., Nakamura, T. and Watanabe, M. (2016) 'The ubiquitin hybrid gene UBA52 regulates ubiquitination of ribosome and sustains embryonic development', *Scientific Reports*, 6, p. 36780.

Koc, A., Wheeler, L.J., Mathews, C.K. and Merrill, G.F. (2004) 'Hydroxyurea arrests DNA replication by a mechanism that preserves basal dNTP pools', *J Biol Chem*, 279(1), pp. 223-30.

Koegl, M., Hoppe, T., Schlenker, S., Ulrich, H.D., Mayer, T.U. and Jentsch, S. (1999) 'A Novel Ubiquitination Factor, E4, Is Involved in Multiubiquitin Chain Assembly', *Cell*, 96(5), pp. 635-644.

Kohen, R. and Nyska, A. (2002) 'Oxidation of Biological Systems: Oxidative Stress Phenomena, Antioxidants, Redox Reactions, and Methods for Their Quantification', *Toxicology Pathology*, 30(6), pp. 620 - 650.

Komander, D. (2009) 'The emerging complexity of protein ubiquitination', *Biochemical Society Transactions*, 37(5), p. 937.

Komander, D., Clague, M.J. and Urbe, S. (2009) 'Breaking the chains: structure and function of the deubiquitinases', *Nat Rev Mol Cell Biol*, 10(8), pp. 550-63.

Kouranti, I., McLean, J.R., Feoktistova, A., Liang, P., Johnson, A.E., Roberts-Galbraith, R.H. and Gould, K.L. (2010) 'A global census of fission yeast deubiquitinating enzyme localization and interaction networks reveals distinct compartmentalization profiles and overlapping functions in endocytosis and polarity', *PLoS biology*, 8(9), p. e1000471.

Kraft, C., Deplazes, A., Sohrmann, M. and Peter, M. (2008) 'Mature ribosomes are selectively degraded upon starvation by an autophagy pathway requiring the Ubp3p/Bre5p ubiquitin protease', *Nat Cell Biol*, 10(5), pp. 602-10.

Krek, W. (1998) 'Proteolysis and the G1-S transition: the SCF connection', *Current Opinion in Genetics & Development*, 8(1), pp. 36-42.

Kritsiligkou, P., Chatzi, A., Charalampous, G., Mironov, A., Jr., Grant, C.M. and Tokatlidis, K. (2017) 'Unconventional Targeting of a Thiol Peroxidase to the Mitochondrial Intermembrane Space Facilitates Oxidative Protein Folding', *Cell Rep*, 18(11), pp. 2729-2741.

Kroetz, M.B. (2005) 'SUMO: a ubiquitin-like protein modifier', *Yale J Biol Med*, 78(4), pp. 197-201.

Kruse, J.P. and Gu, W. (2009) 'MSL2 promotes Mdm2-independent cytoplasmic localization of p53', *J Biol Chem*, 284(5), pp. 3250-63.

Kulak, N.A., Pichler, G., Paron, I., Nagaraj, N. and Mann, M. (2014) 'Minimal, encapsulated proteomic-sample processing applied to copy-number estimation in eukaryotic cells', *Nat Methods*, 11(3), pp. 319-24.

Kulathu, Y., Garcia, F.J., Mevissen, T.E.T., Busch, M., Arnaudo, N., Carroll, K.S., Barford, D. and Komander, D. (2013) 'Regulation of A20 and other OTU deubiquitinases by reversible oxidation', *Nature communications*, 4, p. 1569.

Kulathu, Y. and Komander, D. (2012) 'Atypical ubiquitylation - the unexplored world of polyubiquitin beyond Lys48 and Lys63 linkages', *Nat Rev Mol Cell Biol*, 13(8), pp. 508-23.

Kumar, A., Wu, H., Collier-Hyams, L.S., Hansen, J.M., Li, T., Yamoah, K., Pan, Z.Q., Jones, D.P. and Neish, A.S. (2007) 'Commensal bacteria modulate cullin-dependent signaling via generation of reactive oxygen species', *Embo j*, 26(21), pp. 4457-66.

Lafont, E., Hartwig, T. and Walczak, H. (2018) 'Paving TRAIL's Path with Ubiquitin', *Trends Biochem Sci*, 43(1), pp. 44-60.

Lai, K.P., Cheung, A.H.Y. and Tse, W.K.F. (2017) 'Deubiquitinase Usp18 prevents cellular apoptosis from oxidative stress in liver cells', *Cell Biol Int*, 41(8), pp. 914-921.

Lam, M.H., Urban-Grimal, D., Bugnicourt, A., Greenblatt, J.F., Haguenauer-Tsapis, R. and Emili, A. (2009) 'Interaction of the deubiquitinating enzyme Ubp2 and the e3 ligase Rsp5 is required for transporter/receptor sorting in the multivesicular body pathway', *PLoS One*, 4(1), p. e4259.

Landry, William D. and Cotter, Thomas G. (2014) 'ROS signalling, NADPH oxidases and cancer', *Biochemical Society Transactions*, 42(4), p. 934.

Lassegue, B. and Griendling, K.K. (2010) 'NADPH oxidases: functions and pathologies in the vasculature', *Arterioscler Thromb Vasc Biol*, 30(4), pp. 653-61.

Laun, P., Pichova, A., Madeo, F., Fuchs, J., Ellinger, A., Kohlwein, S., Dawes, I., Frohlich, K.U. and Breitenbach, M. (2001) 'Aged mother cells of Saccharomyces cerevisiae show markers of oxidative stress and apoptosis', *Molecular Microbiology*, 39(5), pp. 1166-73.

Lecona, E., Rodriguez-Acebes, S., Specks, J., Lopez-Contreras, A.J., Ruppen, I., Murga, M., Munoz, J., Mendez, J. and Fernandez-Capetillo, O. (2016) 'USP7 is a SUMO deubiquitinase essential for DNA replication', *Nat Struct Mol Biol*, 23(4), pp. 270-7.

Lee, J.-G., Baek, K., Soetandyo, N. and Ye, Y. (2013) 'Reversible inactivation of deubiquitinases by reactive oxygen species in vitro and in cells', *Nature communications*, 4, p. 1568.

Lee, J., Godon, C., Lagniel, G., Spector, D., Garin, J., Labarre, J. and Toledano, M.B. (1999) 'Yap1 and Skn7 control two specialized oxidative stress response regulons in yeast', *J Biol Chem*, 274(23), pp. 16040-6.

Lemesle-Meunier, D., Brivet-Chevillotte, P., di Rago, J.P., Slonimski, P.P., Bruel, C., Tron, T. and Forget, N. (1993) 'Cytochrome b-deficient mutants of the ubiquinol-cytochrome c oxidoreductase in Saccharomyces cerevisiae. Consequence for the functional and structural characteristics of the complex', *J Biol Chem*, 268(21), pp. 15626-32.

Leroy, C., Mann, C. and Marsolier, M.-C. (2001) 'Silent repair accounts for cell cycle specificity in the signaling of oxidative DNA lesions', *The EMBO Journal*, 20(11), pp. 2896-2906.

Li, K., Ossareh-Nazari, B., Liu, X., Dargemont, C. and Marmorstein, R. (2007) 'Molecular basis for bre5 cofactor recognition by the ubp3 deubiquitylating enzyme', *J Mol Biol*, 372(1), pp. 194-204.

Li, W.-F., Yu, J., Ma, X.-X., Teng, Y.-B., Luo, M., Tang, Y.-J. and Zhou, C.-Z. (2010) 'Structural basis for the different activities of yeast Grx1 and Grx2', *Biochimica et Biophysica Acta (BBA) - Proteins and Proteomics*, 1804(7), pp. 1542-1547.

Liakopoulos, D., Doenges, G., Matuschewski, K. and Jentsch, S. (1998) 'A novel protein modification pathway related to the ubiquitin system', *Embo j*, 17(8), pp. 2208-14.

Lian, F.-M., Yu, J., Ma, X.-X., Yu, X.-J., Chen, Y. and Zhou, C.-Z. (2012) 'Structural Snapshots of Yeast Alkyl Hydroperoxide Reductase Ahp1 Peroxiredoxin Reveal a Novel Two-cysteine Mechanism of Electron Transfer to Eliminate Reactive Oxygen Species', *The Journal of Biological Chemistry*, 287(21), pp. 17077-17087.

Liang, Q., Dexheimer, T.S., Zhang, P., Rosenthal, A.S., Villamil, M.A., You, C., Zhang, Q., Chen, J., Ott, C.A., Sun, H., Luci, D.K., Yuan, B., Simeonov, A., Jadhav, A., Xiao, H., Wang, Y., Maloney, D.J. and Zhuang, Z. (2014) 'A selective USP1-UAF1 inhibitor links deubiquitination to DNA damage responses', *Nat Chem Biol*, 10(4), pp. 298-304.

Lill, R. (2009) 'Function and biogenesis of iron–sulphur proteins', *Nature*, 460, p. 831.

Linghu, B., Callis, J. and Goebl, M.G. (2002a) 'Rub1p processing by Yuh1p is required for wild-type levels of Rub1p conjugation to Cdc53p', *Eukaryot Cell*, 1(3), pp. 491-4.

Linghu, B., Callis, J. and Goebl, M.G. (2002b) 'Rub1p Processing by Yuh1p Is Required for Wild-Type Levels of Rub1p Conjugation to Cdc53p', *Eukaryotic Cell*, 1(3), pp. 491-494.

Liou, G.-Y. and Storz, P. (2010a) 'Reactive oxygen species in cancer', *Free radical research*, 44(5), p. 10.3109/10715761003667554.

Liou, G.Y. and Storz, P. (2010b) 'Reactive oxygen species in cancer', *Free Radic Res*, 44(5), pp. 479-96.

Liu, J. & Zhang, C. (2017) 'The equilibrium of ubiquitination and deubiquitination at PLK1 regulates sister chromatid separation', *Cellular and Molecular Life Sciences*, 74(12) pp. 2127-2134

Longo, V.D., Liou, L.-L., Valentine, J.S. and Gralla, E.B. (1999) 'Mitochondrial Superoxide Decreases Yeast Survival in Stationary Phase', *Archives of Biochemistry and Biophysics*, 365(1), pp. 131-142.

Longtine, M.S., McKenzie, A., 3rd, Demarini, D.J., Shah, N.G., Wach, A., Brachat, A., Philippsen, P. and Pringle, J.R. (1998) 'Additional modules for versatile and economical PCR-based gene deletion and modification in Saccharomyces cerevisiae', *Yeast*, 14(10), pp. 953-61.

Loor, G., Kondapalli, J., Schriewer, J.M., Chandel, N.S., Vanden Hoek, T.L. and Schumacker, P.T. (2010) 'Menadione triggers cell death through ROS-dependent mechanisms involving PARP activation without requiring apoptosis', *Free radical biology & medicine*, 49(12), pp. 1925-1936.

Lu, J. and Holmgren, A. (2014) 'The thioredoxin antioxidant system', *Free Radic Biol Med*, 66, pp. 75-87.

Lu, S.C. (2013) 'GLUTATHIONE SYNTHESIS', *Biochimica et biophysica acta*, 1830(5), pp. 3143-3153.

Luikenhuis, S., Perrone, G., Dawes, I.W. and Grant, C.M. (1998) 'The Yeast Saccharomyces cerevisiae Contains Two Glutaredoxin Genes That Are Required for Protection against Reactive Oxygen Species', *Molecular Biology of the Cell*, 9(5), pp. 1081-1091.

Luk, E., Yang, M., Jensen, L.T., Bourbonnais, Y. and Culotta, V.C. (2005) 'Manganese activation of superoxide dismutase 2 in the mitochondria of Saccharomyces cerevisiae', *J Biol Chem*, 280(24), pp. 22715-20.

Luque-Contreras, D., Carvajal, K., Toral-Rios, D., Franco-Bocanegra, D., Campos, P., xf and a, V. (2014) 'Oxidative Stress and Metabolic Syndrome: Cause or Consequence of Alzheimer's Disease?', *Oxidative Medicine and Cellular Longevity*, 2014, p. 11.

MacDiarmid, C.W., Taggart, J., Kerdsomboon, K., Kubisiak, M., Panascharoen, S., Schelble, K. and Eide, D.J. (2013) 'Peroxiredoxin Chaperone Activity Is Critical for Protein Homeostasis in Zinc-deficient Yeast', *The Journal of Biological Chemistry*, 288(43), pp. 31313-31327.

Magraoui, F.E., Reidick, C., Meyer, H.E. and Platta, H.W. (2015) 'Autophagy-Related Deubiquitinating Enzymes Involved in Health and Disease', *Cells*, 4(4), pp. 596-621.

Malo, M.E., Postnikoff, S.D.L., Arnason, T.G. and Harkness, T.A.A. (2016) 'Mitotic degradation of yeast Fkh1 by the Anaphase Promoting Complex is required for normal longevity, genomic stability and stress resistance', *Aging (Albany NY)*, 8(4), pp. 810-830.

Maniatis, T., Fritsch, E.F., Sambrook, J. and Engel, J. (1985) 'Molecular cloning–A laboratory manual. New York: Cold Spring Harbor Laboratory. 1982, 545 S., 42 $', *Acta Biotechnologica*, 5(1), pp. 104-104.

Mansour, M.A. (2018) 'Ubiquitination: Friend and foe in cancer', *Int J Biochem Cell Biol*, 101, pp. 80-93.

Mao, K. and Klionsky, D.J. (2013) 'Participation of mitochondrial fission during mitophagy', *Cell Cycle*, 12(19), pp. 3131-3132.

Marchenko, N.D., Wolff, S., Erster, S., Becker, K. and Moll, U.M. (2007) 'Monoubiquitylation promotes mitochondrial p53 translocation', *Embo j*, 26(4), pp. 923-34.

Marrot, L. and Meunier, J.-R. (2008) 'Skin DNA photodamage and its biological consequences', *Journal of the American Academy of Dermatology*, 58(5, Supplement 2), pp. S139-S148.

Martins, D. and English, A.M. (2014) 'Catalase activity is stimulated by H(2)O(2) in rich culture medium and is required for H(2)O(2) resistance and adaptation in yeast()', *Redox Biology*, 2, pp. 308-313.

Maupin-Furlow, J.A. (2014) 'Prokaryotic Ubiquitin-Like Protein Modification', *Annual review of microbiology*, 68, pp. 155-175.

Maytal-Kivity, V., Reis, N., Hofmann, K. and Glickman, M.H. (2002) 'MPN+, a putative catalytic motif found in a subset of MPN domain proteins from eukaryotes and prokaryotes, is critical for Rpn11 function', *BMC Biochem*, 3, p. 28.

McClurg, U.L. and Robson, C.N. (2015) 'Deubiquitinating enzymes as oncotargets', *Oncotarget*, 6(12), pp. 9657-68.

McDowell, G.S. and Philpott, A. (2013) 'Non-canonical ubiquitylation: Mechanisms and consequences', *The International Journal of Biochemistry & Cell Biology*, 45(8), pp. 1833-1842.

McGrath, J.P., Jentsch, S. and Varshavsky, A. (1991) 'UBA 1: an essential yeast gene encoding ubiquitin-activating enzyme', *The EMBO Journal*, 10(1), pp. 227-236.

Meek, D.W. (2015) 'Regulation of the p53 response and its relationship to cancer', *Biochem J*, 469(3), pp. 325-46.

Melchior, F. (2000) 'SUMO—Nonclassical Ubiquitin', *Annual Review of Cell and Developmental Biology*, 16(1), pp. 591-626.

Melov, S., Adlard, P.A., Morten, K., Johnson, F., Golden, T.R., Hinerfeld, D., Schilling, B., Mavros, C., Masters, C.L., Volitakis, I., Li, Q.-X., Laughton, K., Hubbard, A., Cherny, R.A., Gibson, B. and Bush, A.I. (2007) 'Mitochondrial

Oxidative Stress Causes Hyperphosphorylation of Tau', *PLoS ONE*, 2(6), p. e536.

Melov, S., Ravenscroft, J., Malik, S., Gill, M.S., Walker, D.W., Clayton, P.E., Wallace, D.C., Malfroy, B., Doctrow, S.R. and Lithgow, G.J. (2000) 'Extension of life-span with superoxide dismutase/catalase mimetics', *Science*, 289(5484), pp. 1567-9.

Messick, T.E., Russell, N.S., Iwata, A.J., Sarachan, K.L., Shiekhattar, R., Shanks, J.R., Reyes-Turcu, F.E., Wilkinson, K.D. and Marmorstein, R. (2008) 'Structural basis for ubiquitin recognition by the Otu1 ovarian tumor domain protein', *J Biol Chem*, 283(16), pp. 11038-49.

Mevissen, T.E.T. and Komander, D. (2017) 'Mechanisms of Deubiquitinase Specificity and Regulation', *Annual Review of Biochemistry*, 86(1), pp. 159-192.

Miotto, B., Marchal, C., Adelmant, G., Guinot, N., Xie, P., Marto, J.A., Zhang, L. and Defossez, P.-A. (2018) 'Stabilization of the methyl-CpG binding protein ZBTB38 by the deubiquitinase USP9X limits the occurrence and toxicity of oxidative stress in human cells', *Nucleic Acids Research*, 46(9), pp. 4392-4404.

Moazed, D. and Johnson, D. (1996) 'A deubiquitinating enzyme interacts with SIR4 and regulates silencing in S. cerevisiae', *Cell*, 86(4), pp. 667-77.

Mocciaro, A. and Rape, M. (2012) 'Emerging regulatory mechanisms in ubiquitin-dependent cell cycle control', *J Cell Sci*, 125(Pt 2), pp. 255-63.

Morano, K.A., Grant, C.M. and Moye-Rowley, W.S. (2012) 'The Response to Heat Shock and Oxidative Stress in Saccharomyces cerevisiae', *Genetics*, 190(4), pp. 1157-1195.

Morgan, B.A., Banks, G.R., Toone, W.M., Raitt, D., Kuge, S. and Johnston, L.H. (1997) 'The Skn7 response regulator controls gene expression in the oxidative stress response of the budding yeast Saccharomyces cerevisiae', *The EMBO Journal*, 16(5), pp. 1035-1044.

Morgan, M.T., Haj-Yahya, M., Ringel, A.E., Bandi, P., Brik, A. and Wolberger, C. (2016) 'Structural basis for histone H2B deubiquitination by the SAGA DUB module', *Science (New York, N.Y.)*, 351(6274), pp. 725-728.

Morillon, A., O'Sullivan, J., Azad, A., Proudfoot, N. and Mellor, J. (2003) 'Regulation of elongating RNA polymerase II by forkhead transcription factors in yeast', *Science*, 300(5618), pp. 492-5.

Moye-Rowley, W.S., Harshman, K.D. and Parker, C.S. (1989) 'Yeast YAP1 encodes a novel form of the jun family of transcriptional activator proteins', *Genes Dev*, 3(3), pp. 283-92.

Muid, K.A., Karakaya, H.Ç. and Koc, A. (2014) 'Absence of superoxide dismutase activity causes nuclear DNA fragmentation during the aging process', *Biochemical and Biophysical Research Communications*, 444(2), pp. 260-263.

Mulford, K.E. and Fassler, J.S. (2011) 'Association of the Skn7 and Yap1 Transcription Factors in the Saccharomyces cerevisiae Oxidative Stress Response', *Eukaryotic Cell*, 10(6), pp. 761-769.

Müller, M., Kötter, P., Behrendt, C., Walter, E., Scheckhuber, C.Q., Entian, K.-D. and Reichert, A.S. (2015) 'Synthetic quantitative array technology identifies the

Ubp3-Bre5 deubiquitinase complex as a negative regulator of mitophagy', *Cell reports*, 10(7), pp. 1215-1225.

Müller, M. and Reichert, Andreas S. (2011) 'Mitophagy, mitochondrial dynamics and the general stress response in yeast', *Biochemical Society Transactions*, 39(5), pp. 1514-1519.

Muller, P.A. and Vousden, K.H. (2013) 'p53 mutations in cancer', *Nat Cell Biol*, 15(1), pp. 2-8.

Murphy, Michael P. (2009) 'How mitochondria produce reactive oxygen species', *Biochemical Journal*, 417(Pt 1), pp. 1-13.

Murphy, R. and DeCoursey, T.E. (2006) 'Charge compensation during the phagocyte respiratory burst', *Biochimica et Biophysica Acta (BBA) - Bioenergetics*, 1757(8), pp. 996-1011.

Nagai, H., Noguchi, T., Homma, K., Katagiri, K., Takeda, K., Matsuzawa, A. and Ichijo, H. (2009) 'Ubiquitin-like Sequence in ASK1 Plays Critical Roles in the Recognition and Stabilization by USP9X and Oxidative Stress-Induced Cell Death', *Molecular Cell*, 36(5), pp. 805-818.

Nagai, M. and Ushimaru, T. (2014) 'Cdh1 is an antagonist of the spindle assembly checkpoint', *Cellular Signalling*, 26(10), pp. 2217-2222.

Nanao, M.H., Tcherniuk, S.O., Chroboczek, J., Dideberg, O., Dessen, A. and Balakirev, M.Y. (2004) 'Crystal structure of human otubain 2', *EMBO Rep*, 5(8), pp. 783-8.

Nayak, A. and Müller, S. (2014) 'SUMO-specific proteases/isopeptidases: SENPs and beyond', *Genome Biology*, 15(7), p. 422.

Nguyen, V.-N., Huang, K.-Y., Huang, C.-H., Chang, T.-H., Bretaña, N.A., Lai, K.R., Weng, J.T.-Y. and Lee, T.-Y. (2015) 'Characterization and identification of ubiquitin conjugation sites with E3 ligase recognition specificities', *BMC Bioinformatics*, 16(Suppl 1), pp. S1-S1.

Nickel, A., Kohlhaas, M. and Maack, C. (2014) 'Mitochondrial reactive oxygen species production and elimination', *Journal of Molecular and Cellular Cardiology*, 73, pp. 26-33.

Nijman, S.M.B., Luna-Vargas, M.P.A., Velds, A., Brummelkamp, T.R., Dirac, A.M.G., Sixma, T.K. and Bernards, R. (2005) 'A Genomic and Functional Inventory of Deubiquitinating Enzymes', *Cell*, 123(5), pp. 773-786.

Nikko, E. and Andre, B. (2007) 'Evidence for a direct role of the Doa4 deubiquitinating enzyme in protein sorting into the MVB pathway', *Traffic*, 8(5), pp. 566-81.

Nostramo, R., Varia, S.N., Zhang, B., Emerson, M.M. and Herman, P.K. (2016) 'The Catalytic Activity of the Ubp3 Deubiquitinating Protease Is Required for Efficient Stress Granule Assembly in Saccharomyces cerevisiae', *Molecular and Cellular Biology*, 36(1), pp. 173-183.

Nozawa, K., Ishitani, R., Yoshihisa, T., Sato, M., Arisaka, F., Kanamaru, S., Dohmae, N., Mangroo, D., Senger, B., Becker, H.D. and Nureki, O. (2013) 'Crystal structure of Cex1p reveals the mechanism of tRNA trafficking between nucleus and cytoplasm', *Nucleic Acids Res*, 41(6), pp. 3901-14.

O'Callaghan, P. (2004) *The regulation of the cell division cycle of Saccharomyces cerevisiae by the oxidative stress response*. Newcastle University.

Ohdate, T., Kita, K. and Inoue, Y. (2010) 'Kinetics and redox regulation of Gpx1, an atypical 2-Cys peroxiredoxin, in Saccharomyces cerevisiae', *FEMS Yeast Res*, 10(6), pp. 787-90.

Ohtake, Y. and Yabuuchi, S. (1991) 'Molecular cloning of the gamma-glutamylcysteine synthetase gene of Saccharomyces cerevisiae', *Yeast*, 7(9), pp. 953-61.

Okatsu, K., Koyano, F., Kimura, M., Kosako, H., Saeki, Y., Tanaka, K. and Matsuda, N. (2015) 'Phosphorylated ubiquitin chain is the genuine Parkin receptor', *J Cell Biol*, 209(1), pp. 111-28.

Oldenburg, K.R., Vo, K.T., Michaelis, S. and Paddon, C. (1997) 'Recombination-mediated PCR-directed plasmid construction in vivo in yeast', *Nucleic Acids Research*, 25(2), pp. 451-452.

Oliveira, A.M., Perez-Atayde, A.R., Dal Cin, P., Gebhardt, M.C., Chen, C.J., Neff, J.R., Demetri, G.D., Rosenberg, A.E., Bridge, J.A. and Fletcher, J.A. (2005) 'Aneurysmal bone cyst variant translocations upregulate USP6 transcription by promoter swapping with the ZNF9, COL1A1, TRAP150, and OMD genes', *Oncogene*, 24(21), pp. 3419-26.

Ordureau, A., Heo, J.M., Duda, D.M., Paulo, J.A., Olszewski, J.L., Yanishevski, D., Rinehart, J., Schulman, B.A. and Harper, J.W. (2015) 'Defining roles of PARKIN and ubiquitin phosphorylation by PINK1 in mitochondrial quality control using a ubiquitin replacement strategy', *Proc Natl Acad Sci U S A*, 112(21), pp. 6637-42.

Ostapenko, D., Burton, J.L. and Solomon, M.J. (2015) 'The Ubp15 deubiquitinase promotes timely entry into S phase in Saccharomyces cerevisiae', *Molecular Biology of the Cell*, 26(12), pp. 2205-2216.

Otomo, C., Metlagel, Z., Takaesu, G. and Otomo, T. (2013) 'Structure of the human ATG12~ATG5 conjugate required for LC3 lipidation in autophagy', *Nat Struct Mol Biol*, 20(1), pp. 59-66.

Ozkaynak, E., Finley, D., Solomon, M.J. and Varshavsky, A. (1987) 'The yeast ubiquitin genes: a family of natural gene fusions', *Embo j*, 6(5), pp. 1429-39.

Padmanabhan, A., Candelaria, N., Wong, K.K., Nikolai, B.C., Lonard, D.M., O'Malley, B.W. and Richards, J.S. (2018) 'USP15-dependent lysosomal pathway controls p53-R175H turnover in ovarian cancer cells', *Nat Commun*, 9(1), p. 1270.

Pal, A., Young, M.A. and Donato, N.J. (2014) 'Emerging Potential of Therapeutic Targeting of Ubiquitin-Specific Proteases in the Treatment of Cancer', *Cancer Research*, 74(18), p. 4955.

Palm-Espling, M.E., Niemiec, M.S. and Wittung-Stafshede, P. (2012) 'Role of metal in folding and stability of copper proteins in vitro', *Biochimica et Biophysica Acta (BBA) - Molecular Cell Research*, 1823(9), pp. 1594-1603.

Paula, O.A. and Uwe, S. (2012) 'The importance of post-translational modifications in regulating Saccharomyces cerevisiae metabolism', *FEMS Yeast Research*, 12(2), pp. 104-117.

Peck, S.C. (2006) 'Analysis of protein phosphorylation: methods and strategies for studying kinases and substrates', *Plant J*, 45(4), pp. 512-22.

Pedrajas, J.R., Kosmidou, E., Miranda-Vizuete, A., Gustafsson, J.A., Wright, A.P. and Spyrou, G. (1999) 'Identification and functional characterization of a novel mitochondrial thioredoxin system in Saccharomyces cerevisiae', *J Biol Chem*, 274(10), pp. 6366-73.

Petroski, M.D. and Deshaies, R.J. (2005) 'Function and regulation of cullin–RING ubiquitin ligases', *Nature Reviews Molecular Cell Biology*, 6, p. 9.

Phaniendra, A., Jestadi, D.B. and Periyasamy, L. (2015) 'Free Radicals: Properties, Sources, Targets, and Their Implication in Various Diseases', *Indian Journal of Clinical Biochemistry*, 30(1), pp. 11-26.

Platta, H.W., Grunau, S., Rosenkranz, K., Girzalsky, W. and Erdmann, R. (2005) 'Functional role of the AAA peroxins in dislocation of the cycling PTS1 receptor back to the cytosol', *Nat Cell Biol*, 7(8), pp. 817-22.

Poole, L.B. (2015) 'The Basics of Thiols and Cysteines in Redox Biology and Chemistry', *Free radical biology & medicine*, 0, pp. 148-157.

Pujol-Carrion, N., Belli, G., Herrero, E., Nogues, A. and de la Torre-Ruiz, M.A. (2006) 'Glutaredoxins Grx3 and Grx4 regulate nuclear localisation of Aft1 and the oxidative stress response in Saccharomyces cerevisiae', *J Cell Sci*, 119(Pt 21), pp. 4554-64.

Pujol-Carrion, N. and de la Torre-Ruiz, M.A. (2010) 'Glutaredoxins Grx4 and Grx3 of Saccharomyces cerevisiae play a role in actin dynamics through their Trx domains, which contributes to oxidative stress resistance', *Appl Environ Microbiol*, 76(23), pp. 7826-35.

Qiao, X., Zhang, L., Gamper, A.M., Fujita, T. and Wan, Y. (2010) 'APC/C-Cdh1: From cell cycle to cellular differentiation and genomic integrity', *Cell Cycle*, 9(19), pp. 3904-3912.

Quinn, J., Findlay, V.J., Dawson, K., Millar, J.B.A., Jones, N., Morgan, B.A. and Toone, W.M. (2002) 'Distinct Regulatory Proteins Control the Graded Transcriptional Response to Increasing H(2)O(2) Levels in Fission Yeast Schizosaccharomyces pombe', *Molecular Biology of the Cell*, 13(3), pp. 805-816.

Ragu, S., Dardalhon, M., Sharma, S., Iraqui, I., Buhagiar-Labarchède, G., Grondin, V., Kienda, G., Vernis, L., Chanet, R., Kolodner, R.D., Huang, M.-E. and Faye, G. (2014) 'Loss of the Thioredoxin Reductase Trr1 Suppresses the Genomic Instability of Peroxiredoxin tsa1 Mutants', *PLoS ONE*, 9(9), p. e108123.

Raitt, D.C., Johnson, A.L., Erkine, A.M., Makino, K., Morgan, B., Gross, D.S. and Johnston, L.H. (2000) 'The Skn7 Response Regulator of Saccharomyces cerevisiae Interacts with Hsf1 In Vivo and Is Required for the Induction of Heat Shock Genes by Oxidative Stress', *Molecular Biology of the Cell*, 11(7), pp. 2335-2347.

Rattanawong, K., Kerdsomboon, K. and Auesukaree, C. (2015) 'Cu/Zn-superoxide dismutase and glutathione are involved in response to oxidative stress induced by protein denaturing effect of alachlor in Saccharomyces cerevisiae', *Free Radical Biology and Medicine*, 89, pp. 963-971.

Ray, P.D., Huang, B.-W. and Tsuji, Y. (2012) 'Reactive oxygen species (ROS) homeostasis and redox regulation in cellular signaling', *Cellular signalling*, 24(5), pp. 981-990.

Refsgaard, H.H.F., Tsai, L. and Stadtman, E.R. (2000) 'Modifications of proteins by polyunsaturated fatty acid peroxidation products', *Proceedings of the National Academy of Sciences of the United States of America*, 97(2), pp. 611-616.

Rehder, D.S. and Borges, C.R. (2010) 'Cysteine sulfenic acid as an intermediate in disulfide bond formation and non-enzymatic protein folding', *Biochemistry*, 49(35), pp. 7748-7755.

Reyes-Turcu, F.E., Horton, J.R., Mullally, J.E., Heroux, A., Cheng, X. and Wilkinson, K.D. (2006) 'The ubiquitin binding domain ZnF UBP recognizes the C-terminal diglycine motif of unanchored ubiquitin', *Cell*, 124(6), pp. 1197-208.

Rhee, S.G., Kang, S.W., Jeong, W., Chang, T.-S., Yang, K.-S. and Woo, H.A. (2005) 'Intracellular messenger function of hydrogen peroxide and its regulation by peroxiredoxins', *Current Opinion in Cell Biology*, 17(2), pp. 183-189.

Richardson, L.A., Reed, B.J., Charette, J.M., Freed, E.F., Fredrickson, E.K., Locke, M.N., Baserga, S.J. and Gardner, R.G. (2012) 'A conserved deubiquitinating enzyme controls cell growth by regulating RNA polymerase I stability', *Cell Rep*, 2(2), pp. 372-85.

Richter, C., Park, J.W. and Ames, B.N. (1988) 'Normal oxidative damage to mitochondrial and nuclear DNA is extensive', *Proc Natl Acad Sci U S A*, 85(17), pp. 6465-7.

Ristow, M. and Schmeisser, K. (2014) 'Mitohormesis: Promoting Health and Lifespan by Increased Levels of Reactive Oxygen Species (ROS)', *Dose-Response*, 12(2), pp. 288-341.

Robzyk, K., Recht, J. and Osley, M.A. (2000) 'Rad6-dependent ubiquitination of histone H2B in yeast', *Science*, 287(5452), pp. 501-4.

Rodrigo-Brenni, M.C. and Morgan, D.O. (2007) 'Sequential E2s drive polyubiquitin chain assembly on APC targets', *Cell*, 130(1), pp. 127-39.

Rodrigo-Moreno, A., Poschenrieder, C. and Shabala, S. (2013) 'Transition metals: A double edge sward in ROS generation and signaling', *Plant Signaling & Behavior*, 8(3), p. e23425.

Rodrigues-Pousada, C.A., Nevitt, T., Menezes, R., Azevedo, D., Pereira, J. and Amaral, C. (2004) 'Yeast activator proteins and stress response: an overview', *FEBS Lett*, 567(1), pp. 80-5.

Rodríguez-Manzaneque, M.T., Ros, J., Cabiscol, E., Sorribas, A. and Herrero, E. (1999) 'Grx5 Glutaredoxin Plays a Central Role in Protection against Protein Oxidative Damage in Saccharomyces cerevisiae', *Molecular and Cellular Biology*, 19(12), pp. 8180-8190.

Rodriguez-Manzaneque, M.T., Tamarit, J., Belli, G., Ros, J. and Herrero, E. (2002) 'Grx5 is a mitochondrial glutaredoxin required for the activity of iron/sulfur enzymes', *Mol Biol Cell*, 13(4), pp. 1109-21.

Rodriguez, M.S., Gwizdek, C., Haguenauer-Tsapis, R. and Dargemont, C. (2003) 'The HECT ubiquitin ligase Rsp5p is required for proper nuclear export of mRNA in Saccharomyces cerevisiae', *Traffic*, 4(8), pp. 566-75.

Rona, G., Herdeiro, R., Mathias, C.J., Torres, F.A., Pereira, M.D. and Eleutherio, E. (2015) 'CTT1 overexpression increases life span of calorie-restricted Saccharomyces cerevisiae deficient in Sod1', *Biogerontology*, 16(3), pp. 343-351.

Ronau, J.A., Beckmann, J.F. and Hochstrasser, M. (2016) 'Substrate specificity of the ubiquitin and Ubl proteases', *Cell Res*, 26(4), pp. 441-56.

Rosser, M.F., Washburn, E., Muchowski, P.J., Patterson, C. and Cyr, D.M. (2007) 'Chaperone functions of the E3 ubiquitin ligase CHIP', *J Biol Chem*, 282(31), pp. 22267-77.

Rothstein, R. (1991) 'Targeting, disruption, replacement, and allele rescue: integrative DNA transformation in yeast', *Methods Enzymol*, 194, pp. 281-301.

Rotin, D. and Kumar, S. (2009) 'Physiological functions of the HECT family of ubiquitin ligases', *Nature Reviews Molecular Cell Biology*, 10, p. 398.

Rouault, T.A. and Tong, W.-H. (2005) 'Iron–sulphur cluster biogenesis and mitochondrial iron homeostasis', *Nature Reviews Molecular Cell Biology*, 6(4), pp. 345-351.

Rudyk, O. and Eaton, P. (2014) 'Biochemical methods for monitoring protein thiol redox states in biological systems', *Redox Biology*, 2, pp. 803-813.

Rytkonen, A. and Holden, D.W. (2007) 'Bacterial interference of ubiquitination and deubiquitination', *Cell Host Microbe*, 1(1), pp. 13-22.

Sadowski, M., Suryadinata, R., Tan, A.R., Roesley, S.N.A. and Sarcevic, B. (2011) 'Protein monoubiquitination and polyubiquitination generate structural diversity to control distinct biological processes', *IUBMB Life*, 64(2), pp. 136-142.

Sahtoe, D.D. and Sixma, T.K. (2015) 'Layers of DUB regulation', *Trends in Biochemical Sciences*, 40(8), pp. 456-467.

Saiz-Baggetto, S., Méndez, E., Quilis, I., Igual, J.C. and Bañó, M.C. (2017) 'Chimeric proteins tagged with specific 3xHA cassettes may present instability and functional problems', *PLoS ONE*, 12(8), p. e0183067.

Salazar G, Falcon-Perez JM, Harrison R, Faundez V, (2009) 'SLC30A3 (ZnT3) oligomerization by dityrosine bonds regulates its subcellular localization and metal transport capacity', *PLoS One*, 4(6) e5896

Salmeen, A., Andersen, J.N., Myers, M.P., Meng, T.-C., Hinks, J.A., Tonks, N.K. and Barford, D. (2003) 'Redox regulation of protein tyrosine phosphatase 1B involves a sulphenyl-amide intermediate', *Nature*, 423, p. 769.

Samoilova, R.I., Crofts, A.R. and Dikanov, S.A. (2011) 'Reaction of superoxide radical with quinone molecules', *J Phys Chem A*, 115(42), pp. 11589-93.

Santos, A.L. and Lindner, A.B. (2017) 'Protein Posttranslational Modifications: Roles in Aging and Age-Related Disease', *Oxid Med Cell Longev*, 2017, p. 5716409.

Sasaki, Y., Sano, S., Nakahara, M., Murata, S., Kometani, K., Aiba, Y., Sakamoto, S., Watanabe, Y., Tanaka, K., Kurosaki, T. and Iwai, K. (2013) 'Defective immune responses in mice lacking LUBAC-mediated linear ubiquitination in B cells', *Embo j*, 32(18), pp. 2463-76.

Schaar, C.E., Dues, D.J., Spielbauer, K.K., Machiela, E., Cooper, J.F., Senchuk, M., Hekimi, S. and Van Raamsdonk, J.M. (2015) 'Mitochondrial and cytoplasmic ROS have opposing effects on lifespan', *PLoS Genet*, 11(2), p. e1004972.

Schaefer, J.B. and Morgan, D.O. (2011) 'Protein-linked ubiquitin chain structure restricts activity of deubiquitinating enzymes', *J Biol Chem*, 286(52), pp. 45186-96.

Schiestl, R.H. and Gietz, R.D. (1989) 'High efficiency transformation of intact yeast cells using single stranded nucleic acids as a carrier', *Curr Genet*, 16(5-6), pp. 339-46.

Schmitz, C., Kinner, A. and Kolling, R. (2005) 'The deubiquitinating enzyme Ubp1 affects sorting of the ATP-binding cassette-transporter Ste6 in the endocytic pathway', *Mol Biol Cell*, 16(3), pp. 1319-29.

Schrader, M. and Fahimi, H.D. (2006) 'Peroxisomes and oxidative stress', *Biochimica et Biophysica Acta (BBA) - Molecular Cell Research*, 1763(12), pp. 1755-1766.

Schulman, B.A. and Harper, J.W. (2009) 'Ubiquitin-like protein activation by E1 enzymes: the apex for downstream signalling pathways', *Nature reviews. Molecular cell biology*, 10(5), pp. 319-331.

Schulze, J.M., Hentrich, T., Nakanishi, S., Gupta, A., Emberly, E., Shilatifard, A. and Kobor, M.S. (2011) 'Splitting the task: Ubp8 and Ubp10 deubiquitinate different cellular pools of H2BK123', *Genes Dev*, 25(21), pp. 2242-7.

Schwertassek, U., Haque, A., Krishnan, N., Greiner, R., Weingarten, L., Dick, T.P. and Tonks, N.K. (2014) 'Reactivation of oxidized PTP1B and PTEN by thioredoxin 1', *Febs j*, 281(16), pp. 3545-58.

Schwob, E., Bohm, T., Mendenhall, M.D. and Nasmyth, K. (1994) 'The B-type cyclin kinase inhibitor p40SIC1 controls the G1 to S transition in S. cerevisiae', *Cell*, 79(2), pp. 233-44.

Seo, M.S., Kang, S.W., Kim, K., Baines, I.C., Lee, T.H. and Rhee, S.G. (2000) 'Identification of a new type of mammalian peroxiredoxin that forms an intramolecular disulfide as a reaction intermediate', *J Biol Chem*, 275(27), pp. 20346-54.

Seol, J.H., Feldman, R.M., Zachariae, W., Shevchenko, A., Correll, C.C., Lyapina, S., Chi, Y., Galova, M., Claypool, J., Sandmeyer, S., Nasmyth, K., Deshaies, R.J., Shevchenko, A. and Deshaies, R.J. (1999) 'Cdc53/cullin and the essential Hrt1 RING-H2 subunit of SCF define a ubiquitin ligase module that activates the E2 enzyme Cdc34', *Genes Dev*, 13(12), pp. 1614-26.

Seth, D. and Rudolph, J. (2006) 'Redox control of cell cycle progression via Cdc25 phosphatase (Mih1p) in S. cerevisiae', *Cell Cycle*, 5(18), pp. 2172-3.

Shackelford, R.E., Kaufmann, W.K. and Paules, R.S. (2000) 'Oxidative stress and cell cycle checkpoint function', *Free Radical Biology and Medicine*, 28(9), pp. 1387-1404.

Sheng, Y., Saridakis, V., Sarkari, F., Duan, S., Wu, T., Arrowsmith, C.H. and Frappier, L. (2006) 'Molecular recognition of p53 and MDM2 by USP7/HAUSP', *Nature Structural &Amp; Molecular Biology*, 13, p. 285.

Shenton, D. and Grant, C.M. (2003) 'Protein S-thiolation targets glycolysis and protein synthesis in response to oxidative stress in the yeast Saccharomyces cerevisiae', *Biochemical Journal*, 374(Pt 2), pp. 513-519.

Shrestha, R.K., Ronau, J.A., Davies, C.W., Guenette, R.G., Strieter, E.R., Paul, L.N. and Das, C. (2014) 'Insights into the mechanism of deubiquitination by JAMM deubiquitinases from cocrystal structures of the enzyme with the substrate and product', *Biochemistry*, 53(19), pp. 3199-217.

Silva, G.M., Finley, D. and Vogel, C. (2015a) 'K63 polyubiquitination is a new modulator of the oxidative stress response', *Nature structural & molecular biology*, 22(2), pp. 116-123.

Silva, G.M., Finley, D. and Vogel, C. (2015b) 'K63 polyubiquitination is a new modulator of the oxidative stress response', 22(2), pp. 116-23.

Simões, T., Schuster, R., den Brave, F. and Escobar-Henriques, M. (2018) 'Cdc48 regulates a deubiquitylase cascade critical for mitochondrial fusion', *eLife*, 7, p. e30015.

Skaar, J.R. and Pagano, M. (2009) 'Control of cell growth by the SCF and APC/C ubiquitin ligases', *Curr Opin Cell Biol*, 21(6), pp. 816-24.

Sliwinska, A., Kwiatkowski, D., Czarny, P., Toma, M., Wigner, P., Drzewoski, J., Fabianowska-Majewska, K., Szemraj, J., Maes, M., Galecki, P. and Sliwinski, T. (2016) 'The levels of 7,8-dihydrodeoxyguanosine (8-oxoG) and 8-oxoguanine DNA glycosylase 1 (OGG1) - A potential diagnostic biomarkers of Alzheimer's disease', *J Neurol Sci*, 368, pp. 155-9.

Song, M.S., Salmena, L., Carracedo, A., Egia, A., Lo-Coco, F., Teruya-Feldstein, J. and Pandolfi, P.P. (2008) 'The deubiquitinylation and localization of PTEN are regulated by a HAUSP-PML network', *Nature*, 455(7214), pp. 813-7.

Spence, J., Sadis, S., Haas, A.L. and Finley, D. (1995) 'A ubiquitin mutant with specific defects in DNA repair and multiubiquitination', *Mol Cell Biol*, 15(3), pp. 1265-73.

Stadtman, E.R. (2006) 'Protein oxidation and aging', *Free Radic Res*, 40(12), pp. 1250-8.

Stadtman, E.R. and Levine, R.L. (2006) 'Protein Oxidation', *Annals of the New York Academy of Sciences*, 899(1), pp. 191-208.

Stankovic-Valentin, N. and Melchior, F. (2018) 'Control of SUMO and Ubiquitin by ROS: Signaling and disease implications', *Molecular Aspects of Medicine*.

Stein, A., Ruggiano, A., Carvalho, P. and Rapoport, T.A. (2014) 'Key steps in ERAD of luminal ER proteins reconstituted with purified components', *Cell*, 158(6), pp. 1375-1388.

Sterner, D.E., Nathan, D., Reindle, A., Johnson, E.S. and Berger, S.L. (2006) 'Sumoylation of the yeast Gcn5 protein', *Biochemistry*, 45(3), pp. 1035-42.

Stewart, M.D., Ritterhoff, T., Klevit, R.E. and Brzovic, P.S. (2016) 'E2 enzymes: more than just middle men', *Cell Res*, 26(4), pp. 423-40.

Sturtz, L.A., Diekert, K., Jensen, L.T., Lill, R. and Culotta, V.C. (2001) 'A fraction of yeast Cu,Zn-superoxide dismutase and its metallochaperone, CCS, localize to the intermembrane space of mitochondria. A physiological role for SOD1 in guarding against mitochondrial oxidative damage', *J Biol Chem*, 276(41), pp. 38084-9.

Sumara I, Giménez-Abián JF, Gerlich D, Hirota T, Kraft C, de la Torre C, Ellenberg and J, Peters JM (2004) 'Roles of polo-like kinase 1 in the assembly of functional mitotic spindles', *Curr Biol*, 14(19) pp.1712-1722

Swaminathan, S., Amerik, A.Y. and Hochstrasser, M. (1999) 'The Doa4 deubiquitinating enzyme is required for ubiquitin homeostasis in yeast', *Mol Biol Cell*, 10(8), pp. 2583-94.

Swaney, D.L., Beltrao, P., Starita, L., Guo, A., Rush, J., Fields, S., Krogan, N.J. and Villen, J. (2013) 'Global analysis of phosphorylation and ubiquitylation cross-talk in protein degradation', *Nat Methods*, 10(7), pp. 676-82.

Swatek, K.N. and Komander, D. (2016) 'Ubiquitin modifications', *Cell Research*, 26(4), pp. 399-422.

Tabernero, L., Aricescu, A.R., Jones, E.Y. and Szedlacsek, S.E. (2008) 'Protein tyrosine phosphatases: structure-function relationships', *Febs j*, 275(5), pp. 867-82.

Tachibana, T., Okazaki, S., Murayama, A., Naganuma, A., Nomoto, A. and Kuge, S. (2009) 'A major peroxiredoxin-induced activation of Yap1 transcription factor is mediated by reduction-sensitive disulfide bonds and reveals a low level of transcriptional activation', *J Biol Chem*, 284(7), pp. 4464-72.

Tanaka, T., Izawa, S. and Inoue, Y. (2005) 'GPX2, encoding a phospholipid hydroperoxide glutathione peroxidase homologue, codes for an atypical 2-Cys peroxiredoxin in Saccharomyces cerevisiae', *J Biol Chem*, 280(51), pp. 42078-87.

Tang, L., Wang, W., Zhou, W., Cheng, K., Yang, Y., Liu, M., Cheng, K. and Wang, W. (2015) 'Three-pathway combination for glutathione biosynthesis in Saccharomyces cerevisiae', *Microbial Cell Factories*, 14, p. 139.

Tang, Y., Zhang, J., Yu, J., Xu, L., Wu, J., Zhou, C.-Z. and Shi, Y. (2014) 'Structure-Guided Activity Enhancement and Catalytic Mechanism of Yeast Grx8', *Biochemistry*, 53(13), pp. 2185-2196.

Tapia, P.C. (2006) 'Sublethal mitochondrial stress with an attendant stoichiometric augmentation of reactive oxygen species may precipitate many of the beneficial alterations in cellular physiology produced by caloric restriction, intermittent fasting, exercise and dietary phytonutrients: "Mitohormesis" for health and vitality', *Medical Hypotheses*, 66(4), pp. 832-843.

Taymaz-Nikerel, H., Cankorur-Cetinkaya, A. and Kirdar, B. (2016) 'Genome-Wide Transcriptional Response of Saccharomyces cerevisiae to Stress-Induced Perturbations', *Frontiers in Bioengineering and Biotechnology*, 4, p. 17.

Titen, S.W.A. and Golic, K.G. (2008) 'Telomere Loss Provokes Multiple Pathways to Apoptosis and Produces Genomic Instability in Drosophila melanogaster', *Genetics*, 180(4), pp. 1821-1832.

Tolbert, B.S., Tajc, S.G., Webb, H., Snyder, J., Nielsen, J.E., Miller, B.L. and Basavappa, R. (2005) 'The active site cysteine of ubiquitin-conjugating enzymes has a significantly elevated pKa: functional implications', *Biochemistry*, 44(50), pp. 16385-91.

Toledano, M.B., Delaunay-Moisan, A., Outten, C.E. and Igbaria, A. (2013) 'Functions and Cellular Compartmentation of the Thioredoxin and Glutathione Pathways in Yeast', *Antioxidants & Redox Signaling*, 18(13), pp. 1699-1711.

Tomalin, L.E., Day, A.M., Underwood, Z.E., Smith, G.R., Dalle Pezze, P., Rallis, C., Patel, W., Dickinson, B.C., Bähler, J., Brewer, T.F., Chang, C.J.-L., Shanley, D.P. and Veal, E.A. (2016) 'Increasing extracellular H(2)O(2) produces a bi-phasic response in intracellular H(2)O(2), with peroxiredoxin hyperoxidation only triggered once the cellular H(2)O(2)-buffering capacity is overwhelmed', *Free Radical Biology & Medicine*, 95, pp. 333-348.

Trotter, E.W. and Grant, C.M. (2005) 'Overlapping roles of the cytoplasmic and mitochondrial redox regulatory systems in the yeast Saccharomyces cerevisiae', *Eukaryot Cell*, 4(2), pp. 392-400.

Tsang, C.K., Liu, Y., Thomas, J., Zhang, Y. and Zheng, X.F.S. (2014) 'Superoxide dismutase 1 acts as a nuclear transcription factor to regulate oxidative stress resistance', *Nature Communications*, 5, p. 3446.

Turcu, F.E.R., Ventii, K.H. and Wilkinson, K.D. (2009) 'Regulation and Cellular Roles of Ubiquitin-specific Deubiquitinating Enzymes', *Annu Rev Biochem*, 78, pp. 363-97.

Turrens, J.F., Alexandre, A. and Lehninger, A.L. (1985) 'Ubisemiquinone is the electron donor for superoxide formation by complex III of heart mitochondria', *Archives of Biochemistry and Biophysics*, 237(2), pp. 408-414.

Uchida, K., Kato, Y. and Kawakishi, S. (1990) 'A novel mechanism for oxidative cleavage of prolyl peptides induced by the hydroxyl radical', *Biochem Biophys Res Commun*, 169(1), pp. 265-71.

Ukai, Y., Kishimoto, T., Ohdate, T., Izawa, S. and Inoue, Y. (2011) 'Glutathione peroxidase 2 in Saccharomyces cerevisiae is distributed in mitochondria and involved in sporulation', *Biochemical and Biophysical Research Communications*, 411(3), pp. 580-585.

Upadhyay, M., Bhadauriya, P. and Ganesh, S. (2016) 'Heat shock modulates the subcellular localization, stability, and activity of HIPK2', *Biochemical and Biophysical Research Communications*, 472(4), pp. 580-584.

Valko, M., Rhodes, C.J., Moncol, J., Izakovic, M. and Mazur, M. (2006) 'Free radicals, metals and antioxidants in oxidative stress-induced cancer', *Chemico-Biological Interactions*, 160(1), pp. 1-40.

van der Veen, A.G. and Ploegh, H.L. (2012) 'Ubiquitin-Like Proteins', *Annual Review of Biochemistry*, 81(1), pp. 323-357.

van Montfort, R.L., Congreve, M., Tisi, D., Carr, R. and Jhoti, H. (2003) 'Oxidation state of the active-site cysteine in protein tyrosine phosphatase 1B', *Nature*, 423(6941), pp. 773-7.

van Wijk, S.J. and Timmers, H.M. (2010) 'The family of ubiquitin-conjugating enzymes (E2s): deciding between life and death of proteins', *The FASEB Journal*, 24(4), pp. 981-993.

Veal, E.A., Day, A.M. and Morgan, B.A. (2007) 'Hydrogen Peroxide Sensing and Signaling', *Molecular Cell*, 26(1), pp. 1-14.

Veal, E.A., Ross, S.J., Malakasi, P., Peacock, E. and Morgan, B.A. (2003) 'Ybp1 is required for the hydrogen peroxide-induced oxidation of the Yap1 transcription factor', *J Biol Chem*, 278(33), pp. 30896-904.

Veen, A.G.v.d. and Ploegh, H.L. (2012) 'Ubiquitin-Like Proteins', *Annual Review of Biochemistry*, 81(1), pp. 323-357.

Ventii, K.H. and Wilkinson, K.D. (2008) 'Protein partners of deubiquitinating enzymes', *Biochem J*, 414(2), pp. 161-75.

Verma, R., Feldman, R.M. and Deshaies, R.J. (1997) 'SIC1 is ubiquitinated in vitro by a pathway that requires CDC4, CDC34, and cyclin/CDK activities', *Molecular Biology of the Cell*, 8(8), pp. 1427-1437.

Visintin, R., Prinz, S. and Amon, A. (1997) 'CDC20 and CDH1: a family of substrate-specific activators of APC-dependent proteolysis', *Science*, 278(5337), pp. 460-3.

Vivancos, A.P., Castillo, E.A., Biteau, B., Nicot, C., Ayté, J., Toledano, M.B. and Hidalgo, E. (2005) 'A cysteine-sulfinic acid in peroxiredoxin regulates H(2)O(2)-sensing by the antioxidant Pap1 pathway', *Proceedings of the National Academy of Sciences of the United States of America*, 102(25), pp. 8875-8880.

von Zglinicki, T. (2000) 'Role of oxidative stress in telomere length regulation and replicative senescence', *Ann N Y Acad Sci*, 908, pp. 99-110.

Vosper, J.M.D., McDowell, G.S., Hindley, C.J., Fiore-Heriche, C.S., Kucerova, R., Horan, I. and Philpott, A. (2009) 'Ubiquitylation on Canonical and Non-canonical Sites Targets the Transcription Factor Neurogenin for Ubiquitin-mediated Proteolysis', *The Journal of Biological Chemistry*, 284(23), pp. 15458-15468.

Walsh Christopher, T., Garneau-Tsodikova, S. and Gatto Gregory, J. (2005) 'Protein Posttranslational Modifications: The Chemistry of Proteome Diversifications', *Angewandte Chemie International Edition*, 44(45), pp. 7342-7372.

Wang, Y., Marotti, L.A., Jr., Lee, M.J. and Dohlman, H.G. (2005) 'Differential regulation of G protein alpha subunit trafficking by mono- and polyubiquitination', *J Biol Chem*, 280(1), pp. 284-91.

Wang, Y., Serricchio, M., Jauregui, M., Shanbhag, R., Stoltz, T., Di Paolo, C.T., Kim, P.K. and McQuibban, G.A. (2015) 'Deubiquitinating enzymes regulate PARK2-mediated mitophagy', *Autophagy*, 11(4), pp. 595-606.

Wang, Z., Zhu, W.-G. and Xu, X. (2017) 'Ubiquitin-like modifications in the DNA damage response', *Mutation Research/Fundamental and Molecular Mechanisms of Mutagenesis*, 803-805, pp. 56-75.

Wäsch, R. and Cross, F.R. (2002) 'APC-dependent proteolysis of the mitotic cyclin Clb2 is essential for mitotic exit', *Nature*, 418, p. 556.

Watts, F.Z. (2013) 'Starting and stopping SUMOylation. What regulates the regulator?', *Chromosoma*, 122(6), pp. 451-63.

Wauer, T., Swatek, K.N., Wagstaff, J.L., Gladkova, C., Pruneda, J.N., Michel, M.A., Gersch, M., Johnson, C.M., Freund, S.M. and Komander, D. (2015) 'Ubiquitin Ser65 phosphorylation affects ubiquitin structure, chain assembly and hydrolysis', *Embo j*, 34(3), pp. 307-25.

Wei, N. and Deng, X.W. (2003) 'The COP9 signalosome', *Annu Rev Cell Dev Biol*, 19, pp. 261-86.

Wei, R., Liu, X., Yu, W., Yang, T., Cai, W., Liu, J., Huang, X., Xu, G.T., Zhao, S., Yang, J. and Liu, S. (2015) 'Deubiquitinases in cancer', *Oncotarget*, 6(15), pp. 12872-89.

Weinert, Brian T., Schölz, C., Wagner, Sebastian A., Iesmantavicius, V., Su, D., Daniel, Jeremy A. and Choudhary, C. (2013) 'Lysine Succinylation Is a Frequently Occurring Modification in Prokaryotes and Eukaryotes and Extensively Overlaps with Acetylation', *Cell Reports*, 4(4), pp. 842-851.

Wenzel, D.M. and Klevit, R.E. (2012) 'Following Ariadne's thread: a new perspective on RBR ubiquitin ligases', *BMC Biology*, 10(1), p. 24.

Wheeler, G.L., Quinn, K.A., Perrone, G., Dawes, I.W. and Grant, C.M. (2002) 'Glutathione regulates the expression of gamma-glutamylcysteine synthetase via the Met4 transcription factor', *Mol Microbiol*, 46(2), pp. 545-56.

Williams, R.L. and Urbé, S. (2007) 'The emerging shape of the ESCRT machinery', *Nature Reviews Molecular Cell Biology*, 8, p. 355.

Wong, C.M., Siu, K.L. and Jin, D.Y. (2004) 'Peroxiredoxin-null yeast cells are hypersensitive to oxidative stress and are genomically unstable', *J Biol Chem*, 279(22), pp. 23207-13.

Wong, C.M., Zhou, Y., Ng, R.W., Kung Hf, H.F. and Jin, D.Y. (2002) 'Cooperation of yeast peroxiredoxins Tsa1p and Tsa2p in the cellular defense against oxidative and nitrosative stress', *J Biol Chem*, 277(7), pp. 5385-94.

Wood, Z.A., Schröder, E., Robin Harris, J. and Poole, L.B. (2003) 'Structure, mechanism and regulation of peroxiredoxins', *Trends in Biochemical Sciences*, 28(1), pp. 32-40.

Xu, X., Blackwell, S., Lin, A., Li, F., Qin, Z. and Xiao, W. (2015) 'Error-free DNA-damage tolerance in Saccharomyces cerevisiae', *Mutat Res Rev Mutat Res*, 764, pp. 43-50.

Xu, Z., Lam, L.S., Lam, L.H., Chau, S.F., Ng, T.B. and Au, S.W. (2008) 'Molecular basis of the redox regulation of SUMO proteases: a protective mechanism of intermolecular disulfide linkage against irreversible sulfhydryl oxidation', *Faseb j*, 22(1), pp. 127-37.

Yan, C., Lee, L.H. and Davis, L.I. (1998) 'Crm1p mediates regulated nuclear export of a yeast AP-1-like transcription factor', *Embo j*, 17(24), pp. 7416-29.

Yang, W. and Hekimi, S. (2010) 'A mitochondrial superoxide signal triggers increased longevity in Caenorhabditis elegans', *PLoS Biol*, 8(12), p. e1000556.

Ye, Y. and Rape, M. (2009) 'Building ubiquitin chains: E2 enzymes at work', *Nat Rev Mol Cell Biol*, 10(11), pp. 755-64.

Yeasmin Khusbu, F., Chen, F.-Z. and Chen, H.-C. (2018) 'Targeting ubiquitin specific protease 7 in cancer: A deubiquitinase with great prospects', *Cell Biochemistry and Function*, 36(5), pp. 244-254.

Yen, James L., Flick, K., Papagiannis, Christie V., Mathur, R., Tyrrell, A., Ouni, I., Kaake, Robyn M., Huang, L. and Kaiser, P. (2012) 'Signal-Induced Disassembly of the SCF Ubiquitin Ligase Complex by Cdc48/p97', *Molecular Cell*, 48(2), pp. 288-297.

Yi, D.G., Kim, M.J., Choi, J.E., Lee, J., Jung, J., Huh, W.-K. and Chung, W.-H. (2016) 'Yap1 and Skn7 genetically interact with Rad51 in response to oxidative stress and DNA double-strand break in Saccharomyces cerevisiae', *Free Radical Biology and Medicine*, 101, pp. 424-433.

Yonashiro, R., Ishido, S., Kyo, S., Fukuda, T., Goto, E., Matsuki, Y., Ohmura-Hoshino, M., Sada, K., Hotta, H., Yamamura, H., Inatome, R. and Yanagi, S. (2006) 'A novel mitochondrial ubiquitin ligase plays a critical role in mitochondrial dynamics', *EMBO J*, 25(15), pp. 3618-26.

Yuan, J., Luo, K., Zhang, L., Cheville, J.C. and Lou, Z. (2010) 'USP10 Regulates p53 Localization and Stability by Deubiquitinating p53', *Cell*, 140(3), pp. 384-396.

Zemirli, N., Morel, E. and Molino, D. (2018) 'Mitochondrial Dynamics in Basal and Stressful Conditions', *International Journal of Molecular Sciences*, 19(2), p. 564.

Zhang, B., Bandyopadhyay, S., Shakamuri, P., Naik, S.G., Huynh, B.H., Couturier, J., Rouhier, N. and Johnson, M.K. (2013) 'Monothiol Glutaredoxins Can Bind Linear [Fe(3)S(4)](+) and [Fe(4)S(4)](2+) Clusters in Addition to [Fe(2)S(2)](2+) Clusters: Spectroscopic Characterization and Functional Implications', *Journal of the American Chemical Society*, 135(40), p. 10.1021/ja407059n.

Zhou, J., Wang, J., Chen, C., Yuan, H., Wen, X. and Sun, H. (2018) 'USP7: Target Validation and Drug Discovery for Cancer Therapy', *Med Chem*, 14(1), pp. 3-18.

Zhu, H., Santo, A. and Li, Y. (2012) 'The antioxidant enzyme peroxiredoxin and its protective role in neurological disorders', *Exp Biol Med (Maywood)*, 237(2), pp. 143-9.

Zou, C. and Mallampalli, R.K. (2014) 'Regulation of histone modifying enzymes by the ubiquitin-proteasome system', *Biochimica et biophysica acta*, 1843(4), pp. 694-702.

Zou, Q., Jin, J., Hu, H., Li, H.S., Romano, S., Xiao, Y., Nakaya, M., Zhou, X., Cheng, X., Yang, P., Lozano, G., Zhu, C., Watowich, S.S., Ullrich, S.E. and Sun, S.C. (2014) 'USP15 stabilizes MDM2 to mediate cancer-cell survival and inhibit antitumor T cell responses', *Nat Immunol*, 15(6), pp. 562-70.